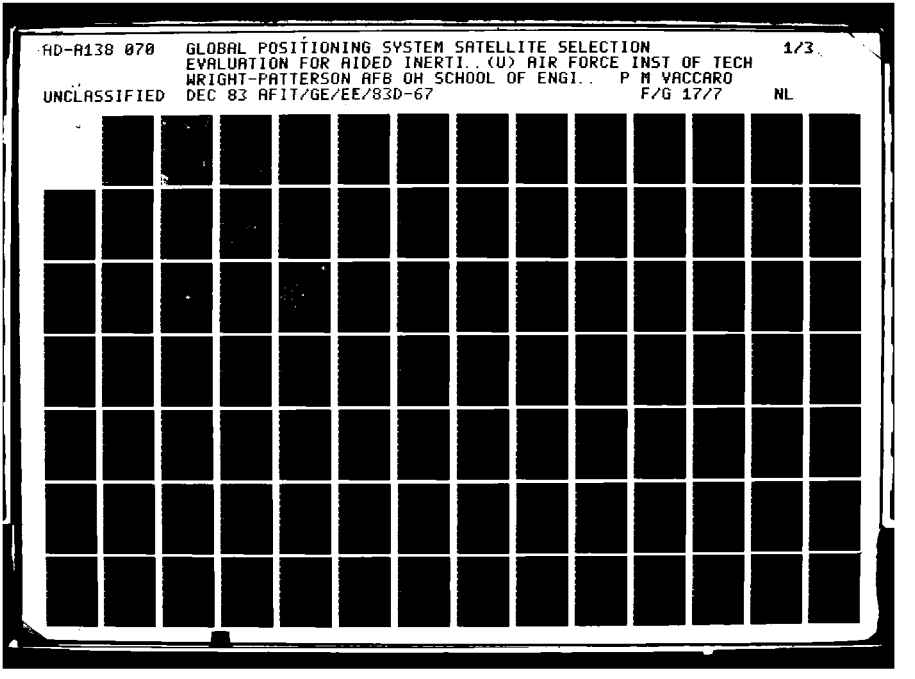
AD-A138 070
GLOBAL POSITIONING SYSTEM SATELLITE SELECTION
EVALUATION FOR AIDED INERTI..(U) AIR FORCE INST OF TECH
WRIGHT-PATTERSON AFB OH SCHOOL OF ENGI.. P M VACCARO
UNCLASSIFIED
DEC 83 AFIT/GE/EE/83D-67
F/G 17/7
NL
1/3

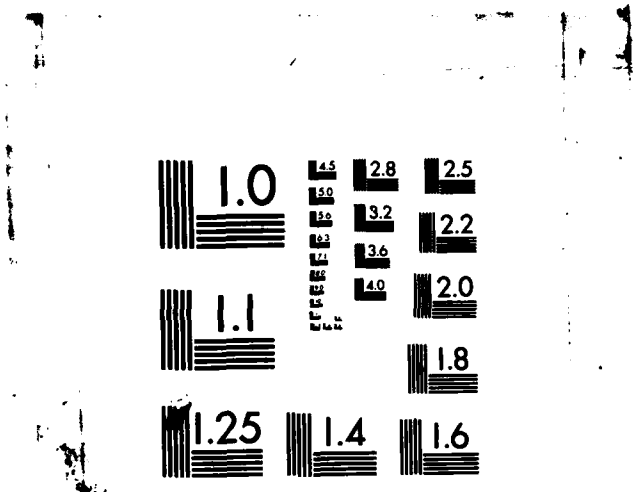

GLOBAL POSITIONING SYSTEM SATELLITE SELECTION EVALUATION FOR AIDED INERTIAL NAVIGATION

THESIS

Peter M. Vaccaro
AFIT/GE/EE/83D-67 1st Lt USAF

DEPARTMENT OF THE AIR FORCE
AIR UNIVERSITY
AIR FORCE INSTITUTE OF TECHNOLOGY

Wright-Patterson Air Force Base, Ohio

AFIT/GE/EE/83D-67

GLOBAL POSITIONING SYSTEM SATELLITE SELECTION EVALUATION FOR AIDED INERTIAL NAVIGATION

THESIS

Peter M. Vaccaro
AFIT/GE/EE/83D-67 1st Lt USAF

Approved for public release; distribution unlimited

AFIT/GE/EE/83D-67

GLOBAL POSITIONING SYSTEM SATELLITE SELECTION EVALUATION FOR AIDED INERTIAL NAVIGATION

THESIS

Presented to the Faculty of the School of Engineering
of the Air Force Institute of Technology
Air University
in Partial Fulfillment of the
Requirements for the Degree of
Master of Science

by

Peter M. Vaccaro, B.S.E.E.
1st Lt USAF
Graduate Electrical Engineering

December 1983

Acknowledgments

I would like to express my thanks to Dr. Peter Maybeck, Mr. Jerry Covert, and Ms. Sandy Berning for all their help with this thesis effort. My special thanks to Lt. Colonel Robert Edwards for his extensive guidance as my thesis advisor and best wishes in his civilian career.

My special appreciation to my wife, Maureen for her patience and understanding during the course of my graduate program.

I dedicate this thesis to my daughter Laura, born September 23, 1983 with the hope that the world she grows up in will be a better place to live in not only because of the advances in science but also the advances in the wisdom of mankind to live together in peace.

Peter M. Vaccaro

Contents

List of Figures

List of Tables

Abstract

The navigation performance of the geometric dilution of precision (GDOP) GPS satellite selection criterion versus an alternate GPS satellite selection criterion for an integrated GPS/INS Navigator in a jamming environment is tested and analyzed.

The theoretical development of GDOP and GDOP-based satellite selection criterion are reviewed. From this review a satellite selection criterion known as the cost criterion (which is a combination of noise-weighted GDOP and the a priori covariance weighted least squares position error) is selected for performance testing against a GDOP satellite selection criterion.

Performance assessment of the two satellite selection criterion is accomplished using a modified version of the integrated GPS/INS (IGI) Computer Simulation. The IGI Simulator is modified to simulate adaptive band-width control of the satellite tracking loops, the use of a null steering antenna, the use of an alternate satellite selection criterion, and the effects due to jammers. The performance assessment is based on simulating a single F-4 Close-Air-Support Mission encountering five different jamming scenarios.

For the five test missions, the cost criterion demonstrates a performance improvement of 10-350 feet in mean radial position error with respect to GDOP performance. However, a performance degradation of 10-30 feet mean radial position error is observed for missions with rapidly varying jamming power.

GLOBAL POSITIONING SYSTEM SATELLITE SELECTION EVALUATION FOR AIDED INERTIAL NAVIGATION

I Introduction

The NAVSTAR Global Positioning System (GPS) is a space-based satellite navigation system that provides highly accurate global navigation capability to suitably equipped users. The GPS User Equipment (UE) set collects and processes GPS satellite navigation signals to determine the user's three dimensional position, velocity and GPS time. The GPS UE set can operate either in a stand-alone mode or an integrated mode (integrated with other navigation systems). Integration of the GPS UE set with navigation systems such as Doppler radar or an inertial navigation system (INS) provides accurate navigation under severe operating conditions (i.e., high jamming levels with respect to the GPS satellite signals) (1:2). The benefits of an integrated GPS/INS have been well documented in a number of reports (Refs 2, 3, 5, 6, and 10). A few of the benefits of an integrated GPS/INS navigator are (3:145):

(1) Increased UE set tolerance to jamming

(2) Increased UE set tolerance to severe aircraft dynamics.

(3) Rapid alignment of the INS, by the UE set

(4) The UE set updated INS: can navigate independently during GPS unavailability and provide initialization data for rapid GPS reacquisition when GPS signal conditions improve.

The concern in the Air Force over GPS unavailability due to jamming has resulted in research to improve the GPS UE sets' anti-jam capability (Refs. 5, 6, and 10). This research resulted in a number of methods for GPS UE set improvements. From the number of methods suggested, three main methods for improving the GPS UE sets' jamming tolerance are (6:297):

(1) adaptive bandwidth control, inertial, and/or Doppler aiding of the GPS UE sets' satellite tracking loops

(2) adaptive (pattern) antennas for increasing the strength of the GPS satellite signal and decreasing the strength of jamming signals

(3) alternate satellite selection criteria to choose satellites which will maintain high navigation accuracy and not be jammed off-the-air.

All three methods of increasing the GPS UE sets' capability in a jamming environment will be discussed in the following pages. The primary emphasis of this report, however, will be on the analysis and testing of an alternate satellite selection criterion (to be known as the "cost criterion") against the normal satellite selection criterion also used in the GPS UE set. The alternate satellite selection criterion versus the standard satellite selection criterion, will be tested using the rigorous and proven integrated GPS/INS

(IGI) computer simulation developed at the Avionics Laboratory at the Air Force Wright Aeronautical Laboratories, Wright-Patterson AFB, Ohio (7).

To understand the GPS UE sets' satellite selection problem, a thorough review of the terminology and theory behind the GPS Program must be accomplished. Therefore, the GPS Program will be reviewed in Chapter II, with particular emphasis on the composition of the satellite constellation, the components of the GPS UE set, and the theory and operation of the UE set. The satellite selection process will be further isolated and analyzed in Chapter III. Chapter III will present a tutorial on the classical satellite selection criterion and extensions to the classical criterion to improve integrated GPS/INS navigation performance. One extension to the classical satellite selection criterion will be identified as the "cost criterion", which will be tested in the IGI computer simulation.

An overview of the integrated GPS/INS (IGI) computer simulation will be presented in Chapter IV. This chapter will present the necessary math models used in the computer simulation as well as other information necessary to follow the data analysis in Chapter V.

The result of this report will be to document conclusive results of the performance of an alternate satellite selection criterion over the standard satellite selection criterion. This comparison will be based on the results of a rigorous computer simulation using a realistic environment

(a tactical aircraft in a highly dyramic, jamming environment). In addition, a valuable tool will have been created (the modified computer simulation) with which to test other satellite selection criteria as well as adaptive receiver and adaptive antenna designs.

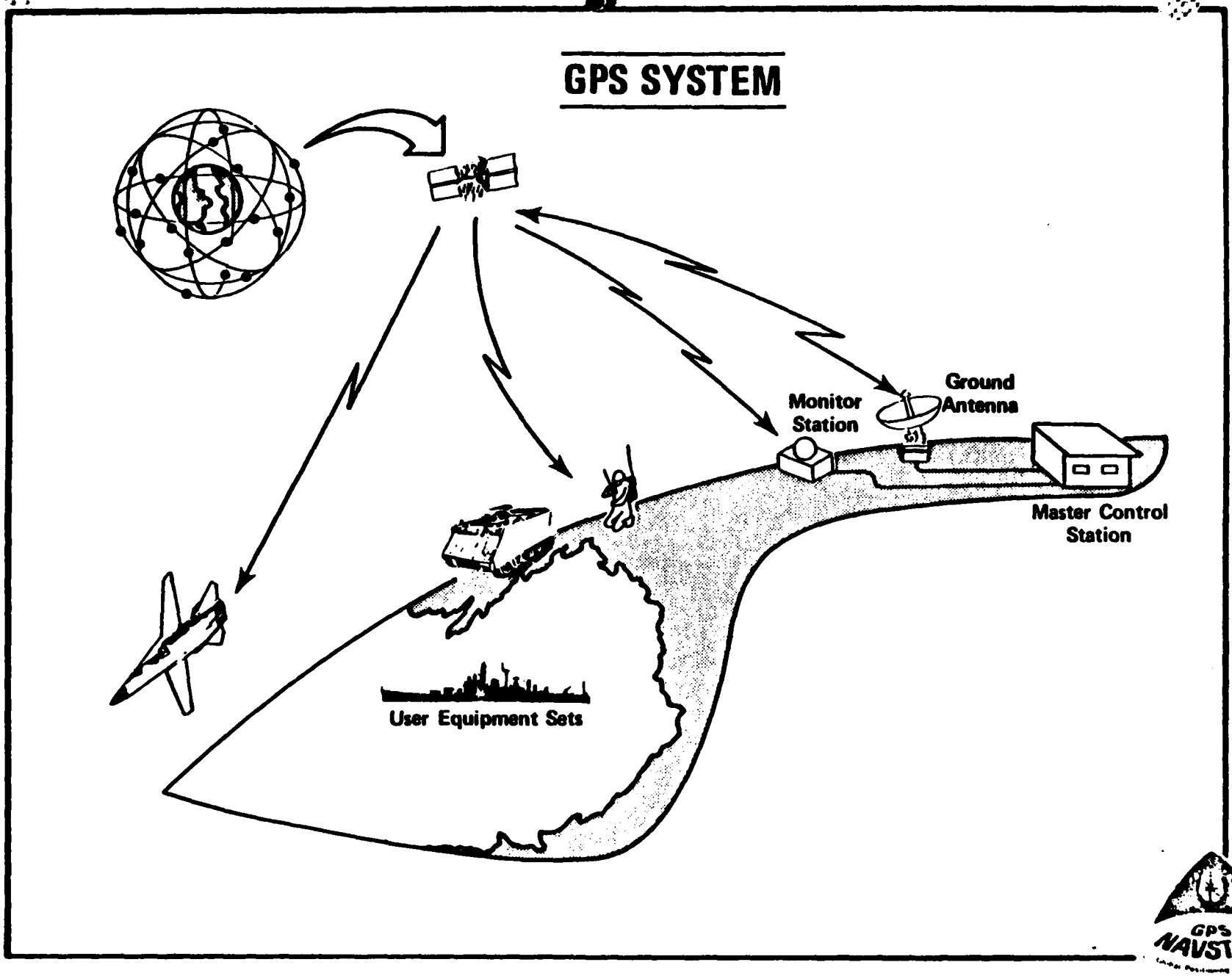

Figure 1. GPS System Overview (1:3)

II NAVSTAR GPS Program Review

Introduction

The NAVSTAR Global Positioning System (GPS) is a space-based satellite navigation system that provides very accurate three dimensional position, velocity, and GPS time, world-wide, to suitably equipped users. The GPS Program is composed of three segments: the Space Segment, the Control Segment, and the User Segment. Each segment plays an important role in maintaining the 24 hour-a-day, all weather, high accuracy global navigation capability that is NAVSTAR/GPS (Figure 1). The following sections in this chapter will discuss each segment, with primary emphasis on the Satellite and User Segments. The level of detail that is covered in each section is determined by the further development of terminology and theory in the next chapter.

Space Segment

The Space Segment is responsible for planning and deployment of the 18 satellites in the GPS constellation. The 18 GPS satellites occupy six different orbital planes with three satellites evenly spaced within each orbital plane. The six orbital planes are inclined at an angle of 55° and each is separated by 60° of longitude. The relative phasing of the satellites from one orbit plane to the next is 40° in an easterly direction. The phasing of satellites means that when a satellite in one orbital plane crosses the equator, the satellite in the next orbital plane (moving in an

easterly direction) is North of the equator by 40° latitude. Each satellite operates at an altitude of 10,900 nautical miles in a circular orbit with a period of one satellite revolution around the earth equal to approximately 12 hours (Figure 2). This particular arrangement of satellites in the GPS constellation was chosen for overall user accuracy, the minimum size and duration of regions of poor navigation performance, and survivability of the satellite constellation. Other factors favorable to this constellation are the ease of replenishment and sparing, ease of build-up to the full constellation, and the constellation's potential to grow to 24 satellites (should funding permit) (Ref 4 and 8).

The GPS satellite navigation signal uses the communication techniques of spread spectrum, pseudo-random noise (PRN) and biphase-shift-keying (BPSK). A spread spectrum signal will typically occupy a signal bandwidth much larger than the information bandwidth (typically greater than 10 times the information bandwidth). Spreading the signal has no adverse effect on performance but provides benefits in signal security, anti-jamming capability (against impulse, continuous, burst, swept, narrowband, and wideband noise), and transmission security (i.e., beyond some range from the satellite the transmitter signal is buried in natural background noise). Pseudo-random-noise (PRN) and biphase-shift-keying (BPSK) of the carrier signal are analogous to time tagging the satellite signal. The phase of the carrier signal is periodically shifted forward or backward as determined

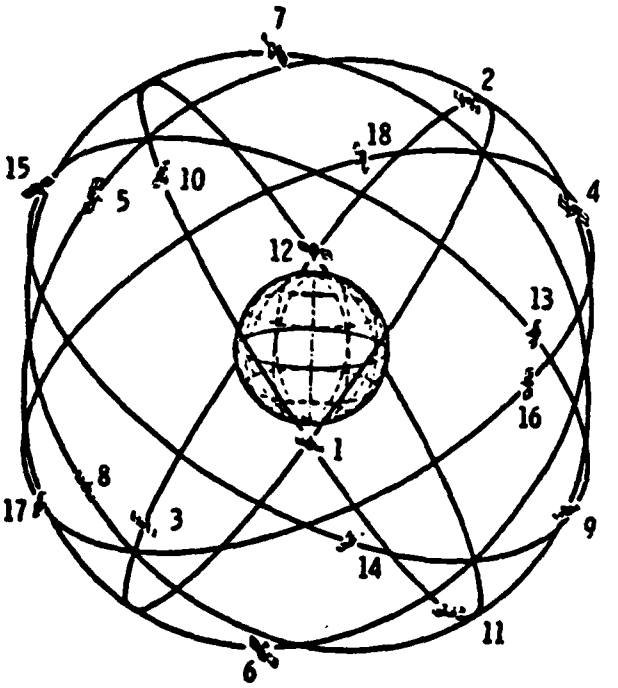

Figure 2. The 6-Plane, 18-Satellite Configuration (4:E9.3.2)

by the instantaneous value of a very long sequence of digital ones and zeros. This sequence is called PRN because, to the casual observer, the ones and zeros appear to occur in a purely random fashion. In actuality, the code generated is predictable relative to the time it was started.

The user can deduce when the code was transmitted by matching his own copy of the code to the incoming signal. The amount the user must shift the code to match the incoming signal determines the estimate of the time that the signal took to reach the user. A range measurement (from the user to the satellite) can be calculated by multiplying the estimate of the satellite signal propagation time to the velocity of an electromagnetic wave (approximately equal to the speed of light).

The GPS satellites transmit navigation signals on two frequencies, 1575.42 MHZ(L1) and 1227.6 MHZ(L2). The reason for transmission on two frequencies is that during daylight hours solar radiation produces a belt of ionized particles in a portion of the atmosphere known as the ionosphere (40-300 miles above the earth surface). Signals passing through this region are refracted resulting in longer than normal propagation of the satellite signals to the user (and a resultant longer time delay estimate). The increase in time delays translate into ranging errors which, if uncorrected, can sometimes lead to relatively large position errors. The ionospheric effect has a predictable, annual pattern of variation. However, the effect is not a totally predictable

phenomena. For high accuracy positioning the phenomena cannot be completely modeled. By making range measurements on both L1 and L2 signals at the same time, a simple mathematical technique can be used to correct the ionospheric error (22:115).

At L1: $$R_1 = R_{TRUE} + (k/f_1^2) \quad (1)$$

At L2: $$R_2 = R_{TRUE} + (k/f_2^2) \quad (2)$$

Combining and rearranging:

$$R_{TRUE} = \frac{R_1 - (f_2/f_1)^2 R_2}{1-(f_2/f_1)^2} \quad (3)$$

Where: R_1 and R_2 are estimates of the true range, R_{TRUE}
f_1 and f_2 are the respective L1 and L2 frequencies
k is a constant associated with the ionospheric error

Superimposed on the L1 frequency are two uniquely coded signals, a precise or P code, and a coarse/acquisition or C/A code. The P code is a very long sequence of digital pulses which does not repeat for approximately 280 days (a PRN code). The pulse train is created by a complex set of equipment on the satellite. The code is generated at 10.23 megabits per second chipping rate, where a chip is the time interval of one pulse in the pulse train (a chip for the P code equals 97.7×10^{-9} seconds). A unique portion of this code (one week) is assigned to each of the GPS satellites. Therefore,

the user can distinguish from the code which of the satellites it is tracking. The C/A code is a short sequence relative to the P code and has a chipping rate of one tenth the P code. The C/A codes are chosen from a family of distinct codes called gold codes. The use of gold codes assures minimum interference between satellites, again allowing unique satellite identification (Ref. 23). The C/A code was chosen to assist the GPS UE set in reducing the time necessary to acquire and track the longer P code (Figure 3) (Ref. 23).

Since the P and C/A codes are chosen not to interfere with each other (i.e., minimum correlation among the codes), they can be modulated onto the same carrier frequencies in the satellite. Transmitters are known to be much more efficient with constant amplitude signals. Therefore, the P and C/A carriers, though derived from the same source, are phase shifted 90° apart, modulated by the P and C/A codes respectively and then combined. This process is known as phased quadrature, and it produces a composite continuous wave (CW) signal at 1575.42 MHZ (L1) (See Figure 4).

Both the P and C/A codes are modulated by a 50 bit-per-second data message by the method of biphase-shift-keying (BPSK). The total block of data transmitted is 1500 bits, thus the user will require at least 30 seconds to read the full block of data for each satellite. The data message contains system time, satellite clock offset and drift errors, satellite position information (ephemerides), C/A to P code handover information, and an almanac of the health and

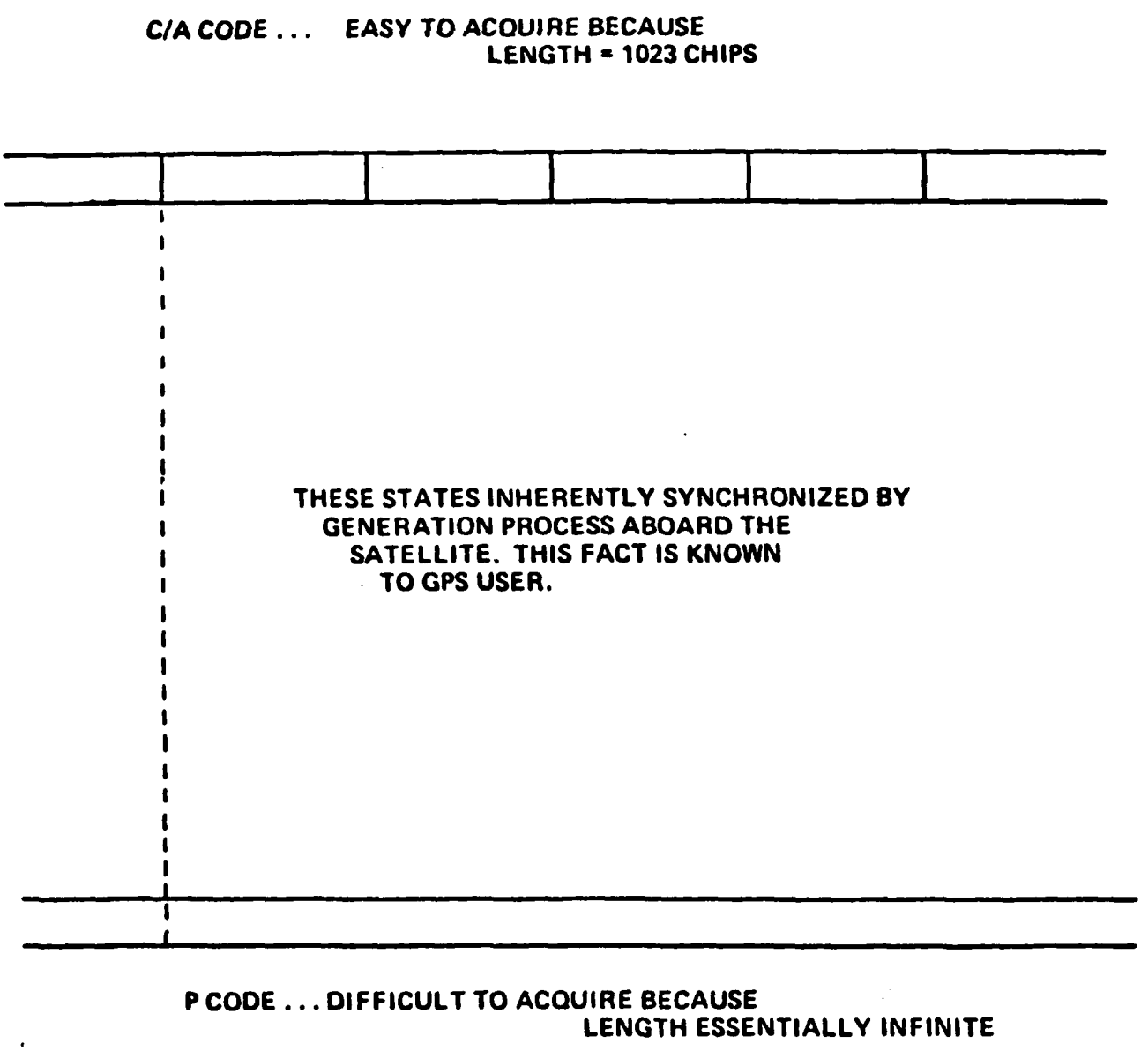

Figure 3. Relationship Between GPS Coarse/Acquisition Code and the GPS Precision Code (23:6).

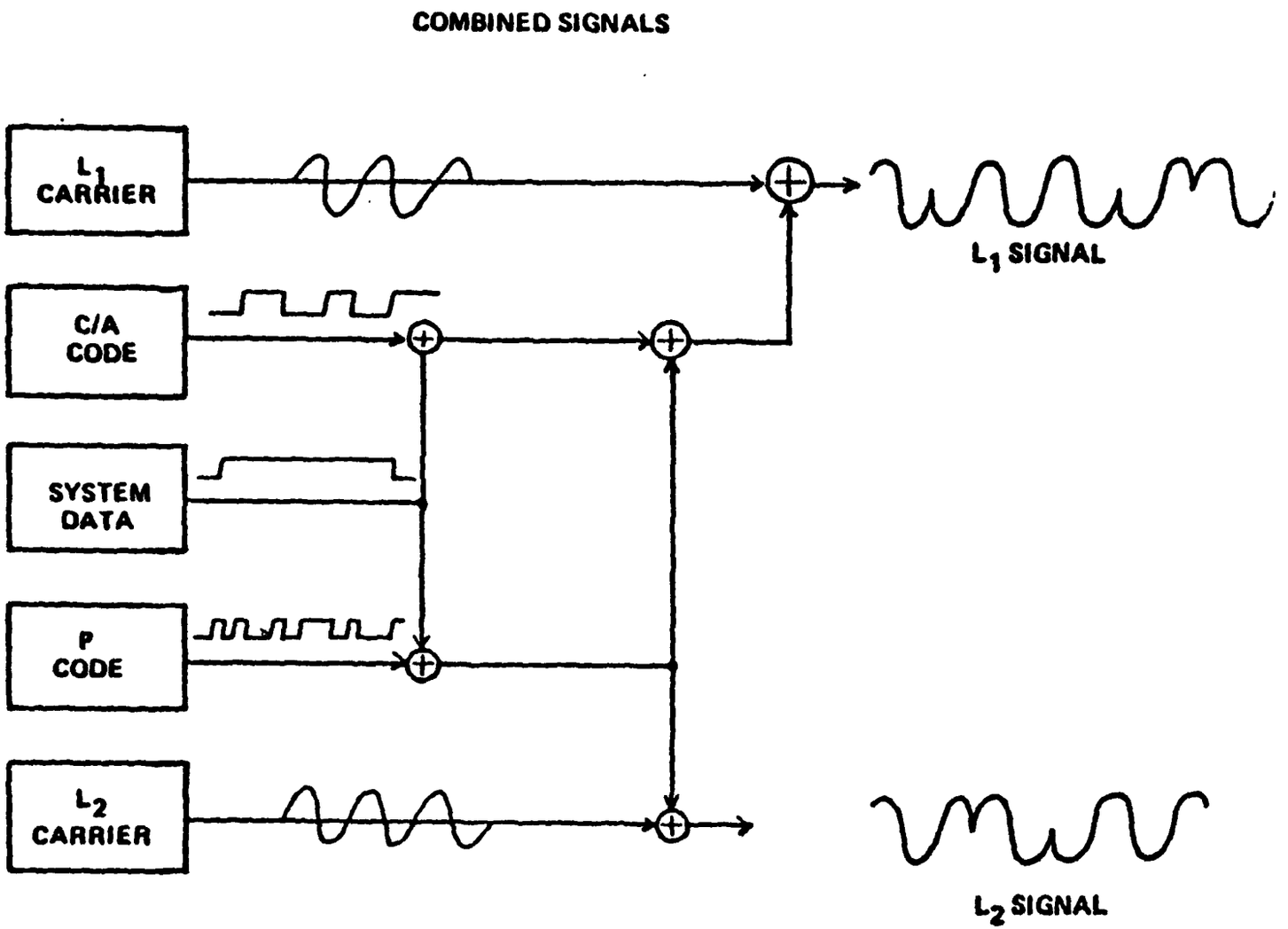

Figure 4. GPS Satellite Signal Formation (23:10).

positions of all other satellites in the GPS constellation. Relative to the ranging codes (P and C/A codes), the data message rate is very slow. It can thus be superimposed on the ranging codes (and separated at the user's receiver) without affecting either the ranging codes or the data message. The particular ranging code and data message are combined prior to modulating the carrier. The combination of the two signals is by modulo-2 addition (exclusive-OR). For convenience, the same set of data that is modulo-2 added to the P code is also added to the C/A code. The generation of the L1 signal (1575.42 MHZ) containing both P code and the C/A code with the data message added to both has just been described. The L2 signal (1227.6 MHZ) is created in the same manner, but contains the P code and data message only (no C/A code).

Control Segment

The Control Segment is composed of seven Monitor Stations (MS), three Ground Antennas (GA), and a Master Control Station (MCS). The Monitor Stations and Ground Antennas are stationed throughout the world on U.S. controlled property. The Master Control Station is located at the Consolidated Space Operations Center (CSOC), outside Colorado Springs, Colorado.

The Monitor Stations continuously collect navigation signals from all the satellites. This information is then transmitted back to the MCS for processing. At the MCS, the satellites' corrected positions and clock error/offset

information are determined. This information is relayed to a Ground Antenna for transmission to the satellites.

In addition to the corrected navigation data the MCS also performs satellite station keeping, health status checks of the satellite hardware, and many other satellite maintenance functions required to keep the satellites working efficiently. This satellite information is transmitted and received on a coded S-band frequency.

User Segment

The purpose of the User Segment is to develop, test, and produce the User Equipment (UE) set. The UE set is composed of the control/display unit (CDU), the receiver/processor unit (RPU), and either a fixed reception pattern antenna (FRPA) or a controlled reception pattern antenna (CRPA), with an antenna control unit.

User Equipment (UE) Operation: Theory. The UE set can locate its three dimensional position by knowing the distance or range from three reference points. In GPS, the reference points at any time are positions of GPS satellites. A UE set can deduce the range to a satellite at any time, because, as stated in the satellite signal description, the time of transmission of the signal can be determined by the code. By noting the time of arrival of the signal, the user can calculate the range (See Figure 5).

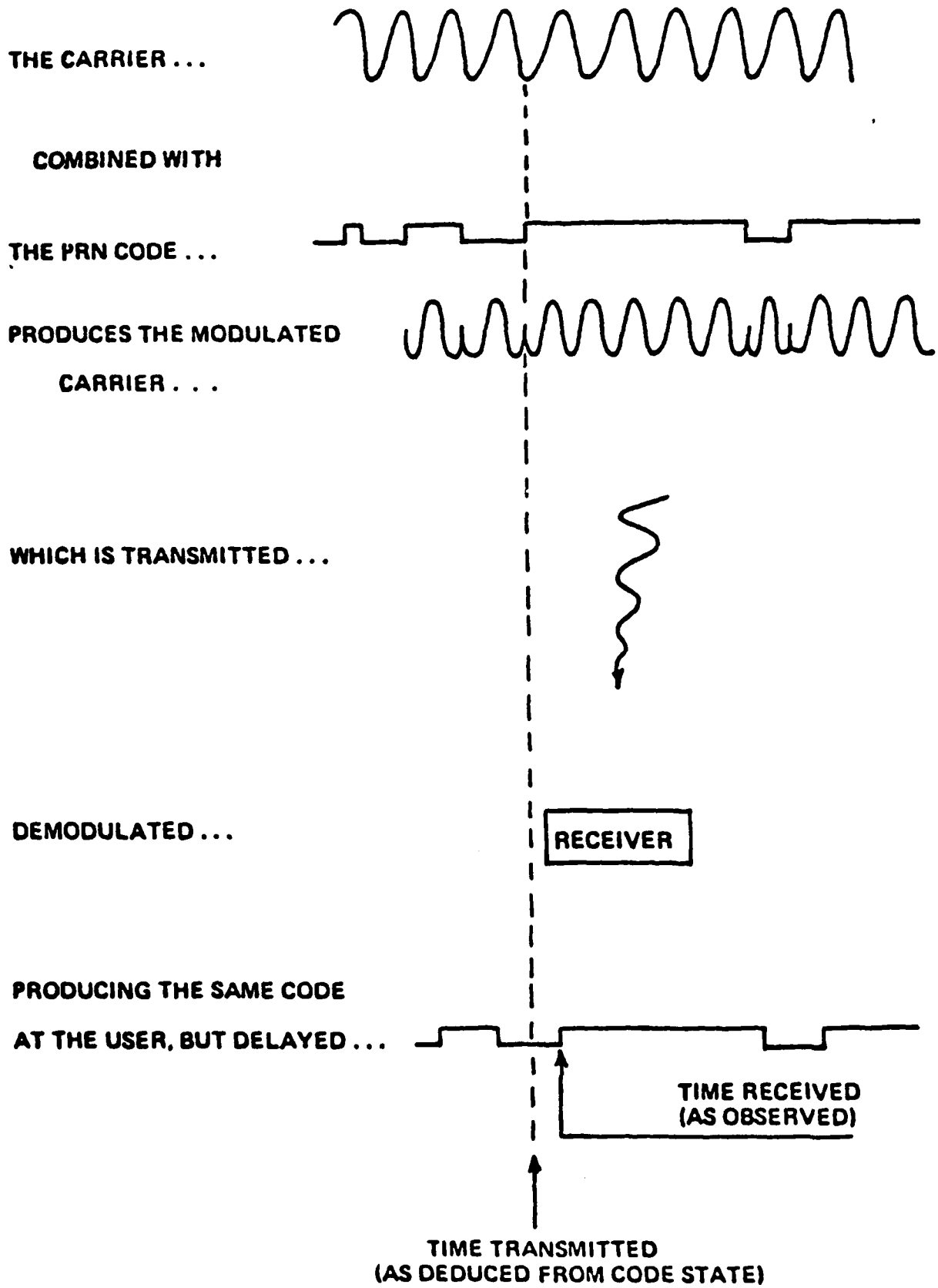

Figure 5. GPS User Equipment Operation (23:14)

Range (R) = Speed of Light (c) x (time of arrival - time transmitted) (4)

Equation (1), however, assumes that the satellite's clock and the UE clock are synchronized. Therefore, the calculated range will be in error by an amount proportional to the time error (or time bias) due to the mismatch of the satellite and receiver clocks. Thus,

$$PR = R_T + R_B = c \times (t_a - t_T + t_B) \quad (5)$$

$$R_B = c \times t_B = \text{time bias ranging error} \quad (6)$$

Where

PR = Pseudo-range measurements

R_T = True Range

R_B = Range Error due to time bias

c = Speed of light in a vacuum

t_a = Time of signal arrival

t_T = Time of signal transmission

t_B = Time bias

The time bias introduces another unknown into the solution of the range equations, in addition to the three desired components of the user's position. To allow instantaneous calculation of these four navigation unknowns, four independent measurements of range are needed to four satellites (Figure 6). Because of the time bias, the range measurements are known as pseudoranges.

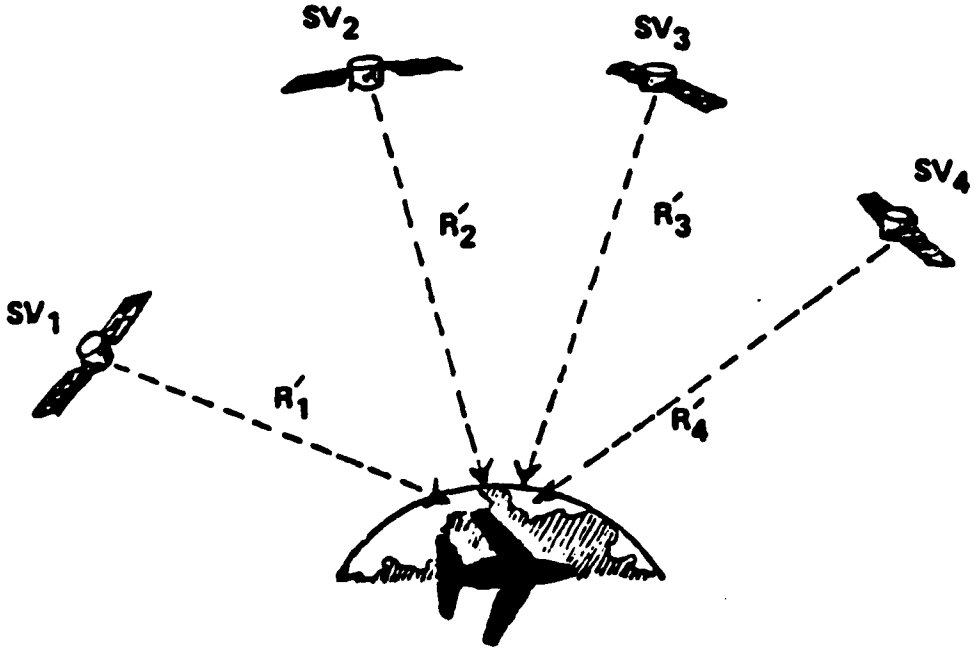

WITH AN UNSYNCHRONIZED CLOCK, THE GPS USER MUST TAKE PSEUDORANGE MEASUREMENTS TO FOUR SATELLITES.

$$R'_1 = R_1 + ct_b$$

$$R'_2 = R_2 + ct_b$$

$$R'_3 = R_3 + ct_b$$

$$R'_4 = R_4 + ct_b$$

Figure 6. GPS User Equipment Operation: Pseudorange Measurements (1:15)

The receiver will collect and calculate pseudorange measurements (simultaneously or sequentially) to four selected satellites as well as changes to the pseudoranges as a function of time. This latter measurement is called a delta pseudorange (or simply a delta range) and may be calculated by counting the number of carrier cycles that occur during a finite interval (usually 0.1 to 0.5 seconds) or by differencing pseudorange measurements at the beginning and end of a finite time interval.

To make pseudorange measurements, the receiver must lock-on and track the incoming signals, determine the time-of-arrival and time-transmitted parameters for pseudorange calculation. To accomplish these tasks, the UE essentially reverses the modulation process of the satellite transmission. The spread spectrum is collapsed back to a single frequency, continuous wave signal. The receiver/processor unit then uses correlation techniques to track the satellite code and carrier. A phase lock loop is used to track the carrier frequency, while a code tracking loop (an internal) code generated to match the transmitted satellite code) is used to track the coded signal (See Figure 7). The receiver detects maximum correlation between the two codes when the internal code generator is perfectly aligned with the received code. Misalignment of the codes causes the correlation of the two codes to decrease to a relatively small value. The precision with which the time-of-arrival can be measured depends on the chip size (pulse width) of the code. The P code has

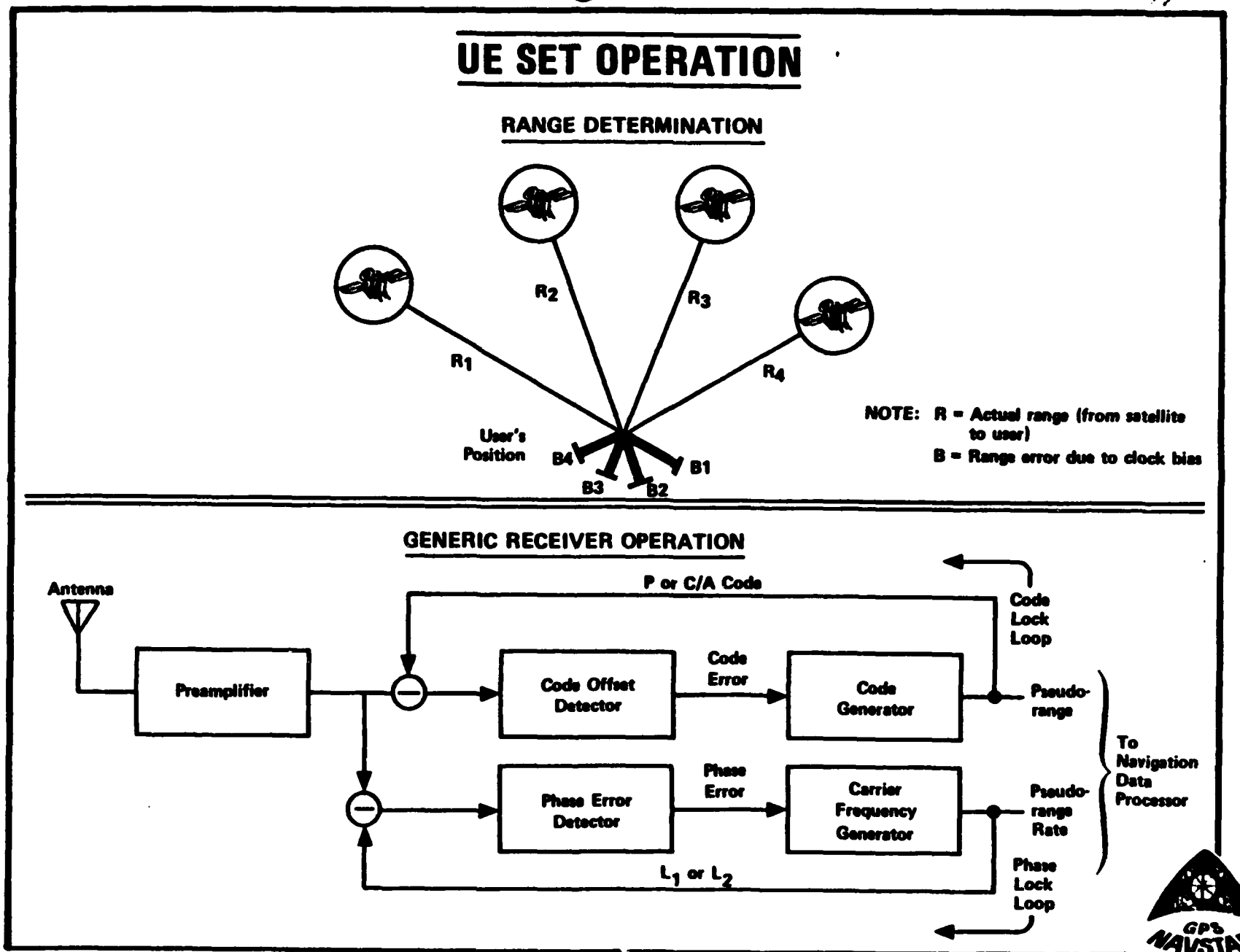

Figure 7. UE Set Operation: Range Determination/Receiver Operation (1:31)

a chip size of ± 97.7 nanoseconds, which is equivalent to ± 29.3 meters ranging error. As stated earlier, synchronizing on the P code is very difficult due to the fact that the P code takes so long to repeat. The C/A code repeats every millisecond and has a pulse width ten times the P code, thus its primary use is for fast acquisition of the satellite signals.

In general, prior to tracking, the signal generated in the code tracking loop will not correlate with the received satellite signal due to the unknown time delay for the satellite signal to reach the user and the unknown UE sets' clock bias errors. Similarly, the signal generated in the phase lock loop differs from the received signal due to an unknown Doppler offset of the carrier frequency caused by the relative velocity between the user and the satellite and a bias in the UE sets' frequency standard (1:30). During satellite acquisition, the UE set shifts a code and carrier search window (the size of the search window is determined by how well the satellites' positions and velocities, and the user's position and velocity are known) until a received signal matches a known satellite signal. Matching a satellite signal in the acquisition phase results in an estimate of the time and frequency bias errors, time delay, and frequency shift of the received satellite signal. Satellite tracking uses the delays, bias errors, and offsets as measurement variables from which user position, velocity, and GPS time are determined. The UE set accomplishes satellite tracking

using two distinct modes of operation: coherent and non-coherent tracking. The following description of satellite tracking is just one method of implementation.

The coherent mode of satellite tracking uses a tau-dithered tracking loop where the code phase is alternately advanced and retarded by half a code chip. The sharpness of the correlation pulse (Figure 8) and the size of the code chip determines how accurately the received signal can be matched to the UE sets' copy of the satellite signal. The dithering of the correlation pulse permits the derivation of an error signal to be used by the code loop to maximize signal correlation (Figure 8). The coherent mode uses one correlator to do tau-dithering and uses the second correlator to remove the code from the signal for carrier tracking (each satellite tracking loop has two correlators) (5:15-18).

The code clock and carrier frequencies of the satellite signals are precisely related, L2 is exactly 120 times the clock frequency. Thus, when the phase lock loop is tracking the carrier, the code clock is further inherently phase locked to the received code. This configuration allows the carrier loop to track the user's dynamics, reducing the dynamics the code loop must track.

The coherent mode is the normal, preferred mode of operation. An alternate mode of operation occurs when the carrier loop breaks lock due to severe user dynamics and/or low signal-to-noise (S/N) ratio (primarily due to jamming noise). In this alternate mode, called the non-coherent

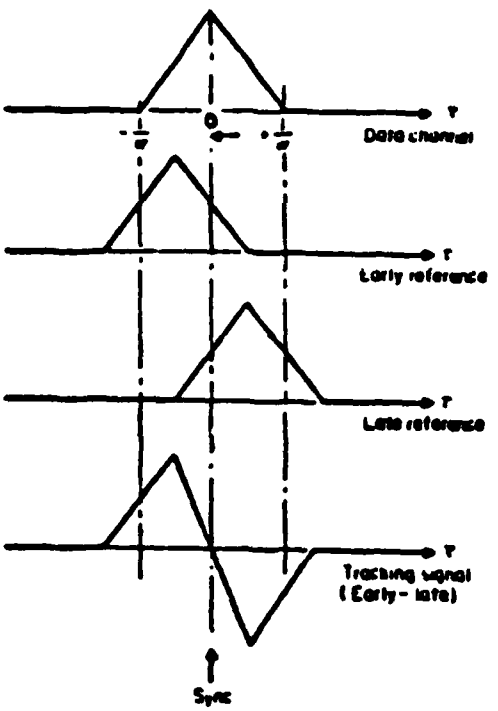

Sync tracking by early-late correlators

Figure 8. Tau-Dither Tracking

mode, the UE set uses a second order code tracking loop. The second order code loop uses simultaneous early-late correlators to track the code. The second order code loop provides much more accurate pseudorange measurements, but must also track-out all residual signal dynamics and jamming noise to maintain code lock. The bandwidth of each code loop greatly affects the performance of the loops. The bandwidth design requires compromise between the conflict of designing to track maximum dynamics (large bandwidth) or to overcome increased noise due to jamming (small bandwidth). Early UE set designs used fixed bandwidths based on the dynamics and jamming levels expected for particular groups of users (low, medium, or high dynamics with low to moderate jamming). More recent designs have employed adaptive bandwidth features (Refs. 5, 6, and 10). The specific bandwidths in an adaptive receiver are determined by the estimate (or measurement) of the users dynamics and/or the jamming noise. In this way the UE set can optimize its operation for the changing environment and increase the set's navigation accuracy (5:14-21).

When a GPS set is integrated with an aircraft's INS, a number of positive changes result (as already mentioned in Chapter I). The INS information provides an accurate estimate of position and velocity for prepositioning of the carrier and code loops for acquisition of the satellites. The code loop uses the position estimate to determine an approximate range to the satellite (or more specifically, a time delay between an incoming satellite code and the user's

version of the code) from which to start searching for the incoming signal. The carrier loop uses the velocity estimate to calculate an approximate Doppler frequency shift from which to start searching for the incoming carrier frequency. The INS aiding of the code and carrier loops as described above result in faster acquisition and tracking of the satellites. Once tracking, the INS continues to provide information on the aircraft's dynamics to the carrier loop, thereby reducing the amount of dynamics the carrier loop will have to track. Therefore, the UE sets' carrier loop can use smaller bandwidths and still maintain lock during severe aircraft dynamics. In the coherent mode (when the coupled carrier loop-INS is tracking), the code loop will benefit from the increased capability of carrier tracking. In the non-coherent mode (when the carrier loop can no longer maintain track even with INS information), the INS will provide open loop, carrier type estimates (derived primarily from the estimates of the aircraft's velocity) and aircraft dynamics to the code loop. The INS open loop information results in considerable improvement in the second-order code loop's tracking capability. The tracking bandwidths (of both code and carrier loops), for an integrated GPS/INS, allow substantially higher jamming tolerance and improved capability to track severe aircraft dynamics as compared to the stand-alone GPS UE set (5:17-18).

UE Satellite Selection. The ultimate objective of any satellite selection scheme for the GPS UE is to pick from the

available satellites the set which minimizes the user's navigation errors. In a normal environment (without jamming) the optimum set of four satellites to track is determined by the geometry between the user and the in-view satellites. For example, without considering an unknown time bias, the best three satellite set for determining the user's position is the set with mutually orthogonal line-of-sight (LOS) unit vectors with the origin at the user's position extending in the direction of the satellite. The orthogonal geometry provides maximum information along all three coordinates of the user's position. If the satellites, instead of being aligned in an orthogonal set, are grouped or clustered closely together, the information along one or more of the directions of the user's position is degraded. In two dimensions for example, the user's position (the "X" or aircraft) in the following diagram is determined by the intersection of the range vector to each satellite. As a result of the inaccuracy in the range measurement to each satellite, the intersection of the two range vectors creates an area of uncertainty within which the user's position is located instead of one unique solution to the user's position.

The shape of the region of uncertainty in the user's position is a result of the user-satellite geometry. For a favorable geometry (when satellite LOS vectors are at or near 90° separated from each other) the region of user position uncertainty is approximately a square with dimensions defined by the inaccuracies of the measurements. An

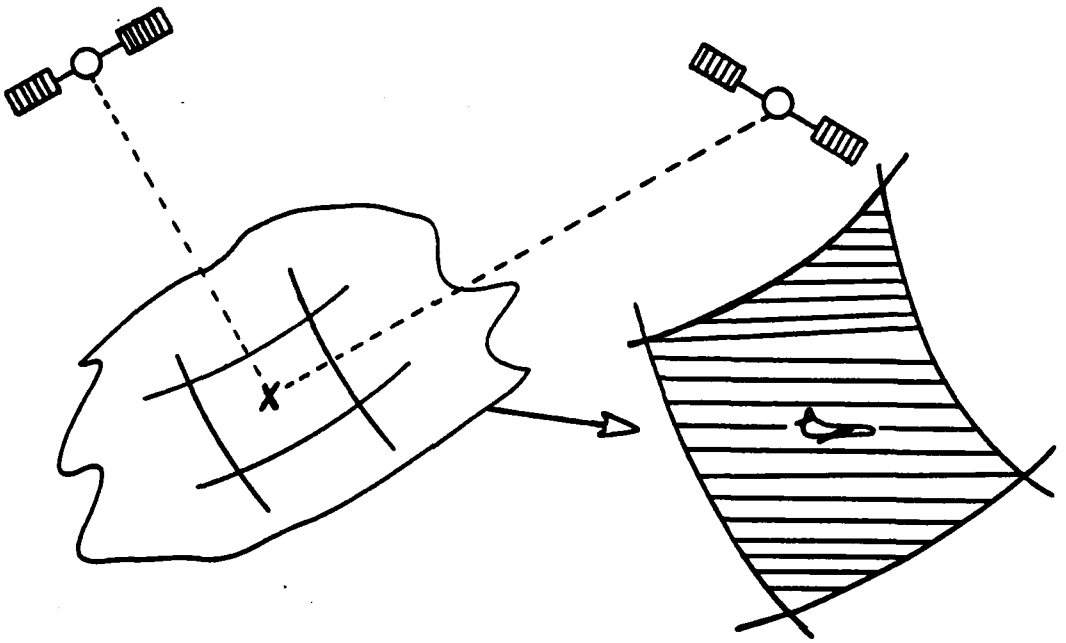

FAVORABLE GEOMETRY

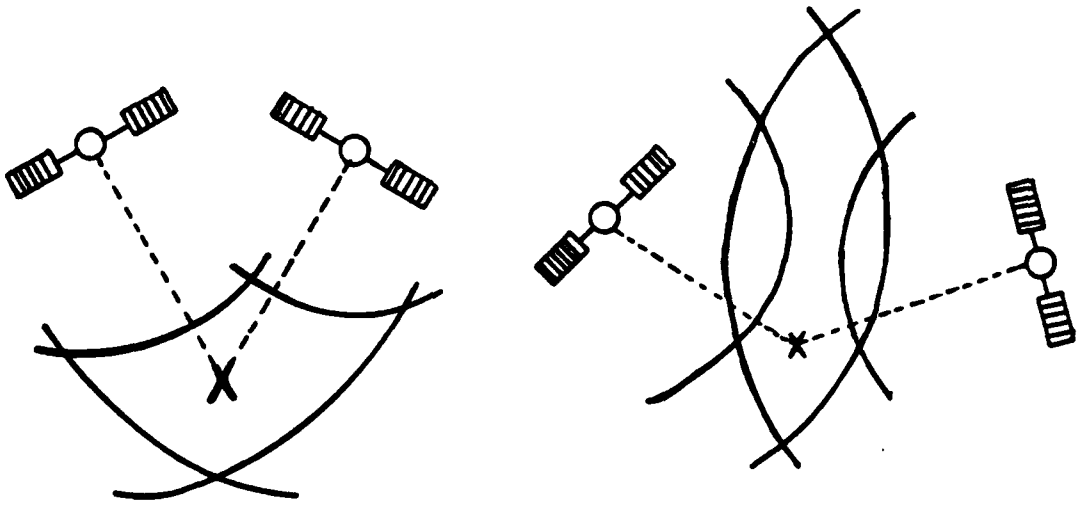

UNFAVORABLE GEOMETRIES

unfavorable geometry creates a region of user position uncertainty that is elongated, indicating increased uncertainty in user position along the direction of elongation. Expanding from two dimensions to three dimensions the region of user position uncertainty changes from an area to a volume. Again, a favorable satellite LOS geometry will place the user on equal distance from the surface of the uncertainty (or error) volume. An unfavorable geometry will have an error volume that is elongated or depressed in shape, resulting in the user's position having greater uncertainty in the direction of the elongation (the direction of the grouped or clustered satellites). As discussed in the Space Segment Section, the satellite constellation was chosen to minimize the clustering or grouping of satellites.

The time bias between the satellite and UE sets' clock adds an additional range error to each satellite measurement. If the time bias is not determined, the size of the three dimensional error volume would grow substantially. To determine and remove the range error due to the time bias, a fourth satellite range measurement is needed. Solving for the time bias, however, adds another unfavorable geometry condition. The unfavorable time bias geometry occurs when all four satellites are close to or on the surface of a cone (7:4). When this unfavorable geometry occurs the information along one or more of the coordinates of the user's position becomes redundant with the time bias, thus effectively reducing the number of range measurements to three and

preventing calculation of the time bias. The loss of observability of the time bias rapidly increases the user's position uncertainty. The unfavorable cone geometry is a function not only of the satellite constellation, but the specific user's location.

The UE set uses a figure of merit known as geometrical dilution of precision (GDOP) to select from the available satellites the four satellite set with the best geometry for tracking.

$$GDOP = SQRT\ (TRACE((\underline{H}^T\underline{H})^{-1})) \tag{7}$$

The visibility matrix (or $\underline{H}$ matrix) is formed by calculating the direction cosines of the line-of-sight unit vector from the user to each in-view satellite (expressed in user local level coordinates) (6:144-145). Each row of the $\underline{H}$ matrix is composed of the three direction cosines of the LOS unit vector and the fourth element for all satellites is a one to account for the equal uncertainty in range due to satellite-user clock time bias for each satellite

$$H = \begin{bmatrix} A_E(1) & A_N(1) & A_u(1) & 1 \\ A_E(2) & A_N(2) & A_u(2) & 1 \\ \cdot & \cdot & \cdot & \cdot \\ \cdot & \cdot & \cdot & \cdot \\ \cdot & \cdot & \cdot & \cdot \\ A_E(j) & A_N(j) & A_u(j) & 1 \end{bmatrix} \tag{8}$$

where

$A_E(\cdot)$, $A_N(\cdot)$, $A_u(\cdot)$ are the respective direction cosines of the line-of-sight unit vector to each satellite expressed in user-local level (EAST-NORTH-UP) coordinates

j = the number of in-view and available satellites

Due to variations in geographical terrain, all satellites below 5° elevation from the horizon are deleted from possible satellite selection (the 5° angle is known as the mask angle) (4:E9.3.2). The GDOP figure of merit (Equation (7)) calculates a scalar value for each possible satellite set. The satellite set with the lowest GDOP is the best user-satellite geometry to provide the smallest navigation errors (7:4). Other useful figures of merit are derived from GDOP. The position dilution of precision (PDOP) is calculated using Equation (7) but with the $\underline{H}$ matrix composed of the direction cosines to the satellites only (time/geometry conditions determined by the fourth column of 1's are deleted). PDOP is used extensively in satellite constellation design and analysis without having to specify the user's position and trajectory. Horizontal dilution of precision is a horizontal plane accuracy descriptor like CEP. Vertical dilution of precision is valuable in terrain avoidance. The next chapter will examine GDOP and other satellite selection criterion in more detail.

UE Adaptive Antenna Theory. The objective behind using an adaptive antenna over a regular antenna is to limit the

noise passed on to the satellite tracking loops, and thereby to increase the performance of the set. This capability is especially critical in a jamming environment. The adaptive antenna designs used with the high performance GPS UE are either a beam steering or a null steering antenna. Both designs are phased array antenna systems. Characteristics of a phased array antenna system are the ability to provide rapid inertialess scanning for high speed angular coverage, a large power handling capability, and their suitability to environments where actual movement of the antenna is difficult or impossible (9:1). Since the satellites may be tracked anywhere from the horizon to the zenith, both antenna designs must provide total coverage of the upper hemisphere. The problem for the antenna is to track the satellite trajectories while limiting jamming power (by either ground or airborne jammers) being passed on to the satellite tracking loops.

Beam Steering Antenna. The beam steering antenna creates and points high gain beams toward each satellite being tracked, providing maximum gain in the direction of the satellite and very low gain in all other directions (10:6). The pointing information for the antenna beams is derived initially from the UE estimate, which may be aided with INS information (for the integrated GPS/INS). Once tracking of the satellites has commenced, pointing directions are provided by the tracking loops and navigation information (to compensate for vehicle dynamics). The antenna beam width and

gain determine the required accuracy of the pointing information and the jamming tolerance of the beam steering antenna. The beam steering antenna has the advantage of being able to overcome moderate jamming levels by pointing narrow, high gain beams at the satellites in order to isolate the GPS signal from jamming noise. The disadvantages are the large, bulky array apertures required to form narrow beams at the L band frequencies, the high computational requirements for beam steering in a high performance aircraft, and the undesirable amplification of jamming noise in the direction of the satellite (10:6).

Null Steering Antenna. The null steering antenna uses the fact that the satellite signal is 30 decibels below thermal noise (10:6). Therefore, any signal that rises above thermal noise must be interference. The antenna algorithm acts to distribute its nulls to minimize the total power out of the antenna (6:139). This process is accomplished by combining the outputs of several individual antenna elements through phase and amplitude controls to minimize the power out of the antenna (10:6). The advantages of the null steering antenna are its smaller array, better jammer suppression, and simplicity of operation (compared to the beam steering antenna). The disadvantages of the null steering antenna are that the number of nulls it can create is limited to the number of antenna array elements minus one (i.e., a seven element array has a maximum of six nulls) and that in an effort to null out strong jammers, other "spurious" nulls may

be formed that null a satellite signal (10:6, 6:139-141). The last disadvantage can be limited by constraining the power inversion process from forming a null in the direction of a satellite (10:6, 6:140). The null steering antenna will be discussed in greater detail in Chapter IV, and in Appendix B.

Summary

This chapter has reviewed the three segments of the GPS Program with particular emphasis on the Satellite and User Segments. The Satellite Segment discussed the satellite constellation and the GPS satellite transmitted signal. The User Segment presented the theory and operation of the User Equipment. The User Equipment operation included a discussion of the GDOP method for satellite selection and adaptive beam and null steering antenna designs used with high performance GPS User Equipment. The next chapter will further analyze the GPS UE satellite selection process.

III GPS UE Satellite Selection

Introduction

The standard procedure for UE satellite selection is based solely on geometrical dilution of precision (GDOP) (as discussed in the User Segment Section of Chapter II). Navigation measurements are dependent on three factors (external to the UE signal processor): the geometry, the incoming signal, and the noise (11:1). GDOP provides a figure of merit to determine the best geometry, but does not address the incoming signal and noise. An optimum satellite selection process must use every available piece of information available to determine the satellite set which will provide the smallest navigation errors over a particular time period. The following sections of this chapter will discuss this problem and possible solutions to the problem in much greater detail. The next section will review previous work in the area of GPS UE satellite selection. The section following the Literature Review will present a tutorial on GDOP and improvements and extensions to GDOP (from a more rigorous stochastic analysis). The material in this section is an excerpt from a report authored by Dr. William L. Brogan, University of Nebraska-Lincoln, under contract to the Avionics Laboratory of the Air Force Wright Aeronautical Laboratories (AFWAL) at Wright-Patterson AFB, Ohio (11). The work in this section coupled with the development in the following section will provide the reader with a thorough

understanding of the concepts and theory behind the UE satellite selection problem and possible solutions to that problem.

Literature Review

ADGINT Study. In February 1981, a summary of the work completed by the Charles Stark Draper Laboratory on the "Advanced GPS/Inertial Integration Technology Program (ADGINT)", was published by the AFWAL Avionics Laboratory (6). In that work a weighted GDOP satellite selection criteria was developed and tested. The weighted GDOP criteria was a simplification of the a-posteriori error covariance $\underline{P}_1$ equation:

$$\underline{P}_1 = (\underline{P}_o^{-1} + \underline{H}^T\underline{R}^{-1}\underline{H})^{-1} \qquad (9)$$

where:

$\underline{H}$ is the user-satellite geometry matrix

$\underline{P}_o$ is the a priori error covariance

$\underline{R}$ is the covariance of the measurement noise

The new satellite selection criterion will select the best satellite set for maximum reduction in the navigation error covariance. The initial error covariance $\underline{P}_o$ was dropped from equation (9), because the new satellite set would not affect $\underline{P}_o$, thus equation (9) reduces to

$$\underline{P}_1 = (\underline{H}^T\underline{R}^{-1}\underline{H})^{-1} \qquad (10)$$

Therefore, by minimizing $TR(\underline{H}^T\underline{R}^{-1}\underline{H})^{-1}$ the a posteriori error covariance $\underline{P}_1$ is minimized (6:145). The further justification of dropping $\underline{P}_o$ from equation (9) was that $\underline{P}_o$ would be very large (therefore the $\underline{P}_o^{-1}$ would be negligible) and that equation (10) would result in a smaller number of computations than equation (9) (6:145).

The assumption of uncorrelated pseudo-range measurements from different satellites yields a diagonal R matrix:

$$\underline{R} = \begin{bmatrix} p_1 & 0 & 0 & 0 \\ 0 & p_2 & 0 & 0 \\ 0 & 0 & p_3 & 0 \\ 0 & 0 & 0 & p_4 \end{bmatrix} \tag{11}$$

The elements of $\underline{R}$ (p_1, p_2, p_3, and p_4) are functions of an estimate of the received signal-to-noise ratio. In the ADGINT study, a signal-to-noise estimation algorithm was derived from outputs of a null steering antenna in order to aid an extended range receiver tracking design. Therefore, the signal-to-noise estimate was readily available for use in the satellite selection criteria (6:29-33). The diagonal R matrix results in easy matrix inversion using a very small number of calculations.

$$\underline{R}^{-1} = \begin{bmatrix} W_1 & 0 & 0 & 0 \\ 0 & W_2 & 0 & 0 \\ 0 & 0 & W_3 & 0 \\ 0 & 0 & 0 & W_4 \end{bmatrix} \tag{12}$$

The weights, W_i, in $\underline{R}^{-1}$ range from zero to one depending on the signal-to-noise ratio. The upper limit of W_i is the signal-to-noise level at which further performance improvements are no longer advantageous (compared to the added complexity of the algorithm). The lower limit of W_i is the signal-to-noise level at which acquisition and tracking is no longer possible (6:146). The resultant weighted-GDOP (WGDOP) figure of merit is,

$$\text{WGDOP} = \text{SQRT}\ (\text{TRACE}(\underline{H}^T\underline{R}^{-1}\underline{H})^{-1}) \qquad (13)$$

The study's conclusions of the performance of WGDOP versus GDOP in a GPS/INS computer simulation determined that (6:152):

(1) The improved signal-to-noise power of the satellite set selection by the WGDOP criterion more than compensates for any degradation in geometry.

(2) The WGDOP criterion is insensitive to small changes in signal-to-noise power, therefore, only a crude estimate of signal-to-noise power is needed for the selected set to be effective.

(3) The WGDOP criterion should be used more frequently than the rate used by GDOP and the rate would be dependent on the expected jamming threat.

(4) Most of the benefits of WGDOP are derived from eliminating the satellites with obviously poor signal-to-noise power. A selection scheme that eliminated satellites with poor signal-to-noise power and then used the standard GDOP would also result in performance improvements.

The ADGINT study based the WGDOP versus GDOP conclusions on a computer simulation with one particular mission in which the jamming threat was encountered at the end of the mission. Encountering the jamming threat after a long period of normal operation would result in a small a priori error covariance $\underline{P}_o$, which is in conflict with the assumption made to eliminate $\underline{P}_o$ from the satellite selection criteria. Therefore, minimizing WGDOP may not in fact result in the smallest a-posteriori error covariance $\underline{P}_1$.

In March 1981, a short study on GPS UE satellite selection was published by the Reference Systems Branch of the AFWAL Avionics Laboratory (7). In that study a combined jamming-to-signal (J/S) estimate and GDOP criteria was used for satellite selection. The study sought to prove the value of incorporating a generalized form of J/S estimate into the satellite selection criteria, and for this reason a generic UE receiver and adaptive antenna were simulated (the generic UE receiver and adaptive antenna were used to make resulting performance improvements applicable to all GPS UE receiver and adaptive antenna designs regardless of the methods for processing the satellite signals inside the set). Navigation performance was judged to be improved if the best GDOP set included one or more satellites above a J/S threshold of 70 decibels while an alternate satellite set existed that had all satellites below the 70 db J/S level and had a GDOP value below 5.0. This procedure for satellite selection is very similar to the procedure proposed in conclusion (4) of the preceding section. The study tested the combined J/S

and GDOP versus GDOP-only satellite selection criterion against a stylized area of jammers (ten rows of ground jammers, paralleling the forward edge of the battle area and extending 80 kilometers deep into enemy territory and stretched beyond the aircraft line-of-sight in both directions (7:7)) broadcasting one kilowatt each. Five different aircraft missions into enemy territory were simulated (Close Air Support, Escort/Intercept, Attack Helicopter, Preplanned Deep Strike, and Intratheater STOL Transport). The results of the simulation for a 24 satellite constillation showed an average performance improvement across all 5 aircraft missions of 42% from a 10° mask angle and 15% for a 20° satellite mask angle (7:15). The results for an 18 satellite constellation showed an average performance improvement across all 5 aircraft missions of 15% for a 10° mask angle and 3% for a 20° mask angle (7:16). Take note here that the 18 satellite constellation referred to is a predecessor of the present 18 satellite constellation. The difference between the two constellations is that originally six satellites would be unevenly spaced within one orbital plane, with a total of three orbital planes, and zero phasing of satellites from one plane to another (phasing is discussed in Chapter II) (4:E9.3.1-E9.3.3). A major concern identified by this study is the importance of satellite availability at the satellite selection time. The 24 satellite constellation provided an average of 8 visible satellites with 70 alternative satellite sets possible. The 18 satellite constellation provides 5-6 visible

satellites; 6 satellites give 15 alternative satellite sets while 5 satellites result in only 5 alternative satellite sets. The satellite visibility effect has some direct consequences on any alternate satellite selection scheme:

(1) The added complexity and computations of an alternate satellite selection scheme may not be justified if there are few or no alternative satellite sets.

(2) The number of computations for a complex satellite selection scheme would also be greatly reduced with the number of visible satellites. The reduction in the number of computations would allow a satellite selection scheme with greater complexity and larger performance improvement. Clearly (1) and (2) pose a degree of conflict in design of an alternate satellite selection criteria that must be addressed as well as any performance improvements.

Satellite Visibility. The present 18 satellite constellation replaced the old satellite constellation because of increased performance of the uniform 3 satellites in 6 different orbits constellation over the non-uniform 6 satellites in 3 different orbits (See Reference 4:E9.3.1-E9.3.8). For further analysis of the satellite visibility of the present 18 satellite constellation the software used in the AFWAL Avionics Laboratory study was obtained and modified to provide Figure 9 (Ref. 7).

For a further discussion of the satellite visibility software used to create the information for Figure 9, see Appendix A. The results of the satellite visibility study

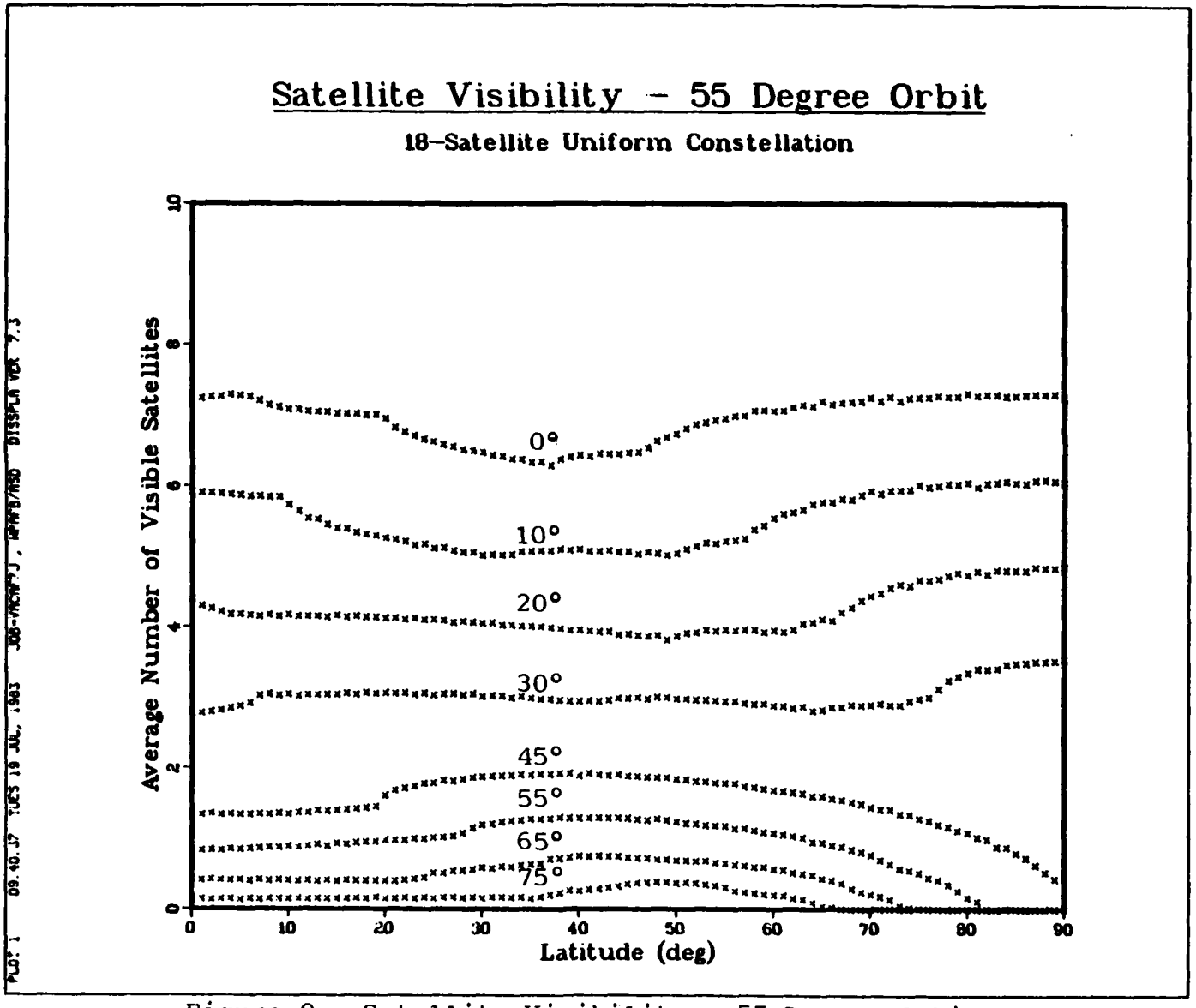

Figure 9. Satellite Visibility - 55 Degree Orbit

using the present 18 satellite constellation show that for a mask angle of 5° (which is typically used in the GPS UE) an average of 6 satellites would be available for tracking over a 24 hour period.

TABLE I

Satellite Availability for a 24 Hour Period

Mask Angle	Average Number of Visible Satellites
0°	7.0
5°	6.0
10°	5.6
15°	4.9
20°	4.2
25°	4.0

These results are in agreement with the "NAVSTAR Global Positioning System Six-Plane 18-Satellite Constellation," data (4:E9.3.1-E9.3.8).

AFWAL Brogan Study. In September 1981, the AFWAL Avionics Laboratory published the study by Dr. William Brogan that included an optimal stochastic approach to an alternate satellite selection criterion. Within this study, a complete, stochastic analysis of the GDOP concept for selecting satellites for navigation measurements was presented. In that development of an alternate satellite selection criterion, not only was the satellite visibility, user-satellite geometry, and jamming noise at the receiver considered, but also the a priori error covariance $\underline{P}_o$ that was deleted from the ADGINT

weighted-GDOP criteria. The value of $\underline{P}_o$ to determine direction(s) of the maximum "need for information" in the satellite selection process adds a great deal of insight into which of the possible satellite range measurements can result in the smallest overall navigation errors. Before discussing the alternate satellite selection criterion that will be implemented and tested in this report, a more detailed review of Dr. Brogan's study is essential. Due to the clarity and insight of Dr. Brogan's work the following section will present excerpts from Dr. Brogan's study (11).

The Cost Criterion for UE Satellite Selection (11)

An Introduction to GDOP Using Least-Squares (11:3-7). Consider a vector of measurement components, $\underline{Z}$, corrupted by additive noise $\underline{N}$ and linearly related to the state vector X.

$$\underline{Z} = \underline{H}\,\underline{X} + \underline{N} \tag{14}$$

An estimate of $\underline{X}$, called $\hat{\underline{X}}$, is sought from the given measurement vector $\underline{Z}$. One approach to this problem is the least-squares estimator $\hat{\underline{X}}$. That is, select $\hat{\underline{X}}$ so as to minimize the sum of the squares of the components of the difference $\underline{Z} - \underline{H}\hat{\underline{X}}$. This $\hat{\underline{X}}$ would then minimize

$$J_1 = (\underline{Z}-\underline{H}\hat{\underline{X}})^T(\underline{Z}-\underline{H}\hat{\underline{X}}) \tag{15}$$

Differentiating J_1 with respect to $\hat{\underline{X}}$ and setting the result to zero gives

$$-\underline{H}^T\underline{Z} + \underline{H}^T\underline{H}\hat{\underline{X}} = \underline{0} \tag{16}$$

so that the well known least-squares estimate is

$$\hat{\underline{X}} = (\underline{H}^T\underline{H})^{-1}\underline{H}^T\underline{Z} \tag{17}$$

The quality of this estimate can be assessed by forming the error

$$\tilde{\underline{X}} = \hat{\underline{X}} - \underline{X} \tag{18}$$

Using equation (14) and (17) gives

$$\tilde{\underline{X}} = (\underline{H}^T\underline{H})^{-1}\underline{H}^T\underline{H}\underline{X} + (\underline{H}^T\underline{H})^{-1}\underline{H}^T\underline{N} - \underline{X}$$

$$= (\underline{H}^T\underline{H})^{-1}\underline{H}^T\underline{N} \tag{19}$$

If the noise $\underline{N}$ has zero mean, taking the expected value $E[\ ]$ of equation (19) shows that the estimator error $\tilde{\underline{X}}$ also has a zero mean. The covariance of the estimation error can be related to the covariance of the noise $\underline{N}$ by:

$$E[\tilde{\underline{X}}\tilde{\underline{X}}^T] = (\underline{H}^T\underline{H})^{-1}\underline{H}^T E\ \underline{N}\underline{N}^T\ \underline{H}(\underline{H}^T\underline{H})^{-1} \tag{20}$$

If all components of $\underline{N}$ are pairwise uncorrelated and have unit variance, i.e.,

$$E[N_i N_j] = [\delta_{ij}] = \begin{cases} 1 & \text{if } i = j \\ 0 & \text{if } i \neq j \end{cases}$$

then $E[\underline{N}\underline{N}^T] = I$ so that

$$E[\tilde{\underline{X}}\tilde{\underline{X}}]^T = (\underline{H}^T\underline{H})^{-1}(\underline{H}^T\underline{H})(\underline{H}^T\underline{H})^{-1}$$

$$= (\underline{H}^T\underline{H})^{-1} \qquad (21)$$

The matrix $(\underline{H}^T\underline{H})^{-1}$ is called the GDOP matrix. Various scalar figures of merit can be derived from this matrix, and are frequently used. For example, the trace of $(\underline{H}^T\underline{H})^{-1}$, is the sum of the squares of all error components when $E[N_i N_j] = [\delta_{ij}]$. The square root, $[\text{TRACE}(\underline{H}^T\underline{H})^{-1}]^{\frac{1}{2}}$, is usually called GDOP. The square root of the sum of all diagonal terms which correspond to position components is called PDOP. If the horizontal plane diagonal components of $(\underline{H}^T\underline{H})^{-1}$ are summed, the square root is called HDOP. In this study, major attention is directed to $\text{TRACE}(\underline{H}^T\underline{H})^{-1}$. Omission of the square root will not alter any conclusions regarding the minimization of GDOP.

It is clear that all GDOP-related performance measures indicate the error in an estimated navigation quantity "per unit of measurement noise" covariance. Deviations from this assumption will be considered in the next subsection.

All of the above GDOP-related measures depend solely on the geometry matrix $\underline{H}$. Smaller GDOP values indicate stronger or more robust geometric solutions to the estimation

problem. For these reasons, when some freedom exists in the choice of measurements, good (i.e., small) GDOP is often used as the selection criteria. It will be shown later that this criterion is not always the best choice.

Weighted Least Squares Solution (11:5-7). The "per unit noise" concept inherent in GDOP is not so useful (or more bluntly, invalid) when certain measurement components are much noisier than others. When a choice exists between two possible sets of measurements, the set with poorer GDOP may be preferable if they are of sufficiently lower measurement noise. This trade-off was pointed out in conjunction with an Integrated GPS/Inertial Navigation System (12). There, the desire to achieve good GDOP suggested selection of range measurements separated by angles near 90°. However, this choice caused an increase in atmospheric diffraction errors in those measurements with low elevation angles. Another potentially more severe problem is non-uniform noise in a jamming environment. Some of the highly directional antennas may receive large amounts of noise pollution. This degradation may well overcome any GDOP advantages.

If the measurement noise covariance is not just the unit matrix, but rather is $E[\underline{N}\underline{N}^T] = \underline{I}\,\sigma^2$ then the GDOP matrix just increases by the scalar σ^2. If all potential measurements have this same variance σ^2, the choice of the best measurement set will still be the best GDOP set. The multiplication scalar σ^2 will not affect the relative rankings.

The measurement noise is called non-uniform when different measurements have different noise levels, as indicated

by their variances. In this case a weighted least-squares approach to estimation is often used (19). The quadratic form of equation (15) is modified by inserting a weighting matrix $\underline{W}$.

$$J_2 = (\underline{Z}-\underline{H}\hat{\underline{X}})^T\underline{W}(\underline{Z}-\underline{H}\hat{\underline{X}}) \tag{22}$$

It is customary to select the weighting matrix as the inverse of the noise covariance matrix (i.e., $\underline{W} = \underline{R}^{-1}$ where $\underline{R} = E[\underline{N}\underline{N}^T]$). This choice weights the accurate measurements more, the noisy ones less. Minimizing this modified cost function leads to a modification of equation (15).

$$\hat{\underline{X}} = (\underline{H}^T\underline{R}^{-1}\underline{H})^{-1}\underline{H}^T\underline{R}^{-1}\underline{Z} \tag{23}$$

and a corresponding modification of equation (20) or (21)

$$E[\tilde{\underline{X}}\tilde{\underline{X}}^T] = (\underline{H}^T\underline{R}^{-1}\underline{H})^{-1} \tag{24}$$

Equation (24), and generalizations of it, are known as noise-weighted GDOP. It is presented here to contrast against the traditional GDOP, but will be discussed further in the next subsection.

Thus far, no mention has been made of the knowledge about the navigation states which may exist prior to making GPS measurements. In almost all real situations prior knowledge of the navigation states will exist because of previous

measurements or for other reasons. The uncertainty volume of $\underline{X}$ need not be spherical (an uncertainty volume of $\underline{X}$ is a set of points enclosed within an equi-probability surface). An example of an error volume would be the case where X, Y, and Z components of position uncertainty are equal. In two dimensions, since X and Y are equal the conic is a circle with a radius equal to X and Y. Expanding to three dimensions, the equi-probability ellipsoid is a sphere with a radius equal to X, Y, and Z. Some components of $\underline{X}$ can have much more uncertainty associated with them, leading to elongated ellipsoidal uncertainty volumes. Those components with the largest uncertainty are said to have "maximum need" for improvement. A GPS measurement which provides maximum information along the elongated axis will likely lower navigation uncertainty the most regardless of classical GDOP considerations.

The treatment of a priori information in estimation can be approached in several ways. One way is to modify equation (15), this time to

$$J_3 = (\underline{Z}-\underline{H}\hat{\underline{X}})^T\underline{R}^{-1}(\underline{Z}-\underline{H}\hat{\underline{X}}) + (\underline{X}_o-\hat{\underline{X}})^T\underline{P}_o^{-1}(\underline{X}_o-\hat{\underline{X}}) \qquad (25)$$

where $\underline{X}_o$ represents an a priori estimate of $\underline{X}$ and the covariance of $\underline{X}_o$ is $\underline{P}_o$ (13). Minimizing J_3 amounts to a trade-off between measurement residuals and deviations from $\underline{X}_o$. This approach leads to a modified estimator

$$\hat{\underline{X}} = [\underline{H}^T\underline{R}^{-1}\underline{H} + \underline{P}_o^{-1}]^{-1}[\underline{H}^T\underline{R}^{-1}\underline{Z} + \underline{P}_o^{-1}\underline{X}_o] \qquad (26a)$$

$$= \underline{X}_o + \underline{P}_o\underline{H}^T[\underline{H}\underline{P}_o\underline{H}^T + \underline{R}]^{-1}[\underline{Z} - \underline{H}\underline{X}_o] \qquad (26b)$$

Form (26a) is most commonly used in weighted least-squares analysis, while form (26b) is one of the well known Kalman Filter equations (Ref. 14). The corresponding forms of the a priori estimation error covariance matrix are

$$E[\underline{\tilde{X}}\underline{\tilde{X}}^T] = \underline{P}_1 = [\underline{H}^T\underline{R}^{-1}\underline{H} + \underline{P}_o^{-1}]^{-1} \qquad (27a)$$

$$= \underline{P}_o - \underline{P}_o\underline{H}^T[\underline{H}\underline{P}_o\underline{H}^T + \underline{R}]^{-1}\underline{H}\underline{P}_o \qquad (27b)$$

Note that equation (26a) looks most like the GDOP matrix in that it reduces to equation (24) if $\underline{P}_o$ approaches infinity (very large navigation position uncertainties) and it reduces to equation (21) if, in addition to $\underline{P}_o$ being very large, $\underline{R} = \underline{I}$ or $\underline{R} = \underline{I}\sigma^2$.

Generalizations and Extensions of GDOP (11:15-16). A major part of the Brogan study was devoted to the question of how best to select measurements at a given point in time. This static measurement selection problem, so called because only one point in time is considered, is a useful simplification to the dynamic measurement selection problem for theoretical development of extensions to GDOP.

In the GPS problem we are concerned with three position components and a clock bias, which converts to an

equivalent user range error. So for the most part a four component state vector will be of ultimate interest. Making the usual assumptions about mean values being zero, attention turns to the second statistical moments of the estimation errors, i.e., the covariance terms. Subject to the usual assumptions, equation (26a) or equation (26b) tells the entire story. Given an a priori state geometry matrix $\underline{H}$ and a noise covariance matrix $\underline{R}$, the a priori covariance $\underline{P}_1$ is uniquely computable.

It is awkward to use a 4 x 4 matrix to describe the accuracy or effectiveness of a given set of measurements. An attractive alternative is to use a single scalar figure of merit to describe the result. In the past, various terms such as circular error probable (CEP) or spherical error probable (SEP) have been used. The a posteriori covariance matrix P_1 can be viewed geometrically as a hyperellipsoid (similar to the error volume discussed earlier but expanded to a larger dimension) with principal axes oriented in space according to the directions of the orthonormal eigenvectors $\underline{\epsilon}_i$ of P_i and with the dimensions of the semimajor axes as the eigenvalues λ_i of P_i. The interior of this ellipsoid can be thought of as a one-sigma error volume, and in this respect it is related to CEP and SEP although much more complicated. Two very simple scalar measures derived from P_1 can be used. The determinant of $\underline{P}_1$, is equal to the product of the eigenvalues (15)

$$\det(\underline{P}_1) = \lambda_1\lambda_2\ldots\lambda_n \tag{28}$$

and is therefore related to the volume of the elipsoid. This measure is not preferred here for two reasons. First, determinants are not as easy to evaluate as the trace, which is used in the next performance measure. Second, and more important, $\det(\underline{P}_1) = 0$ does not mean the error is zero. All it means is that one or more dimensions of the hyper-ellipsoid has degenerated to zero, but very large errors in other coordinates may still exist. The $\det(\underline{P}_1)$ is not very descriptive or discriminating in this regard.

The preferred scalar performance measure is based on the trace of $\underline{P}_1$

$$TR(\underline{P}_1) = \sum_{i=1}^{N} P_1{}^{ii} = \sum_{i=1}^{N} \lambda_i \tag{29}$$

The trace is simply computed as the sum of the diagonal elements, but it is known that it also equals the sum of the eigenvalues (15). Therefore $TR(\underline{P}_1)$ can not equal zero unless <u>all</u> error variance components are zero. Also the trace of $\underline{P}_1$ is analogous to the radius squared value of a representative one sigma hyper-sphere whereas $\det(\underline{P}_1)$ is the volume of the hyper-sphere. The trace functions just described are natural extensions of GDOP. In the following section two extensions of GDOP will be considered: noise-weighted GDOP and the Cost Criterion.

The Cost Criterion for Alternate Satellite Selection. In the second section of this chapter, equation (24) was called the noise-weighted GDOP. The trace of equation (24) may also be called noise-weighted GDOP.

$$\text{Noise-Weighted GDOP} = \text{TRACE}\,[\underline{H}^T\underline{R}^{-1}\underline{H}]^{-1} \qquad (30)$$

Noise-Weighted GDOP penalizes noisy measurements in the satellite selection process. As stated in the first section of this chapter, in the discussion of WGDOP, Noise-weighted GDOP assumes that $\underline{P}_o^{-1}$ can be neglected from equation (30) without loss of performance. For $\underline{P}_o^{-1}$ to be neglected would mean that $\underline{P}_o$ is very large, which could be expected very early in a mission (before the accuracy of GPS has been achieved) or after a long period of GPS unavailability (which could occur from extended periods of severe jamming). For most examples of interest this simply will not be the case (11:18). Therefore, $\underline{P}_o^{-1}$ should be included in an optimum satellite selection criteria, as in equation (27a). Equation (27a) was one of two forms of the a-posteriori estimation error covariance matrix. The trace of equation (27a) will henceforth be known as the cost criterion.

$$\text{Cost Criterion} = \text{TRACE}(\underline{P}_1)$$

$$= \text{TRACE}\,[\underline{H}^T\underline{R}^{-1}\underline{H} + \underline{P}_o^{-1}]^{-1} \qquad (31)$$

The term "cost criterion" is chosen to reflect the fact that this equation is a result of the cost function J_3, equation (25). The cost criterion is a tradeoff between noise-weighting of the user-satellite geometry with the directions of the "need for information" contained in $\underline{P}_o$. The added computations from the noise-weighted GDOP criterion are minimal because $\underline{P}_o$ should already be known by the UE set.

As in the GDOP error volume discussion (in the UE Satellite Selection Section of Chapter II) as the GDOP value increases the error volume becomes elongated and distorts the UE sets' navigation accuracy. A similar result occurs by including $\underline{P}_o$ as part of equation (31). As the estimation error covariance hypervolume elongates $\underline{P}_o$ will become more dominant in determining the best satellite measurements. Then as the estimation error covariance hypervolume equalizes the $(\underline{H}^T\underline{R}^{-1}\underline{H})$ term would become more dominant in satellite measurement selection (an equalized hyper-volume would be similar to a sphere in three dimensions).

The cost criterion is a sound, thorough, and promising approach for an optimal solution to the static GPS UE satellite selection problem. It is, however, unclear whether the cost criterion will result in the smallest mean square user position error for the dynamic measurement selection problem. For this reason the cost criterion will be tested against GDOP-only criteria by means of an integrated GPS/INS computer simulation for a realistic high dynamic (both aircraft and jamming dynamics) flight trajectory.

One caveat on the cost criterion is that it is one approach for an optimal satellite selection process, not the optimal satellite selection process. The cost criterion was based on the cost function J_3 (equation (25)). Additional numbers, locations, power levels, and types of jamming signal and a penalty function for acquiring satellites with moderate to high signal-to-noise levels could be added to J_3. A cost function with this type of additional information would mean a substantial increase in complexity and computational loading that may be unwarranted for the limited satellite visibility of the 18 satellite constellation. Analysis of the cost criterion versus GDOP performance should indicate whether added complexity and computational loading of an alternate satellite selection criterion is warranted.

Summary

This chapter has presented a detailed analysis of the static measurement selection problem with particular emphasis on GDOP and extensions to GDOP for satellite selection. One extension to GDOP uses estimates of the measurement noise to each satellite and the a priori user position error covariance matrix as well as satellite geometry information to select the best satellite set. This extension to GDOP is called the cost criterion. Analysis of the cost criterion in a static measurement selection problem has indicated significant improvement in navigation accuracy (11:36-37).

It is unclear, however, whether the cost criterion will result in the smallest mean square user position error for the dynamic measurement selection problem. This report will implement the cost criterion in an integrated GPS/INS computer simulation to analyze the cost criterion versus GDOP navigation performance and verify the results of the static measurement case.

IV Integrated GPS/INS Computer Simulation

Overview

The Air Force Avionics Laboratory (AFAL) developed a digital simulation computer program for an integrated GPS/INS aircraft navigation system (IGI simulator) in 1976 (16:841). The IGI simulator was a result of a number of in-house (AFWAL) computer simulations in support of the Generalized Development Model (GDM) of GPS User Equipment. The GDM was designed to be used as a flight test bed to evaluate high anti-jam system techniques for military applications and to expand the technology base for GPS User Equipment. The IGI simulator is based on the GDM and is designed to support a variety of GPS User Equipment design trade-off studies and mission analyses (16:841). Thus the IGI simulator is a logical choice for evaluation of a cost criterion versus GDOP satellite selection criterion. The following section of this chapter will analyze the functions, math models, and operation of the IGI simulator. Also, the modifications to the IGI simulator necessary to evaluate the cost criterion versus GDOP satellite selection criterion in a jamming environment will be presented in the final section of this chapter. The level of detail presented in this chapter will be limited to the necessary material for an understanding of the IGI simulator's operation and performance outputs that will be analyzed in the next chapter.

IGI Operation

IGI Description (17:3-5). The IGI simulator uses a direct linear simulation approach in which the differential equations of the INS algorithm are linearized about a pre-computed flight trajectory to describe the propagation of INS errors in position, velocity, and attitude. The INS indicated data is then processed together with GPS pseudo-range and delta pseudo-range measurements in a linearized Kalman filter (21:23-67) to obtain estimates of the errors in the INS-indicated position and velocity, and of other variables describing error sources that might affect navigation performance. The user's new navigation parameters (the INS-indicated data) are updated by combining the Kalman filter error estimates with the old INS-indicated data. This direct linear simulation approach was chosen as a compromise between the less realistic covariance analysis approach (where the equations describing all of the state variables are a linear combination of the state variables) and the more computationally demanding non-linear simulation approach (16:842).

A Functional Look at IGI. The IGI simulator consists of a three-program package; PROFGEN, IGI, and PLOTTER. PROFGEN (Ref. 24) is an aircraft profile generator which generates a realistic flight trajectory data file. This flight trajectory data file along with a set of user-determined configuration and initialization parameters are input to IGI. The PLOTTER program processes the IGI plot output

file to create time history plots of navigation errors. The IGI program consists of the main code (or executive) and three levels of subroutines. Level one subroutines perform the major functions in IGI. Level two and three subroutines provide specialized processing of data (such as storing a block of data for printed or plotted output) and/or utility routines (such as matrix multiplication, addition, and inversion). The executive determines when and which of the major functions must be performed. The major functions of IGI are,

(1) Initialization and Configuration

(2) Satellite Propagation and Selection

(3) State (Truth and Filter) Propagation

(4) Measurement Update

(5) Store Output Data

A graphical view of the IGI simulator (input data, flight trajectory file, the IGI executive, and the five major functions within the IGI program) is presented in Figure 10.

The initialization function reads data from the input data file to determine the simulation user's desired configuration and initialization parameters. For instance, the input data file specifies the number of truth and filter states, the time interval for storing printed and plotted output, the time interval for satellite selection, the number and type of external measurements (i.e., pseudo-range and/or delta pseudo-range GPS measurements), and the statistics of the simulation's error models.

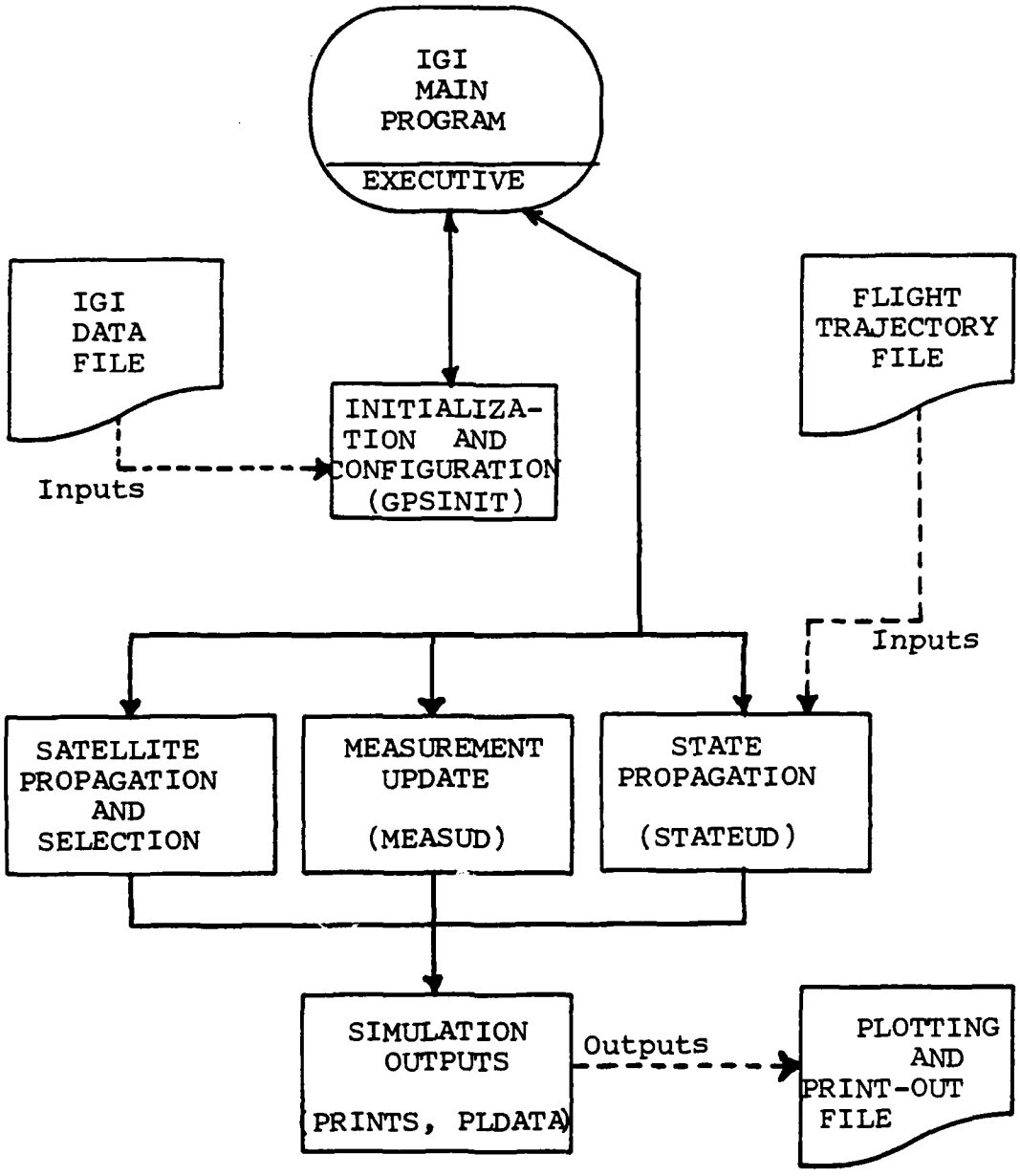

Figure 10. Structure of the IGI Simulation

The second major IGI function simulates the GPS satellite's positions and velocities at the simulation time. The satellite selection process uses the GDOP criterion to determine the best four satellite set for tracking (See UE Satellite Selection Section of Chapter II). Satellite selection is carried out once every five minutes to insure the best satellite set is being tracked (modeling of the satellites' positions and velocities will be discussed further in Chapter IV).

The state propagation function for both the truth and filter states is accomplished by continuously updating the truth and filter states with INS-derived data alone. State propagation occurs between GPS measurements or during periods of GPS nonavailability (as would be expected during severe jamming conditions). (A more detailed discussion will be presented in the IGI Operation Section of Chapter IV).

The measurement update function creates the true measurements (satellite-user ranges and range-rates) then corrupts the true measurements with various error sources (such as satellite-user clock bias, atmospheric delay, ionospheric errors, and environmental noise errors) to create the four GPS pseudo-range and delta psdueo-range measurements. The measurement information is used to correct the filter state estimates by sequentially using Carlson's upper triangular square root algorithm for scalar measurements (19) (discussed in more detail in the Satellite Measurement Generation and Incorporation Subsection of the IGI Operation Section of Chapter IV).

The simulator outputs are of two forms, printed and plot data output. The printed output echoes the data from the input files (both the flight trajectory and configuration - initialization data files) and the program-generated outputs before and after a measurement update. The program-generated outputs include the following (17:68),

(1) True, INS-indicated, and filter-estimated whole value user position and velocity variables.

(2) The square root of the filter covariance diagonal elements.

(3) The elements of the filter error state vector.

(4) The elements of the filter estimation error.

(5) The elements of the true error state vector.

(6) The satellites in view at the satellite selection time.

(7) The set of four satellites with the minimum GDOP.

(8) The GDOP value of the optimum satellite set.

The simulation plot data file contains a series of navigation data records. A navigation data record contains the time, the elements of the filter estimation errors, the elements of the square root of the covariance diagonal, and the INS-indicated position and velocity errors.

IGI Truth and Filter States (16:842-843). The basic inertial navigation system is described by a nine dimensional state vector $\underline{X}$ consisting of position, velocity, and aircraft attitude angles with respect to the navigation frame. An east-north-up orientation of the navigation frame is used in the IGI simulator.

$$\underline{X} = \begin{bmatrix} \lambda \\ L \\ h \\ V_e \\ V_N \\ V_Z \\ \epsilon_e \\ \epsilon_N \\ \epsilon_Z \end{bmatrix} = \begin{bmatrix} \text{Aircraft Longitude} \\ \text{Aircraft Latitude} \\ \text{Aircraft Altitude} \\ \text{Aircraft East Velocity} \\ \text{Aircraft North Velocity} \\ \text{Aircraft Up Velocity} \\ \text{Aircraft Angular Orientation about East axis} \\ \text{Aircraft Angular Orientation about North axis} \\ \text{Aircraft Angular Orientation about Up axis} \end{bmatrix} \quad (32)$$

Evolution of the states is described by the following system of nonlinear differential equations

$$\dot{\underline{X}} = \underline{F}(\underline{X}, \underline{f}, t) + \underline{u}(t) \quad (33)$$

where $\underline{f}$ is the specific force and $\underline{u}(t)$ are the continuous or discontinuous rates of correction in an aided-inertial implementation. For example, vertical channel stabilization is accomplished by altitude and vertical velocity rates from the aircraft altimeter.

In lieu of integrating the nonlinear equations in (33) for each IGI simulation run, the approach is to linearize equation (33) about the specified (and precomputed) nonlinear flight trajectory. The errors are propagated as perturbations to the reference trajectory and added to the whole-valued reference trajectory quantities in succeeding runs to obtain a first order approximation to the actual

inertial navigation system outputs. The true nonlinear flight trajectory consists of the vector $\underline{X}_t$ (output from PROFGEN is expressed in a level wander angle coordinate frame, as opposed to the East-North-Up geographic frame) (See Figure 11).

$$\underline{X}_t = \begin{bmatrix} \lambda_t \\ L_t \\ h_t \\ V_{et} \\ V_{Nt} \\ V_{Zt} \\ f_{et} \\ f_{Nt} \\ F_{Zt} \\ \alpha_t \\ \phi_t \\ \theta_t \\ Y_t \end{bmatrix} = \begin{bmatrix} \text{True Longitude} \\ \text{True Latitude} \\ \text{True Altitude} \\ \text{True East Velocity} \\ \text{True North Velocity} \\ \text{True Up Velocity} \\ \text{True East Specific Force} \\ \text{True North Specific Force} \\ \text{True Up Specific Force} \\ \text{True Wander Angle} \\ \text{True Aircraft Roll Angle} \\ \text{True Aircraft Pitch Angle} \\ \text{True Aircraft Yaw Angle} \end{bmatrix} \tag{34}$$

The linearized errors $\delta\underline{X}_t$ are computed from equations (33) and (34) using the following set of differential equations,

$$\dot{\delta\underline{X}}_t = \underline{A}_t(t)\delta\underline{X}_t + \underline{w}(t) + \underline{w}^1(t) + \underline{u}(t) \tag{35}$$

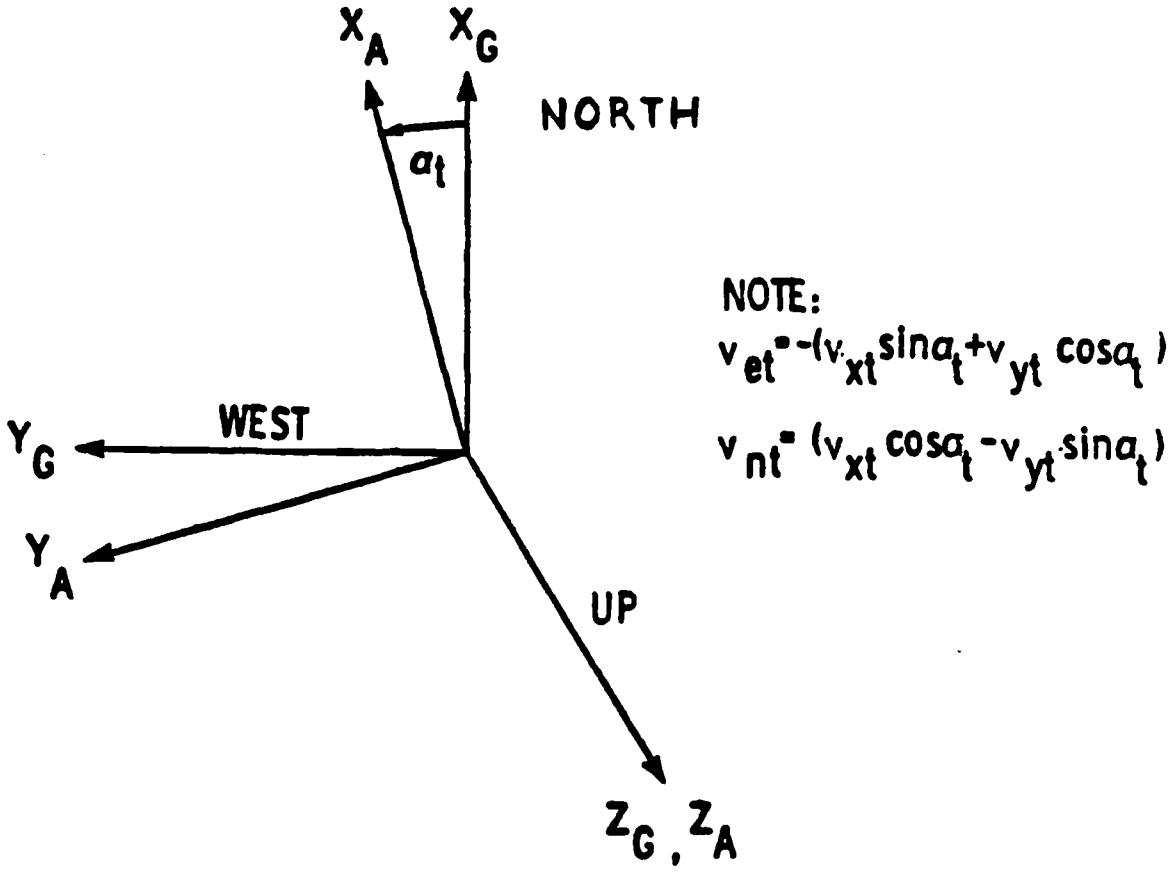

Figure 11 Definition of PROFGEN Geographic (X_G,Y_G,Z_G) and Wander Angle (X_A,Y_A,Z_A) Coordinate Frame (17:7)

where

$$\underline{A}_t(t) = (\delta \underline{F}/\delta \underline{X}) \Big|_{\underline{X}_t} \tag{36}$$

are the partial derivatives of $\underline{F}$ (from equation (33)) evaluated on $\underline{X}_t$. The $\underline{w}(t)$ and $\underline{W}^1(t)$ represent stochastic error forcing functions which perturb the linear system dynamics (e.g. gravity anomalies, gyro biases, and accelerometer errors).

The IGI direct simulation is currently configured for an altimeter-aided LN-15 inertial navigation system error model. The functions $\underline{w}(t)$, $\underline{w}^1(t)$, and $\underline{u}(t)$ for this system are derived in Reference 18. The $\underline{w}(t)$ can be written as follows,

$$\underline{w}(t) = \begin{bmatrix} \underline{w}_R \\ \underline{w}_V \\ \underline{w}_\epsilon \end{bmatrix} = \begin{bmatrix} \underline{0} \\ C_P^N \underline{\delta f}^P + \underline{\delta g}^{1N} \\ C_P^N \underline{\delta w}_{iP}^P \end{bmatrix} = \begin{bmatrix} \text{Position Error Components} \\ \text{Velocity Error Components} \\ \text{Attitude Error Components} \end{bmatrix} \tag{37}$$

where C_P^N is the small angle transformation matrix from platform to navigation coordinates (East-North-Up); $\underline{\delta f}^P$ is the specific force measurement error in platform coordinates; $\underline{\delta g}^{1N}$ is the gravity model error in navigation coordinates; and $\underline{\delta w}_{ip}^P$ is the platform angular velocity error in inertial coordinates. These INS error models contain a total of 48 states in the referenced report (17:16). In addition to the 48 states from the INS error model, seven states have been

added to simulate the GPS UE crystal clock errors, two additional barometric altimeter errors have been added, and four external pseudo-range error states have been added (to account for the small inaccuracies in the GPS Control and Space Segments) for a total truth state vector dimension of 61. A list of the total truth states is provided in Table II (17:6-50). The time propagation of the filter states is performed with the upper left 16 x 16 portion of the $\underline{A}_t(t)$ matrix. This upper left matrix is referred to as $\underline{A}_f(t)$ and is generated using nominal position, velocity and specific force. Since specific force is not directly measurable in an inertial system an approximation based on velocity differencing is used (16:844). The generation of $\underline{A}_f(t)$ as just described, serves to isolate the user's inertial system state estimates from the truth state values, lending added realism to the simulation.

IGI Trajectory and Navigation Error Formulation (16: 843-845). A number of trajectories and navigation errors are employed in the IGI simulation to create and maintain the distinction between the user's inertial system estimates and the truth state variables;

(1) True Trajectory, $\underline{X}_t$

(2) True Navigation Errors, $\delta\underline{X}_t$

(3) Nominal Trajectory, $\underline{X}_N$

(4) Filter Estimated Navigation Errors, $\delta\underline{X}_f$

(5) Filter Estimated Trajectory, $\underline{X}_f$

TABLE II

Error Model State Variables (17:16)

Basic Inertial Navigation Errors

1. $\delta\lambda$ Error in east longitude
2. δL Error in north latitude
3. δh Error in altitude
4. δv_e Error in east velocity
5. δv_n Error in north velocity
6. δv_u Error in vertical velocity
7. ϵ_e Attitude error east component
8. ϵ_n Attitude error north component
9. ϵ_u Attitude error up component

Barometric Altimeter Error

10. ∇_{baf} Altimeter scale factor error

Vertical Channel Error Variable

11. δa Vertical acceleration error variable in altitude channel

Clock Errors

12. δt_u User clock phase error
13. δt_{ru} User clock frequency bias

G-Insensitive Gyro Drift

14. DR_x X gyro drift rate
15. DT_y Y gyro drift rate
16. DZ_z Z gyro drift rate

G-Sensitive Gyro Drift Coefficients

17. DR_x X gyro input axis g-sensitivity
18. DR_y X gyro spin axis g-sensitivity
19. DT_x Y gyro spin axis g-sensitivity
20. DT_y Y gyro input axis g-sensitivity
21. DZ_y Z gyro spin axis g-sensitivity
22. DZ_z Z gyro input axis g-sensitivity

G²-Sensitive Gyro Drift Coefficients

23. DR_{xy} X gyro spin-input g^2-sensitivity
24. DT_{xy} Y gyro spin-input g^2-sensitivity
25. DZ_{yz} Z gyro spin-input g^2-sensitivity

Gyro Scale Factor Errors

26. GSF_x X gyro scale factor error
27. GSF_y Y gyro scale factor error
28. GSF_z Z gyro scale factor error

Gyro Input Axis Misalignments

29. RG_y X gyro input axis misalignment about Y
30. RG_z X gyro input axis misalignment about Z
31. YG_x Y gyro input axis misalignment about X
32. YG_z Y gyro input axis misalignment about Z
33. ZG_x Z gyro input axis misalignment about X
34. ZG_y Z gyro input axis misalignment about Y

Accelerometer Biases

35. AB_x X accelerometer bias
36. AB_y Y accelerometer bias
37. AB_z Z accelerometer bias

Accelerometer Scale Factor Errors

38. ASF_x X accelerometer scale factor error
39. ASF_y Y accelerometer scale factor error
40. ASF_z Z accelerometer scale factor error

Accelerometer Input Axis Misalignments

41. RA_y X accelerometer input axis misalignment about Y
42. RA_z X accelerometer input axis misalignment about Z
43. YA_x Y accelerometer input axis misalignment about X
44. YA_z Y accelerometer input axis misalignment about Z

Accelerometer Input Axis Misalignments (Cont.)

45. ZA_x Z accelerometer input axis misalignment about X
46. ZA_y Z accelerometer input axis misalignment about Y

Additional Barometric Altimeter Error

47. ϵ_{po} Error due to variation in altitude of a constant pressure surface

Gravity Deflections and Anomaly

48. $\delta\eta_e$ East deflection of gravity
49. $\delta\eta_n$ North deflection of gravity
50. $\delta\eta_z$ Gravity anomaly

Additional Clock Errors

51. δt_{bu} Clock aging bias
52. δt_{ru} Clock random frequency bias

Additional Barometric Altimeter Errors

53. c_{op} Coefficient of static pressure measurements
54. τ_b Altimeter lag

Clock Frequency g Sensitivities

55. C_r r axis specific force sensitivity
56. C_f f axis specific force sensitivity
57. C_n n axis specific force sensitivity

External Pseudo-Range Errors

58. δt_{e1} External Pseudo-Range error to Satellite 1
59. δt_{e2} External Pseudo-Range error to Satellite 2
60. δt_{e3} External Pseudo-Range error to Satellite 3
61. δt_{e4} External Pseudo-Range error to Satellite 4

The true trajectory, $\underline{X}_t$ is generated a priori by the program PROFGEN (Ref. 24). PROFGEN processes realistic flight profiles (path accelerations, altitude rates, headings, etc.) to create a data file of the true aircraft state $\underline{X}_t$ as a function of time. The processing of the realistic flight profile input is accomplished by integrating the nonlinear equations of motion over a WGS-72 (World Geodectic Survey-1972) reference ellipsoid with a Kutta-Merson fifth-order numerical integration routine with step-size control (Ref. 24).

The true nonlinear reference data from PROFGEN is used to "drive" the linear error model in equation (35). Note that the true specific force f is employed directly in $\underline{A}_t(t)$ to simulate the true acceleration "felt" by the accelerometers. The stochastic disturbances in $\underline{w}^1(t)$ are generated by means of a Gaussian random number generator with variances as specified in Reference 18. Since the stepsize in equation (35) is small, typically 0.1 seconds, integration of the equations for the state transition matrix $\underline{\Phi}_t(t_{i+1}, t_i)$ is carried out with the linear approximation,

$$\underline{\Phi}_t(t_{i+1}, t_i) \tilde{=} \underline{I} + \underline{A}_t(t_i)(t_{i+1} - t_i) \qquad (38)$$

and the resultant true error is given by

$$\delta \underline{X}_t^{i+1} = \underline{\Phi}_t(t_{i+1}, t_i)\delta \underline{X}_t^i + \bar{\underline{W}}^{1L} \qquad (39)$$

where $E[\bar{\underline{W}}^{1L}] = 0$, $E[\bar{\underline{W}}^{1i}\bar{\underline{W}}^{1jT}] = \underline{Q}_f(t_i)\delta_{ij}$ and $\bar{\underline{W}}^{1i}$ are the integrated contributions of the noise $\underline{W}^1$ in analytical form. The true initial condition errors $\delta\underline{X}^{\circ}_t$ and the noise covariance $\underline{Q}_f$ are specified in the input initialization and configuration file.

The nominal trajectory $\underline{X}_N$, which represents the user's INS-indicated position and velocity, is created by the difference between the true navigation error $\delta\underline{X}_t$ and the true reference trajectory $\underline{X}_t$.

$$\underline{X}_n = \underline{X}_t - \delta\underline{X}_t \tag{40}$$

Without external measurement data, or between measurement updates, $\underline{X}_N$ represents the user's best estimate of his navigation parameters based solely on the user's internal navigation aids; namely the IMU, altimeter, and clock.

The nominal nonlinear reference trajectory $\underline{X}_N$ is used to "drive" the user's 16 state filter error model. The inputs required for the fundamental matrix $\underline{A}_t(t)$ include nominal position, velocity, and specific force $\underline{f}_N$. Since the specific force $\underline{f}_N$ is not directly measurable in an inertial system, velocity pulses (or differences) are utilized to derive an approximation as follows

$$\underline{f}_N(t) = [\underline{V}_N(t) - \underline{V}_N(t - \Delta t)]/\Delta t \tag{41}$$

where Δt is the velocity pulse integration stepsize. This duplicates the procedure employed in a real inertial system.

Therefore, the effects of integration errors and time lags (due to the stepsize) in obtaining correct specific force data from the computer will be reflected in the simulation. Since Δt is small, the following approximation is made for the user's estimate of the state transition matrix,

$$\underline{\Phi}_f(t_{i+1}, t_i) = \underline{I} + \underline{A}_f(t_i)(t_{i+1} - t_i) \tag{42}$$

and the user's estimated navigation error is

$$\delta\underline{X}_f^{i+1} = \underline{\Phi}_f(t_{i+1}, t_i)\ \delta\underline{X}_f^i + \bar{\underline{W}}_f^{1i} \tag{43}$$

At the initial time, $\delta\underline{X}_f^\circ = 0$, since the user has no better information than has initial nonlinear state estimate. When satellite measurements are available, the error estimate $\delta\underline{X}_f$ is updated (measurement update will be discussed further later in this section).

The user's best estimate of his nonlinear trajectory is obtained by adding the error estimate $\delta\underline{X}_f$ from the filter to the nominal reference trajectory, $\underline{X}_N$.

$$\underline{X}_f = \underline{X}_N + \delta\underline{X}_f \tag{44}$$

which is referred to as the estimated trajectory. The true navigation error can then be computed by taking the difference between the estimated and true reference trajectories as follows,

$$\underline{e}_t = \underline{X}_f - \underline{X}_t \tag{45}$$

or using equations (40) and (44),

$$\underline{e}_t = \delta\underline{X}_f - \delta\underline{X}_t \tag{46}$$

Satellite Measurement Generation and Incorporation (17: 42-50). The IGI simulator assumes that the 18 GPS satellites are point masses moving in circular orbits of 12 hour period above a spherical earth. Two-body orbit equations and angular transformations are used to compute the position $\underline{X}_s$ and velocity $\underline{V}_s$ of the selected satellites. The position and velocity components in earth centered earth fixed (ECEF) coordinates at a given time are computed according to the following equations (See Ref. 29:51-143).

$$\begin{aligned} X_{s1} &= R_s \sin W \sin i \\ X_{s2} &= -R_s (\sin W \cos i \cos \Omega + \cos W \sin \Omega) \\ X_{s3} &= -R_s (\sin W \cos i \sin \Omega - \cos W \cos \Omega) \end{aligned} \tag{47}$$

$$\begin{aligned} V_{s1} &= V_s \cos W \sin i \\ V_{s2} &= -V_s (\cos W \cos i \cos \Omega - \sin W \sin \Omega) + \Omega_e X_{s3} \\ V_{s3} &= -V_s (\cos W \cos i \sin \Omega + \sin W \cos \Omega) + \Omega_e X_{s2} \end{aligned}$$

where

R_s = radius from earth center to the satellite orbit

V_s = orbital velocity

i = orbital inclination

W = argument of latitude (See Figure 12)

Ω = nodal longitude (See Figure 12)

Ω_e = earth rotation rate

The ECEF coordinate frame is defined by an axis that is along the earth's axis of rotation (through the north pole), an axis in the equatorial plane at a longitude of -90° from Greenwich, and the third axis in the equational plane at a longitude equal to the Greenwich meridian. The simulated truth state satellite pseudo-range measurement is defined by the following

$$PR_m(t) = R_t(t) + \delta t_u(t) + \delta t_e(t) + E_{pr} \qquad (49)$$

where

$PR_m(t)$ = Measured pseudo-range

$R_t(t)$ = Geometric Range from the user-to-satellite based on the true user's position

$\delta t_u(t)$ = True user-clock phase error

$\delta t_e(t)$ = External pseudo-range error due to satellite clock errors, satellite ephemeaides errors, and atmospheric delays

E_{pr} = Pseudo-range additive random error (due to multipath random error, receiver noise, etc.)

t = Pseudo-range measurement time

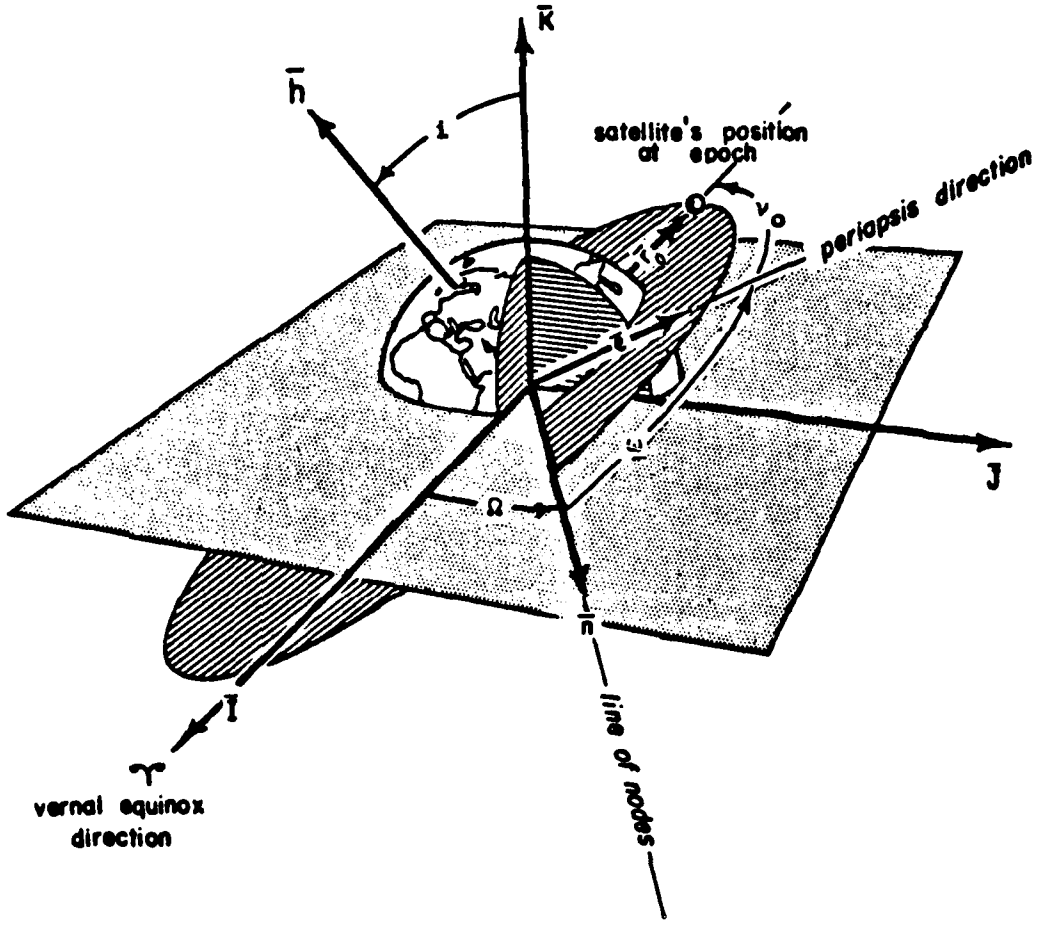

where:

Periapsis Direction = the direction of closest orbital approach to the earth

$\bar{h}$ = the specific angular momentum = $\underline{r} \times \underline{V}$

$\bar{e}$ = eccentricity vector

$\bar{I}$, $\bar{J}$, and $\bar{K}$ denote the Geocentric-Equational Coordinate System

ν_o = True Anomaly at epoch

Ω = Longitude of the ascending node

ω = Argument of periapsis

Figure 12. Classical Orbital Element Description (29:59).

The clock phase errors δt_u and external pseudo-range error δt_e are included as states in the truth model (17:35-36). The pseudo-range additive random error E_{pr} is generated by a random number generator (Gaussian distributed with zero mean and unit variance) times the one-sigma value of a pseudo-range additive random error (7 feet). The simulated filter state pseudo-range measurement, however, does not have δt_u and δt_e available in the filter states. To account for the added uncertainty in the simulated filter state pseudo-range due to the lack of knowledge of δt_u and δt_e, the one-sigma value of pseudo-range additive random error E_{pr} has a value of 12 feet (17:44).

Measurement information is processed in the Kalman filter by using the measurement residual. The measurement residual is calculated by differencing the pseudo-range measurement with the expected value for the pseudo-range conditioned on the previous measurements taken. The expected value is computed based on the INS-indicated position corrected by the Kalman filter estimates of error in the indicated position ($\delta\hat{\lambda}_f$, $\delta\hat{L}_f$, $\delta\hat{h}_f$) and the given satellite ephemeris. The equation for the expected value of the pseudo-range measurement is (the detailed development of equation (50) is available in Reference 17, page 45-48),

$$\hat{PR}_f(t) = g_{PR}(\underline{r}_N(t), \delta\hat{\underline{X}}_f(t)) + h_{PR}^T(\delta\hat{\underline{X}}_f(t))E[(\delta\underline{X}_f(t) - \delta\hat{\underline{X}}_f(T))] + E[V_{PR}] \quad (50a)$$

or

$$\hat{PR}_f(t) = g_{PR}(\underline{r}_N(t), \delta\hat{\underline{X}}_f(t)) \tag{50b}$$

where

$\underline{r}_N(t)$ = INS-indicated position vector

$\delta\underline{X}_f(t)$ = filter error state vector

$\delta\hat{\underline{X}}_f(t)$ = filter's best prediction of the state before the measurement is incorporated

$\underline{h}_{PR}^T(\delta\hat{\underline{X}}_f(t)$ = the pseudo-range measurement gradient vector

V_{PR} = additive random measurement error

The pseudo-range measurement redisual is

$$\Delta Z_{PR} = PR_m - \hat{PR}_f \tag{51}$$

The pseudo-range and delta pseudo-range measurement residuals and the associated measurement gradient vectors are used to correct the filter estimates of the state using Carlson's upper triangular square root algorithm (19). The scalar measurements are incorporated sequentially according to the following equations.

$$P_f(-) = S_f(-)S_f^T(-) \tag{52}$$

$$\underline{f} = S_f^T(-)\underline{h}_i \qquad \text{for } i = 1 \rightarrow m \qquad (53a)$$

$$\alpha_o = \sigma_i^2 \qquad (53b)$$

$$\underline{b}_o = \underline{o} \qquad \text{for } j = 1 \rightarrow N_f \qquad (53c)$$

$$\alpha_j = \alpha_{j-1} + f_j^2 \qquad (53d)$$

$$\underline{b}_j = \underline{b}_{j-1} + S_{fj}(-)f_j \qquad (53e)$$

$$S_{fj}(+) = [S_{fj}(-) - \underline{b}_{j-1}f_j/\alpha_{j-1}]\sqrt{\alpha_{j-1}/\alpha_j} \qquad (53f)$$

$$\underline{K} = \underline{b}_N/\alpha_N \qquad (53g)$$

$$\delta\hat{\underline{X}}_f(+) = \delta\hat{\underline{X}}_f(-) + \underline{K}\,\Delta Z_i \qquad (53h)$$

$$P_f(+) = S_f(+)S_f^T(+) \qquad (54)$$

where

$P_f(\cdot)$ = filter covariance matrix before (-) or after (+) measurement incorporation

$S_f(\cdot)$ = the upper triangular square root matrix of the filter covariance (using Cholesky decomposition)

S_{fj} = the j^{th} column of S_f

fj = the j^{th} element of $\underline{f}$ (specific force)

ΔZ_i = the i^{th} measurement residual

h_i = the measurement gradient vector of the i^{th} measurement

σ_i^2 = variance of the noise in the i^{th} measurement

N_f = dimension of the filter state

M = number of measurements

$\underline{K}$ = Kalman gain vector

Modifications to the IGI Simulator

The modifications to the IGI Simulator necessary to test the cost criterion satellite selection algorithm fall into two categories, functions supporting the cost criterion and functions to increase the realism of the computer simulation. The increased realism will allow the results of this study to be more applicable to the present hardware design. Also, the increased realism and capability of the modified IGI simulator will make it an effective design/analysis tool. The major functions added to the IGI simulator are: the cost criterion (for satellite selection), an adaptive null steering antenna algorithm, the air and/or ground jammers, and an adaptive bandwidth control of the GPS satellite signal tracking loops. A brief discussion of each function follows, with references to the appropriate appendix for a more detailed analysis of each function.

The Cost Criterion. The cost criterion function added to the IGI simulator modifies the satellite selection algorithm to minimize equation (33) instead of GDOP for each possible satellite set. In order to calculate equation (33), the covariance matrix values for three position errors and

one time bias error are needed to fill the a priori covariance matrix $\underline{P}_o$. Also, the one-sigma measurement noise values for each satellite (in the set being examined) are needed to create the measurement noise matrix $\underline{R}$. The information needed for the $\underline{P}_o$ matrix is readily available from the IGI simulator. The information for the $\underline{R}$ matrix, however, is a function of satellite signal level at the antenna, the jamming power level at the antenna, the type of antenna, and the type of satellite tracking loop, none of which are available in the IGI simulator, but are added in the modifications to be discussed. For analysis purposes, the cost criterion value of the satellite set with the minimum cost criterion value is stored for output with the printed data as well as the GDOP value for that particular satellite set. Then by comparing the cost and GDOP values for a simulation run using the cost criterion and a simulation run using GDOP, conclusive results can be made of the effectiveness of the alternate versus standard satellite selection criterion on mean square position error.

The Null Steering Antenna. The objective of the null steering antenna algorithm is to maximize the GPS satellite signals, minimize interference, and estimate the signal carrier-to-noise density (C/No) values for each in view satellite. To accomplish these objectives the null steering algorithm uses a power inversion process to determine the directions of the strongest interference sources. The null steering controller thereby forms nulls in the direction of

the interference sources to reduce their jamming power. The implemented null steering antenna model uses a seven element phased array antenna arranged in a circular pattern (Figure 13). A seven element null steering antenna is capable of forming a maximum of six nulls with approximately 30db watts of jammer suppression (6:141). The satellite signals are protected from spurious nulls by using the estimate of the satellites direction in the null steering controller.

The estimate of signal-to-noise density (C/No) values for each satellite is an inherent quantity in the null steering algorithm which limits the unwanted signals and maximizes the satellite signals.

For a more detailed analysis of the processes implemented in the modified IGI simulator, the reader is directed to Appendix B.

Jamming Field. The jamming field parameters are input through the initialization and configuration input file. The simulation user may specify the number of jammers (1-25), the position of the jammers (in degrees latitude, degrees longitude, and altitude in feet), the velocity of the jammers (in feet-per-second), and the effective isotropic radiating power (EIRP) out of the jammer. The above format was implemented to allow land, sea, and airborne jammers that are stationary or mobile. The jammers are omni-directional radiating sources that transmit the full EIRP into the GPS L1 frequency. The GPS user-to-jammer line-of-sight is

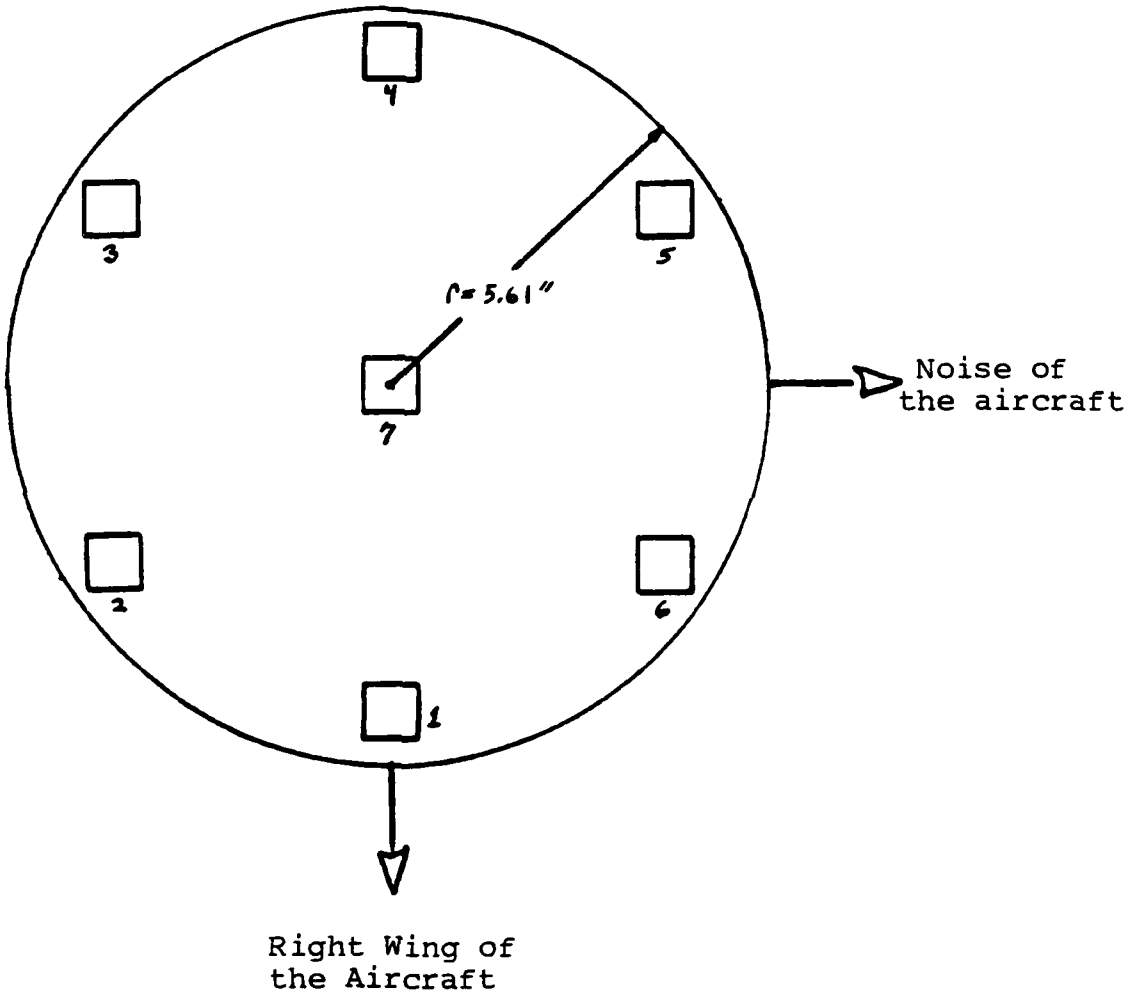

Figure 13. Seven Element Null Steering Antenna Geometry

obstructed by blockage from the earth only (which is again assumed to be spherical) (See Appendix B).

Adaptive Bandwidth Control of Satellite Tracking. As discussed in Chapter III, the bandwidth of the satellite tracking loops is very important in limiting jamming related navigation errors. The C/No estimates from the null steering algorithm allow the implementation of adaptive control of the bandwidth of the satellite tracking loops. The bandwidth of the code loops is determined by four separate quadratic functions that use the C/No estimate. The software implementation covers both coherent and non-coherent code loop modes, as well as loss-of-lock thresholds. The carrier loop was not implemented due to the very small amount of error associated with the carrier loop estimates ($\tilde{\sim}$ 1 cm of position error) (5:25-26). A more detailed discussion of the adaptive bandwidth control of satellite tracking is addressed in Appendix B.

V Simulation Analysis

Introduction

This chapter will present the results from the modified IGI computer simulation runs. The results will be presented in a pictorial and tabular form to increase readability. From the abundance of IGI output information four parameters will be highlighted:

(1) The number of times the cost criterion chooses a satellite set other than the set chosen using GDOP.

(2) The user position and clock phase errors for both GDOP and the cost criterion for the times when an alternate satellite set was chosen from GDOP.

(3) The measurement error estimate for each satellite at the satellite selection time.

(4) The noise level at each satellite selection time when GDOP and the cost criterion don't agree on the same satellite set.

These four parameters will be the basis for an assessment of the performance of GDOP versus the cost criterion in satellite selection.

The Simulated Mission

The mission used in all of the simulation runs is an F-4 Close Air Support (CAS) flight profile, provided by the Reference Systems Branch, AFWAL Avionics Laboratory, Wright-Patterson AFB, Ohio. This flight profile was chosen because of the high aircraft dynamics associated with the

tactical mission and the increased realism of the mission by locating a jamming field around the target area. A 24 minute segment of the total F4 CAS mission was used in the simulation runs in order to cover the aircraft's maneuver's in the target area, while keeping the simulation outputs to a manageable level. The time history of the 24 minute F4 CAS mission is presented in Table III. The target is assumed to be located at the position where the F-4 is at its lowest altitude (time = 760.0 seconds).

The jamming field patterns for each simulation run (simulation runs are identified as missions 1-5) were modeled as stylized jamming arrays (as in Ref. 20) to easily vary the maximum jamming power, to move the maximum jamming power points, and to increase or decrease the rate of change of jamming power. The location and transmitted power for each jammer in each mission in shown in Table IV.

Mission Parameters

Each simulated mission has a duration of 1400 seconds. At time = 0.0 seconds the truth state terms and the filter covariance terms of east, north, and up user position error and the clock phase error are set to a value of 50 feet (that is a 50 ft one-sigma for the covariance terms). This is consistent with an integrated GPS/INS that is within its steady state performance accuracy, attained enroute to the target area. The GPS measurements are incorporated every five seconds, but the truth and filter state's and the filter covariance data is printed out once every 100 seconds. While

TABLE III

F4 CAS Mission

TIME	LATITUDE	LONGITUDE	ALTITUDE	MANEUVER	HEADING
0-300 sec	38.00000000°	-90.00000000°	27500.0 ft	STRAIGHT/LEVEL	90.0°
300-305	38.00000000	-89.02823787	17710.7	1g. VERT. TURN	90.0°
305-341	38.00000000	-89.01286603	17356.2	4.5g HOR. TURN	90.0°
341-377	37.99988087	-89.01402387	13913.2	4.5g HOR. TURN	75.0°
377-387	37.99975728	-89.01520037	10470.2	2g VERT. TURN	90.0°
387-487	37.99975728	-88.98592818	10498.7	25s JINKING	90.0°
487-667	37.99975713	-88.70057322	12857.6	30s JINKING	90.0°
667-682	37.99975773	-88.17834075	17103.7	1g HOR. TURN	90.0°
682-707	37.99702820	-88.13456426	17457.5	0.5g VERT. TURN	95.0°
707-712	37.99197757	-88.06161573	17503.0	STRAIGHT/LEVEL	95.0°
712-714.5	37.99096743	-88.04702639	17506.0	1g HOR. TURN	95.0°
714.5-740.5	37.99032542	-88.03974968	17507.5	1.6g VERT. TURN	97.0°
740.5-745	37.98392310	-87.97386683	8945.3	STRAIGHT/LEVEL	97.0°
745-750	37.98302315	-87.86460641	6258.9	5g HOR. TURN	97.0°
750-760	37.97930273	-87.95560263	3274.1	7.5g VERT. TURN	127.0°
760-775	37.96624533	-87.93371384	2028.6	7.5s JINKING	127.0°

TABLE III CONTINUED

TIME	LATITUDE	LONGITUDE	ALTITUDE	MANEUVER	HEADING
775-778	37.94541682°	-87.89880594	3141.9	2g VERT. Turn	127.0°
778-874	37.94125483	-87.89183101	3423.5	16s JINKING	127.0°
874-884	37.80973269	-87.67165256	12661.1	3.75g HOR. TURN	127.0°
884-1076	37.78939539	-87.66416777	13623.3	24s JINKING	-161.0°
1076-1136	37.37530301	-87.74333152	32098.4	0.1g VERT. TURN	-161.0°
1136-1436	37.2[illegible]420201	-87.89985007	34804.4	STRAIGHT/LEVEL	-161.0°
1400	36.66596914	-88.14795691	34960.2	STRAIGHT/LEVEL	-161.0°
1436 sec	36.58711517°	-88.18164506°	34981.4^{ft}	STRAIGHT/LEVEL	-161.0°

$23.9\bar{3}$ minutes elapsed time in total flight profile

$23.3\bar{3}$ minutes elapsed time in simulation runs

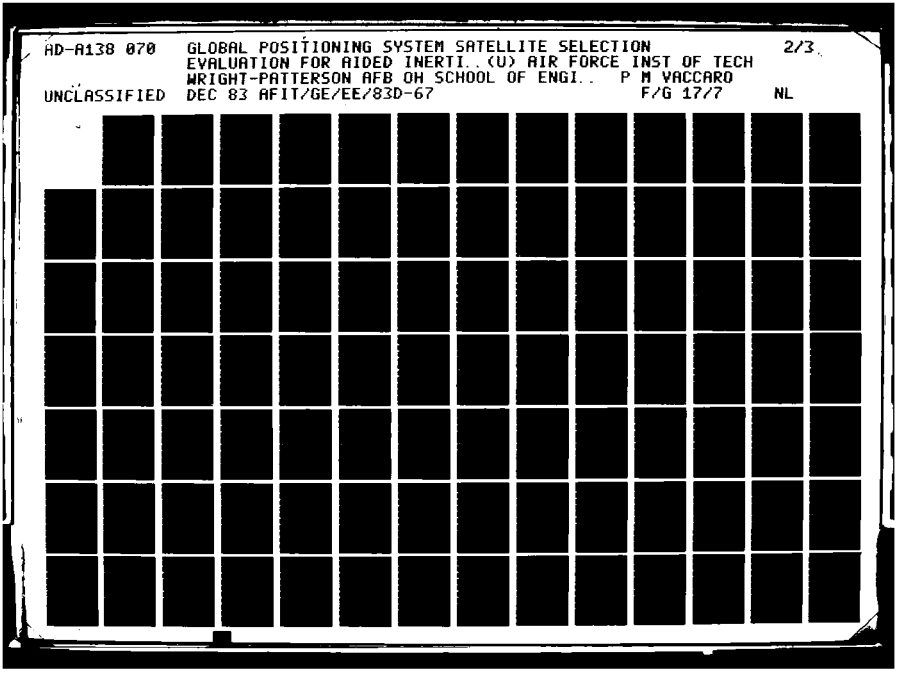
AD-A138 070 GLOBAL POSITIONING SYSTEM SATELLITE SELECTION 2/3
EVALUATION FOR AIDED INERTI..(U) AIR FORCE INST OF TECH
WRIGHT-PATTERSON AFB OH SCHOOL OF ENGI.. P M VACCARO
UNCLASSIFIED DEC 83 AFIT/GE/EE/83D-67 F/G 17/7 NL

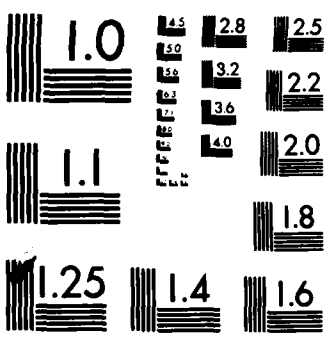

MICROCOPY RESOLUTION TEST CHART
NATIONAL BUREAU OF STANDARDS-1963-A

TABLE IV

Jamming Field Patterns

Mission # 1					
LONGITUDE / LATITUDE	-87.0°	-88.0°	-88.5°	-89.0°	-90.0°
36.0°	1.0kw	0.1kw	0.1kw	0.1kw	1.0kw
37.0°	1.0kw	0.1kw	0.1kw	0.1kw	1.0kw
37.5°	1.0kw	0.1kw	0.2kw	0.1kw	1.0kw
38.0°	1.0kw	0.1kw	0.1kw	0.1kw	0.1kw
39.0°	1.0kw	0.1kw	0.1kw	0.1kw	1.0kw
Mission # 2					
LONGITUDE / LATITUDE	-87.0°	-88.0°	-88.5°	-89.0°	-90.0°
36.0°	0.5kw	0.5kw	0.5kw	0.5kw	0.5kw
37.0°	0.5kw	0.5kw	0.5kw	0.5kw	0.5kw
37.5°	0.5kw	0.5kw	0.5kw	0.5kw	0.5kw
38.0°	0.5kw	0.5kw	0.5kw	0.5kw	0.5kw
39.0°	0.5kw	0.5kw	0.5kw	0.5kw	0.5kw
Mission # 3					
LONGITUDE / LATITUDE	-87.0°	-88.0°	-88.5°	-89.0°	-90.0°
36.0°	0.1kw	0.1kw	0.1kw	0.1kw	0.1kw
37.0°	0.1kw	0.1kw	0.1kw	0.1kw	0.1kw
37.5°	0.1kw	0.1kw	0.1kw	0.1kw	0.1kw
38.0°	0.1kw	0.1kw	0.1kw	0.1kw	0.1kw
39.0°	0.1kw	0.1kw	0.1kw	0.1kw	0.1kw

* All jammers have an elevation of 10 feet and are stationary with respect to the earth's surface.

TABLE IV CONTINUED

Mission # 4					
LONGITUDE / LATITUDE	-87.0°	-88.0°	-88.5°	-89.0°	-90.0°
37.995°	1.0 kw	0.001kw	0.1 kw	0.001kw	1.0 kw
37.990°	0.001kw	0.1 kw	0.001kw	0.1 kw	0.001kw
37.965°	1.0 kw	0.001kw	0.1 kw	0.001kw	1.0 kw
37.950°	0.001kw	0.1 kw	0.001kw	0.1 kw	0.001kw
37.945°	1.0 kw	0.001kw	0.1 kw	0.001kw	1.0 kw
Mission # 5					
LONGITUDE / LATITUDE	-88.05°	-87.95°	-97.90°	-87.85°	-87.75°
37.995°	0.1kw	0.1kw	0.1kw	0.1kw	0.1kw
37.990°	0.1kw	1.0kw	1.0kw	1.0kw	0.1kw
37.965°	0.1kw	1.0kw	2.0kw	1.0kw	0.1kw
37.950°	0.1kw	1.0kw	1.0kw	1.0kw	0.1kw
37.945°	0.1kw	0.1kw	0.1kw	0.1kw	0.1kw

* All jammers have an elevation of 10 feet and are station-are with respect to the earth's surface.

in the jamming field, satellite selection using both the GDOP and cost criterion is executed every 100 seconds. There is no measurement incorporation or satellite selection at the final time (1400 seconds).

Mission # 1

The satellite selection in Mission # 1 between GDOP and the cost criterion was in agreement until 700 seconds into the flight. For next 6 satellite selection times, a set other than the best GDOP set was chosen by the cost criterion. Table Va shows the measurement noise estimates for the satellites chosen by the cost criterion and the associated noise density at the 6 satellite selection times of interest. The noise density (No) value is $N_T + N_J$ from Equation (74) in Appendix B. The N_J term is the difference of the total jammer power at the antenna output (J_a) and the p-code processing gain (6) when both J_a and G are expressed in decibels. The noise density (No) is related to another commonly used term J/S. The term J.S is defined as the jammer-to-signal power ratio (typically expressed in dBs). A noise density, No = 190 db relates to J/S values of 45-58. J/S values are typically associated with satellite signal and jammer power estimates with respect to the antenna input (i.e., the anti-jam performance gained from a null steering antenna, adaptive bandwidth control, and the p-code processing gain is lost), therefore, the C/No or No terms provide much more insight into the UE sets' performance with respect to jamming power.

Table Vb presents the same data as Table Va for the GDOP selected satellite set. Note that the cost criterion will almost always choose satellites that have measurement errors that are less than the measurement errors for the GDOP selected satellites. The performance of the integrated GPS/INS with the cost criterion versus the GDOP satellite selection algorithm is presented in Figures 14-17. broken into the three components of filter estimation (filter-truth states) position error and filter estimation clock phase error (note that plot a in each figure is the IGI using the cost criterion, and plot b in each figure is the IGI using GDOP). Included in the plots of Figures 14-17 are the ± 1 sigma values of the related filter covariance terms. The figures show the cost criterion exhibiting smaller errors in all three components of position error than the GDOP plots, with the clock phase errors being roughly equal during the 700-1200 second interval when an alternate satellite set is being tracked. The maximum noise density is -186.93dB and occurs at approximately 1053 seconds. The composite statistics for the filter estimation radial position errors averaged over the 700-1200 second interval are:

Cost Criterion		versus	GDOP	
Mean	Std. Dev.		Mean	Std. Dev.
241.77	262.38		627.80	855.04

Including time-bias range errors:

Mean	Std. Dev.	Mean	Std. Dev.
294.81	262.38	627.80	855.04

where all units are in feet.

TABLE Va

Mission 1 Statistics
(Cost Only)

700	800	900	1000	1100	1200	1300	SECONDS
18.88	15.41	19.11	22.49	22.70	20.15	x	R_{meas} (1)
17.66	17.87	18.45	20.29	20.55	18.61	x	R_{meas} (2)
15.21	15.47	15.55	15.53	15.27	15.19	x	R_{meas} (3)
***	***	***	***	***	20.41	x	R_{meas} (4)
-190.58	-190.21	-189.30	-187.35	-187.15	-189.16	-191.87	NOISE DENSITY

TABLE Vb

Mission 1 Statistics
(GDOP Only)

700	800	900	1000	1100	1200	1300	SECONDS
18.69	15.41	17.29	21.46	21.04	29.31	x	R_{meas} (1)
22.33	18.79	19.11	19.60	18.34	17.69	x	R_{meas} (2)
15.21	15.47	18.45	20.29	20.55	18.61	x	R_{meas} (3)
***	***	***	***	***	***	x	R_{meas} (4)
-190.58	-190.21	-189.30	-187.35	-187.15	-189.16	-191.87	NOISE DENSITY

NOTE: (1) "***" indicates that the C/N_o level for this satellite is below tracking limits, therefore $R_{meas} = 1.0 \times 10^8$ feet.
(2) "x" indicates that GDOP and cost criterion satellite sets agreed during this time period.
(3) All R_{meas} values are expressed in feet.

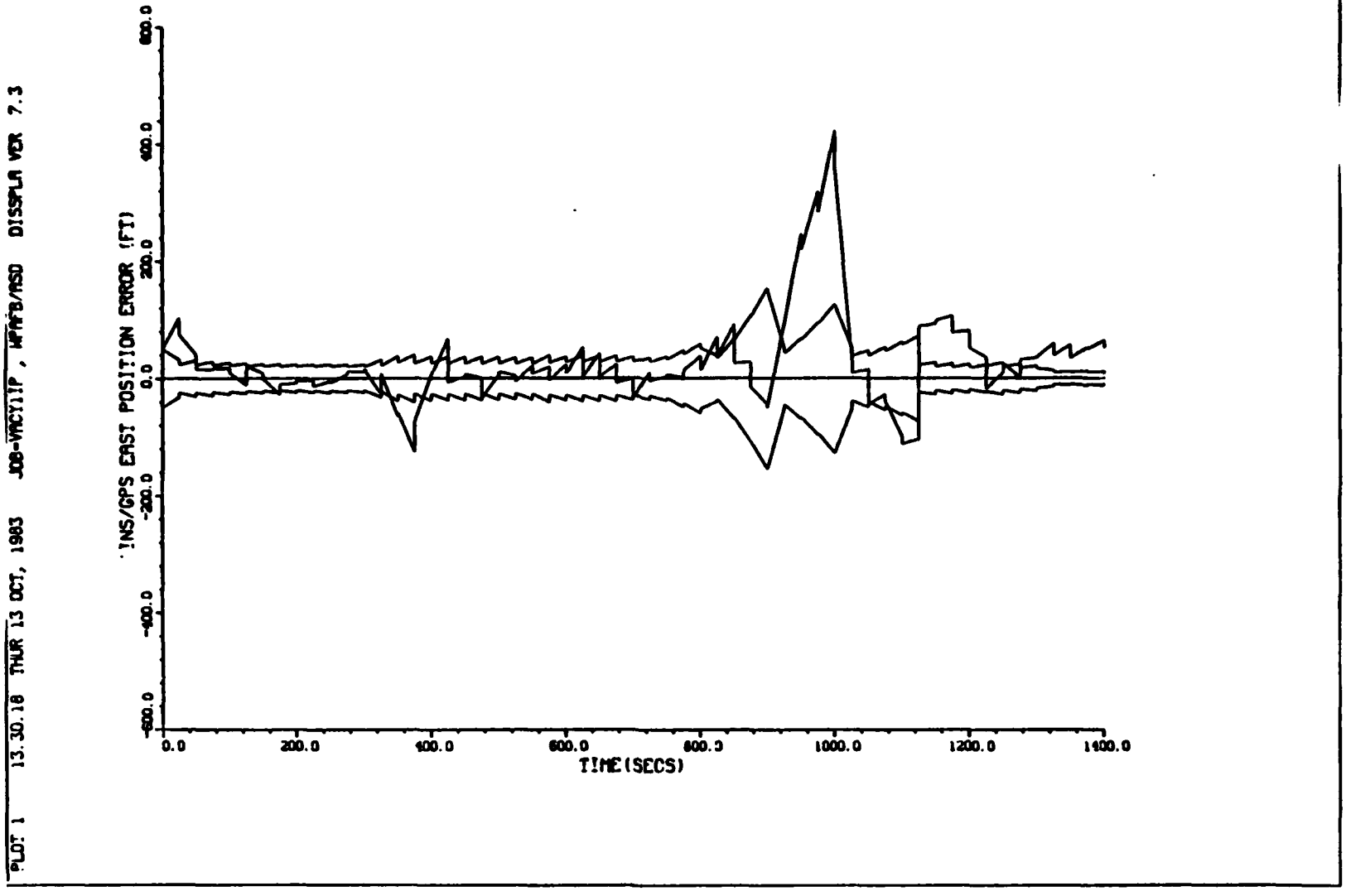

Figure 14a. Mission # 1: Cost Criterion; East Position Error

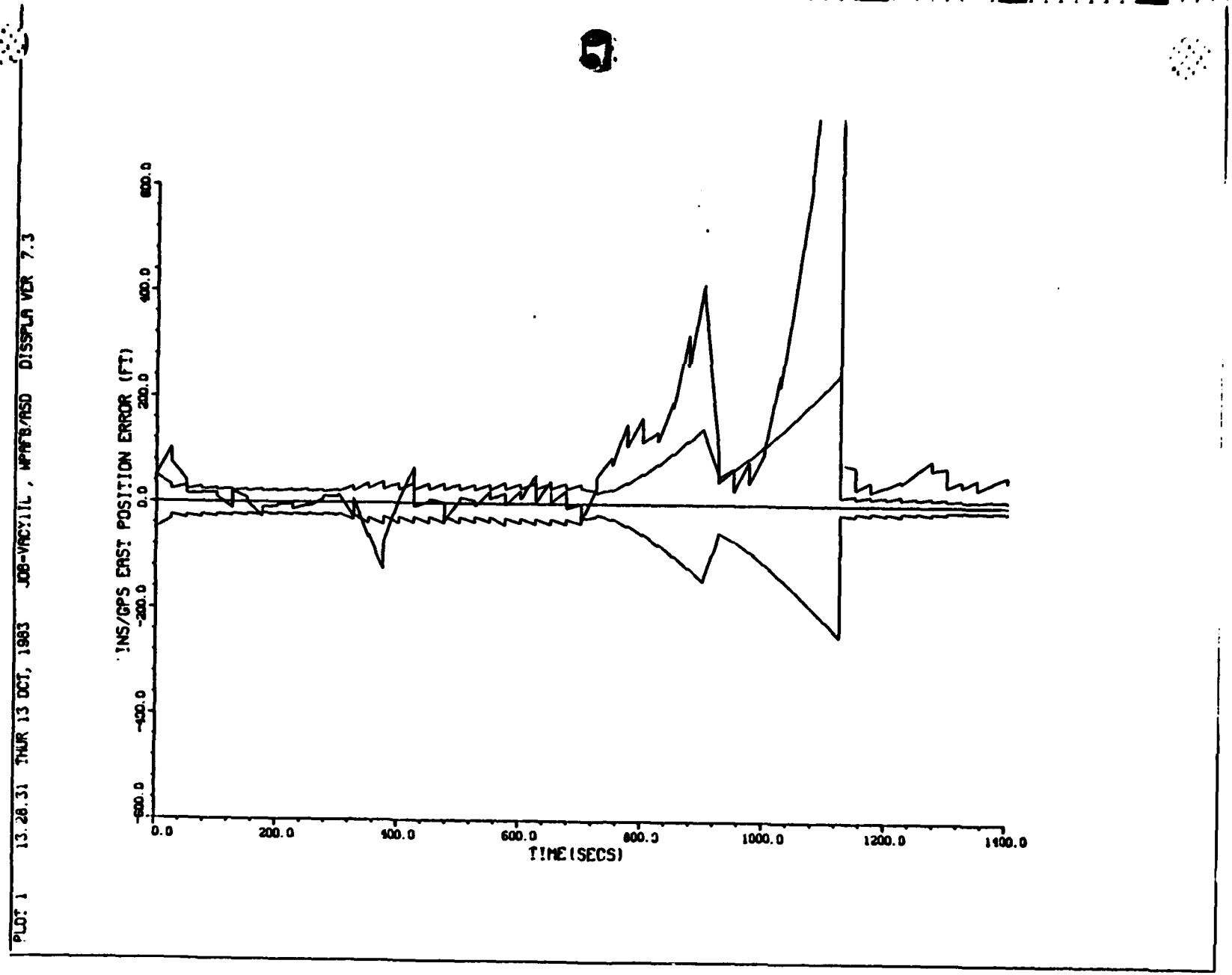

Figure 14b. Mission # 1: GDOP; East Position Error

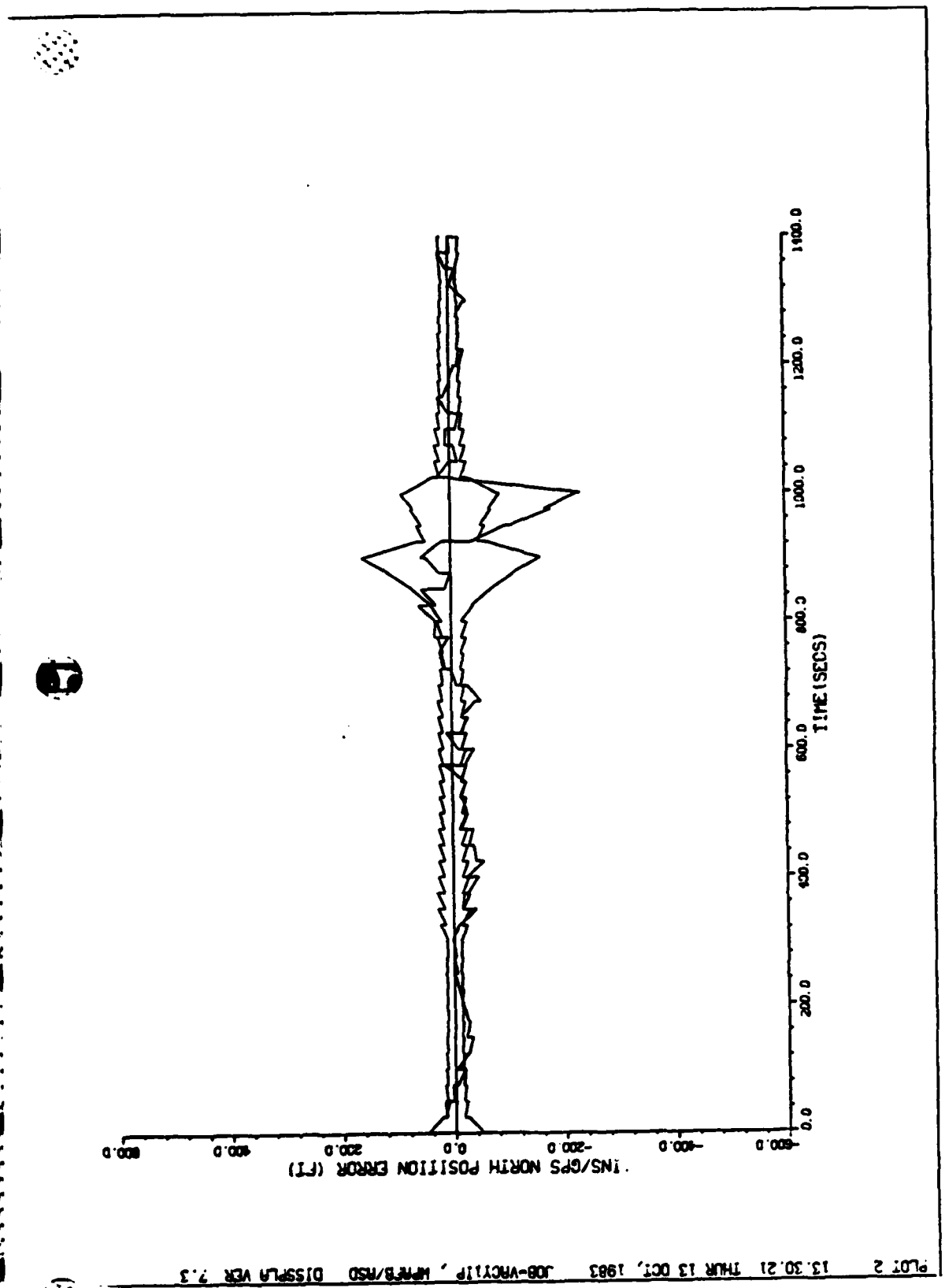

Figure 15a. Mission # 1: Cost Criterion; North Position Error

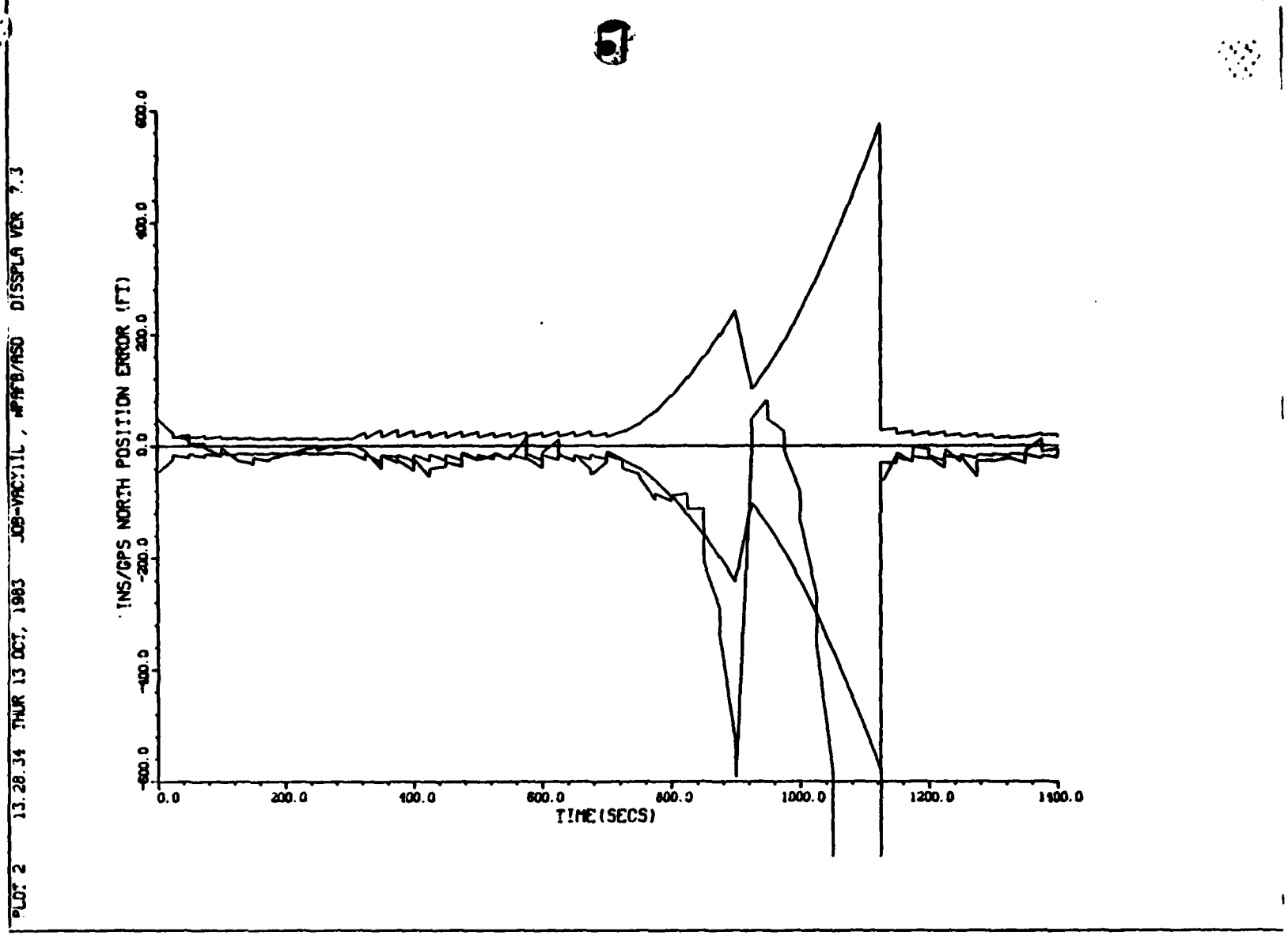

Figure 15b. Mission # 1: GDOP; North Position Error

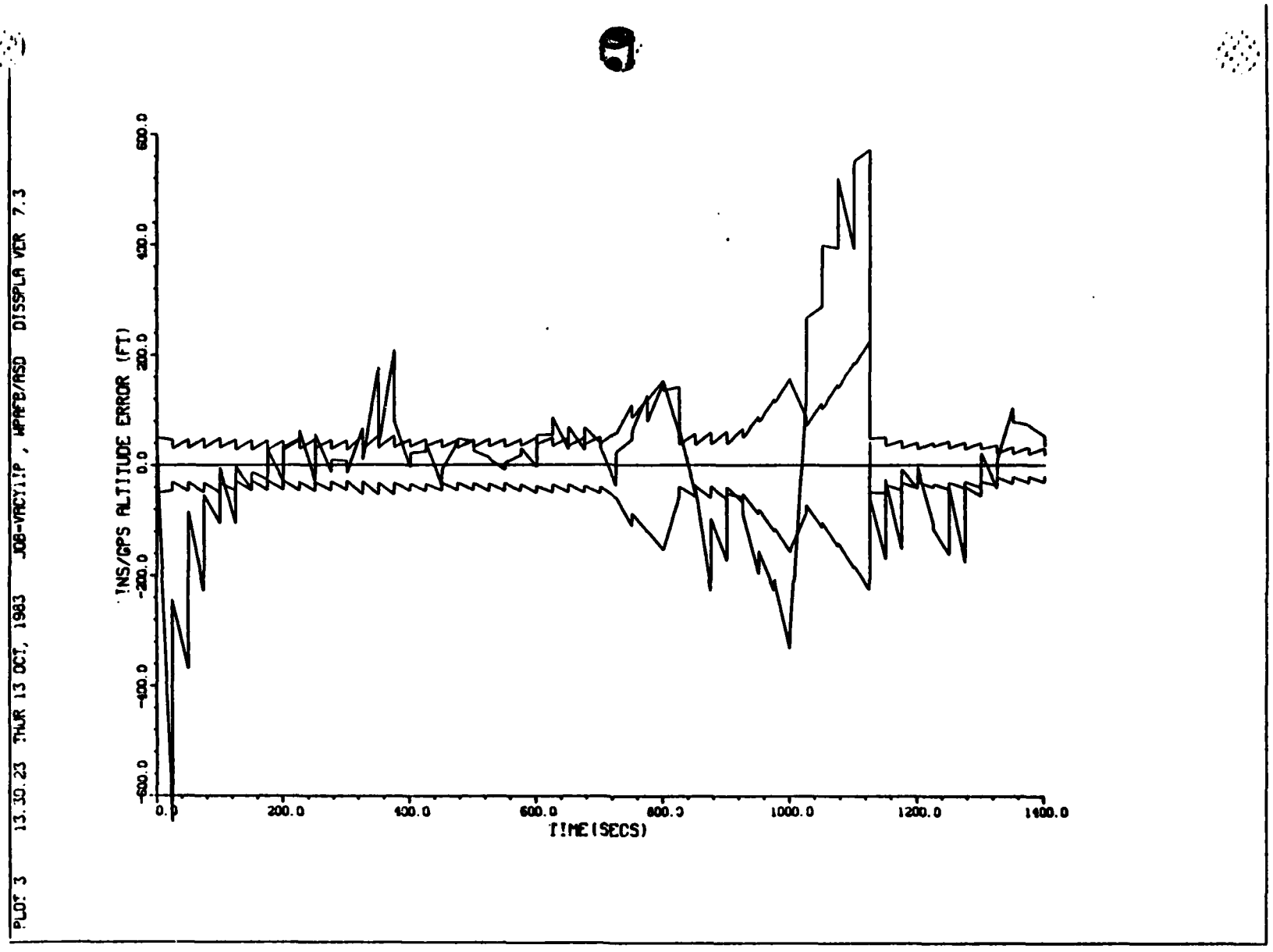

Figure 16a. Mission # 1: Cost Criterion; Altitude Error

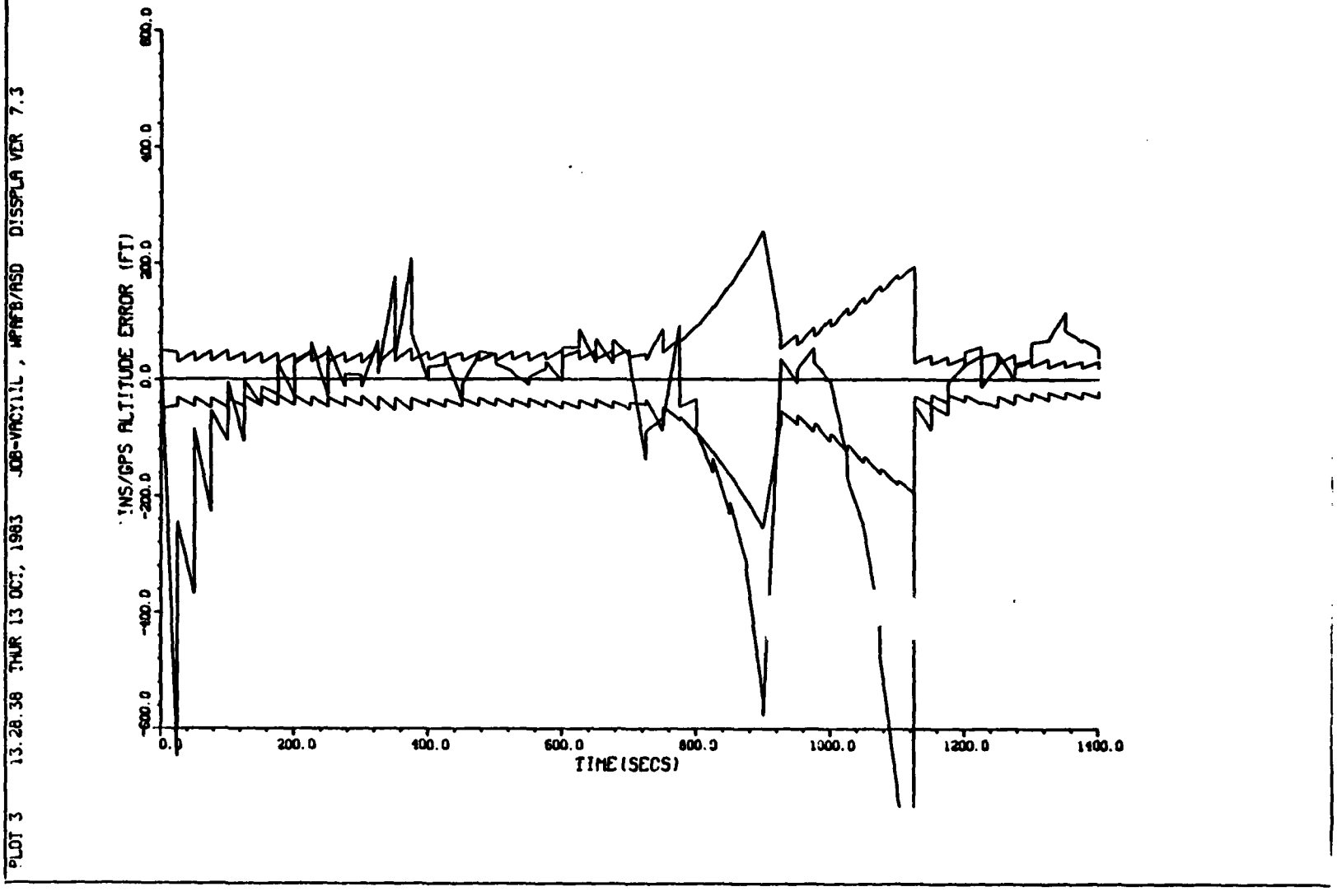

Figure 16b. Mission # 1: GDOP; Altitude Error

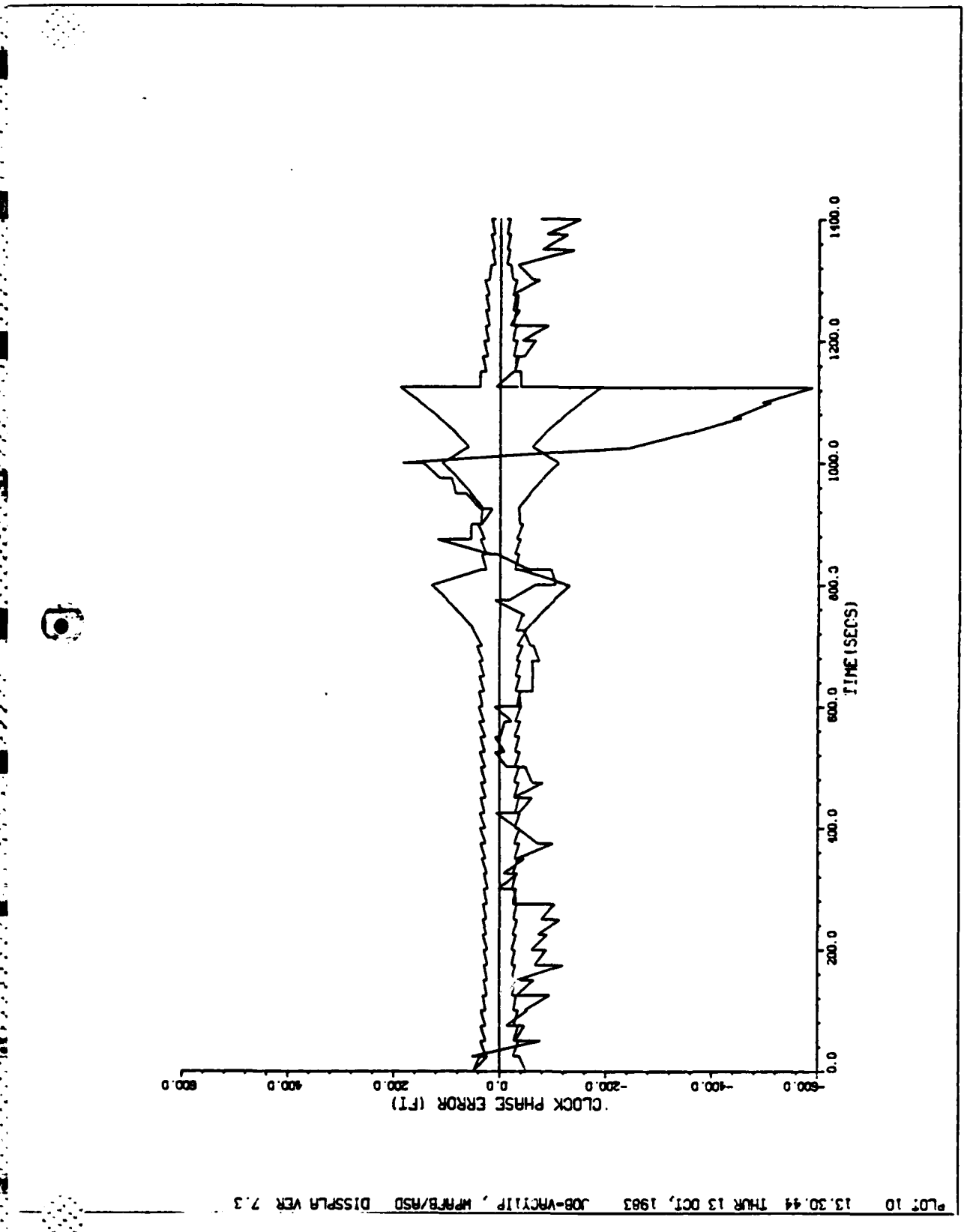

Figure 17a. Mission # 1: Cost Criterion; Clock Phase Error

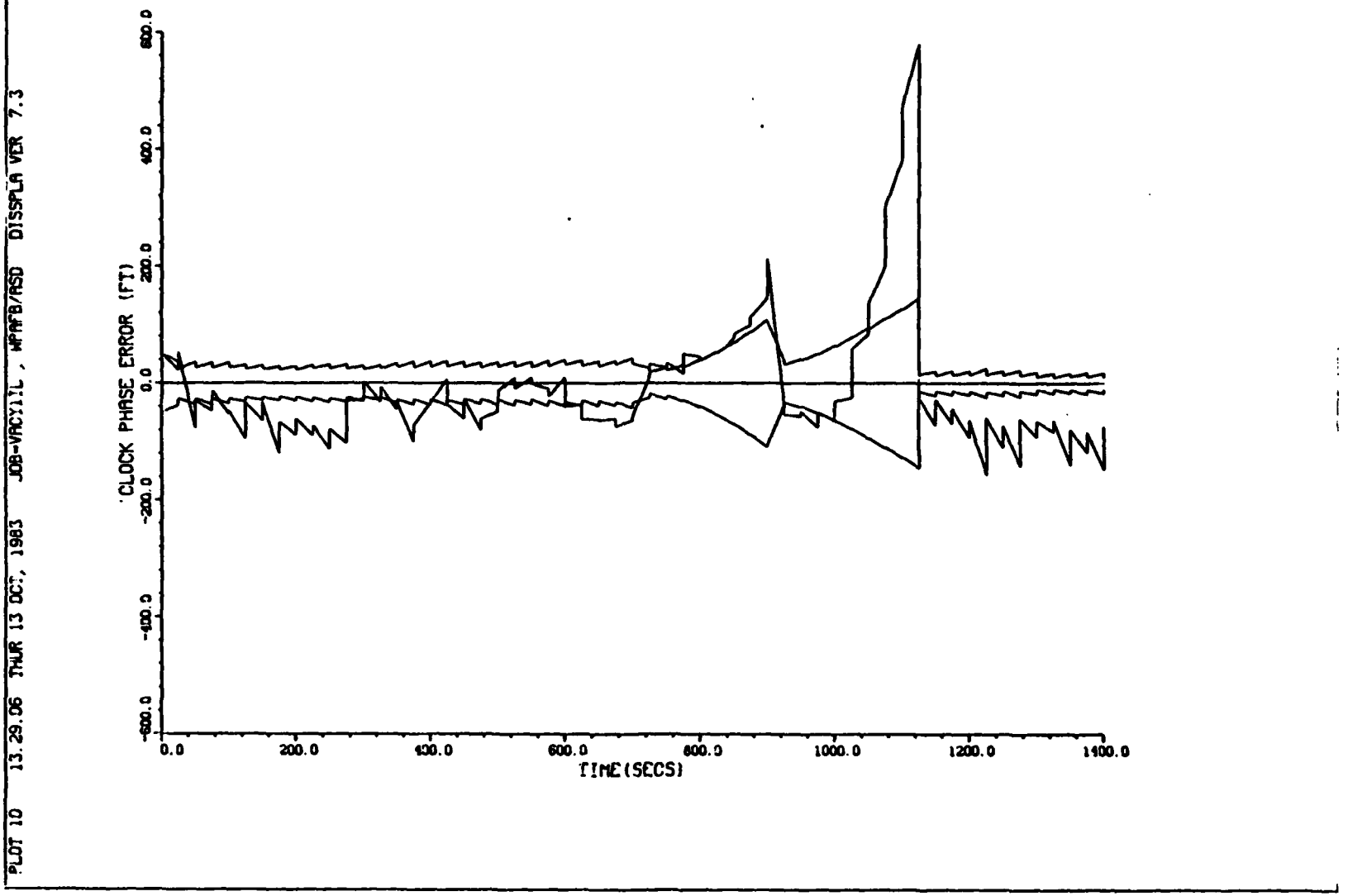

Figure 17b. Mission # 1: GDOP; Clock Phase Error

Mission # 2

The satellite selection in Mission # 2 varied from 700-1100 seconds and 1200-1300 seconds in the flight. Table VIa and b shows measurement error estimates for the cost criterion and GDOP satellite sets respectively. Note that the noise density peaks much earlier in Mission # 2 than in Mission # 1 (max noise density for Mission # 2 is -179.24 dB and occurs at 747 seconds in the mission), then remains relatively low for the duration of the mission. As was the case in Mission # 1, the cost criterion has chosen a satellite set with a lower composite measurement error than the GDOP satellite set.

Figures 18-21 present the time history performance of position and clock phase errors. The figures show that the cost criterion exhibits smaller position and clock phase errors than the corresponding GDOP errors, but that the difference is much less than appears in Mission # 1. The composite statistics for the filter estimation radial position errors averaged over the 700-1300 second interval (excluding 1100 seconds) are:

Cost Criterion		versus	GDOP	
Mean	Std. Dev.		Mean	Std. Dev.
73.81	34.35		94.20	45.13

Including time-bias range errors:

Mean	Std. Dev.	Mean	Std. Dev.
91.12	34.46	116.13	38.69

where all units are in feet. Again, the cost criterion significantly out-performs the GDOP criterion.

TABLE VIa

Mission 2 Statistics
(Cost Only)

700	800	900	1000	1100	1200	1300	SECONDS
16.49	15.58	15.10	18.70	x	17.69	15.21	R_{meas} (1)
15.16	18.03	15.29	17.62	x	16.21	15.08	R_{meas} (2)
15.02	15.66	15.19	15.16	x	15.15	15.08	R_{meas} (3)
28.44	***	28.75	25.72	x	17.90	19.25	R_{meas} (4)
-193.65	-189.94	-193.20	-190.66	-192.62	-192.09	-194.62	NOISE DENSITY

TABLE VIb

Mission 2 Statistics
(GDOP Only)

700	800	900	1000	1100	1200	1300	SECONDS
16.16	15.58	15.10	18.18	x	23.25	15.21	R_{meas} (1)
18.81	19.02	15.79	17.26	x	15.20	15.21	R_{meas} (2)
15.02	15.66	15.29	17.62	x	16.21	15.08	R_{meas} (3)
28.44	***	28.75	25.72	x	17.90	19.25	R_{meas} (4)
-193.65	-189.94	-193.20	-190.66	-192.61	-192.09	-196.62	NOISE DENSITY

NOTE: (1) "***" indicates that the C/N_o level for this satellite is below tracking limits, therefore $R_{meas} = 1.0 \times 10^8$ feet.
(2) "x" indicates that GDOP and cost criterion satellite sets agreed during this time period.
(3) All R_{meas} values are expressed in feet.

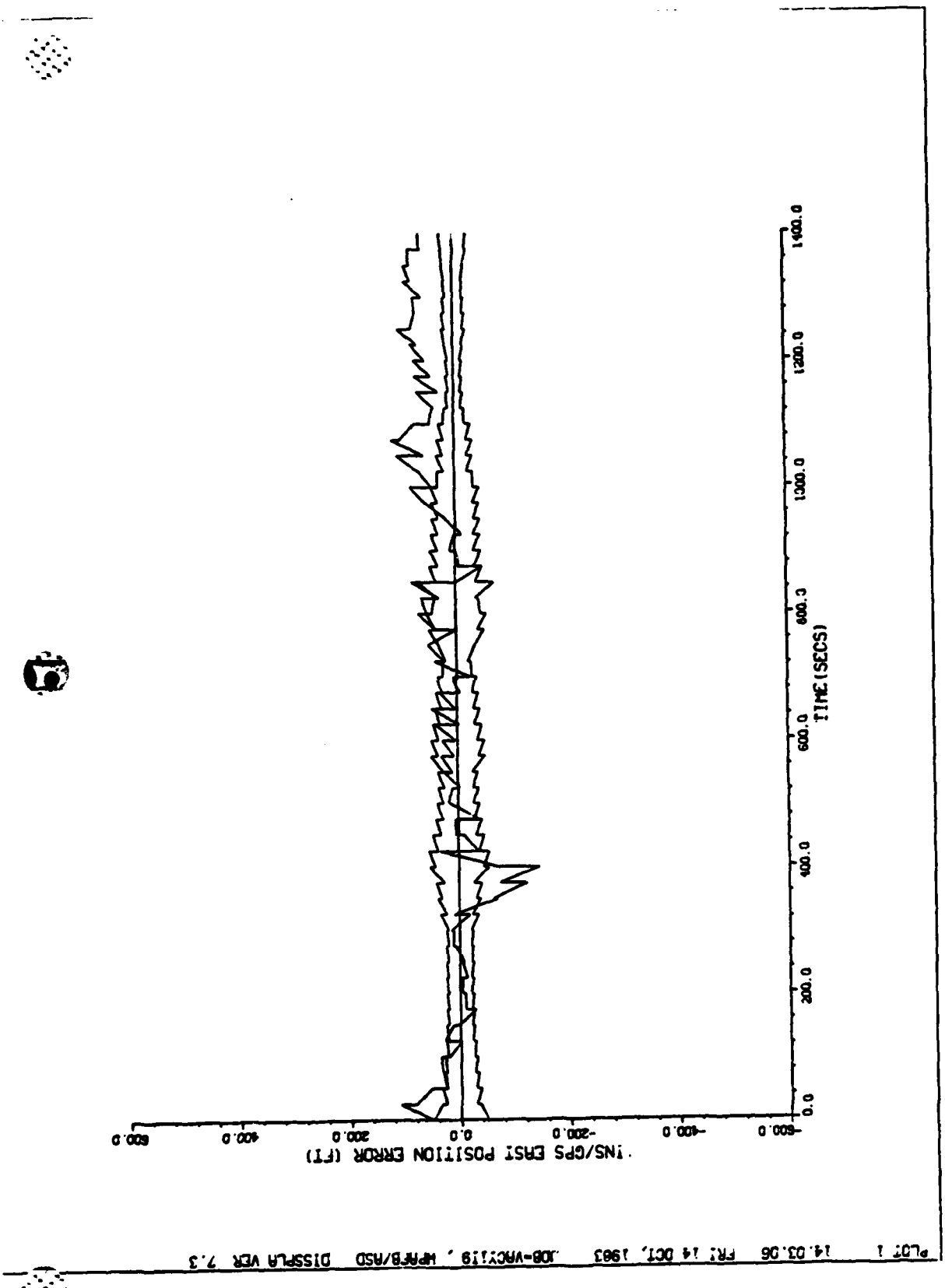

Figure 18a. Mission # 2: Cost Criterion; East Position Error

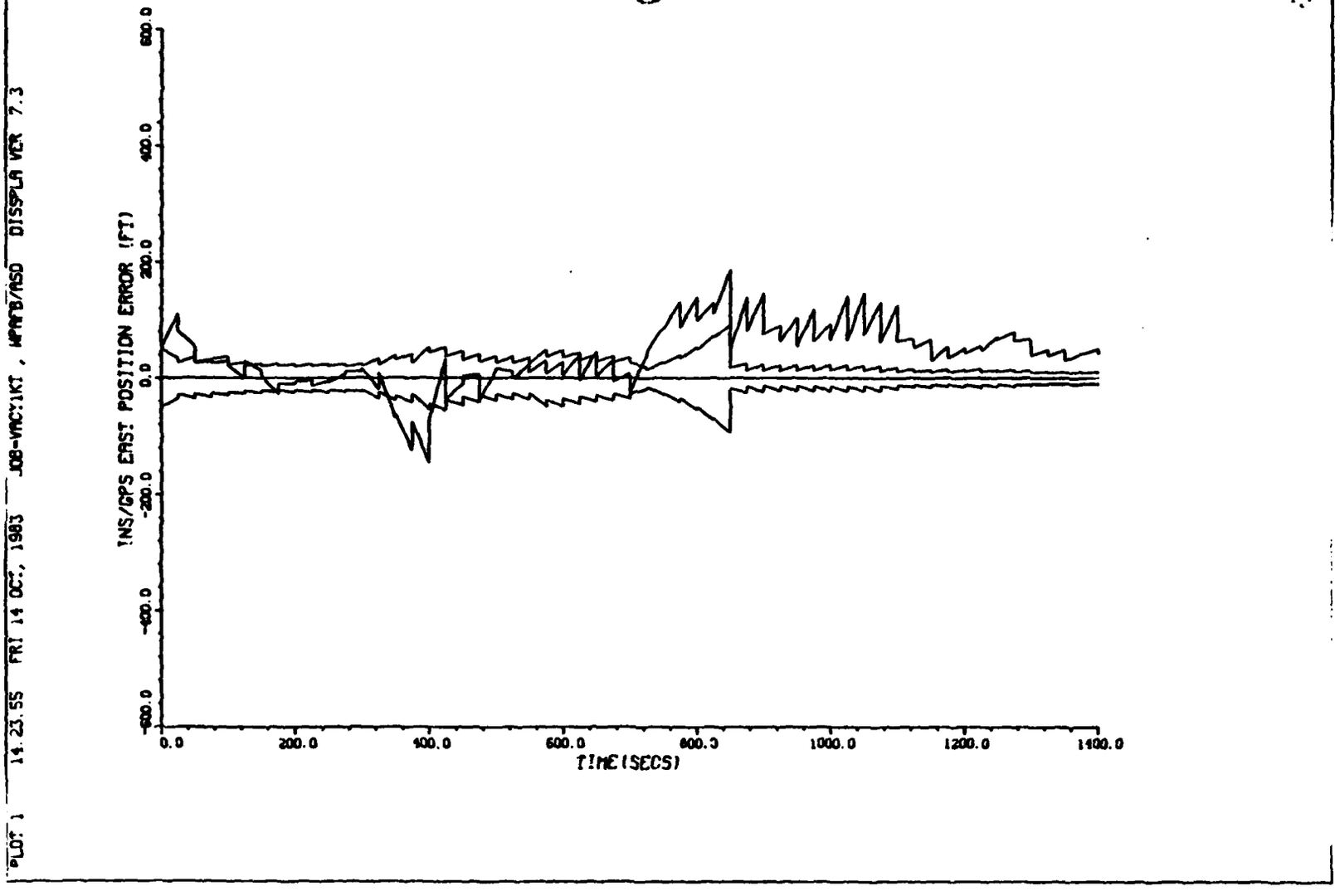

Figure 18b. Mission # 2: GDOP; East Position Error

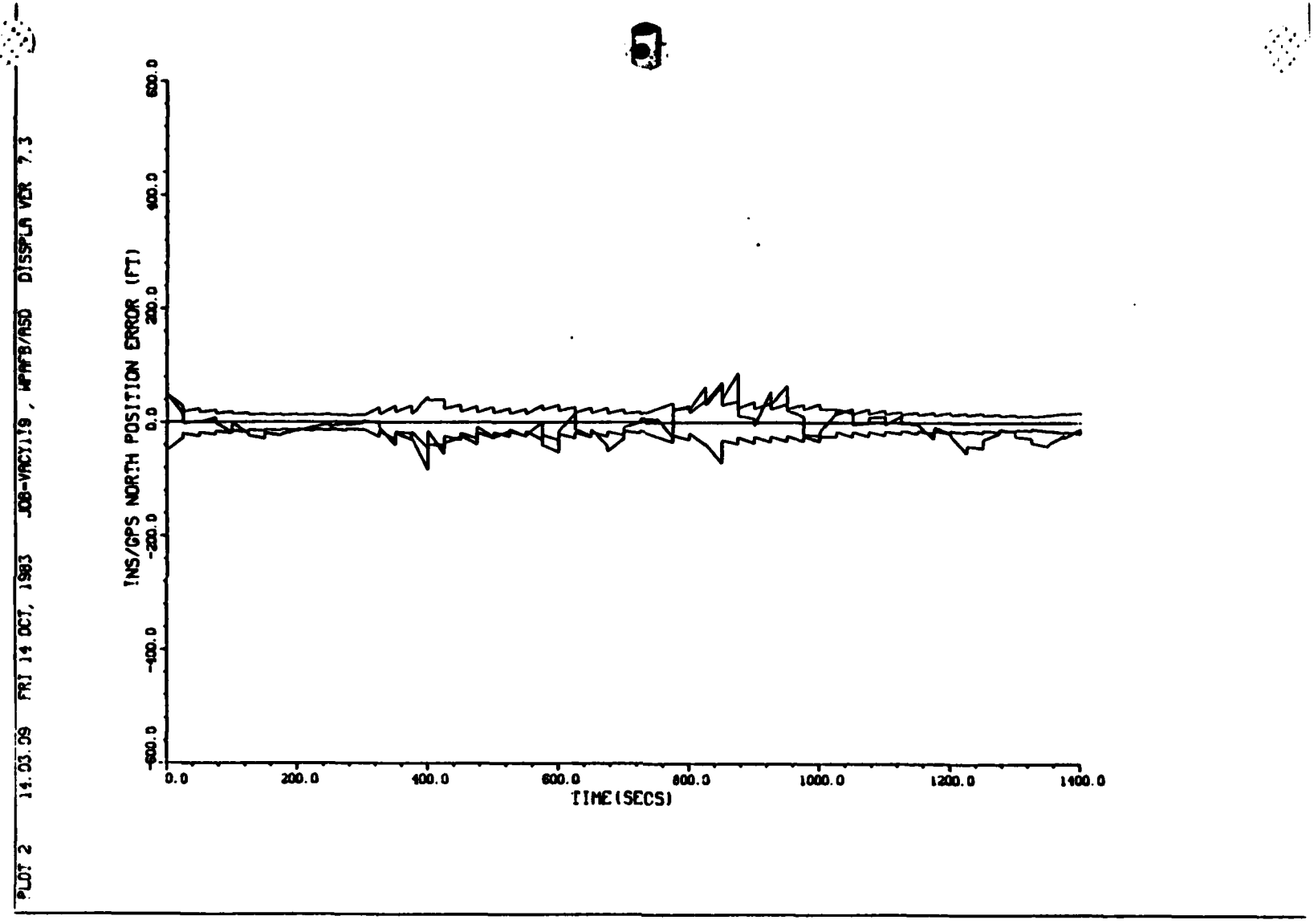

Figure 19a. Mission # 2: Cost Criterion; North Position Error

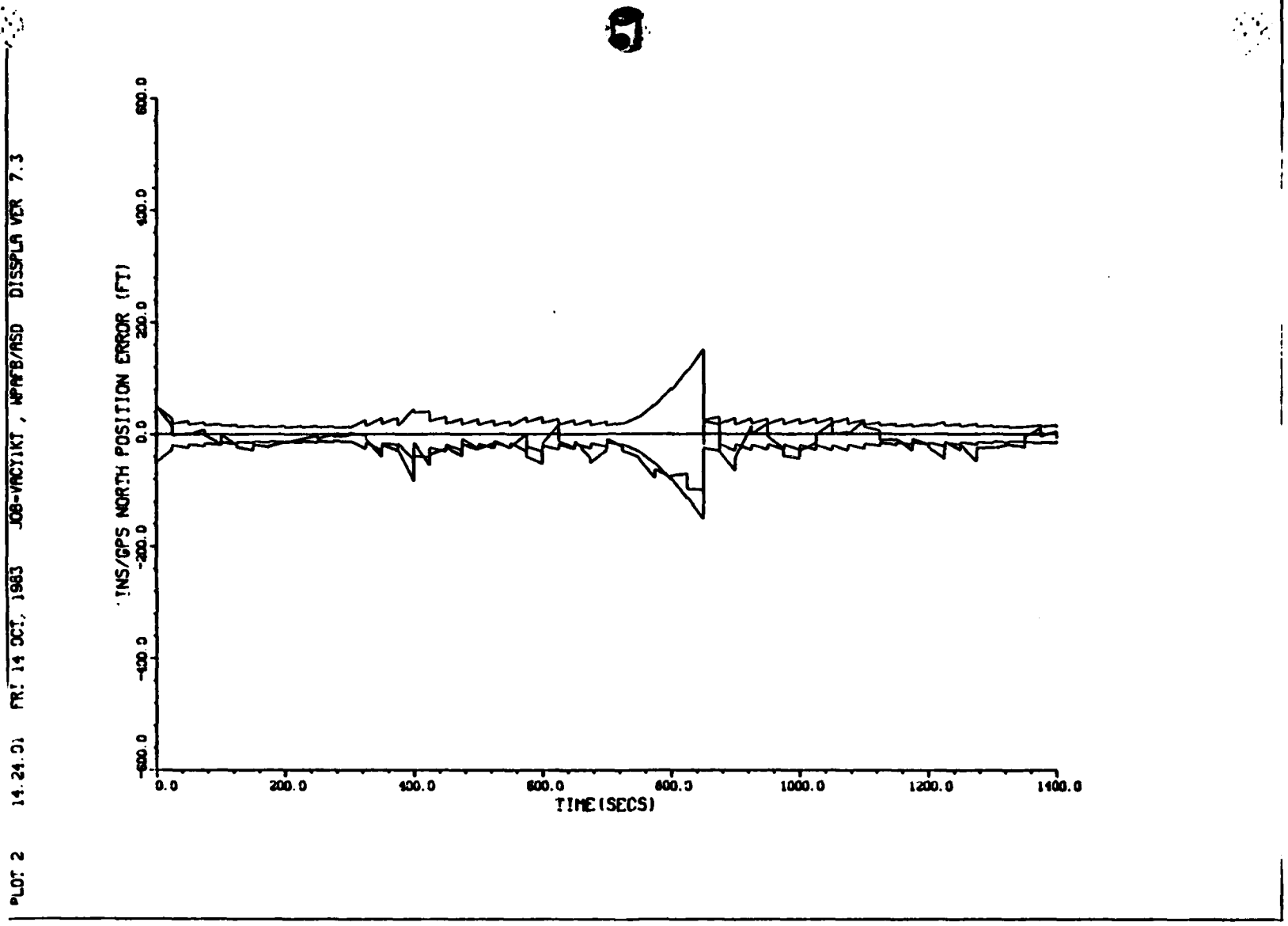

Figure 19b. Mission # 2: GDOP; North Position Error

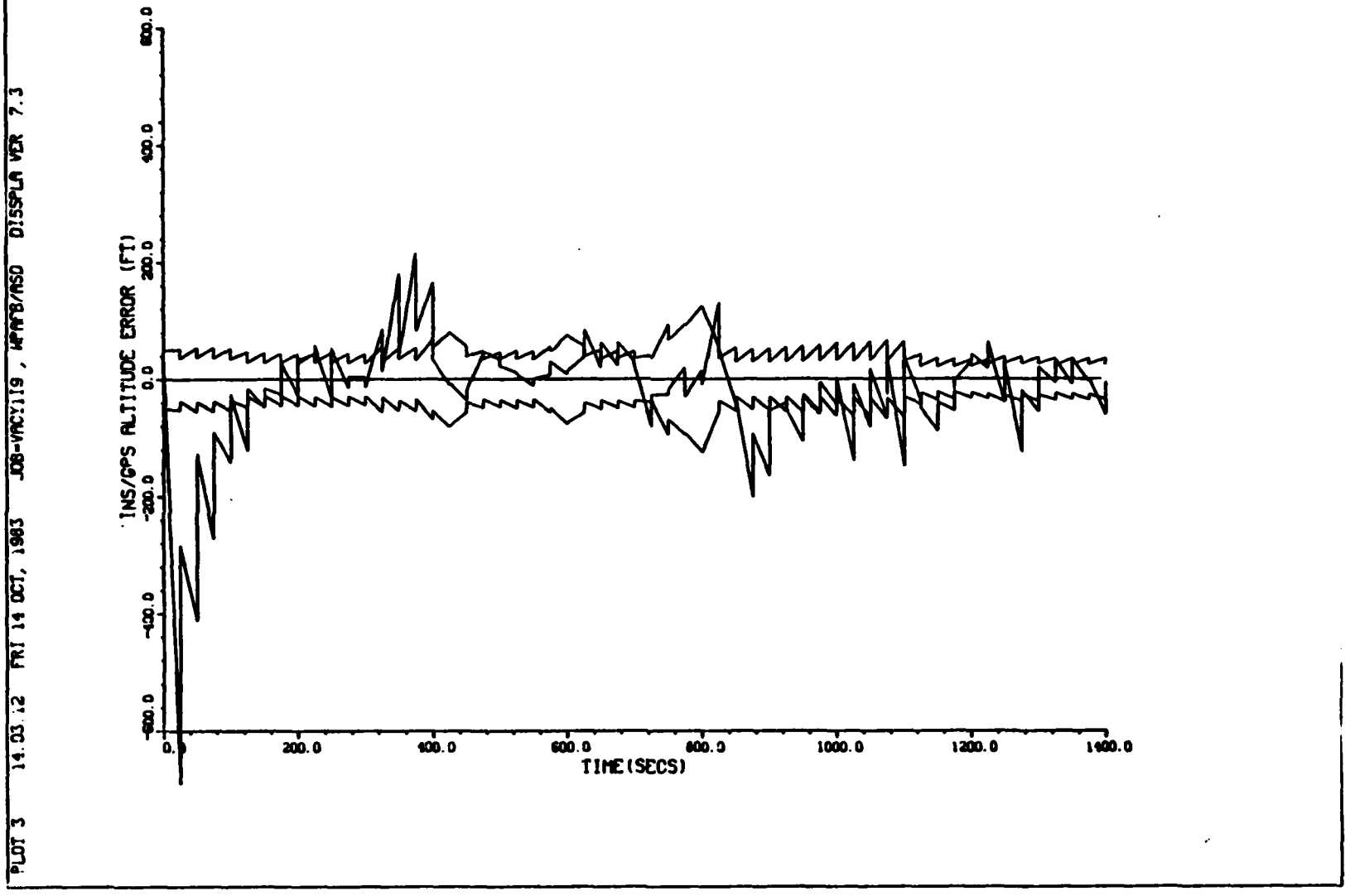

Figure 20a. Mission # 2: Cost Criterion; Altitude Error

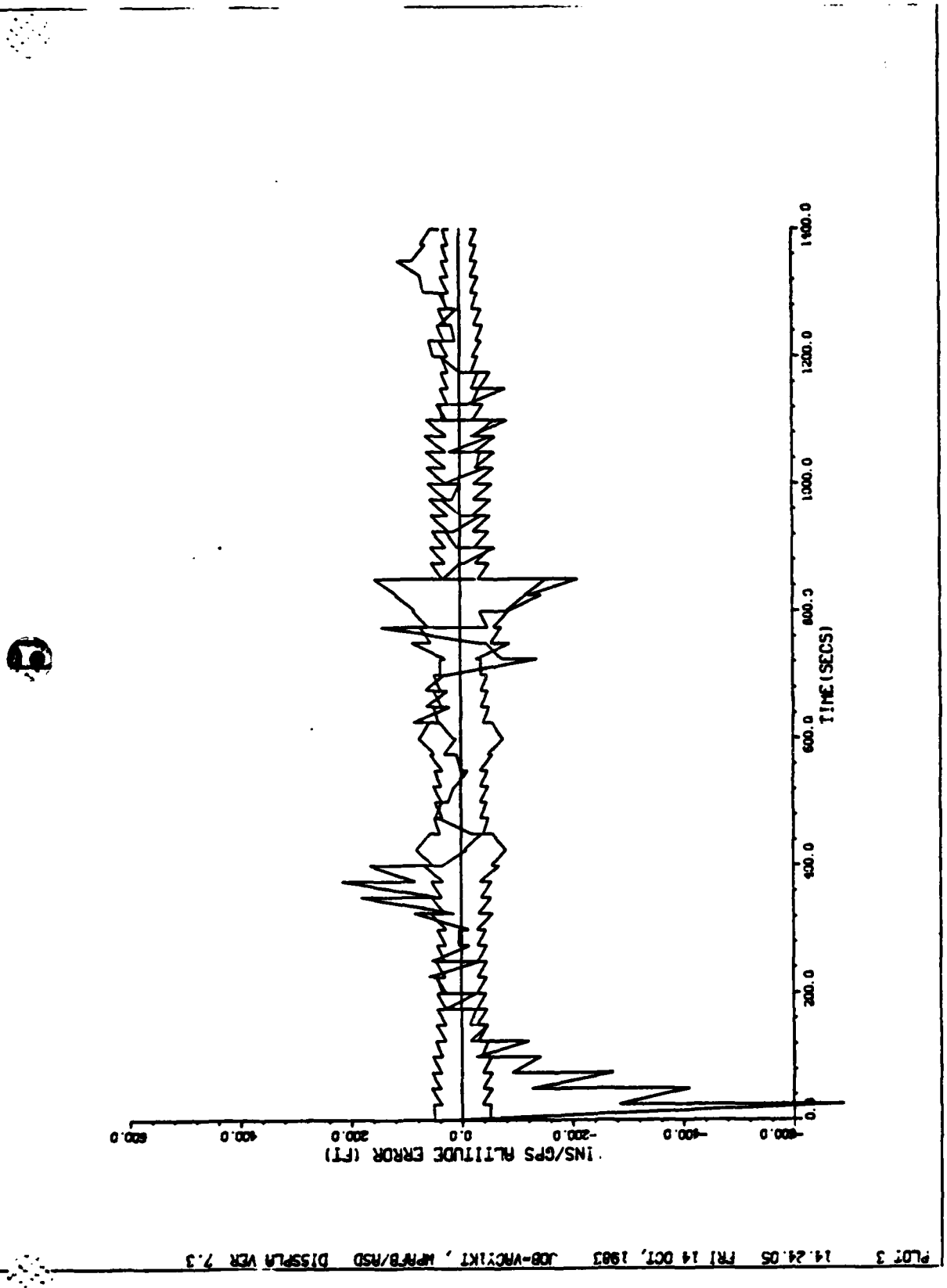

Figure 20b. Mission # 2: GDOP; Altitude Error

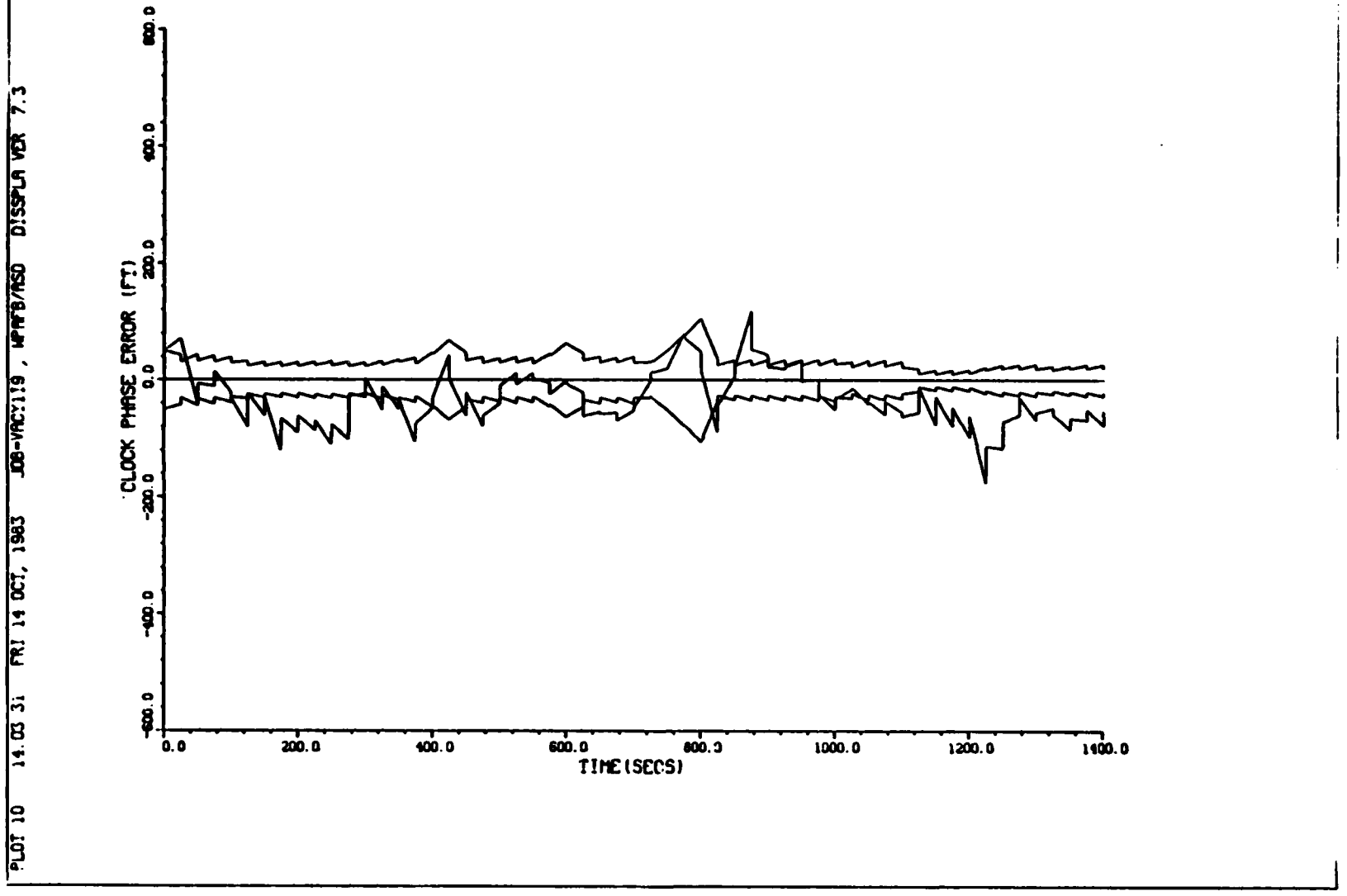

Figure 21a. Mission # 2: Cost Criterion; Clock Phase Error

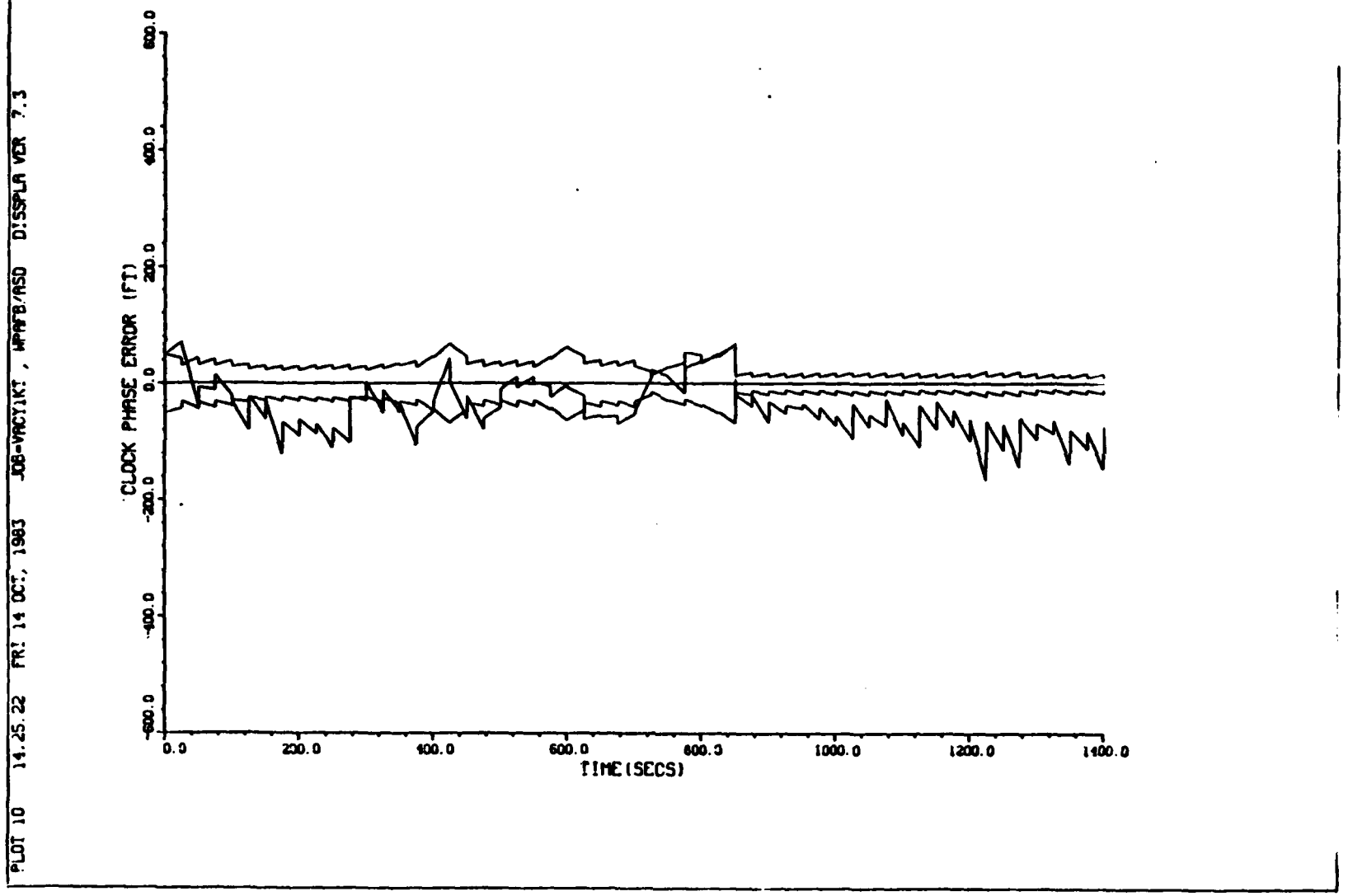

Figure 21b. Mission # 2: GDOP; Clock Phase Error

Mission # 3

The satellite selection using the cost criterion varied from the GDOP choice at 700 seconds and for the following 6 satellite selection times. Table VIIa and b shows the measurement errors for the cost criterion and GDOP satellite sets respectively.

The cost criterion chose a satellite set with a lower composite measurement error than the GDOP satellite set for every selection time except at 1300 seconds. The maximum noise density is -194.50dB at 747 seconds. Note the slow changes in the noise density from one satellite selection time to the next. Also, the measurement error estimates for the four satellite sets are roughly equivalent (i.e., $R_{meas}(1) \approx R_{meas}(2) \approx R_{meas}(3) \approx R_{meas}(4)$. This effect would make the $\underline{R}$ matrix approximately a scalar multiple of the identity matrix. As stated in Chapter III for noise weighted GDOP, if the $\underline{R}$ matrix is the identity matrix or a scalar multiple of the identity matrix then the satellite selection criterion is the same as GDOP values but increased by the scalar multiple. Applying this effect to the cost criterion means that there is a trade-off between the GDOP effect and the filter covariance's need for information in a particular direction. Since the satellite set chosen by the cost interior differs from the GDOP selection, the cause can be attributed to the filter covariance terms outweighing the GDOP terms.

Figures 22-25 present the time history performance of position and clock phase errors for this mission. The

TABLE VIIa

Mission 3 Statistics
(Cost Only)

700	800	900	1000	1100	1200	1300	SECONDS
15.15	14.79	14.89	15.17	15.15	15.15	15.12	R_{meas} (1)
14.99	15.07	15.00	15.05	15.01	15.03	14.99	R_{meas} (2)
14.11	14.79	14.69	14.57	14.38	14.15	14.29	R_{meas} (3)
17.53	19.03	17.23	15.17	15.09	15.17	17.56	R_{meas} (4)
-201.42	-200.63	-201.35	-200.83	-201.25	-201.15	-201.55	NOISE DENSITY

TABLE VIIb

Mission 3 Statistics
(GDOP Only)

700	800	900	1000	1100	1200	1300	SECONDS
15.15	14.79	14.89	15.11	15.12	15.09	14.93	R_{meas} (1)
15.18	15.17	15.06	14.97	14.66	14.86	15.13	R_{meas} (2)
14.11	14.79	15.00	15.05	15.01	15.03	14.99	R_{meas} (3)
17.53	19.03	17.23	15.17	15.09	15.17	17.56	R_{meas} (4)
-201.42	-200.63	-201.35	-200.83	-201.25	-201.15	-201.55	NOISE DENSITY

NOTE: (1) "***" indicates that the C/N_o level for this satellite is below tracking limits, therefore $R_{meas} = 1.0 \times 10^8$ feet.
(2) "x" indicates that GDOP and cost criterion satellite sets agreed during this time period.
(3) All R_{meas} values are expressed in feet.

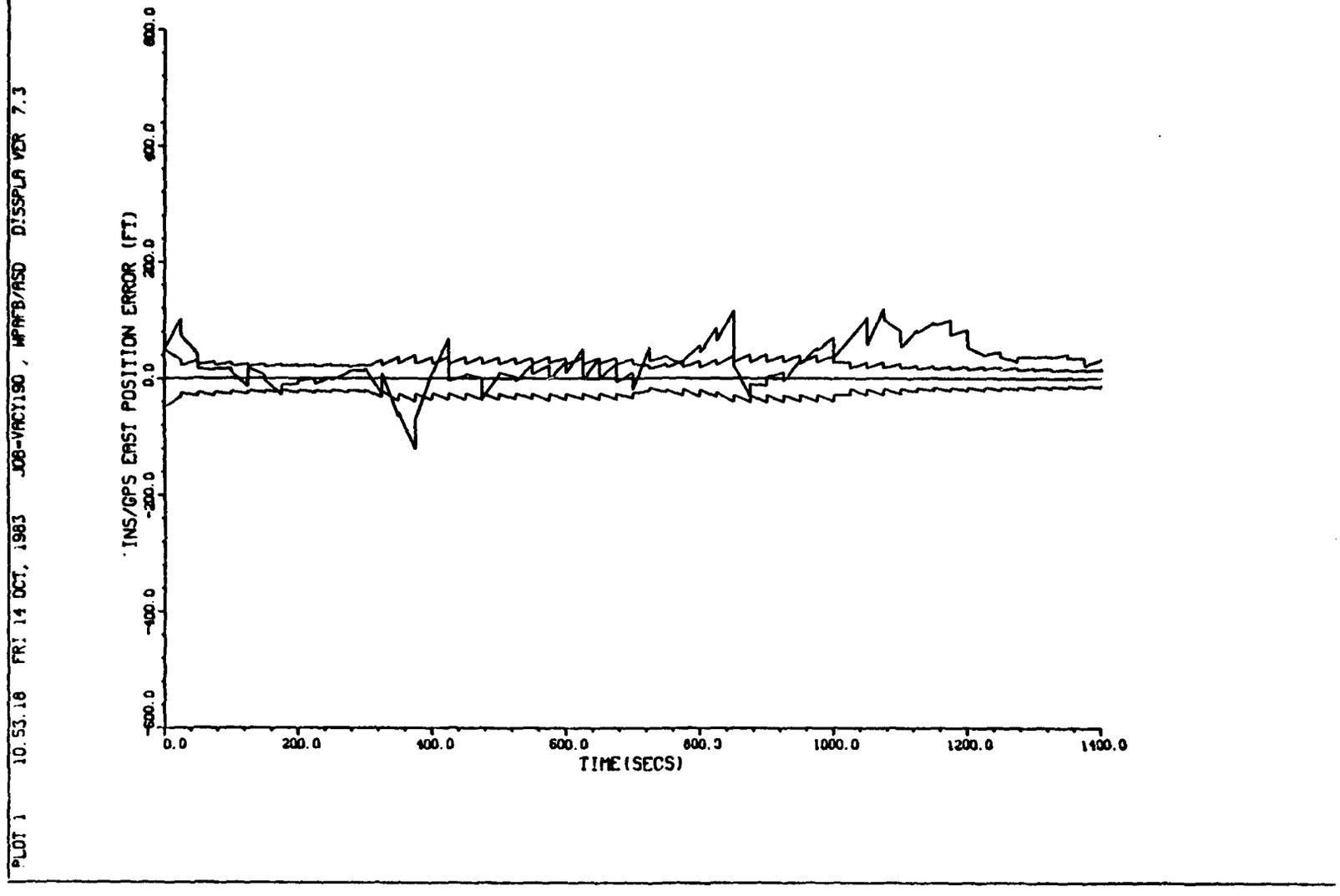

Figure 22a. Mission # 3: Cost Criterion; East Position Error

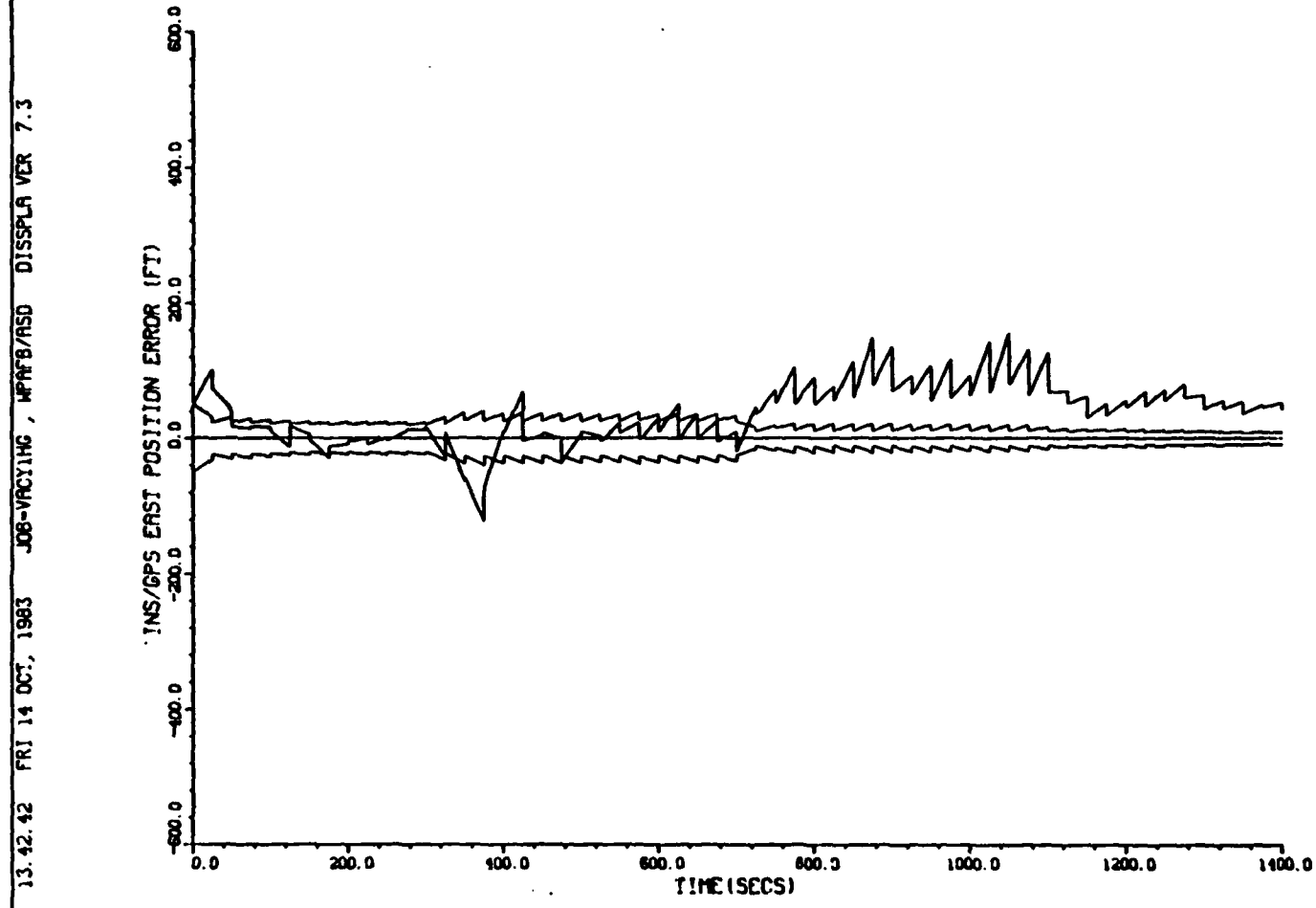

Figure 22b. Mission # 3: GDOP; East Position Error

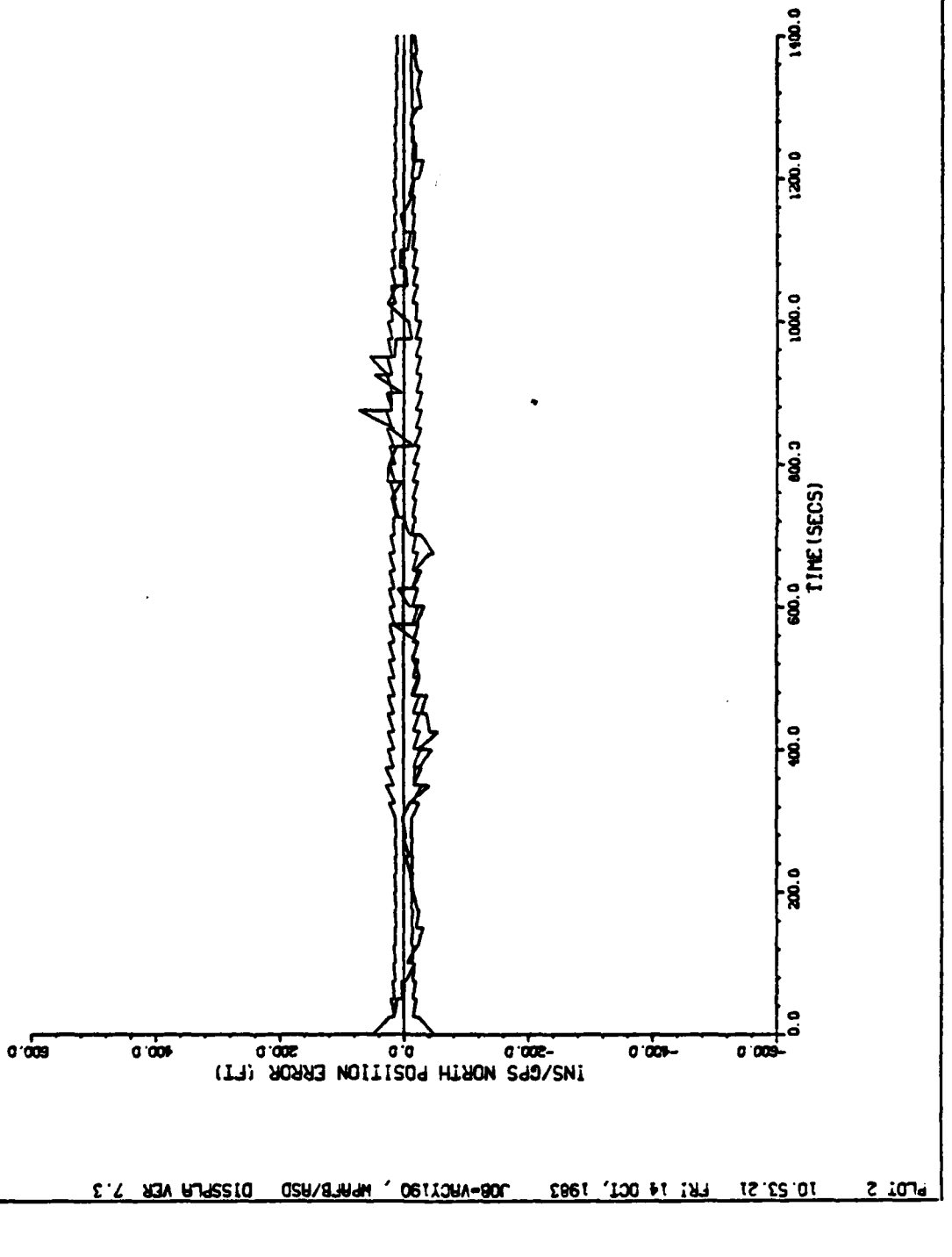

Figure 23a. Mission # 3: Cost Criterion; North Position Error

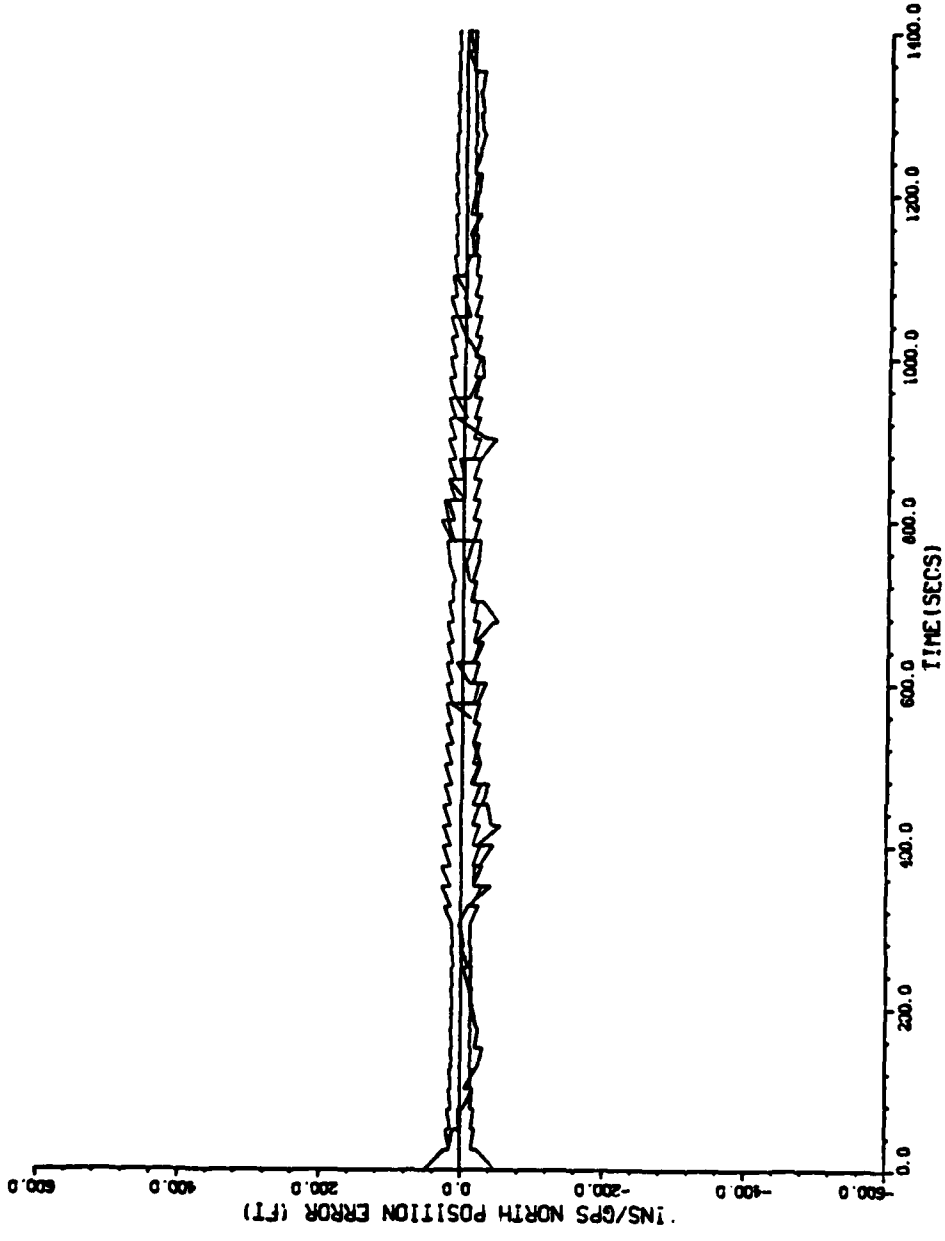

Figure 23b. Mission # 3: GDOP; North Position Error

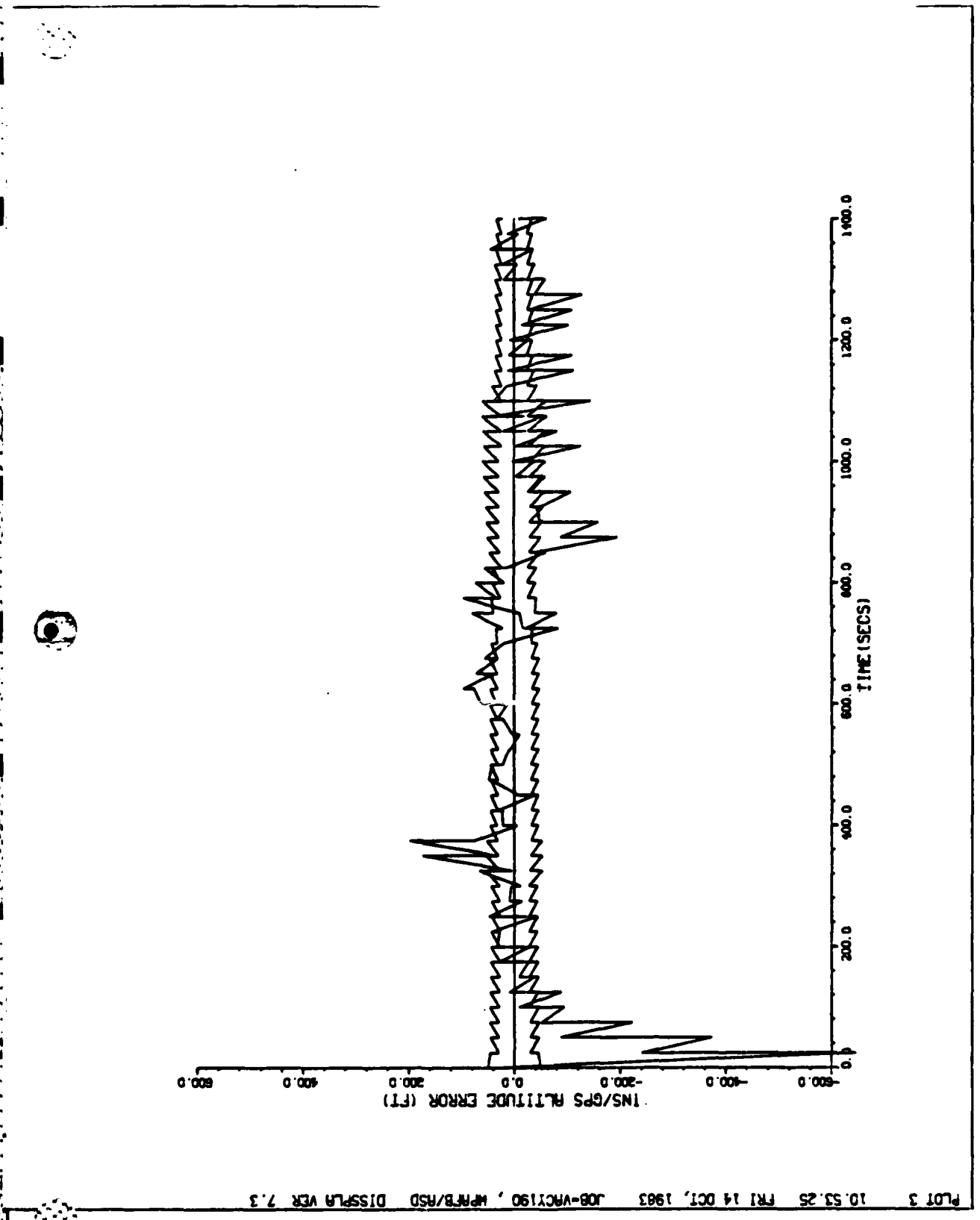

Figure 24a. Mission # 3: Cost Criterion; Altitude Error

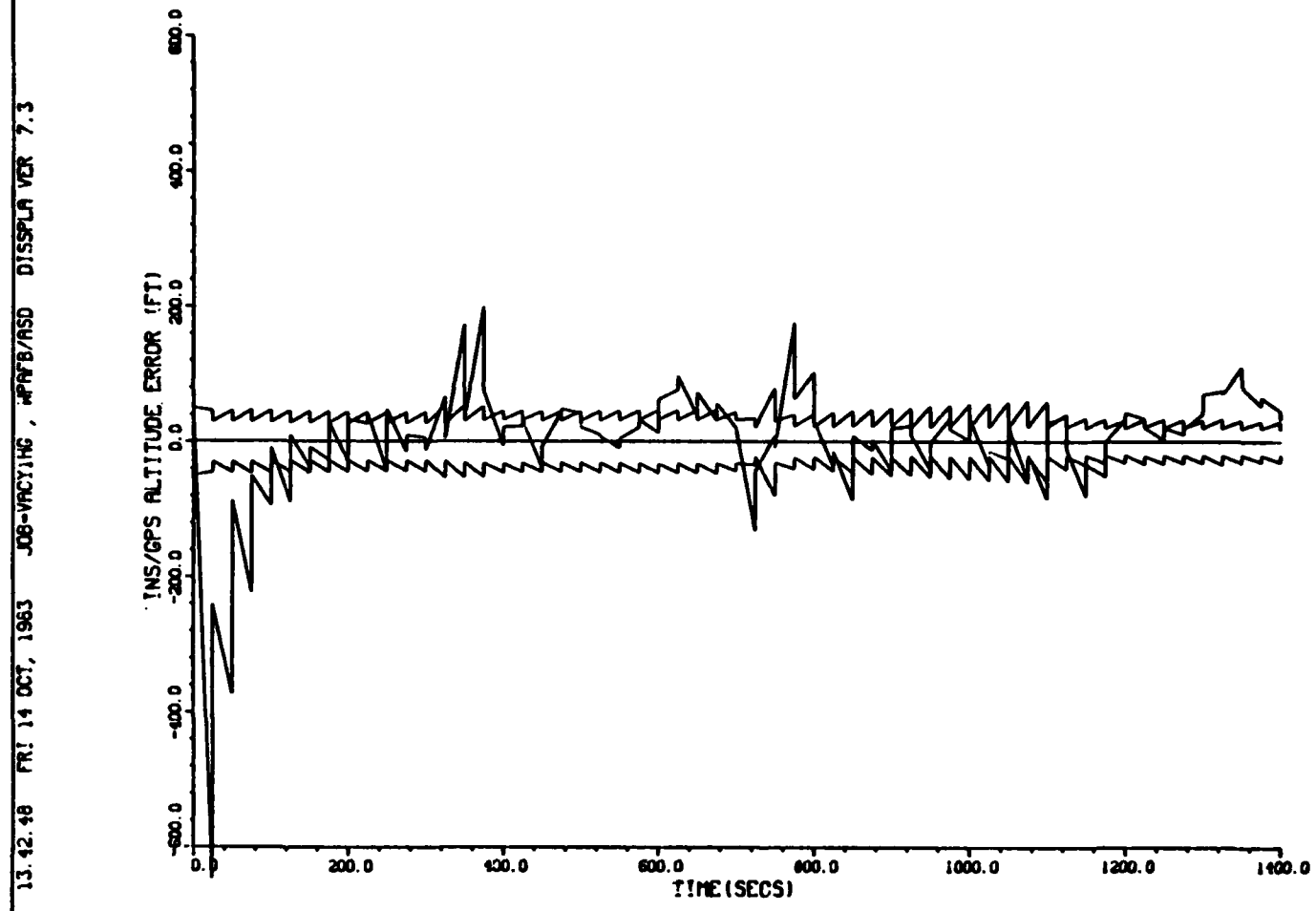

Figure 24b. Mission # 3: GDOP; Altitude Error

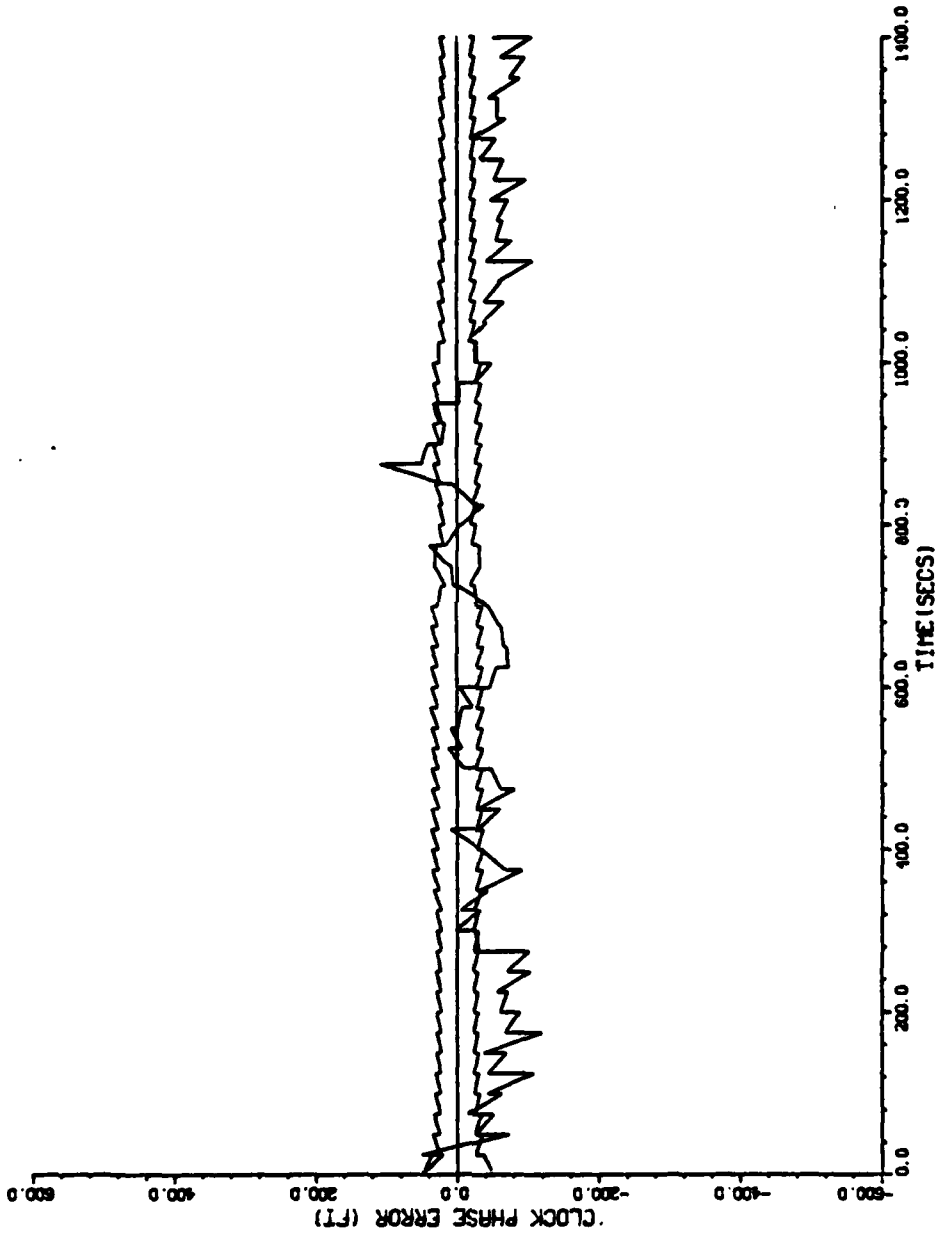

Figure 25a. Mission # 3: Cost Criterion; Clock Phase Error

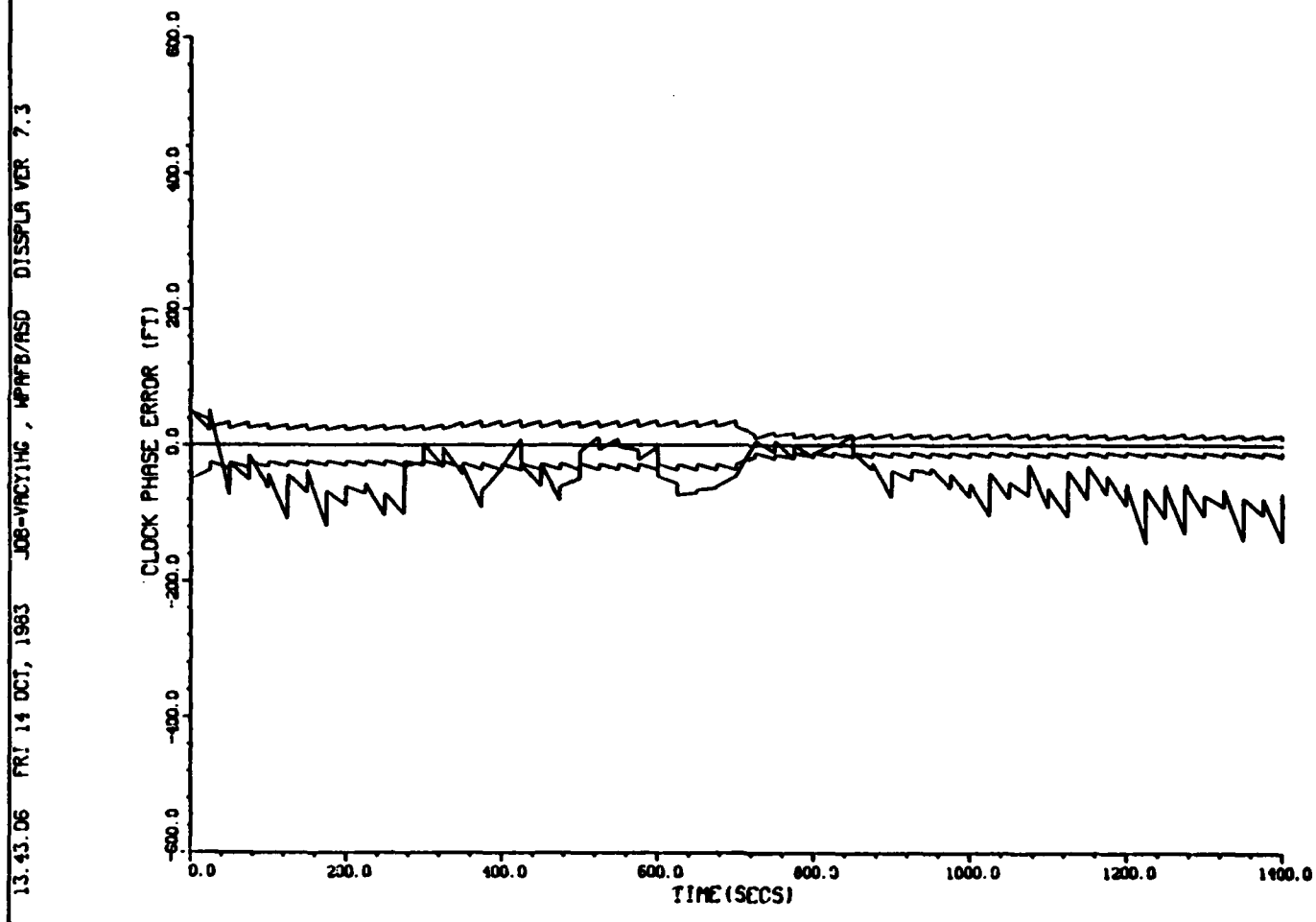

Figure 25b. Mission # 3: GDOP; Clock Phase Error

figures show a small improvement in performance for the cost criterion over the GDOP case. The composite statistics for the filter estimation radial position errors averaged over the 700-1300 second interval are:

Cost Criterion		versus	GDOP
Mean	Std. Dev.	Mean	Std. Dev.
74.88	42.23	85.03	37.95

Including the time-bias range errors:

Mean	Std. Dev.	Mean	Std. Dev.
89.49	40.33	107.07	37.96

where all units are in feet. The cost criterion shows a small performance improvement over GDOP, but the larger standard deviation of the cost criterion would reduce the significance of the difference in mean values.

Mission # 4

As in Mission # 3, the satellite set chosen using the cost criterion varied from the GDOP choice from 700 seconds to 1300 seconds in the mission. The maximum noise density is -172.40db at 740 seconds into the mission. Table VIIIa and b shows the measurement errors for the cost criterion and GDOP satellite sets respectively. The cost criterion chose a satellite set with larger composite measurement error than the GDOP satellite set at the 800 and 900 second selection times. This choice may be a result of the rapid change in the noise density and encountering the maximum noise density unexpectedly (i.e., without some significant build-up in noise density at 700 seconds).

TABLE VIIIa

Mission 4 Statistics
(Cost Only)

700	800	900	1000	1100	1200	1300	SECONDS
14.65	23.94	24.94	18.13	15.11	15.21	15.16	R_{meas} (1)
15.21	***	***	18.99	14.68	14.37	14.07	R_{meas} (2)
15.20	30.98	24.10	16.71	14.79	14.50	14.24	R_{meas} (3)
15.10	***	***	***	15.09	15.20	15.08	R_{meas} (4)
-197.40	-179.68	-184.11	-191.45	-195.62	-199.08	-200.85	NOISE DENSITY

TABLE VIIIb

Mission 4 Statistics
(GDOP Only)

700	800	900	1000	1100	1200	1300	SECONDS
15.29	24.67	18.48	20.17	15.31	15.19	15.19	R_{meas} (1)
16.07	34.94	24.94	17.53	16.17	15.11	15.17	R_{meas} (2)
15.20	30.98	***	18.99	14.68	14.37	14.07	R_{meas} (3)
15.10	***	***	***	15.09	15.20	15.08	R_{meas} (4)
-197.40	-179.68	-184.11	-191.45	-195.62	-199.08	-200.85	NOISE DENSITY

NOTE: (1) "***" indicates that the C/N_o level for this satellite is below tracking limits, therefore $R_{meas} = 1.0 \times 10^8$ feet.
(2) "x" indicates that GDOP and cost criterion satellite sets agreed during this time period.

Figures 26-29 present the time history performance of the position and clock phase errors for this mission. The figures show that the performance is roughly comparable between the cost criterion and GDOP. The cost criterion filter covariance reaction to the increased noise density from 700-960 seconds probably accounts for the roughly equivalent performance errors with respect to GDOP, even though a noisier measurement set is chosen at 800 and 900 seconds. The filter covariance reaction to increasing or decreasing noise density can be viewed as the way the cost criterion keeps track of the time history of the noise density. For instance, small a priori filter covariance values with large measurement errors would indicate entry into the jamming field. When both a priori filter covariance values and measurement errors are large the user is operating within the jamming field. When the a priori filter covariances values are large and the measurement errors are small the user is leaving the jamming field. How effectively the cost criterion uses the jamming information seems to be dependent on the rate of change of the noise density. The slower the variation in noise density the more significant the improvement in performance for the cost criterion with respect to GDOP.

The composite statistics for the filter estimation position errors for the 700-1300 second interval are:

Cost Criterion		versus	GDOP	
Mean	Std. Dev.		Mean	Std. Dev.
120.31	81.14		123.64	109.12

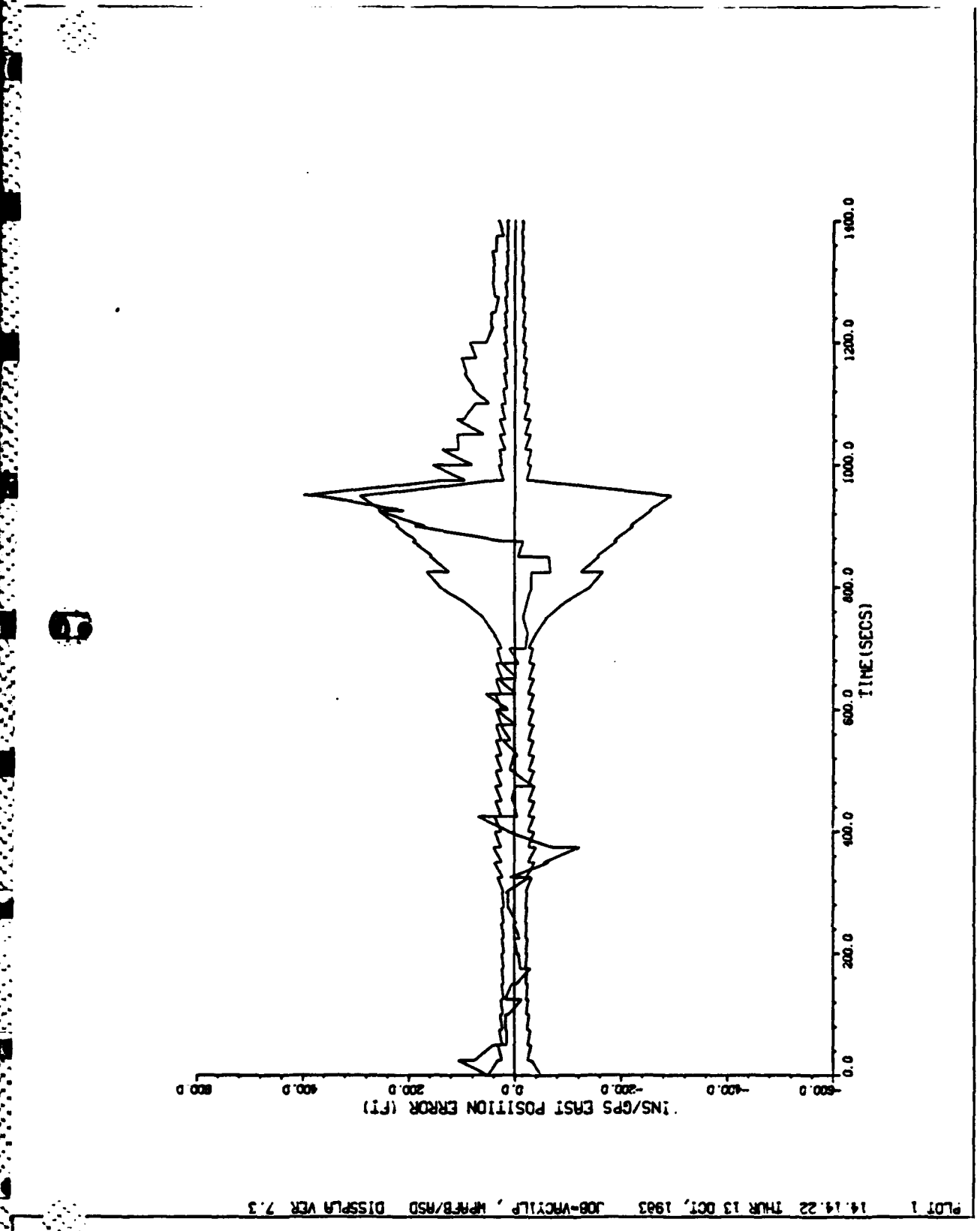

Figure 26a. Mission # 4: Cost Criterion; East Position Error

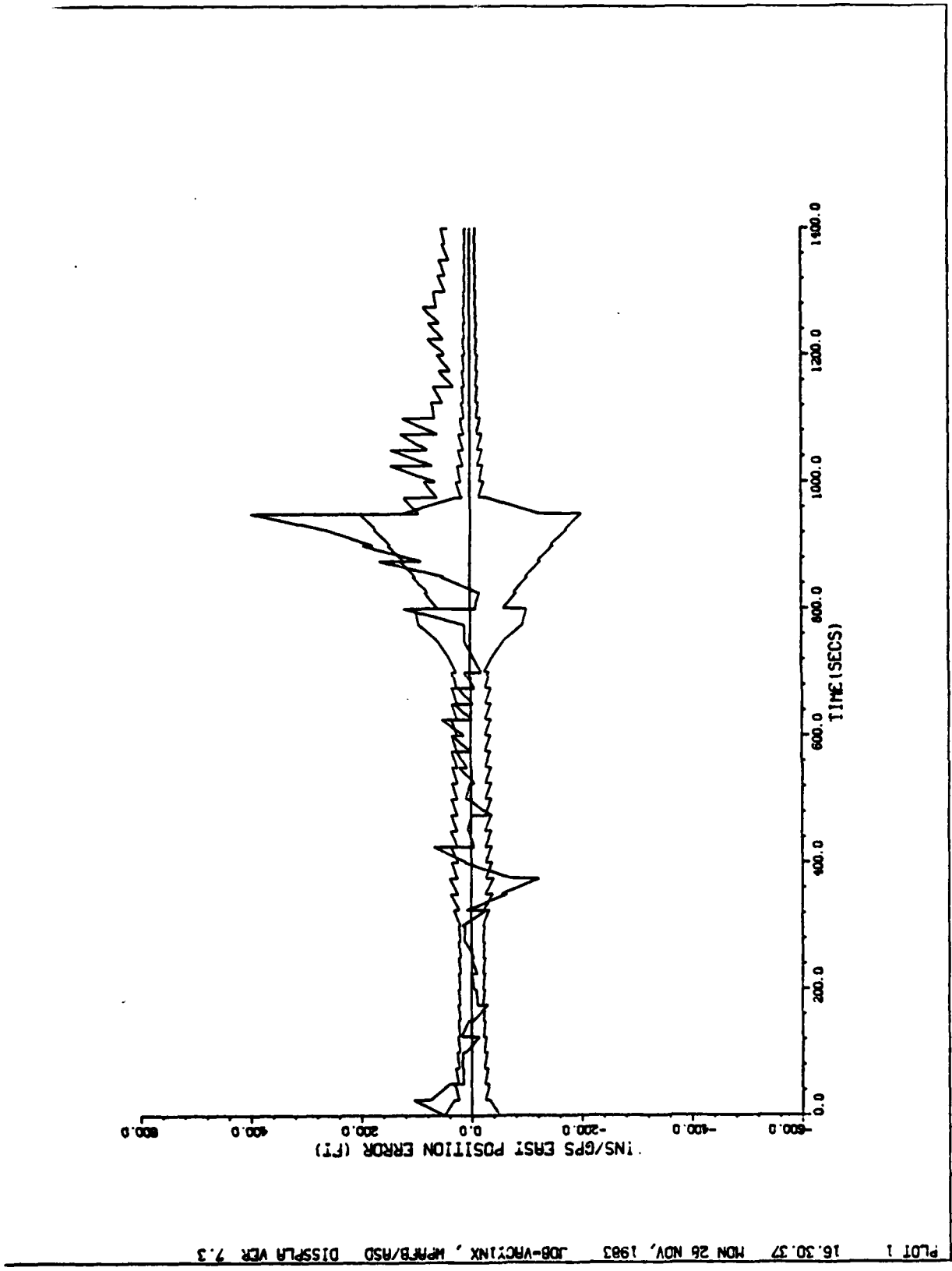

Figure 26b. Mission # 4: GDOP; East Position Error

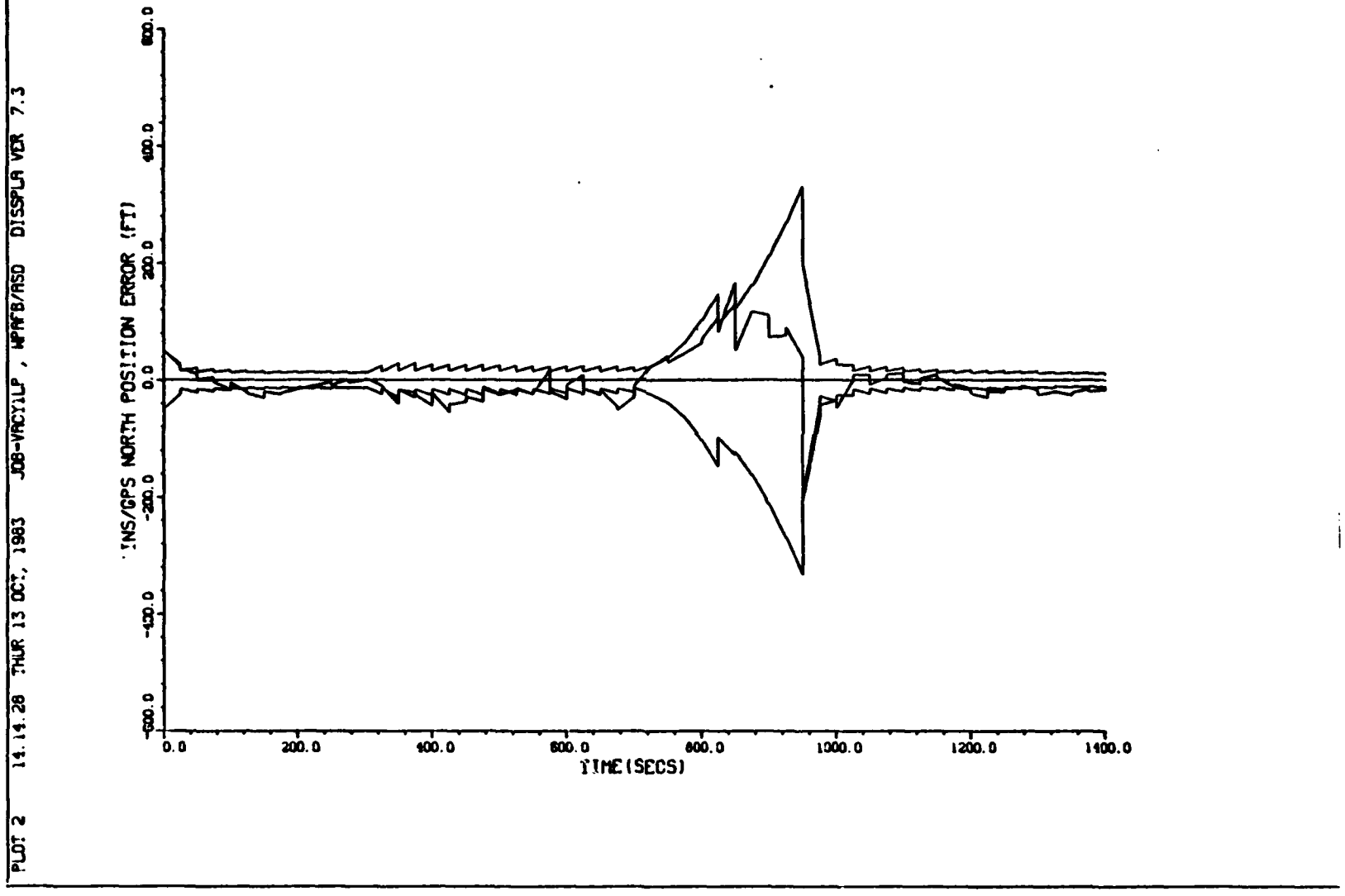

Figure 27a. Mission # 4: Cost Criterion; North Position Error

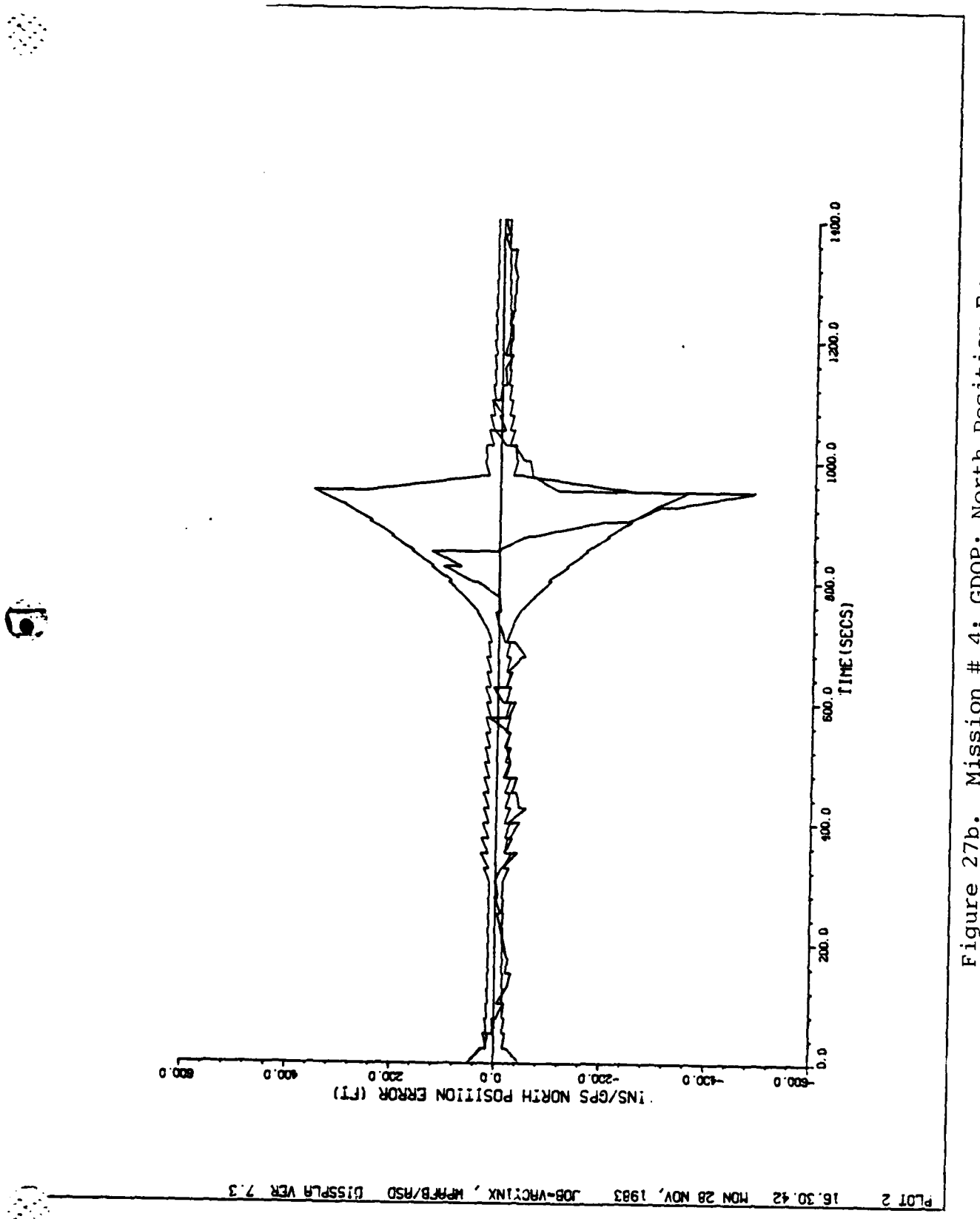

Figure 27b. Mission # 4: GDOP; North Position Error

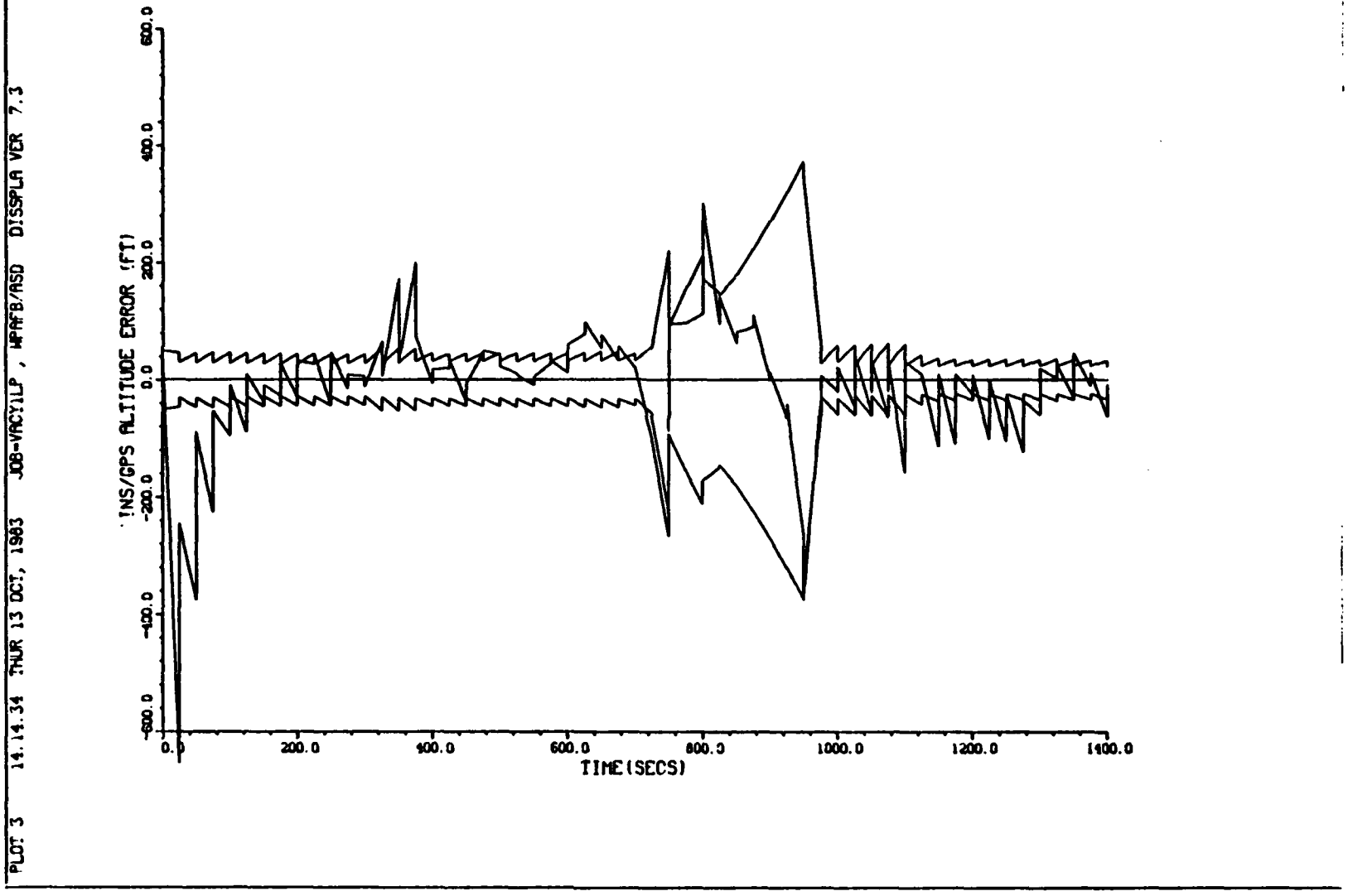

Figure 28a. Mission # 4: Cost Criterion; Altitude Error

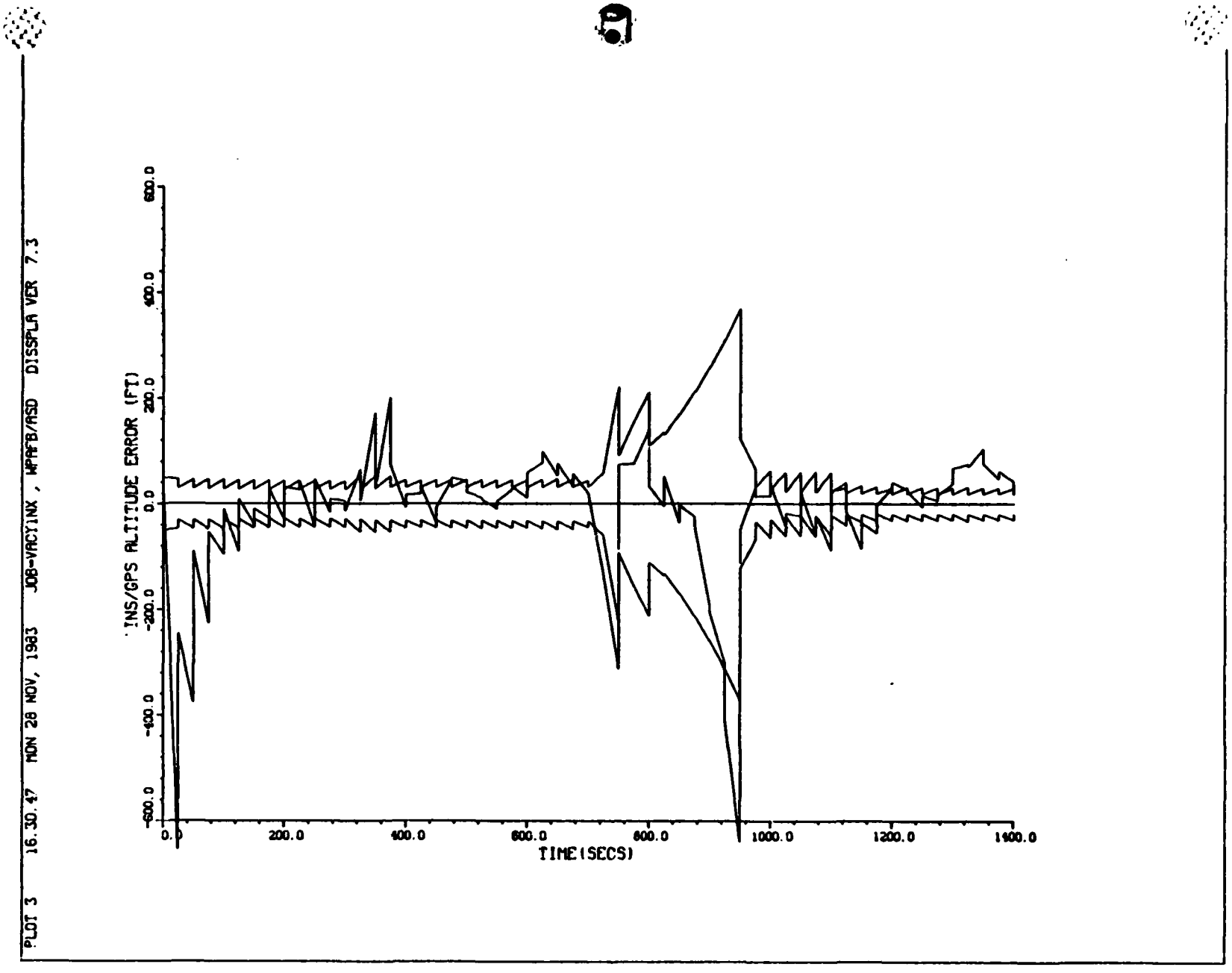

Figure 28b. Mission # 4: GDOP; Altitude Error

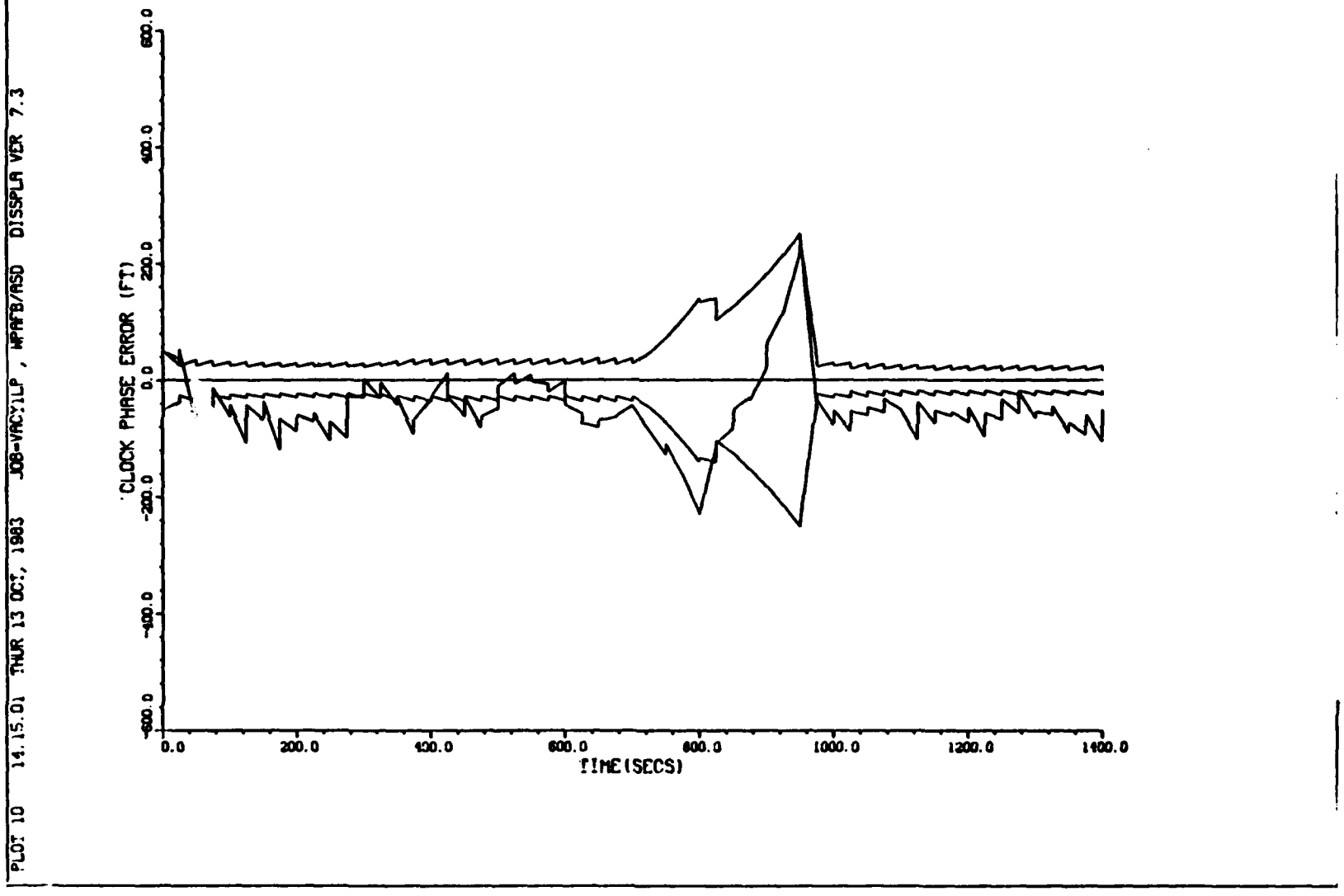

Figure 29a. Mission # 4: Cost Criterion; Clock Phase Error

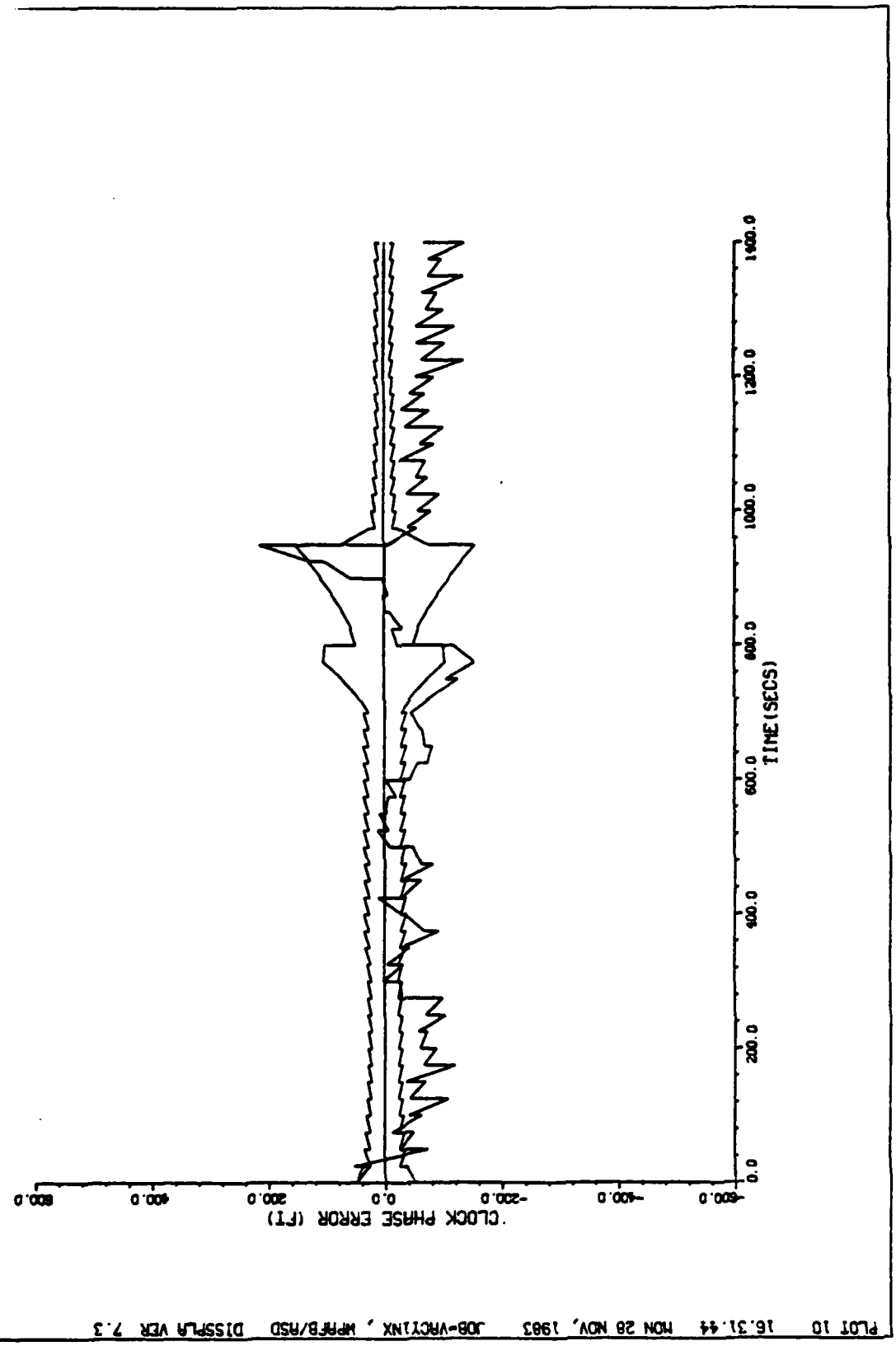

Figure 29b. Mission # 4: GDOP; Clock Phase Error

Including the time-bias range errors:

Mean	Std. Dev.	Mean	Std. Dev.
164.38	86.74	146.05	98.76

where all units are in feet. In Missions 1-3 the time-bias range errors were roughly equal for both the cost criterion and GDOP, or they did not significantly affect the performance comparison. In this mission the time-bias range errors change the performance assessment significantly. The large time bias range errors for the cost criterion can be explained by the $(\underline{H}^T\underline{R}^{-1}\underline{H})$ term in the cost criterion. When a satellite set with poor time-bias related geometry has a composite measurement error much smaller than a more favorable time-bias geometry, the first set will be selected. Adding the filter covariance terms into the selection process further increases the desire to select the poor time-bias related geometry. This last effect is due to the fact that under the influence of increased noise density, the filter covariance position terms reflect much larger errors than does the filter covariance clock phase error. The direct result in the cost criterion is a need for information for position errors that significantly outweigh the clock phase errors.

Mission # 5

The satellite set chosen using the cost criterion varied from the GDOP choice during 700-1000 seconds and 1100-1300 seconds in the mission. The maximum noise density was -163.60db at 780 seconds in the flight. The satellite

set's measurement errors are presented in Table IXa and b. Note that at 80 seconds the GPS signal is jammed-off-the air and at 900 seconds only one satellite is being tracked for either the cost criterion or GDOP case. At 700,1100, 1200, and 1300 seconds the cost criterion has selected a satellite set with lower composite measurement error than the GDOP selected set. The encounter with the maximum noise density results in over a 30db increase in noise density from 700-800 seconds. Figures 30-33 plot the time history performance of the filter estimation position and clock phase errors. In all cases the GDOP performance is better than the cost criterion. The composite statistic of the 700-1300 second time interval are:

Cost Criterion		versus	GDOP
Mean	Std. Dev.	Mean	Std. Dev.
125.59	114.50	87.84	37.92

Including the time-bias range errors:

Mean	Std. Dev.	Mean	Std. Dev.
142.21	110.01	117.50	39.34

where all units are in feet. The performance degradation of the cost criterion with respect to GDOP is even more pronounced in this mission than in Mission # 4. The rapid variation in the noise density is also more pronounced than in Mission # 4. The time-bias range errors are not significant in performance assessment in this mission as they were in Mission # 4.

TABLE IXa

Mission 5 Statistics
(Cost Only)

700	800	900	1000	1100	1200	1300	SECONDS
14.08	***	***	x	15.75	15.20	15.19	R_{meas} (1)
14.94	***	***	x	14.91	14.45	14.15	R_{meas} (2)
14.98	***	35.10	x	14.99	14.57	14.32	R_{meas} (3)
15.15	***	***	x	15.65	15.21	15.12	R_{meas} (4)
-201.92	-169.06	-179.88	-186.99	-194.08	-198.58	-200.40	NOISE DENSITY

TABLE IXb

Mission 5 Statistics
(GDOP Only)

700	800	900	1000	1100	1200	1300	SECONDS
15.21	***	23.54	x	16.85	15.17	15.21	R_{meas} (1)
15.19	***	***	x	17.64	15.08	15.15	R_{meas} (2)
14.98	***	***	x	14.91	14.45	14.15	R_{meas} (3)
15.15	***	***	x	15.65	15.21	15.12	R_{meas} (4)
-201.92	-169.06	-179.88	-186.99	-194.08	-198.58	-200.40	NOISE DENSITY

NOTE: (1) "***" indicates that the C/N_o level for this satellite is below tracking limits, therefore $R_{meas} = 1.0 \times 10^8$ feet.
(2) "x" indicates that GDOP and cost criterion satellite sets agreed during this time period.
(3) All R_{meas} values are expressed in feet.

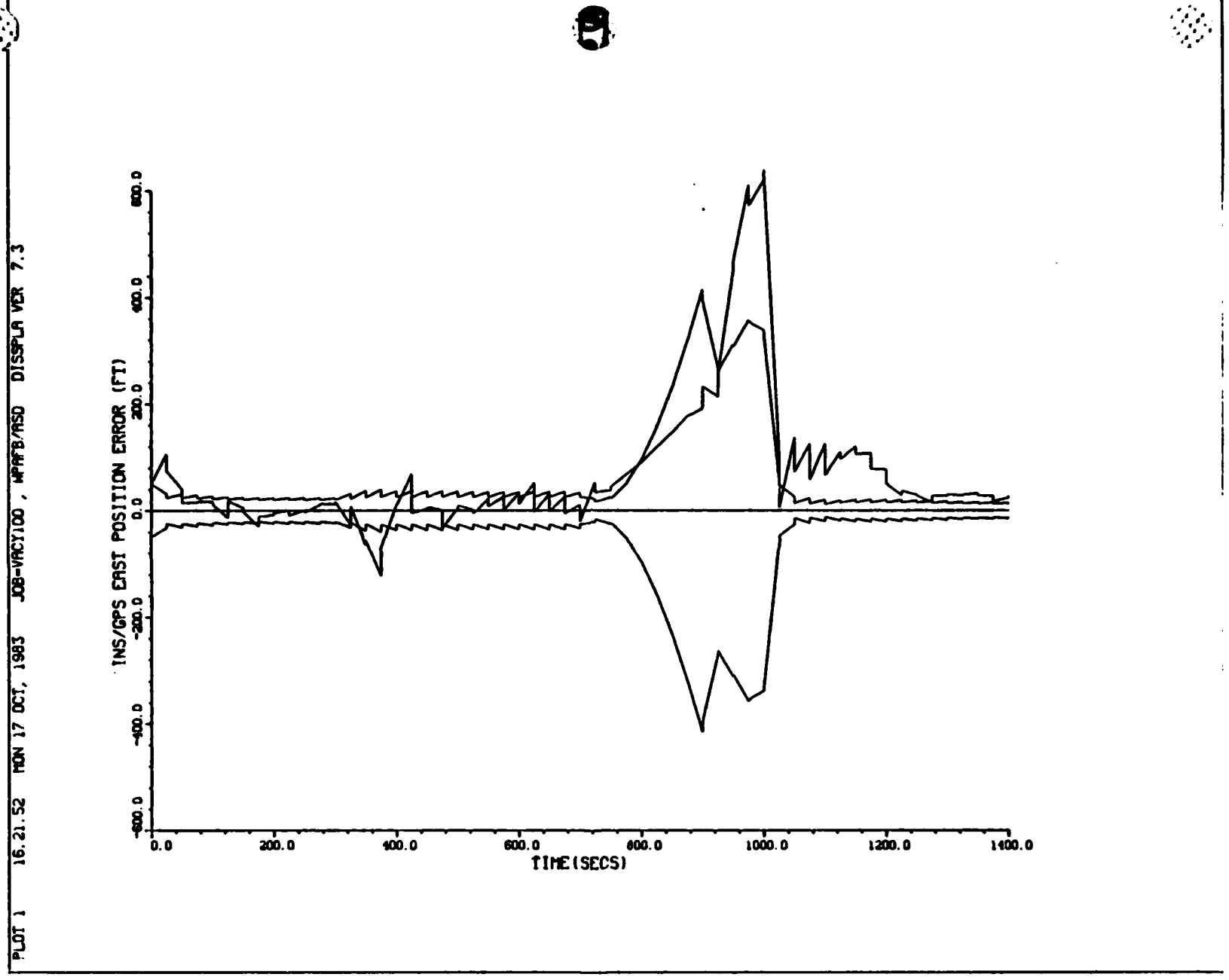

Figure 30a. Mission # 5: Cost Criterion; East Position Error

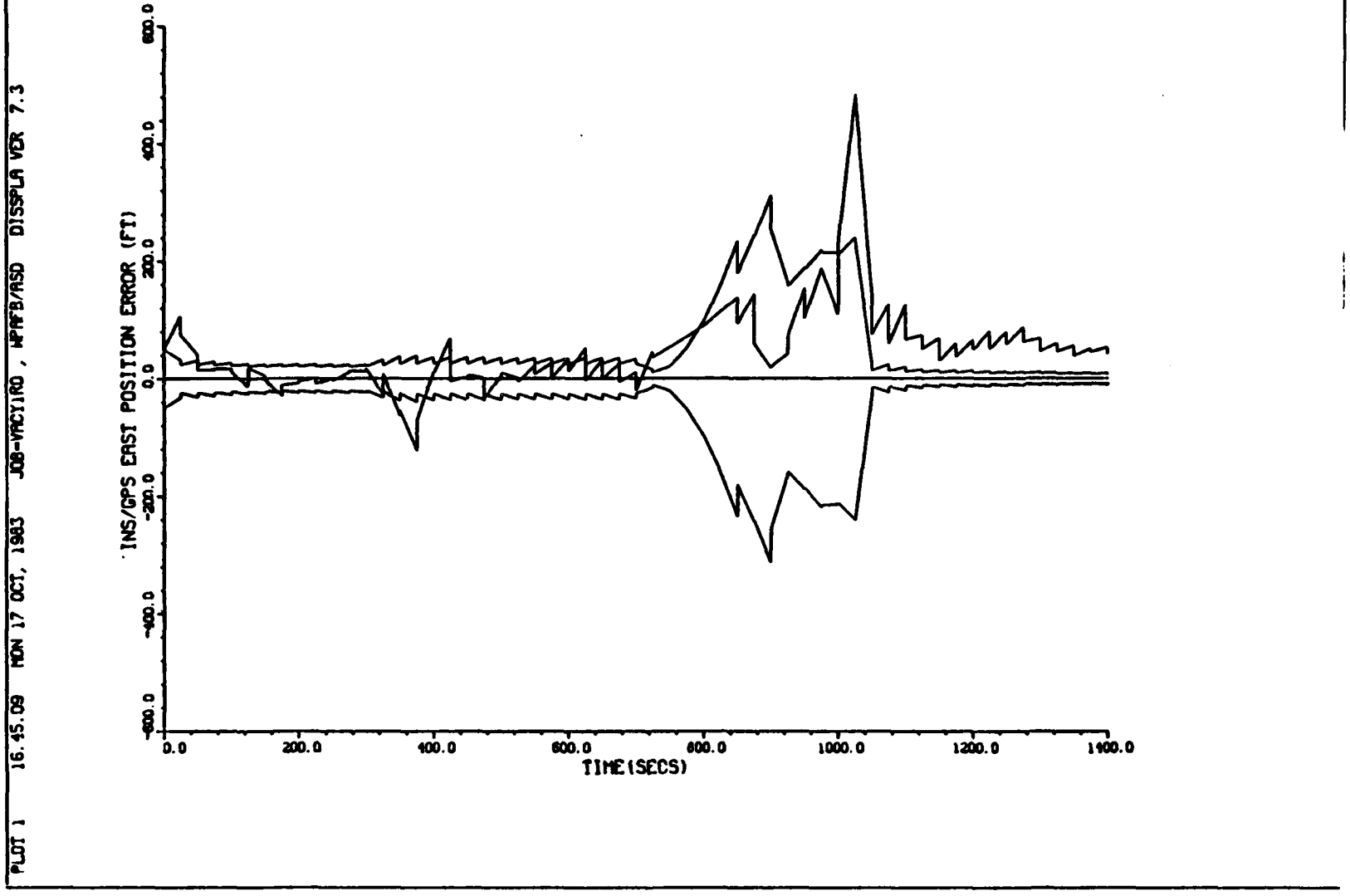

Figure 30b. Mission # 5: GDOP; East Position Error

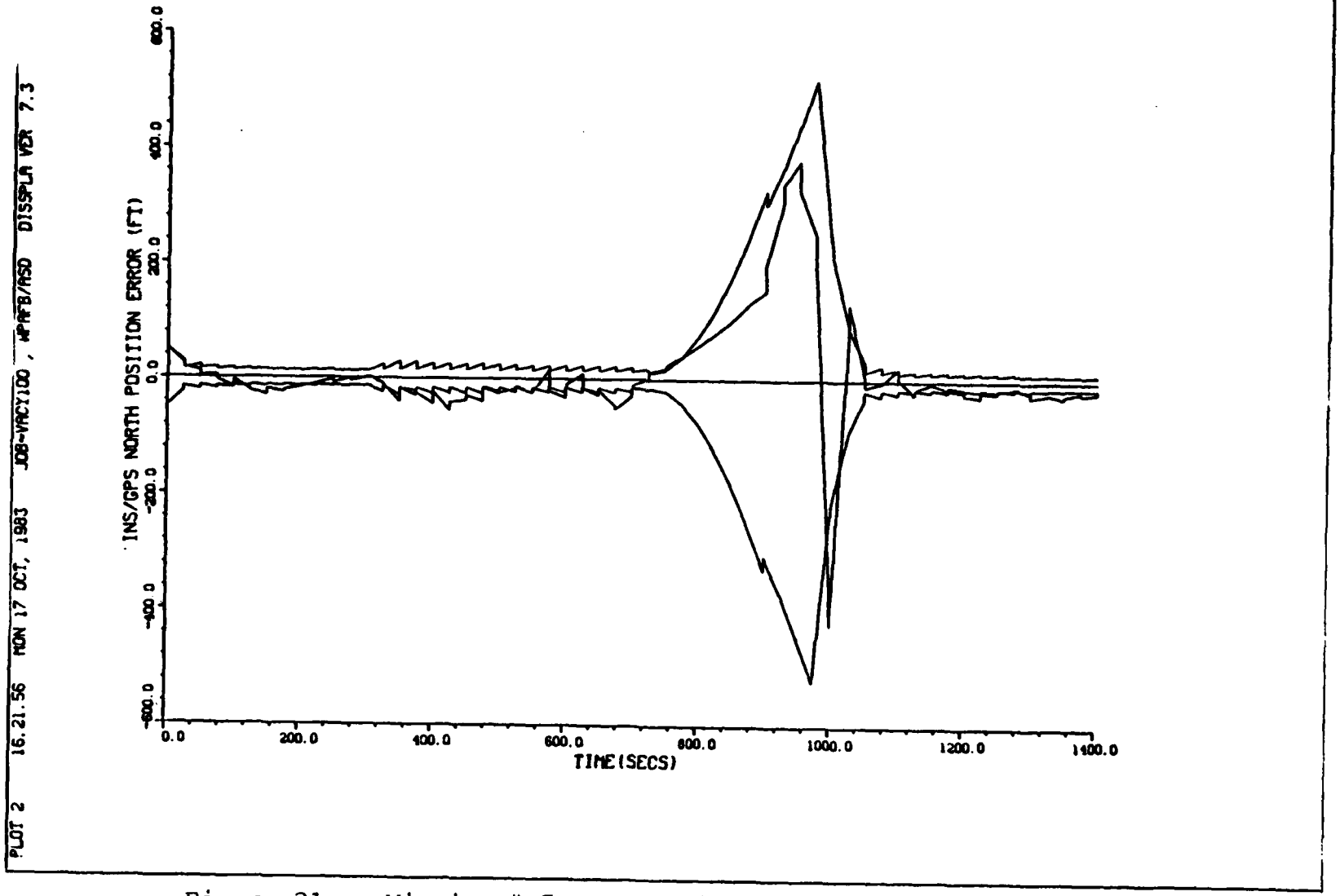

Figure 31a. Mission # 5: Cost Criterion; North Position Error

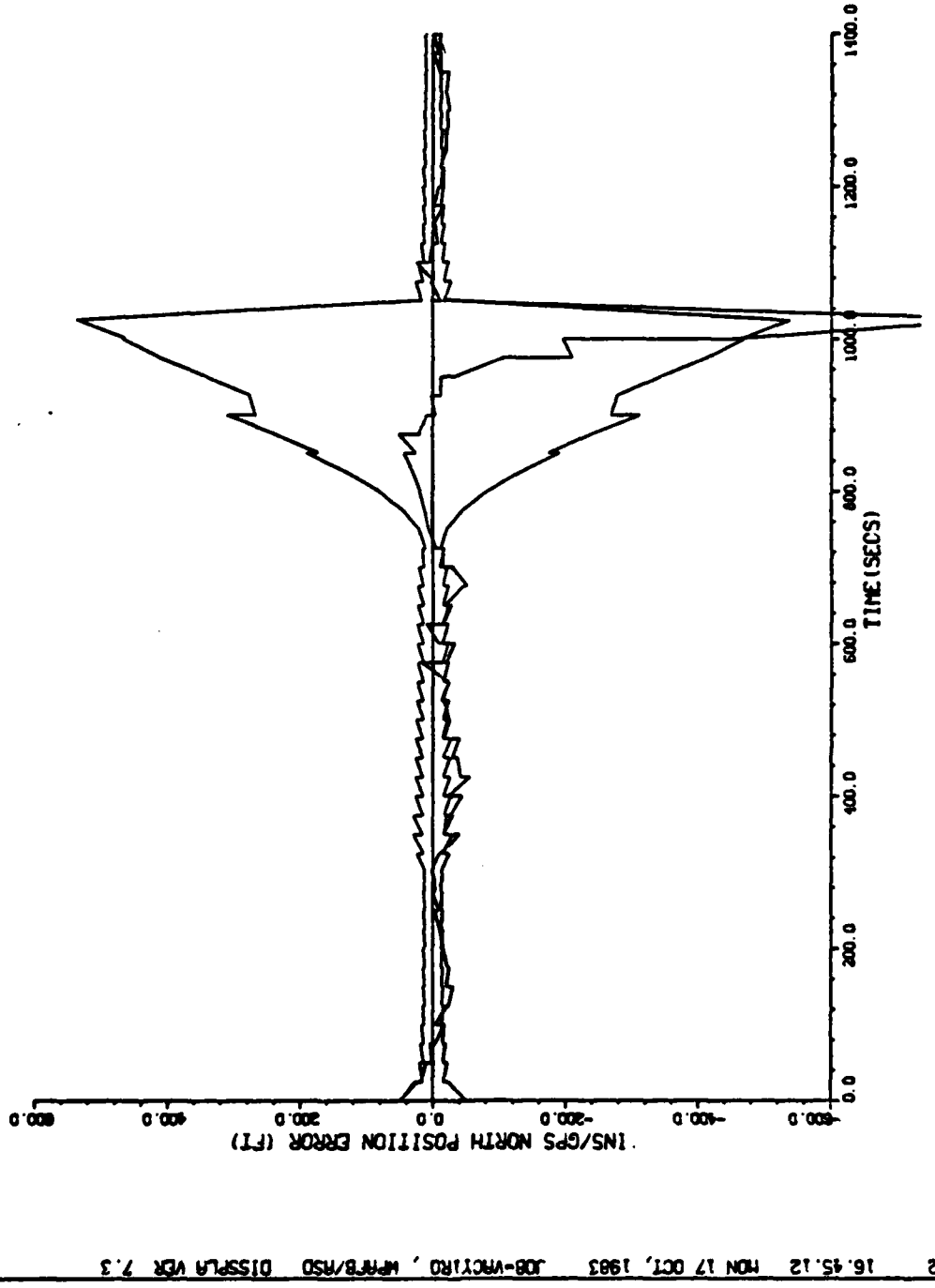

Figure 31b. Mission # 5: GDOP; North Position Error

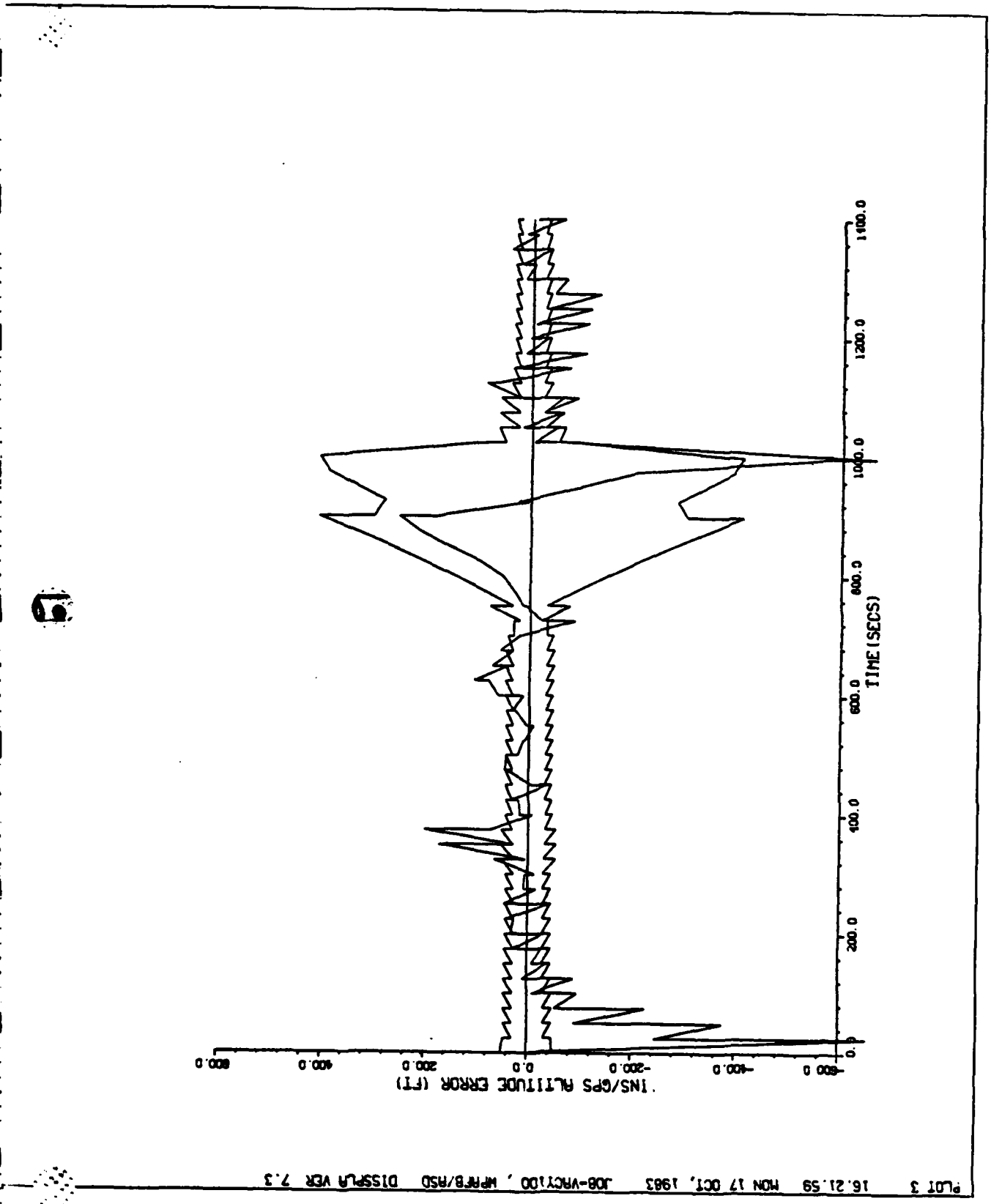

Figure 32a. Mission # 5: Cost Criterion; Altitude Error

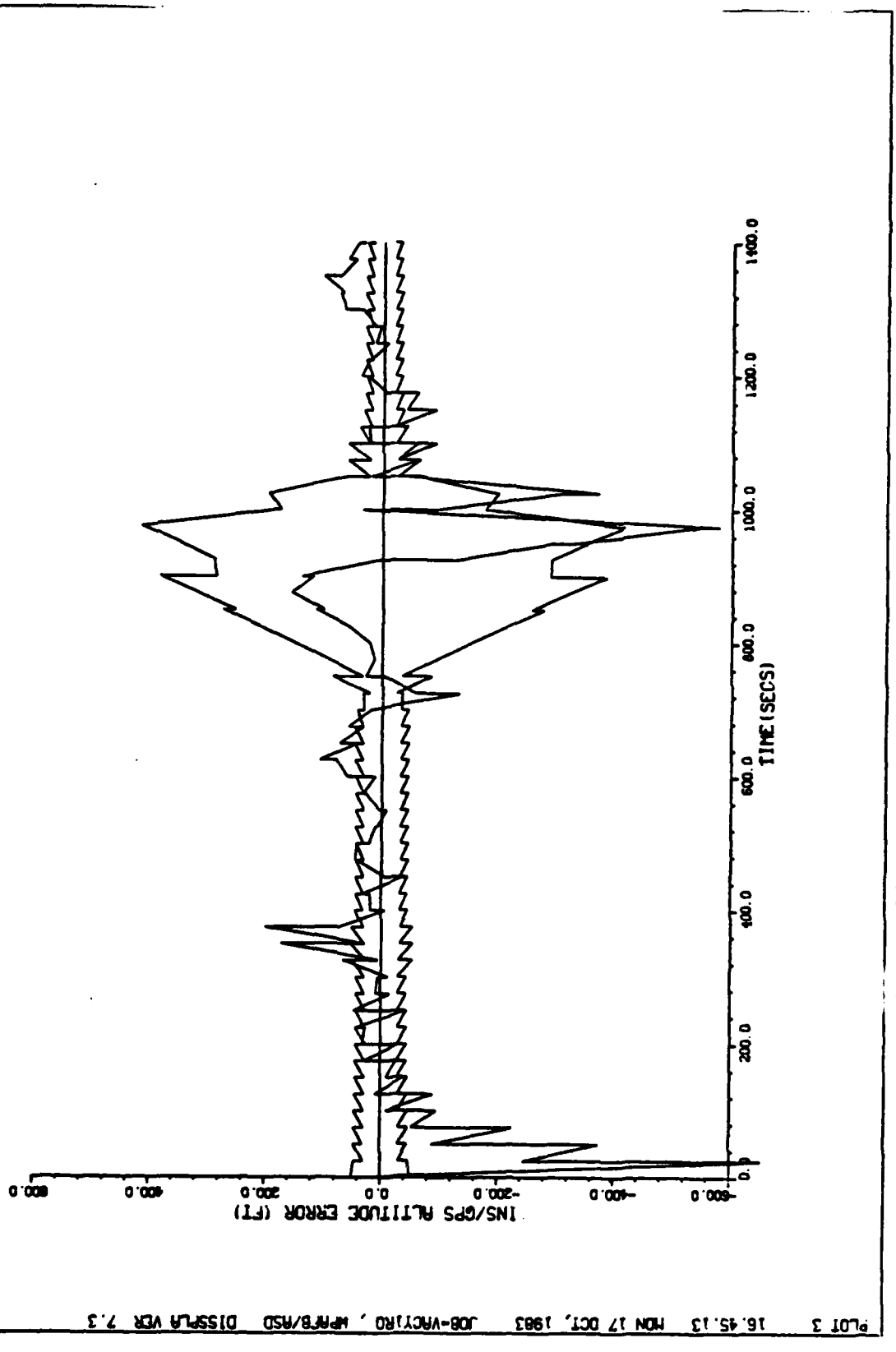

Figure 32b. Mission # 5: GDOP; Altitude Error

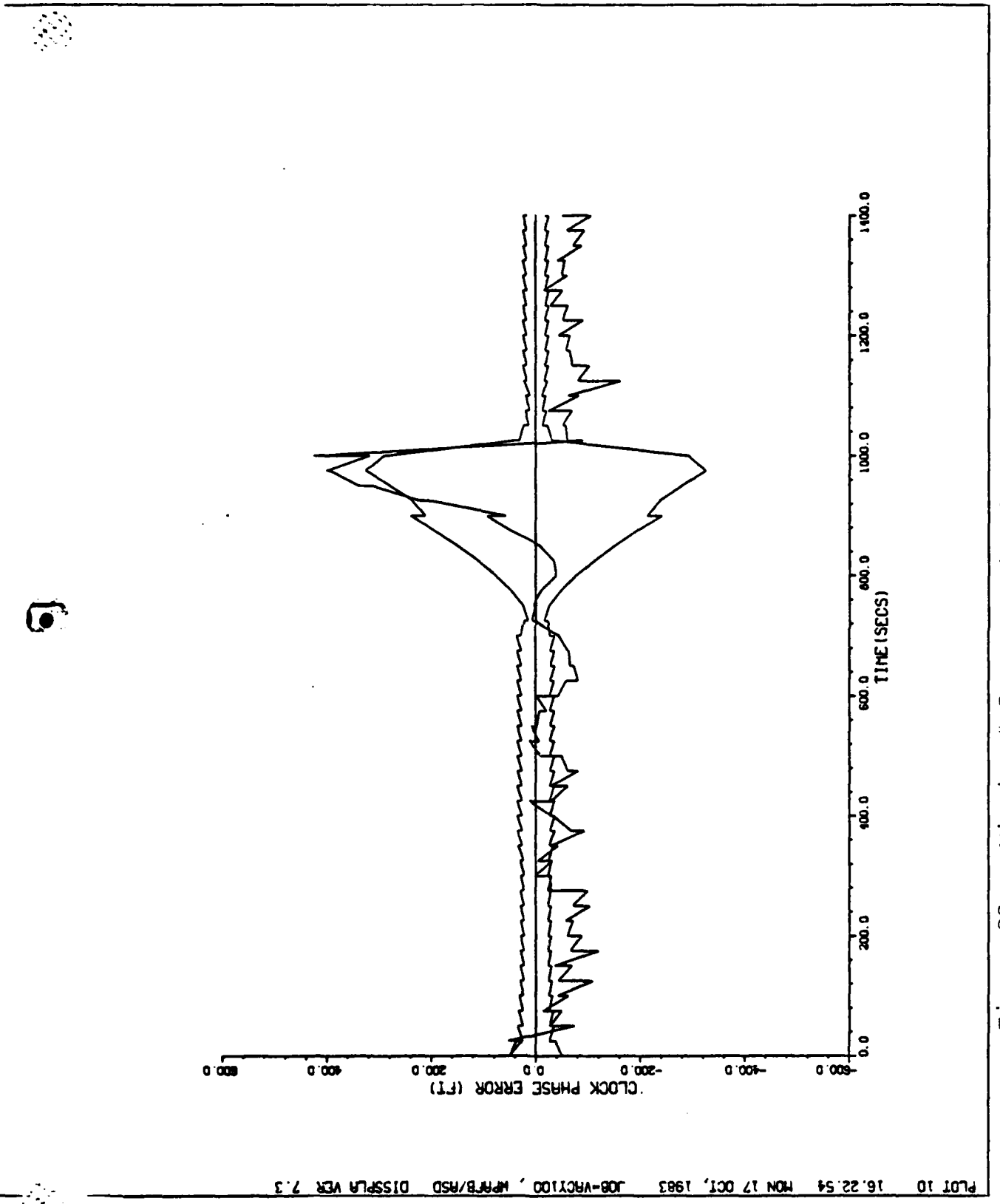

Figure 33a. Mission # 5: Cost Criterion; Clock Phase Error

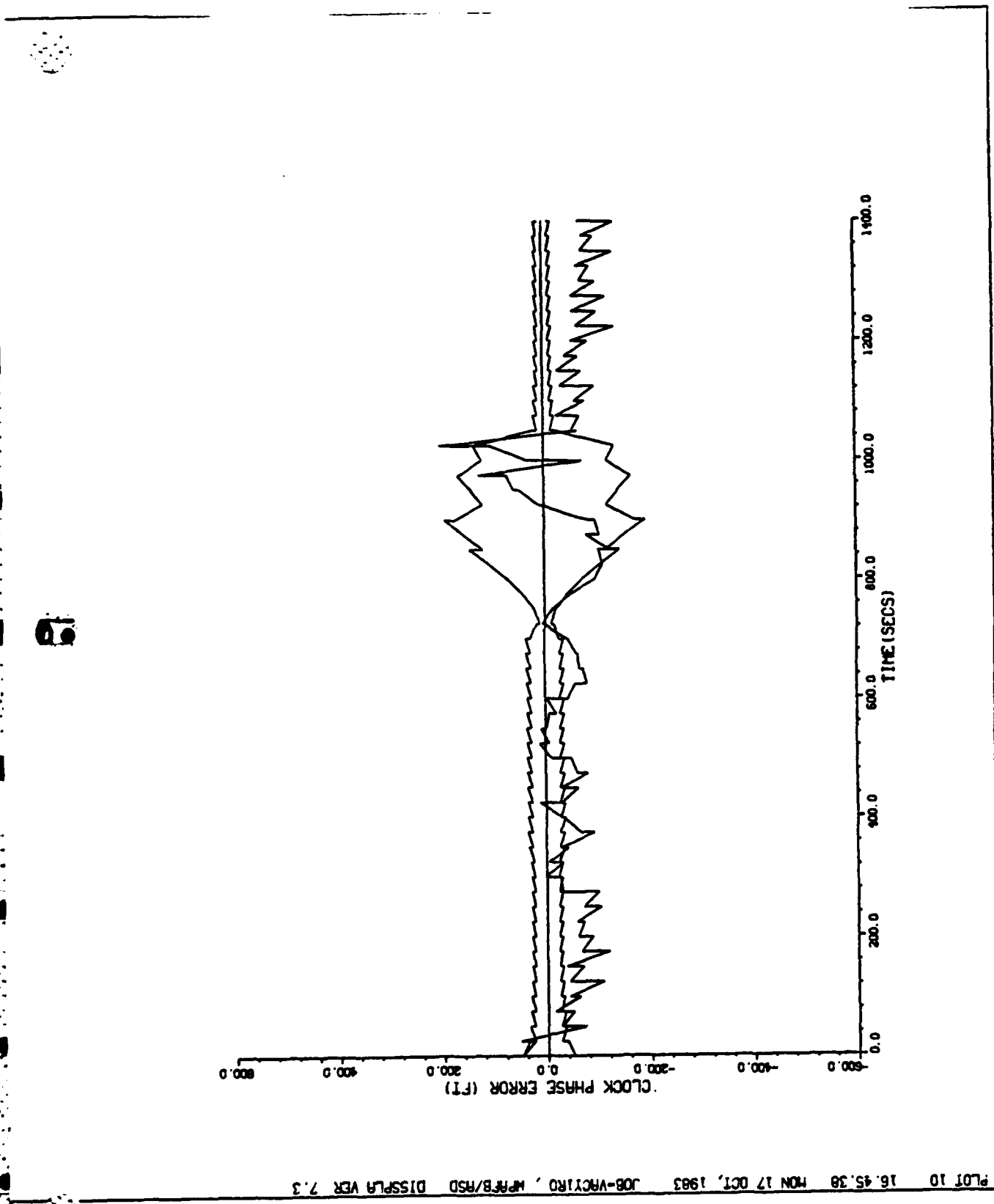

Figure 33b. Mission # 5: GDOP; Clock Phase Error

Summary

This chapter has reviewed the data from 5 simulated close-air-support missions with an integrated GPS/INS navigator in a jamming environment. Each mission was run twice, once using the cost criterion and once using the GDOP criterion for satellite selection. Several parameters are of particular interest in the assessment of the performance improvement of the cost criterion with respect to the GDOP method for satellite selection. Table X presents a review of the composite statistics for all five missions. It is clear from Table Xb and c that on Missions 1 and 2 the cost criterion yields a performance improvement with respect to GDOP; on Mission 3 performance is equivalent to GDOP; and Missions 4 and 5 indicate performance degradation of the cost criterion with respect to GDOP. The performance degradation of the cost criterion in Missions 4 and 5 can be explained by the rapid variation in noise density and the larger measurement errors of the selected satellite set from 800 to 1000 seconds. This would suggest that the cost criterion would have to be tested against realistic jamming scenarios to determine its value for a particular mission. Note that in all 5 missions for the first 600 seconds only 5 satellites are in-view, but during the next 700 seconds of the mission (700-1400 seconds) 6 satellites are in-view. This accounts for the fact that all five missions have alternate satellite sets chosen at 700 seconds and for the next six selection times as well (with the exception of Missions 1, 2, and 5

TABLE Xa

Composite Statistics

Mission #	No. of Alternative Sets	Max. Noise Density	Time of Max. Noise
1.	6 out of 14	-186.93 db watts	1053 seconds
2.	6 out of 14	-179.24 db watts	747 seconds
3.	7 out of 14	-194.50 db watts	747 seconds
4.	7 out of 14	-172.40 db watts	740 seconds
5.	6 out of 14	-163.60 db watts	780 seconds

0-700 sec = 5 satellites 700-1400 seconds = 6 satellites

TABLE Xb

Performance Comparison of User Position Error
(Without Time-Bias Range Errors)

	Cost Criterion		versus GDOP	
	Mean	Std. Dev.	Mean	Std. Dev.
1.	241.77	214.65	604.09	848.80
2.	73.81	34.35	94.20	45.13
3.	74.88	42.23	85.03	37.95
4.	120.31	81.14	123.64	109.12
5.	125.59	114.50	87.83	37.92

≠ all units are in feet

TABLE Xc

Performance Comparison of User Position Error
(With Time-Bias Range Errors)

	Cost Criterion		versus GDOP	
	Mean	Std. Dev.	Mean	Std. Dev.
1.	294.81	262.38	627.80	855.04
2.	91.12	34.46	116.13	38.69
3.	89.49	40.33	107.07	37.96
4.	164.38	86.74	146.05	98.76
5.	142.21	110.01	117.50	39.34

≠ all units are in feet

that chose an alternate satellite set five out of the next six selection times). The limited satellite visibility was a concern that was discussed in Chapter III's analysis of satellite visibility for the 3 satellites x 6 orbits constellation. Increasing the number of in-view satellites (by either scheduling missions during periods of high visibility or by increasing the number of active satellites in the GPS constellation) increases the number of choices available to the cost criterion and the performance improvement over the GDOP satellite selection criterion.

VI Conclusions/Recommendations

Conclusions

This report has tested and analyzed an alternate satellite selection criterion for an integrated GPS/INS navigator to document performance improvements with respect to the standard GDOP criterion. Testing was accomplished using a version of the IGI computer simulation, modified specifically to test satellite selection criterion. The modifications to the simulation included the addition of a null steering antenna algorithm, adaptive bandwidth control of the satellite tracking loops, the parameters that describe the jamming field, and the implementation of the new satellite selection criterion (known as the cost criterion). The computer simulated missions were created by running a single F-4 Close-Air-Support (CAS) flight profile against five different jamming field patterns (where the power of the jammer's and/or the dimensions of the jamming field were varied from mission to mission). The results from the five missions indicated that the performance of the cost criterion was dependent on the rate of change in noise density at the GPS receiver and the number of satellites available.

For a slowly varying noise density, the cost criterion showed performance improvement of 10-350 feet in mean radial position error (with respect to GDOP performance). For rapidly varying noise density the cost criterion showed a performance degradation of 10-30 feet in mean radial position error (with respect to GDOP performance). The cost criterion

was tested in Reference 11 (Brogan Study) using a static measurement analysis to assess the performance of GPS UE. The static versus dynamic measurement analysis looks at satellite measurement selection for one point in time as opposed to satellite measurement selection as a function of the time history (and the associated variations in the noise density) of the mission. The performance degradation observed in this study is in sharp contrast to performance improvements suggested by the static measurement analysis of the cost criterion in Reference 11. The reason for the contradiction in performance between the static and dynamic analysis is that the static measurement case made no attempt to account for rapid variations in noise density. During rapid variations in the noise density, the cost criterion could make worse decisions than GDOP (i.e., choose a satellite set resulting in larger position errors than the satellite set chosen by GDOP) due to satellite selection based on measurement noise estimates that are low at the satellite selection time, that become very large after the selection time. Thus, the satellite set has larger position errors over the interval between satellite selection times. This effect could also occur for a satellite set chosen by GDOP, although GDOP has no knowledge of the measurement noise to use in satellite selection.

The cost criterion also was significantly affected by the number of satellites visible at the satellite selection times. In all five missions the cost criterion did not

choose an alternate satellite set (with respect to the GDOP selected satellite set) when five satellites were visible, but did choose an alternate set when six satellites were visible, even under widely varying noise conditions. This result can be explained by the fact that 5 feasible satellites give the cost criterion only 5 satellite sets to choose from. For most realistic geometry and jamming scenarios for 5 visible satellites, the geometrical affects will outweigh the measurement noise and filter covariance weights of the cost criterion. Thus, for 5 visible satellites the cost criterion will tend to choose the same satellite set as the GDOP criterion. The cost criterion, therefore, should be used when six or more satellites are visible. This satellite visibility problem poses a constraint on when missions could be flown (in order to achieve the smallest possible navigation errors) unless the number of satellites in the GPS constellation could be increased.

Recommendations

The conclusions of this report indicate that shortcomings of the cost criterion (the limitations of satellite visibility and the rate of change of the noise density) must be addressed before it could significantly impact the GDOP criterion used in the present GPS design. Specifically, further research into the performance of the cost criterion in a rapidly varying noise density environment is needed. Such research would greatly aid in modifying the cost

criterion to overcome the noise density problem, or aid in development of another satellite selection algorithm.

This study has developed a valuable design and analysis tool in the modified Integrated GPS/INS Computer Simulation. It is strongly recommended that the modified IGI be used to understand the satellite selection problem thoroughly, to aid in the design of new satellite selection algorithms, and to test these new algorithms against realistic aircraft dynamics and jamming threats. Requests for the modified IGI Computer Simulator code should be addressed to the Reference Systems Branch of the Avionics Laboratory, (AFWAL/AAAN), Wright-Patterson AFB, Ohio 45433.

Appendix A: Satellite Visibility Study

Introduction

The following sections of this appendix will present the satellite visibility study completed in support of this report. This satellite visibility study is based on earlier satellite visibility studies of the 24 satellite constellation (7:28, 31-33) and the 18 satellite constellation (non-uniformly spaced satellites within each of the 3 orbits) (7:29, 34-36). This satellite visibility study will determine the number of GPS satellites that are visible to the user for the present 18 satellite constellation (uniformly spaced satellites within each of the 6 orbits). Since the number of satellites available to the user is a function of the user's position and satellite mask angle, these parameters will be emphasized in the satellite visibility discussion.

Purpose

The purpose for a satellite visibility analysis as part of this report is to determine if the number of satellites available to the user would support the added complexity and computational loading of an alternate satellite selection criterion (with respect to the standard GDOP satellite selection criterion). The number of visible satellites determines the number of four satellite sets from which the best satellite set (with respect to the satellite selection criterion employed) is chosen. If there is a large number of satellites visible, there is a very large number of satellite

sets available and the large number of computations associated with an alternate satellite selection criterion may be unacceptable for analysis and/or implementation. If there are only four or five satellites visible the small number of four satellite sets (0 or 5 respectively) effectively precludes any choice of an alternate satellite set regardless of the satellite selection criterion. Also, most jammers will be either ground-based or at relatively low elevation angles with respect to the GPS satellites. Therefore, by masking out all signals at low elevation angles satellites with high noise levels (due to jamming) and/or deceptive jammers (i.e., that simulate GPS signals) are excluded from satellite selection. Therefore, satellite visibility is of major importance in the selection and analysis of any alternate satellite selection criterion.

Method

The method used to determine satellite visibility was a computer program used in the satellite visibility studies of Reference 7. The computer program was obtained through the Avionics Laboratory's Reference Systems Branch (Air Force Wright Aeronautical Laboratories, Wright-Patterson AFB, Ohio). The program is composed of software modules extracted from the Integrated GPS/Inertial Simulator Computer Program (IGI) (17).

The major modification to the satellite visibility computer program was the conversion to parameter values that describe the present 18 satellite constellation. The

parameters that describe the 18 satellite constellation are:

(1) 6 orbital planes; 3 satellites evenly spaced within each plane

(2) circular orbits with an inclination of 55°

(3) the period for one orbit is approximately 12 hours

(4) the altitude of the satellites is 10,500 nautical miles

(5) the orbital phasing is 40° (in an eastward direction).

In addition to the satellite constellation parameters the desired mask angles (there are 8 possible mask angles that can be specified each run) were varied in the computer program.

Satellite Visibility Analysis

As stated in the introduction, the satellite visibility is dependent on the user's position and the desired mask angles. The satellite visibility discussion will look at the average number of satellites for a 24 hour observation period for latitudes of 0° to 90° and longitudes of 10° and -90°.

Case 1. The satellite visibility for a user's position of -90° longitude and a range from 0° to 90° latitude (for 1° increments of latitude) is examined in Figure A-1. From Figure A-1 the number of satellites visible for mask angles of 0°, 10°, and 20° is approximately 7, 5.5, and 4 satellites respectively (for 0° to 90° latitude). The satellite visibility for mask angles of 0° to 20° is of

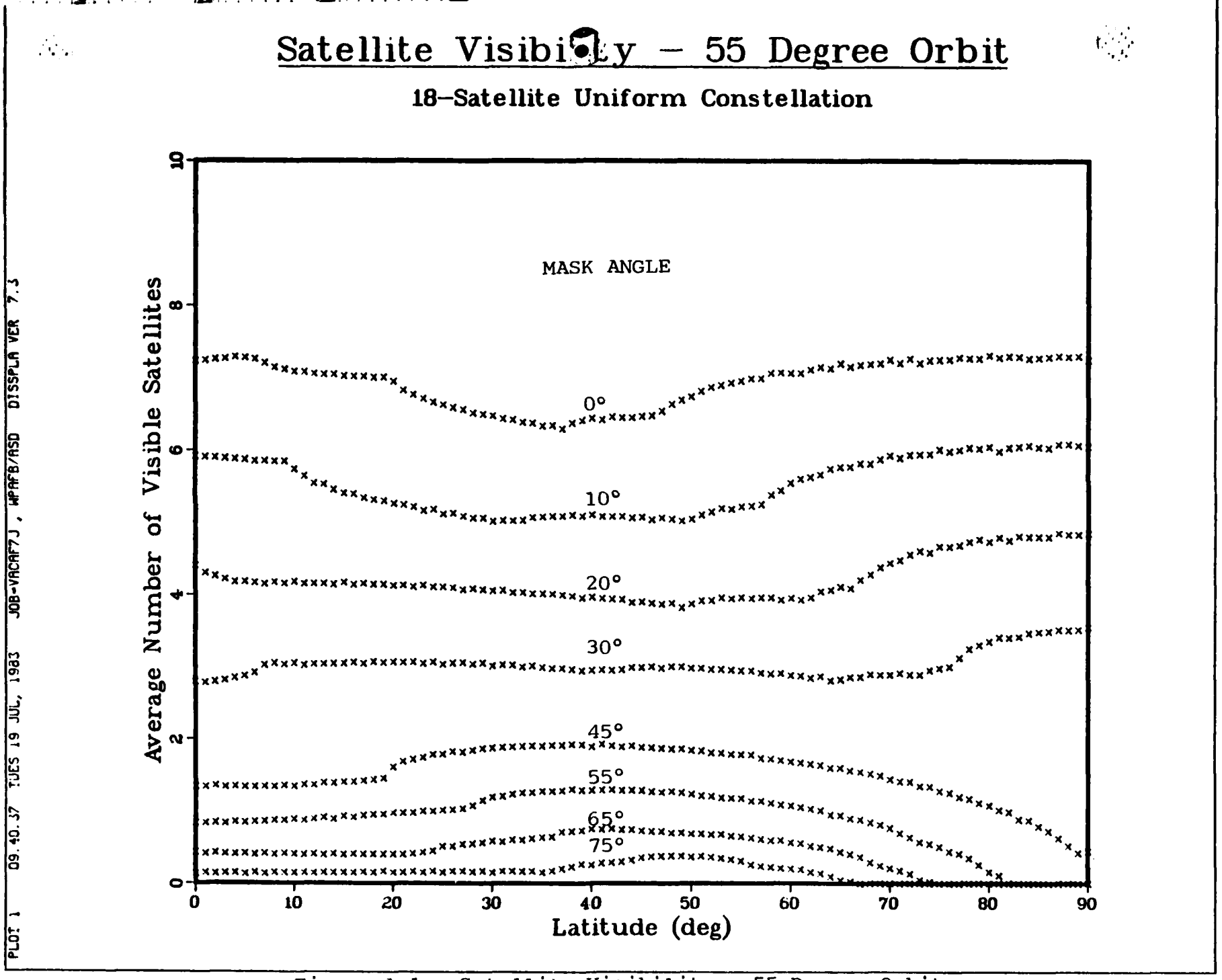

Figure A-1. Satellite Visibility - 55 Degree Orbit

particular interest in determining the number of four satellite sets available to a satellite selection criterion. Figure A-2 examines satellite visibility for mask angles between 0° and 25°. Note that for mask angles between 5° and 15° the average number of visible satellites for all latitudes is between 5 and 6 satellites. This indicates that mask angles for 10° to 20° are undesirable for use in an alternate satellite selection criterion because the number of satellite sets prevents any decisions (other than geometry factors) from being made (See the Purpose Section of this Appendix). Also, for mask angles between 5° to 10° there is very little difference in the number of visible satellites for increments of the mask angle. Therefore, since the present GPS UE uses a mask angle of 5°, it is appropriate to use this mask angle for analysis of alternate satellite selection criterion.

From the data in Figures A-1 and A-2 an analysis of satellite visibility for a user's position of 38° Latitude, -90° Longitude is possible. This location is of particular importance to this report because it is the initial user's position in the F4 Close-Air-Support flight trajectory used in the modified IGI Simulator as discussed in Chapters IV, V, and Appendix B. The number of visible satellites for mask angles from 0° to 75° is shown in Table A-1.

Satellite Visibility – 55 Degree Orbit

18–Satellite Uniform Constellation

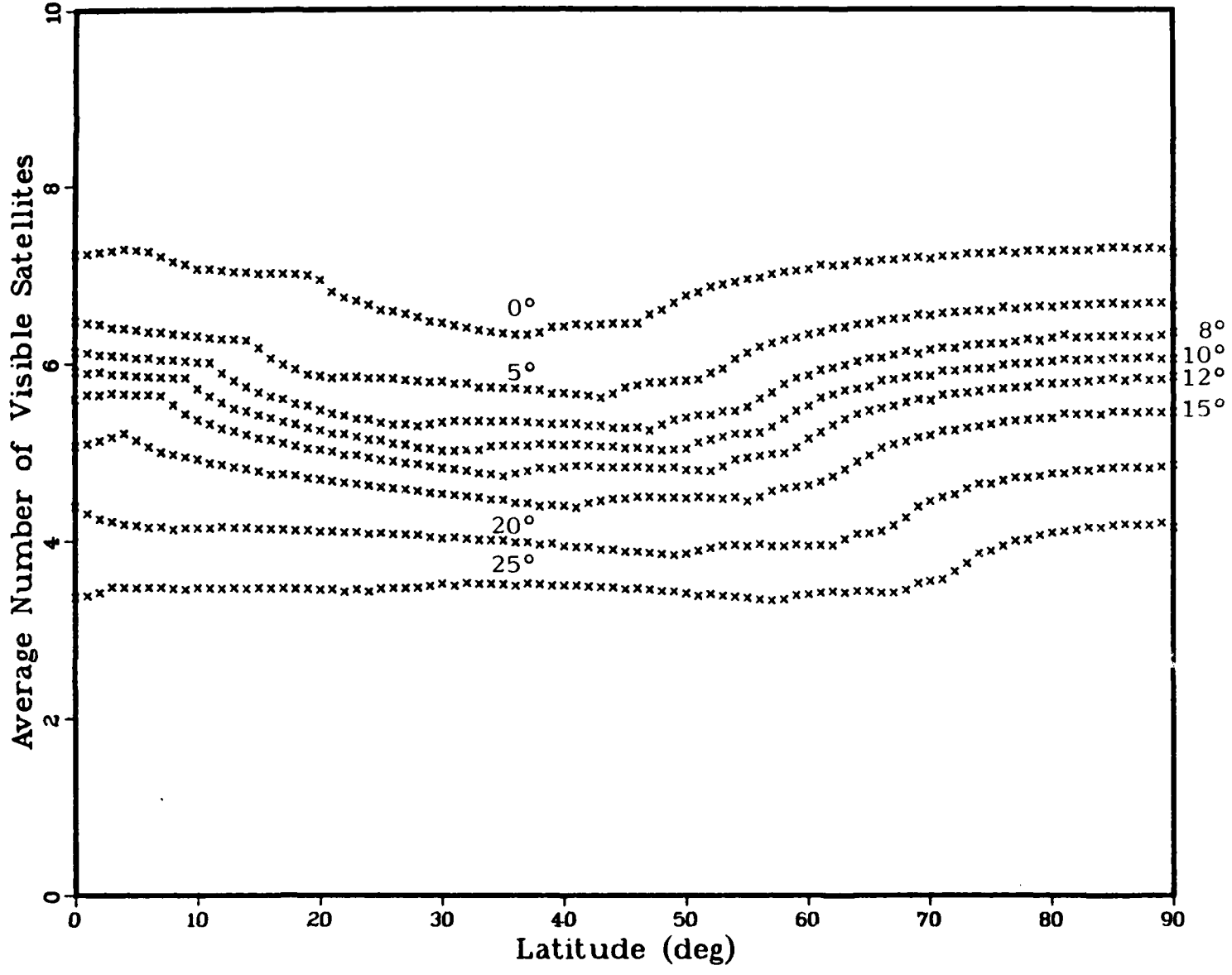

Figure A-

TABLE A-1

Mapping of Satellite Visibility for a 24 hr. Period
Latitude 38° Longitude -90°

Mask Angle	0°	5°	8°	10°	12°	15°	20°	25°	30°	45°	55°	65°	75°
Av. # of Sat.	6.6	5.9	5.4	5.0	4.6	4.0	3.7	3.4	3.0	2.1	1.5	0.5	0.0

Again the number of visible satellites for mask angles from 10° to 15° would result in the average number of satellite sets between 1 and 5, undesirable for use with an alternate satellite selection criterion. For a mask angle of five degrees the user could anticipate an average of about six visible satellites (15 possible satellite sets) for the analysis of an alternate satellite selection criterion. With 15 satellite sets the alternate satellite selection criterion should be effective without unacceptable computational loading.

Case 2. An analysis of the satellite visibility for user positions of 10° Longitude and 0° to 90° Latitude is displayed in Figure A-3. Figure A-3 shows some variation of satellite visibility from that shown in Figure A-2, but the number of visible satellites is consistent with the values seen previously. A tabular view of the number of visible satellites for mask angles from 0° to 75° is shown in Table A-2.

TABLE A-2

Mapping of Satellite Visibility for a 24 hr. Period
Latitudes 0°-90° Longitude 10°

Mask Angle	0°	5°	8°	10°	15°	20°	25°	30°	45°	55°	65°	75°
Av. # of Sat.	7.0	6.0	6.0	5.6	4.9	4.2	4.0	3.0	1.5	0.5	0.3	0.0

Satellite Visibility – 55 Degree Orbit

18–Satellite Uniform Constellation

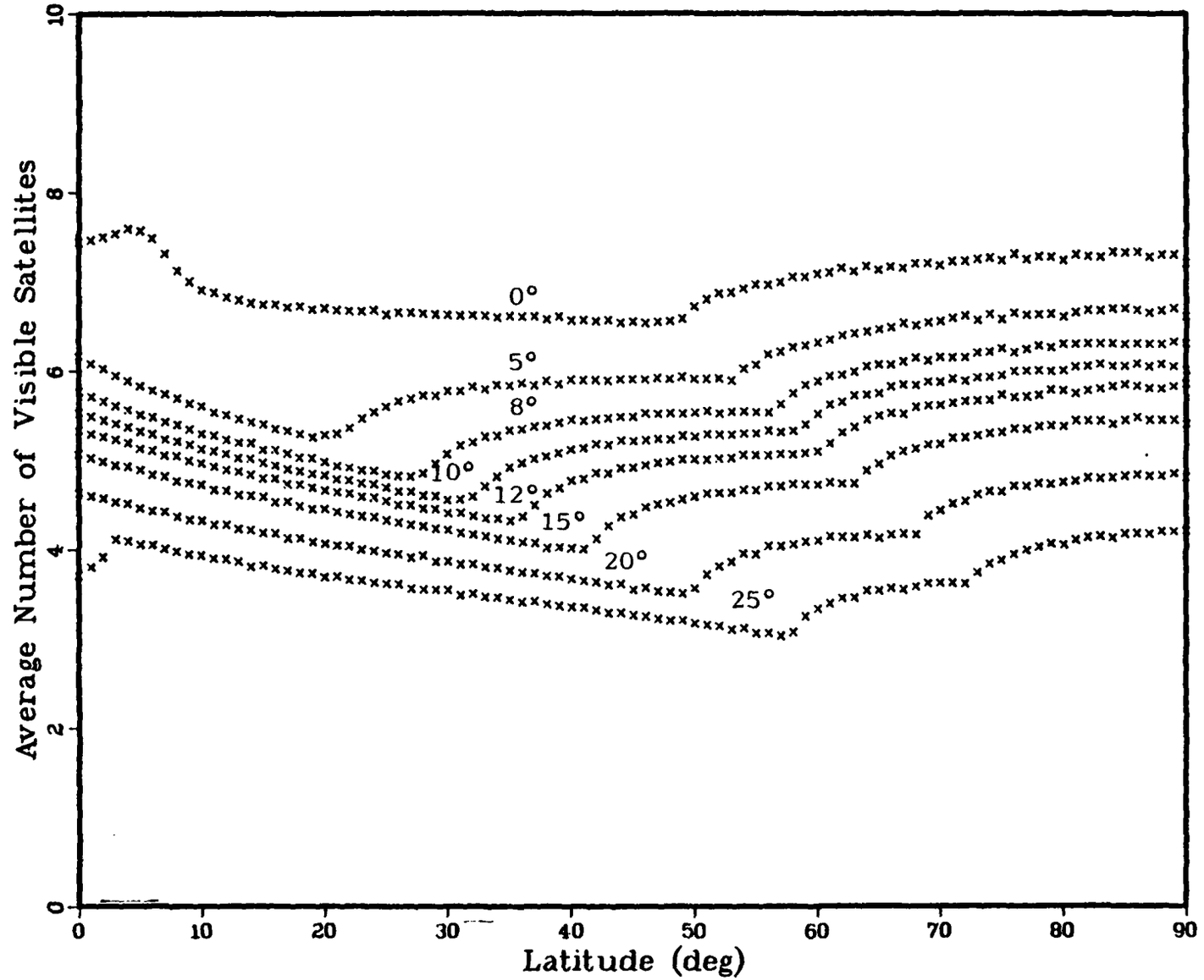

PLOT 1 16.23.11 MON 18 JUL, 1983 JOB=VACAFD1 , WPAFB/ASD DISSPLA VER 7.3

155

Figure A-3

Comparisons of Table A-1 and A-2 show a slight variation in the number of visible satellites with varying longitudes. The variations may be significant for a particular mission but are not significant for the analysis of alternate satellite selection criterion.

Summary

The results of a satellite visibility study have been presented in this Appendix. The purpose for this study was to determine if an alternate satellite selection criterion would be acceptable for analysis and/or implementation (in an integrated GPS/INS) given the number of visible satellites. Satellite visibility implies two constraints on an alternate satellite selection criterion. The first constraint occurs when there are four or five satellites visible. This small number of satellites means there are few or no decisions for the alternate satellite selection criterion to make (other than a simple geometry decision). For this case an alternate satellite selection criterion would not be warranted. The second constraint occurs when too many satellites are visible. A large number of satellites means a very large number of possible satellite sets. For such very large numbers of satellite sets, the increased computational loading of an alternate satellite selection criterion would be unacceptable for analysis and implementation.

The satellite visibility results in Case 1 and 2 show that an average of 6 satellites could be expected for a mask angle of 5° (for two sets of user position: 10° Longitude

0° to 90° Latitude and -90° Longitude 0° to 90° Latitude). The satellite visibility number is however, an average over a 24 hour observation period, this means that periods of less than 6 satellite visibility occur, and that during these periods the alternate satellite selection criterion would probably be ineffective.

Although the satellite visibility analysis that is presented in this appendix examines only two sets of user positions the results are consistent with satellite constellation analyses of Reference 4.

Appendix B: Modifications to the IGI Simulator

The following sections in this appendix will present the assumptions, algorithms, and equations used to modify the IGI Computer Program Simulator. The modifications fall into three main areas; the null steering antenna, adaptive bandwidth control of the satellite tracking loops, and the jamming field. The implementation of the cost criterion (Equation 31) will not be discussed in this appendix.

Null Steering Antenna

Introduction. As stated in Chapter II's User Segment discussion the null steering antenna algorithm acts to distribute its nulls to minimize the total power out of the antenna (6:139). This process is accomplished by combining the outputs of several individual antenna elements through phase and amplitude controls to minimize the power out of the antenna (10:6). The maximum number of nulls that may be formed by the null steering antenna is dependent on the number of antenna elements. The implemented null steering antenna model uses a seven element phased array antenna arranged in a circular pattern (Figure B-1). This seven element, circular pattern is consistent with the null steering antenna being used in GPS High Performance Aircraft Development and Operational Test and Evaluation (25:1-3). A seven element phased array antenna may create a maximum of six nulls (6:139). Each of the antenna elements is omnidirectional in azimuth only. The antenna elevation gain for the

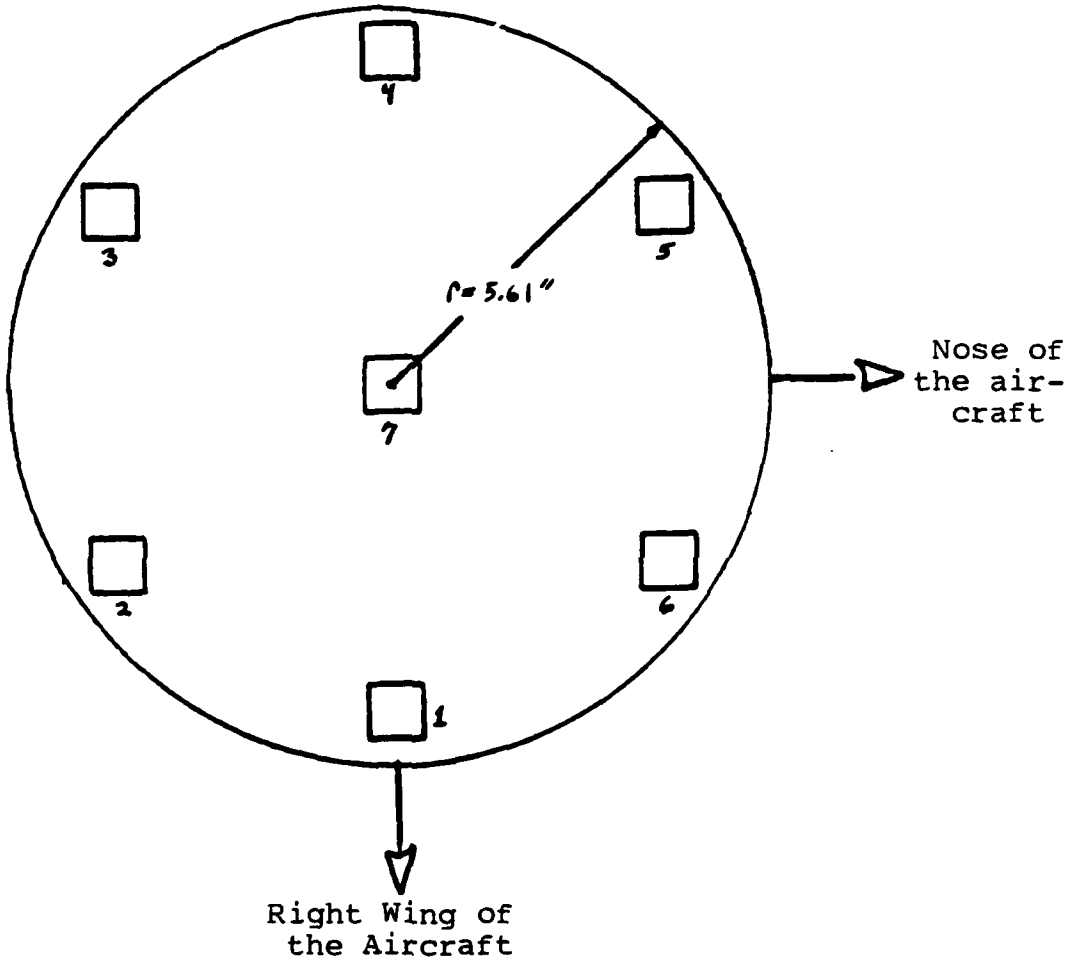

Figure B-1. Seven Element Null Steering Antenna Geometry

individual antenna elements is given by the following equation (6:139):

$$\text{for } \theta < 80^\circ \quad g(\theta) = 4 \cos \theta \quad \text{(in dB)} \tag{55a}$$

$$\text{for } \theta > 80^\circ \quad g(\theta) = 1/3(90-\theta) - 2.64 \text{ dB} \tag{55b}$$

where the angle θ represents the depression from the normal (vertical) to the aircraft. Equation 55b) accounts for blockage caused by the aircraft (6:139-140). The angular orientation of the antenna aperature is assumed to be fixed with respect to local level (i.e., the aircraft may be oriented other than straight (the pitch axis) and level (the roll axis), but the antenna apperature is always straight and level with respect to the local level coordinate frame). This assumption was made to simplify the software to describe the null steering antennas physical characteristics. A more accurate representation of the physical model of the antenna will require coordinate transformation of the antenna elements' position from aircraft frame to local level. This transformation must be calculated using filter estimated angular orientation. The null steering algorithm would then have to keep track of measurement noise estimates based on the true antenna elements' position and the filter estimated antenna elements' position. This level of complexity and impact on computer processing time was deemed unappropriate for this analysis.

Output Power Minimization Algorithm. The process of minimizing the total power out of the antenna is accomplished by combining the outputs of several individual antenna elements through phase and amplitude controls (10:6). This type of phase and amplitude control is based on the concept of mutual coupling between receiving elements in a phased array. For example, two elements in proximity to each other induce voltages at the terminals of each other and the reflected voltage in each line depends upon the phase of the driven voltage in the other. Thus in a phased array of many elements, the reflection coefficient in any one element is unavoidably influenced by mutual coupling and the total effect will depend upon the phase programming of all the elements in the phased array (26:1662). The phase and amplitude programming is accomplished by weighting the input signal to each antenna element. The input signal vector ($\underline{x}$) to the antenna is a function of the jamming power (J), the satellite signal power (S), and the environment noise level (σ_b) at the antenna (6:140).

$$\underline{X} = \sigma_b + \sum_m J_m \underline{V_m} + \sum_N S_N \underline{Y_N} \tag{56}$$

The vectors $\underline{V_m}$ and $\underline{Y_N}$ are complex vectors for the jammers and satellites respectively, which contain the phase shift due to the antenna element geometry (6:140).

$$V_m^i = \exp(j\underline{l_m} \cdot \underline{r}^i) = i^{th} \text{ element of vector } \underline{V_m} \tag{57a}$$

$$Y_N^i = \exp(j\underline{p}_n \cdot \underline{r}^i) = i^{th} \text{ element of vector } \underline{Y}_N \qquad (57b)$$

where:

$\underline{r}^i$ = position of the i^{th} omni element expressed in the local level coordinate frame

$\underline{l}_m$ = line-of-sight to the m^{th} jammer expressed in the local level coordinate frame

$\underline{p}_n$ = line-of-sight to the n^{th} satellite expressed in the local level coordinate frame

The background noise level, σ_b, is set to -133dBw and the nominal value of S_N = -162dBw (6:140 and 5:148).

The input signal vector $\underline{X}$ (Equation 56) may now be used to form the signal autocorrelation matrix $\underline{R}_X$ (6:104, 27:81).

$$\underline{R}_X = E(\underline{X}\underline{X}^*) \qquad (58a)$$

$$\underline{R}_X = \sigma_b{}^2 I + \sum_m J_m{}^2 \underline{V}_m \underline{V}_m{}^* + \sum_N S_N{}^2 \underline{Y}_N \underline{Y}_N{}^* \qquad (58b)$$

where the "*" indicates the conjugate transpose. The weights W_i are formed from the inverse of $\underline{R}_X$ and a control law dependent vector $\hat{\underline{e}}$.

$$\underline{W} = \underline{R}_X{}^{-1} \hat{\underline{e}} \qquad (59)$$

$$\hat{\underline{e}} = [0,0,0,0,0,0,1]^T \qquad (60)$$

The vector $\hat{\underline{e}}$ imposes the constraint that one of the elements have unity weight and the remaining elements have complex weights (the unity weight is the center element of Figure 13) (6:141). For computer implementation Equation (59) is rearranged to an $\underline{AX} = \underline{B}$ form for solution by a high accuracy, complex matrix, linear equation solver (28). The weighting vector in Equation (59) is normalized every time the null steering algorithm is called to prevent degradation of the GPS signals due to old weights (serious degradation of the GPS signals could result when in a rapidly varying jamming environment antenna element weights are used for a relatively long time before recalculation (usually to reduce computational loading).

Carrier-to-Noise Power Density (C/No) Estimation

The Jammer Power Estimate. The jammer power estimate at the antenna output (J_a) is a function of the jammer power received at the antenna input (J_R) and the gain associated with the received jammer power ($G(\theta)$).

$$J_a = J_R + G(\theta) \quad \text{(db)} \tag{61}$$

$$J_R = \sum_m (J_{T_m} + L_{S_m}) \quad \text{(db)} \tag{62}$$

$$G(\theta) = \left|g(\theta)\right|^2 \left|\underline{W}^* \underline{V}_M\right|^2 \quad \text{(db)} \tag{63}$$

where:

J_{T_m} = the power of the m^{th} jammer at transmission

L_{s_m} = the transmission (space) loss of the radiated jamming signal.

$g(\theta)$ = as defined in Equation (55a and b)

$\underline{W}^*$ = the conjugate transpose of the antenna element weighting vector

$\underline{V}_m$ = the complex power vector for the m jammers (see Equation (57a)).

The received power from each jammer, $J_R{}^m$, is calculated using the following equation (20:6-7):

$$J_R{}^m = \frac{J_T{}^m G(\emptyset,\theta)A}{4\pi R^2} \tag{64}$$

where:

$J_R{}^m$ = the received power of the m^{th} jammer in watts

$J_T{}^m$ = the transmitted power of the m^{th} jammer in watts

$G(\emptyset,\theta)$ = the gain of the transmitting antenna in the direction $\emptyset,\theta$ of the receiving antenna (unit less)

A = the effective area of the receiving antenna in square feet

R = the transmitter to receiver distance in feet.

From basic antenna theory, the effective area of an ideal isotropic antenna is (20:7),

$$A = \lambda^2/4\pi \quad \text{(in square feet)} \tag{65}$$

$$\lambda = {}^{c}/_{f} = \text{wavelength in feet} \qquad (66)$$

where:

c = speed of an electromagnetic wave in a vacuum = 9.8357119×10^{8} feet

f = frequency of transmitted jammer power, assumed to be GPS L1 = 1.57542×10^{9} Hertz

For an antenna with onmidirectional gain in the upper hemisphere the gain ($G(\emptyset,\theta)$ is a constant. The constant gain effect permitted the use of Effective Radiating Power (ERP) as the input to the computer simulation of the jammer's transmitted power (20:7).

$$ERP = J_T{}^{m}G(\emptyset,\theta) = \text{a constant input by the computer simulation user} \qquad (67)$$

Using Equations (65) - (67) and substituting back into Equation (64) results in the following:

$$J_R{}^{m}(dB) = ERP(dB) + [10 \log(\lambda^2/(4\pi)^2)]-20 \log R \qquad (68a)$$

$$= ERP(dB) - (26.076dB)-20 \log R \qquad (68b)$$

Rewriting Equation (61) by substituting in Equations (68b) and (63) results in the following:

$$J_a = \sum_{i=1}^{m} (ERP_i - (26.076) - 20 \log R + \left| g_i(\theta) \right|^2 \left| W^* V_i \right|^2) \quad (69)$$

The gain associated with Equation (63), that appears as the last term in Equation (69) is limited to a maximum null depth of 30db watts (gain = 30db watts) based on estimates of broadband jammer power (6:141).

The Signal Power Estimate. The signal power estimate at the antenna output (S_a) is similar to the approach used in the jammer power estimate.

$$S_a = S_R + G(\theta) \qquad \text{(dB)} \qquad (70)$$

$$S_R = S_T + L_S - \ell(\theta) \qquad \text{(dB)} \qquad (71)$$

$$G(\theta) = g(\theta)^2 \, \underline{W}^* \underline{Y}_N^2 \qquad \text{(dB)} \qquad (72)$$

where:

S_T = satellite power at transmission
= ERP (P-Code) - 23.8db watts (Ref. 5:148)

L_S = Space Loss
= -101.75 - 20 log R (Ref 6:30)

R = satellite to user range

$\ell(\theta)$ = atmospheric loss
= $(0.006)[[(6371 \sin \theta)^2 + 127520]^{\frac{1}{2}} - 6371 \sin \theta])$
(Ref 6:30)

θ = user to satellite elevation angle

$g(\theta)$ = as defined in Equation (55a and b)

$\underline{Y}_N$ = the complex power vector for GPS satellite signal (See Equation (57b))

The space loss, L_s, is a constant -183.5db for most near earth missions (L_s varies less than 0.2 dB for user altitudes up to 200 miles). The atmospheric loss accounts for added satellite attenuation at or near the horizon. This term can be dropped due to the UE set masking out all satellites from the horizon to 5° above the horizon ($\ell(\theta)$ above 5° from the horizon is negligible (less than -2db)). Substituting the above simplifications into Equation (71), results in a received satellite signal of -159.7db, slightly better than the nominal value of -162.0db used in Equation (52b). For simplicity and to account for any overly optimistic simplifications, the value -162.0db was used for S_R. The resulting equation for the signal power is,

$$S_a = (-162.0) + |g(\theta)|^2 |\underline{W}^* \underline{Y}_N|^2 \qquad (73)$$

As in the jammer power estimation algorithm, when the antenna places a null on top of a GPS signal source, the null depth is limited to 30db. In addition, the satellite signal gain is increased 10db in the range $-10db \leq G(\theta) \leq -30db$ to simulate the effect of increased gain due to the use of directional information of the satellite's position in the null steering controller (reducing the chance of a null being put on a satellite signal, thus increasing the gain on the satellite signal).

The C/No Estimate. The carrier-to-noise density (C/No) is a function of the signal power estimate (S_a), the jamming power estimate (J_a), the UE set front-end noise power density (N_T), and the UE set processing gain (G) as shown in the following equation (5:150):

$$C/N_o = \frac{S_a/N_T}{1 + (J_a/S_a)(S_a/N_T)(1/G)} \quad (dB\text{-}H_Z) \qquad (74a)$$

$$= \frac{S_a}{N_T + (J_a/G)} \quad (dB\text{-}H_Z) \qquad (74b)$$

where

$N_T = -202.0 dbw/H_Z$ (Ref 5:148)

$G = 70db\text{-}H_Z$ (P-code)

The term, J_a/G, is subject to the assumptions of the type of jamming signal. In this implementation it is assumed that all of the jamming power is transmitted into the satellite signal 20MHZ bandwidth, centered at the frequency of L2(1.57542×10^9 HZ). For this type of jamming signal the full 70db-HZ of the P-code processing gain is used. For jamming signals that replicate the GPS satellite signal structure the processing gain may be reduced significantly.

Adaptive Bandwidth Control of the Satellite Tracking Loops.

Introduction. The purpose of incorporating adaptive bandwidth control of the satellite tracking loops is to simulate the contribution this algorithm has toward the GPS UE Anti-Jam capability, simulate the two modes of operation

(coherent and non-coherent tracking), and to increase the realism and capability of the computer simulation.

The Adaptive Bandwidth Process. In the User Segment Section the importance of the proper satellite tracking loop bandwidth on anti-jam performance was discussed. The adaptive bandwidth process attempts to minimize the mean squared error caused by all disturbances (noise, jamming, clock instability, and aircraft residual dynamics) affecting the receiver by varying bandwidth as a function of C/No (5:20). A graphical representation of the adaptive bandwidth functions for the coherent and non-coherent mode are presented in Figures B-2a dnd B-2b respectively. For implementation purposes the functions were simulated by two second order quadratic equations of the form

$$B_c = A(C/N_o)^2 + B(C/N_o) + C \qquad (75)$$

For the coherent mode:

For (35.0db-HZ) > C/N_o > (29db-HZ)

A = -0.0133

B = 1.1567

C = 21.20

(max. error in $B_c \leq 0.04$HZ)

For (29.0db-HZ) > C/N_o > (17db-HZ)

A = 0.0094

B = 0.3411

C = 3.1494

(max. error in $B_c \leq 0.07$HZ)

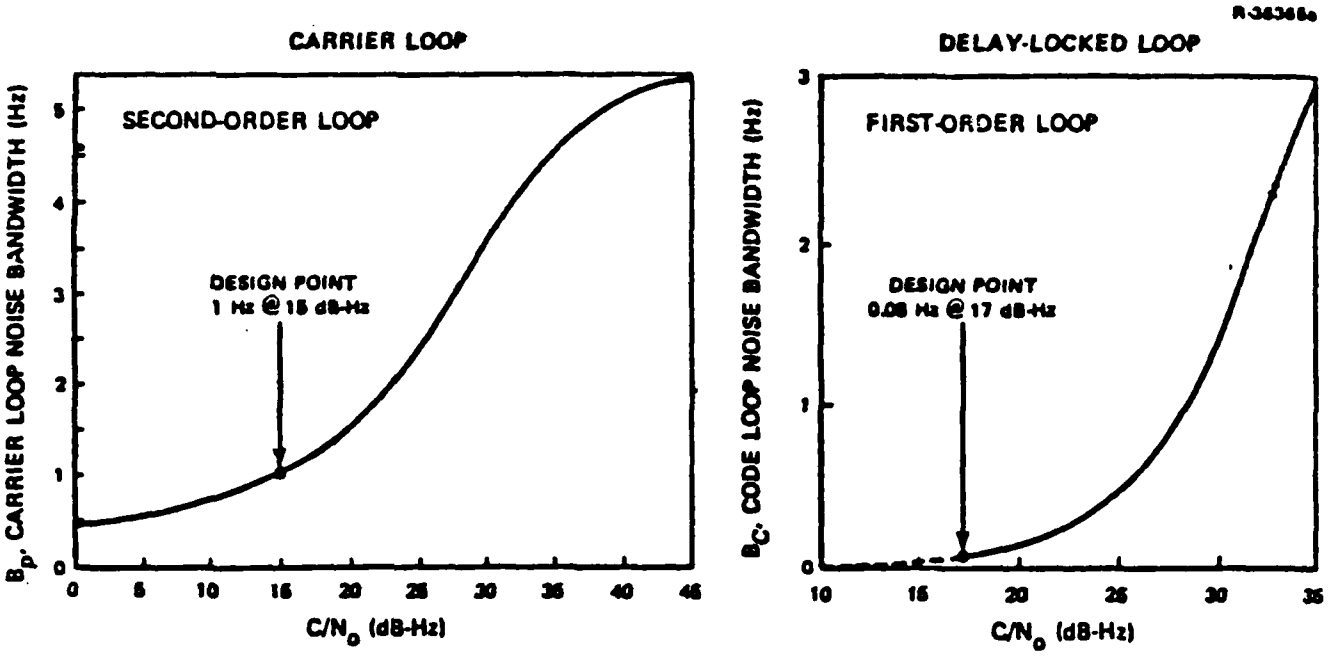

Figure B-2a Bandwidth Variation with C/N_0 for the Coherent Mode (5:20)

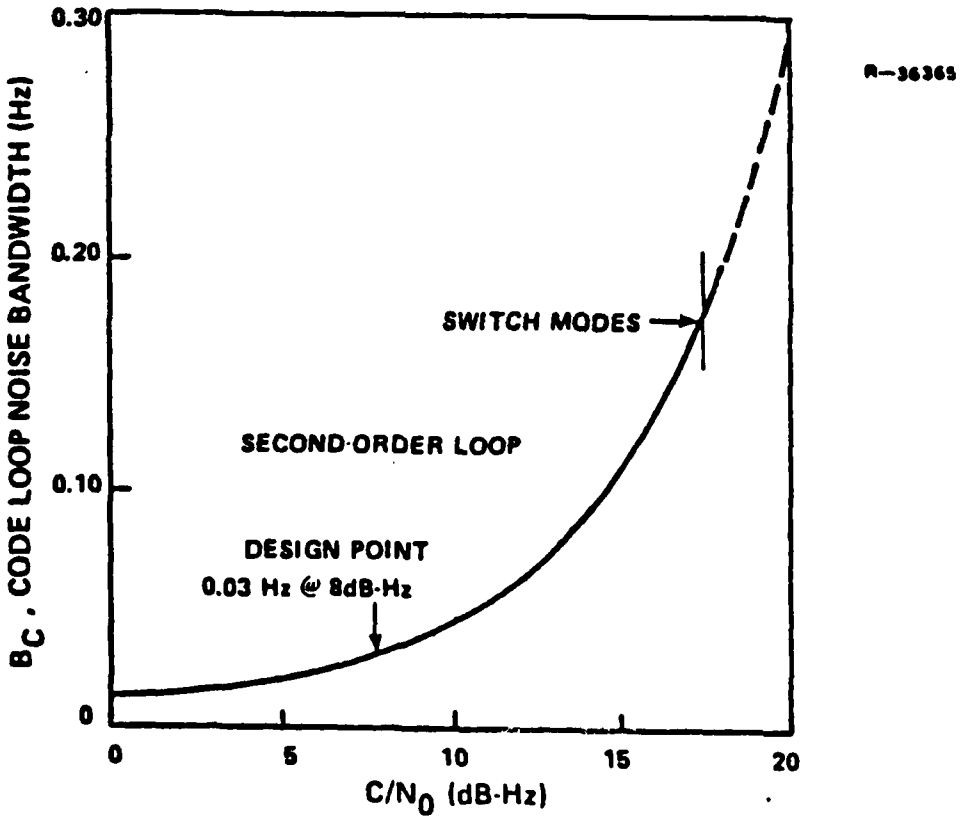

Figure B-2b Bandwidth Variation with C/N_0 for the Noncoherent Mode (5:21)

For the non-coherent mode:

For (17.0db-HZ) > C/N_o > (13db-HZ)

A = 0.003625

B = 0.0845

C = 0.563875

(max. error in $B_c \leq 0.0056$HZ)

For (13.0db-HZ) > C/N_o > (6.0db-HZ)

A = 0.00079167

B = -0.007583

C = 0.04

(max. error in $B_c \leq 0.0021$HZ)

From the figures and above data the tracking loop limits are readily obvious. Above 35dB-HZ the tracking loops are operating in an environment with little or no jammer interference. From 17.0 to 35.0dB-HZ (and above) the UE is in the coherent mode. From 6.0 to 17.0dB-HZ the UE set is in the non-coherent mode. Below 6.0dB-HZ no tracking is possible (for both satellites being tracked or for acquisition of alternate satellites). In reality, studies have shown the possibility of tracking a satellite below 6.0dB-HZ until correlation errors grow beyond the tracking limits (5:34-43). The modifications to this computer simulation, however, implement a sharp cut-off at each lock limit to deny usage of satellites with marginal signal strength in this performance analysis.

Measurement Error Estimate. The measurement error for each individual satellite measurement is directly related to the RMS error of the tracking loop output. The RMS error of

a tracking loop output is composed of two components: σ_N due to noise and jamming (jitter), and σ_D due to residual dynamics and oscillator instabilities (5:25). The total RMS error is given by:

$$\sigma_e = (\sigma_N^2 + \sigma_D^2)^{\frac{1}{2}} \tag{76}$$

The jitter term, σ_N, can be approximated by an analytical expression. The σ_D term is known in the simulation, but is approximated by a constant 1-σ value in the IGI Simulator. The RMS jitter due to noise and jamming for the coherent mode can be approximated by the following expression (5:25):

$$\sigma_N \approx (98.424) \frac{B_C}{C/N_o} \left[1 + \frac{2B_{lp}}{C/N_o}\right]^{\frac{1}{2}} \text{(feet)} \tag{77}$$

where B_{lp} is the bandwidth of the low pass filters (these filters separate the coded signal from the carrier signal). The expression for the non-coherent mode is given by multiplying the $(B_C/(C/N_o))$ term in Equation (77) by 0.5. For computer implementation the measurement error estimate (R_m) is approximated by the RMS error of the track loop (σ_e). The one sigma truth and filter measurement errors used in the IGI simulator are 7.0 feet and 12.0 feet respectively (for an environment without jamming). These one sigma errors are associated with the σ_D term in Equation (76). The one sigma filter measurement error is larger than the true error to account for measurement errors associated with atmospheric disturbances and inaccuracies in the satellites

emphemeries that are represented in the truth model as one sigma position errors of 10 feet (truth states 58-61), but are not modeled in the filter state. Therefore the equation for the filter measurement error (R_{mf}) is,

$$R_{mf} = (\sigma_N^2 + \sigma_D^2 + 95.0)^{1/2} \text{ (feet)} \qquad (78)$$

As stated in the previous section the code tracking loop lock limit is a C/N_o value equal to 6.0dB-HZ. The measurement error estimate for any satellite that is below this lock limit is set to a value of 1.0×10^8 feet. This measurement error value is at least five orders of magnitude higher than the largest filter measurement error, which should adequately simulate signal loss-of-lock and appropriately deweight the satellite's pseudo-range and delta pseudo-range measurements during a filter update.

The Jamming Field

Introduction. The IGI simulator does not model any jamming field related parameters. Therefore, the modifications to the simulator could exercise a great deal of flexibility in modeling the jamming field. The goal behind the modifications to be discussed in the next subsection is to add a capability that is consistent with this analysis, but capable of supporting future analysis (using realistic jamming scenarios) without major modifications.

Jamming Field Parameters. The jamming field parameters added to the IGI Simulator are:

(1) up to 25 jammers can be transmitting at one time

(2) the jammers may be on the ground or airborne

(3) the jammers may be moving or stationary.

Each jammer's position is specified in degrees of latitude and longitude, and altitude in feet. Each jammer's velocity is specified in units of feet-per-second in the three components of the local level coordinate frame (i.e., V_{jeast}, V_{jnorth}, and V_{jup}). Power (EIRP or sometimes just ERP) is specified in kilowatts. The jammer's have an omni-directional radiating pattern in both azimuth and elevation. The geographical terrain (i.e., mountains, valleys, foliage) that might obstruct the user-jammer line-of-sight (LOS) is not modeled. Instead, the LOS limit from the user-to-jammer is determined by the following equation (20:9):

$$\text{LOS LIMIT} = (8.0\ R/3.0)^{\frac{1}{2}}((H_1)^{\frac{1}{2}} + (H_2)^{\frac{1}{2}}) \qquad (79)$$

where:

R = Radius of the earth (2.09×10^7 feet)

H_1 = Jammer height (in feet

H_2 = The user's true height (in feet)

All of the specified jammer parameters are listed in the initialization portion of the IGI's printed output.

This appendix has presented the assumptions, algorithms, and equations associated with the three major modifications to the IGI Simulator. Of the three modifications the null steering antenna algorithm was the most difficult to implement in software.

Appendix C: Extracts from the Modified IGI Simulator Output File

```
100=1BATCH       CREATED 11/21/83  TODAY IS 11/23/83
110=
120=
130=
140= FOR INFORMATION ABOUT PHASE 2 PF REDUCTION,TYPE: SYSBULL,NEWS
150=
160=#EOR
170=0 FLIGHT TRAJECTORY DATA INFORMATION
180=
190=
200=
210=
220=
230=
240= PROBLEM TITLE:  F4 COMBAT ZONE FLIGHT--TIMES 4728-5564 IN COMPLETE MISSION$
250=
260=
270=
280=
290=
300= DATA GENERATED ON  06/23/83  AT  15.39.17. HOURS
```

```
320=1$FDTINIT
330=0NSEGT   = 22,
340=0TSTART  = 0.0,
350=0VTO     = .935E+03,
360=0ROLLO   = 0.0,
370=0PITCHO  = -.2E+01,
380=0HEADO   = .9E+02,
390=0ALFAO   = 0.0,
400=0GLATO   = .38E+02,
410=0TLONO   = -.9E+02,
420=0ALTO    = .275E+05,
430=0IPRNT   = 0,
440=0IRITE   = 1,
450=0IPLOT   = 0,
460=0ROLRAT  = .45E+03,
470=0ROLTC   = .5E+00,
480=0LLMECH  = 1,
490=0LUNIT   = 1,
500=0RELERR  = 0.0,
510=0ABSERR  = 0.0,
520=0IPRSET  = 1, 2, 3, 4, 5, 6, 7, 8, 9, 10, 11, 12, 13, 14, 15, 16, -1, -1, -1,
530=0IRTSET  = 1, 2, 4, 3, 5, 6, 7, 13, 15, -1, -1, -1, -1, -1, -1, -1, -1, -1, -1,
540=0$END
```

```
550=1$FDTSEGS
560=0SEGLNT  = .3E+03, .5E+01, .36E+02, .36E+02, .1E+02, .1E+03, .18E+03, .15E+02,   .25E+02, .5E+01, .25E+01, .26E+02,
570=           .45E+01, .5E+01, .1E+02, .15E+02, .3E+01, .96E+02, .1E+02, .192E+03,  .6E+02, .3E+03, .16E+03, .6E+03, .6E+02,
580=           .65E+03, .6E+02, .29E+04, .3E+02, .136E+03, .6E+02, .481E+03, .4E+03, .5E+01, .6E+02, 0.0, 0.0, 0.0, 0.0,
590=           0.0, 0.0, 0.0, 0.0, 0.0, 0.0, 0.0, 0.0, 0.0, 0.0, 0.0,
600=0KTURN   = 4, 1, 2, 2, 1, 3, 3, 2, 1, 4, 2, 1, 4, 2, 1, 3, 1, 3, 2, 3, 1, 4, 2,  2, 2, 4, 2, 4, 1, 2, 4, 1, 4, 1, 4, 4,
610=           4, 4, 4, 4, 4, 4, 4, 4, 4, 4, 4, 4, 4, 4,
620=0NPATH   = 2, 2, 2, 2, 2, 2, 2, 2, 2, 2, 2, 2, 2, 2, 2, 2, 2, 2, 2, 2, 2, 2, 2, 2,  2, 2, 2, 2, 2, 2, 2, 2, 2, 2, 2, 2,
630=           2, 2, 2, 2, 2, 2, 2, 2, 2, 2, 2, 2, 2, 2,
640=0PACC    = 0.0, -.56E+00, 0.0, 0.0, 0.0, 0.0, 0.0, 0.0, 0.0, 0.0, 0.0, 0.0, 0.0, 0.0, 0.0, 0.0, 0.0, 0.0, 0.0, 0.0, 0.0,
650=           0.0, 0.0, -.1272E-01, 0.0, -.7615E-01, 0.0, .7615E-01, 0.0, 0.0, 0.0, 0.0, -.1185E+00, -.2E-01, 0.0, 0.0, -.124446666E+
660=           0.0, 0.0, 0.0, 0.0, 0.0, 0.0, 0.0, 0.0, 0.0, 0.0, 0.0, 0.0, 0.0, 0.0, 0.0, 0.0, 0.0,
670=0TACC    = 0.0, .1E+01, .45E+01, .45E+01, .2E+01, 0.0, 0.0, .1E+01, .5E+00, 0.0, .1E+01, .16E+01, 0.0, .5E+01, .75E+01,
680=           0.0, .2E+01, 0.0, .375E+01, 0.0, .1E+00, 0.0, .3E+00, .1E+00, .1E+00, 0.0, .1E+00, 0.0, .1E+00, .1E+00, 0.0,
690=           .3E-01, 0.0, .1E+00, 0.0, 0.0, 0.0, 0.0, 0.0, 0.0, 0.0, 0.0, 0.0,     0.0, 0.0, 0.0, 0.0, 0.0, 0.0, 0.0,
700=0ROLL    = 0.0, 0.0, 0.0, 0.0, 0.0, 0.0, 0.0, 0.0, 0.0, 0.0, 0.0, 0.0, 0.0, 0.0, 0.0, 0.0, 0.0, 0.0, 0.0, 0.0, 0.0,
710=           0.0, 0.0, 0.0, 0.0, 0.0, 0.0, 0.0, 0.0, 0.0, 0.0, 0.0, 0.0, 0.0, 0.0, 0.0, 0.0, 0.0, 0.0, 0.0, 0.0, 0.0,
720=           0.0, 0.0, 0.0, 0.0, 0.0, 0.0, 0.0, 0.0,
730=0PITCH   = 0.0, -.45E+01, 0.0, 0.0, .81E+01, .25E+02, .3E+02, 0.0, -.156E+01,     0.0, 0.0, -.45E+02, 0.0, 0.0, .5E+02,
740=           .75E+01, .15E+01, .16E+02, 0.0, .24E+02, -.65E+01, 0.0, 0.0, 0.0,     0.0, 0.0, 0.0, -.7E+01, 0.0, 0.0, .4180107E+
750=           0.0, .2819893E+01, 0.0, 0.0, 0.0, 0.0, 0.0, 0.0, 0.0, 0.0, 0.0, 0.0, 0.0,  0.0, 0.0, 0.0, 0.0, 0.0, 0.0, 0.0,
760=0HEAD    = 0.0, 0.0, .36E+03, -.36E+03, 0.0, .25E+02, -.15E+02, .5E+01, 0.0,     0.0, .2E+01, 0.0, 0.0, .3E+02, 0.0,
770=           -.6E+01, 0.0, .17E+02, .72E+02, -.15E+02, 0.0, 0.0, .35E+02, .44E+02, .1E+01, 0.0, .26798E+00, 0.0, 0.0,
780=           -.31207E+02, 0.0, 0.0, 0.0, 0.0, 0.0, 0.0, 0.0, 0.0, 0.0, 0.0, 0.0,  0.0, 0.0, 0.0, 0.0, 0.0, 0.0, 0.0,
790=           0.0, 0.0,
800=0DTPR    = .1E+26, .1E+26, .1E+26, .1E+26, .1E+26, .1E+26, .1E+26, .1E+26,       .1E+26, .1E+26, .1E+26, .1E+26, .1E+26,
810=           .1E+26, .1E+26, .1E+26, .1E+26, .1E+26, .1E+26, .1E+26, .1E+26,       .1E+26, .1E+26, .1E+26, .1E+26, .1E+26,
820=           .1E+26, .1E+26, .1E+26, .1E+26, .1E+26, .1E+26, .1E+26, .1E+26,       .1E+26, .1E+26, .1E+26, .1E+26, .1E+26,
830=           .1E+26, .1E+26, .1E+26, .1E+26, .1E+26, .1E+26, .1E+26, .1E+26,       .1E+26, .1E+26, .1E+26,
840=0DTRI    = .5E+00, .5E+00, .5E+00, .5E+00, .5E+00, .5E+00, .5E+00, .5E+00,       .5E+00, .5E+00, .5E+00, .5E+00, .5E+00,
850=           .5E+00, .5E+00, .5E+00, .5E+00, .5E+00, .5E+00, .5E+00, .5E+00,       .5E+00, .1E+09, .1E+09, .1E+09, .1F09,
860=           .1E+09, .1E+09, .1E+09, .1F+09, .1E+09, .1F09, .1E+09, .1E+09,        .1E+09, .1E+09, .1E+09, .1E+09, .1E+09,
870=           .1E+09, .1E+09, .1E+09, .1E+09, .1E+09, .1E+09, .1E+09, .1E+09,       .1E+09, .1E+09, .1E+09,
880=0DTPL    = .1E+26, .1E+26, .1E+26, .1E+26, .1E+26, .1E+26, .1E+26, .1E+26,       .1E+26, .1E+26, .1E+26, .1E+26, .1E+26,
890=           .1E+26, .1E+26, .1E+26, .1E+26, .1E+26, .1E+26, .1E+26, .1E+26,       .1E+26, .1E+26, .1E+26, .1E+26, .1E+26,
900=           .1E+26, .1E+26, .1E+26, .1E+26, .1E+26, .1E+26, .1E+26, .1E+26,       .1E+26, .1E+26, .1E+26, .1E+26, .1E+26,
910=           .1E+26, .1E+26, .1E+26, .1E+26, .1E+26, .1E+26, .1E+26, .1E+26,       .1E+26, .1E+26, .1E+26,
920=0KRSTRT  = 0, 0, 0, 0, 0, 0, 0, 0, 0, 0, 0, 0, 0, 0, 0, 0, 0, 0, 0, 0, 0, 0, 0, 0,  0, 0, 0, 0, 0, 0, 0, 0, 0, 0, 0, 0,
930=           0, 0, 0, 0, 0, 0, 0, 0, 0, 0, 0, 0, 0, 0,
940=0MODE    = 1, 1, 1, 1, 1, 1, 1, 1, 1, 1, 1, 1, 1, 1, 1, 1, 1, 1, 1, 1, 1, 1, 1, 1,  1, 1, 1, 1, 1, 1, 1, 1, 1, 1, 1, 1,
950=           1, 1, 1, 1, 1, 1, 1, 1, 1, 1, 1, 1, 1, 1, 1, 1,
960=0ERROR   = .1E-05, .1E-05, .1E-05, .1E-05, .1E-05, .1E-05, .1E-05, .1E-05,       .1E-05, .1E-05, .1E-05, .1E-05, .1E-05,
970=           .1E-05, .1E-05, .1E-05, .1E-05, .1E-05, .1E-05, .1E-05, .1E-05,       .1E-05, .1E-05, .1E-05, .1E-05, .1E-05,
980=           .1E-05, .1E-05, .1E-05, .1E-05, .1E-05, .1E-05, .1E-05, .1E-05,       .1E-05, .1E-05, .1E-05, .1E-05, .1E-05,
990=           .1E-05, .1E-05, .1E-05, .1E-05, .1E-05, .1E-05, .1E-05, .1E-05,       .1E-05, .1E-05, .1E-05,
1000=0HMAX   = .1E+05, .1E+05, .1E+05, .1E+05, .1E+05, .1E+05, .1E+05, .1E+05,       .1E+05, .1E+05, .1E+05, .1E+05, .1E+05,
1010=          .1E+05, .1E+05, .1E+05, .1E+05, .1E+05, .1E+05, .1E+05, .1E+05,       .1E+05, .1E+05, .1E+05, .1E+05, .1E+05,
1020=          .1E+05, .1E+05, .1E+05, .1E+05, .1E+05, .1E+05, .1E+05, .1E+05,       .1E+05, .1E+05, .1E+05, .1E+05, .1E+05,
1030=          .1E+05, .1E+05, .1E+05, .1E+05, .1E+05, .1E+05, .1E+05, .1E+05,       .1E+05, .1E+05, .1E+05,
1040=0HMIN   = .2E-03, .2E-03, .2E-03, .2E-03, .2E-03, .2E-03, .2E-03, .2E-03,       .2E-03, .2E-03, .2E-03, .2E-03, .2E-03,
1050=          .2E-03, .2E-03, .2E-03, .2E-03, .2E-03, .2E-03, .2E-03, .2E-03,       .2E-03, .1E+01, .1E+01, .1E+01, .1E+01,
1060=          .1E+01, .1E+01, .1E+01, .1E+01, .1E+01, .1E+01, .1E+01, .1E+01,       .1E+01, .1E+01, .1E+01, .1E+01, .1E+01,
1070=          .1E+01, .1E+01, .1E+01, .1E+01, .1E+01, .1E+01, .1E+01, .1E+01,       .1E+01, .1E+01, .1E+01,
1080=0$END
```

```
1090=1$INDICES
1100=0NF       = 16,
1110=0NT       = 61,
1120=0N1F      = 136,
1130=0M        = 8,
1140=0NPPUD    = 25,
1150=0NREC     = 0,
1160=0NPPUD1   = 20,
1170=0NCLOCKP  = 10,
1180=0$END
1190=1$CLOCK1
1200=0T0       = 0.0,
1210=0TF       = .14E+04,
1220=0DT       = .5E+00,
1230=0DTINV    = .2E+01,
1240=0DRINT    = .1E+01,
1250=0$END
1260=1$JAMINP
1270=0TLOSS    = .6E+01,
1280=0TREAQ    = .17E+02,
1290=0DTMEAS   = .5E+01,
1300=0AJMLVL   = .35E+02,
1310=0AJMASK   = .18E+03,
1320=0NUMJAMS  = 25,
1330=0$END
1340=1$CLOCK2
1350=0DTPRNT   = .1E+03,
1360=0DTPLOT   = .5E+01,
1370=0DTPICK   = .3E+03,
1380=0STARTPL  = 0.0,
1390=0TREC     = 0.0,
1400=0$END
1410=1$AUXVAR
1420=0RNSEED   = .3E+00,
1430=0VIEWANG  = .85E+02,
1440=0$END
1450=1$JAMMR2
1460=0AJLAT    = .37995E+02, .3799E+02, .37965E+02, .3795E+02, .37945E+02, .37995E+02, .3799E+02, .37965E+02, .3795E+02, .37945E+02
1470=            .37995E+02, .3799E+02, .37965E+02, .3795E+02, .37945E+02, .37995E+02, .3799E+02, .37965E+02, .3795E+02, .37945E+02
1480=            .37995E+02, .3799E+02, .37965E+02, .3795E+02, .37945E+02,
1490=0AJLON    = -.8805E+02, -.8805E+02, -.8805E+02, -.8805E+02, -.8805E+02,           -.8795E+02, -.8795E+02, -.8795E+02,
1500=            -.8795E+02, -.8795E+02, -.879E+02, -.879E+02, -.879E+02, -.879E+02,  -.879E+02, -.8785E+02, -.8785E+02,
1510=            -.8785E+02, -.8785E+02, -.8785E+02, -.8775E+02, -.8775E+02,          -.8775E+02, -.8775E+02, -.8775E+02,
1520=0AJELEV   = .1E+02, .1E+02, .1E+02, .1E+02, .1E+02, .1E+02, .1E+02, .1E+02,      .1E+02, .1E+02, .1E+02, .1E+02, .1E+02,
1530=            .1E+02, .1F+02, .1F+02, .1E+02, .1E+02, .1E+02, .1E+02, .1E+02,      .1F+02, .1E+02, .1F+02, .1E+02,
1540=0AJVE     = 0.0, 0.0, 0.0, 0.0, 0.0, 0.0, 0.0, 0.0, 0.0, 0.0, 0.0, 0.0, 0.0, 0.0, 0.0, 0.0, 0.0, 0.0, 0.0, 0.0, 0.0, 0.0,
1550=            0.0, 0.0, 0.0, 0.0,
1560=0AJVN     = 0.0, 0.0, 0.0, 0.0, 0.0, 0.0, 0.0, 0.0, 0.0, 0.0, 0.0, 0.0, 0.0, 0.0, 0.0, 0.0, 0.0, 0.0, 0.0, 0.0, 0.0, 0.0,
1570=            0.0, 0.0, 0.0, 0.0,
1580=0AJVZ     = 0.0, 0.0, 0.0, 0.0, 0.0, 0.0, 0.0, 0.0, 0.0, 0.0, 0.0, 0.0, 0.0, 0.0, 0.0, 0.0, 0.0, 0.0, 0.0, 0.0, 0.0, 0.0,
1590=            0.0, 0.0, 0.0, 0.0,
1600=0AJPWER   = .1F+00, .1E+00, .1E+00, .1E+00, .1E+00, .1E+00, .1E+01, .1E+01,      .1E+01, .1E+00, .1E+00, .1E+01, .2E+01,
1610=            .1E+01, .1E+00, .1E+00, .1E+01, .1F+01, .1E+01, .1E+00, .1F+00,      .1E+00, .1E+00, .1E+00, .1E+00,
1620=0$END
```

```
1630=0 INITTAL TRUE ERROR STATE;DXT =
1640=
1650=  2.3923E-06  2.3923E-06  5.0000E+01  1.0000E+00  1.0000E+00  1.0000E-01 -2.1200E-04  2.2100E-04  7.5400E-04  3.0000E-02
1660=  1.0720E-02  5.0000E+01  5.0000E-02  1.4554E-08  1.4554E-08 -1.4300E-06  4.5200E-08  4.5200E-08  4.5200E-08  4.5200E-08
1670=  4.5200E-08  4.5200E-08  1.8740E-10  1.8740E-10  1.8740E-10  3.0000E-04  3.0000E-04  1.0000E-03  1.9400E-04 -1.9400E-04
1680= -1.9400E-04  1.9400E-04  1.9400E-04 -1.9400E-04  1.6100E-03  1.6100E-03  3.2200E-03  1.5000E-04  1.5000E-04  1.5000E-04
1690= -1.4600E-04  8.7200E-04  1.4600E-04 -8.7200E-04 -1.4200E-04  1.4200E-04  5.0000E+02  8.3720E-04  5.4700E-04  1.1270E-03
1700=  2.0700E-07  1.0000E+01  1.5400E-04  2.5000E-01  3.1000E-02  3.1000E-02  3.1000E-02  1.0000E+01  1.0000E+01  1.0000E+01
1710=  1.0000E+01
1720=0 INITIAL FILTER ERROR STATE;DXF =
1730=
1740=  0.          0.          0.          0.          0.          0.          0.          0.          0.          0.
1750=  0.          0.          0.          0.          0.          0.
1760=1$MEASTYP
1770=0MEASID  = 1, 2, 1, 2, 1, 2, 1, 2, 0,
1780=0$END
1790=1$OBSSTAT
1800=0SIGRT   = .7E+01,
1810=0SIGRRT  = .7E+00,
1820=0SIGRF   = .15E+02,
1830=0SIGRRF  = .15E+01,
1840=0$END
```

```
1850=0 INITIAL FILTER COVARIANCE MATRIX;PF =
1860=
1870=   5.72E-12   0.          0.          0.          0.          0.          0.          0.          0.          0.
1880=   0.         0.          0.          0.          0.          0.
1890=   0.         5.72E-12    0.          0.          0.          0.          0.          0.          0.          0.
1900=   0.         0.          0.          0.          0.          0.
1910=   0.         0.          2.50E+03    0.          0.          0.          0.          0.          0.          0.
1920=   0.         0.          0.          0.          0.          0.
1930=   0.         0.          0.          1.00E+00    0.          0.          0.          0.          0.          0.
1940=   0.         0.          0.          0.          0.          0.
1950=   0.         0.          0.          0.          1.00E+00    0.          0.          0.          0.          0.
1960=   0.         0.          0.          0.          0.          0.
1970=   0.         0.          0.          0.          0.          1.00E-02    0.          0.          0.          0.
1980=   0.         0.          0.          0.          0.          0.
1990=   0.         0.          0.          0.          0.          0.          1.00E-08    0.          0.          0.
2000=   0.         0.          0.          0.          0.          0.
2010=   0.         0.          0.          0.          0.          0.          0.          1.00E-08    0.          0.
2020=   0.         0.          0.          0.          0.          0.
2030=   0.         0.          0.          0.          0.          0.          0.          0.          2.50E-07    0.
2040=   0.         0.          0.          0.          0.          0.
2050=   0.         0.          0.          0.          0.          0.          0.          0.          0.          2.50E+03
2060=   0.         0.          0.          0.          0.          0.
2070=   0.         0.          0.          0.          0.          0.          0.          0.          0.          0.
2080=   5.00E+00   0.          0.          0.          0.          0.
2090=   0.         0.          0.          0.          0.          0.          0.          0.          0.          0.
2100=   0.         2.12E-16    0.          0.          0.          0.
2110=   0.         0.          0.          0.          0.          0.          0.          0.          0.          0.
2120=   0.         0.          2.12E-16    0.          0.          0.
2130=   0.         0.          0.          0.          0.          0.          0.          0.          0.          0.
2140=   0.         0.          0.          5.86E-16    0.          0.
2150=   0.         0.          0.          0.          0.          0.          0.          0.          0.          0.
2160=   0.         0.          0.          0.          1.15E-04    0.
2170=   0.         0.          0.          0.          0.          0.          0.          0.          0.          0.
2180=   0.         0.          0.          0.          0.          2.50E+05
2190=I$GAINS
2200=0XK1       = .3E-01,
2210=0XK2       = .3E-03,
2220=0XK3       = .1E-05,
2230=0$END
2240=I$STATIST
2250=0STAT12    = .1E+01,
2260=0STAT14    = .242E-09,
2270=0STAT15    = .242E-09,
2280=0STAT16    = .403E-09,
2290=0STAT35    = .537E-04,
2300=0STAT36    = .537E-04,
2310=0STAT37    = .537E-04,
2320=0STAT4     = .5E+03,
2330=0STAT40    = .83648E-04,
2340=0STAT41    = .54695E-03,
                  .12603E-02,
                  .1E+02,
                  .15190B7E+07,
                  .2611E+05,
                  .2611E+05,
```

AD-A138 070 GLOBAL POSITIONING SYSTEM SATELLITE SELECTION 3/3
EVALUATION FOR AIDED INERTI..(U) AIR FORCE INST OF TECH
WRIGHT-PATTERSON AFB OH SCHOOL OF ENGI.. P M VACCARO
UNCLASSIFIED DEC 83 AFIT/GE/EE/83D-67 F/G 17/7 NL

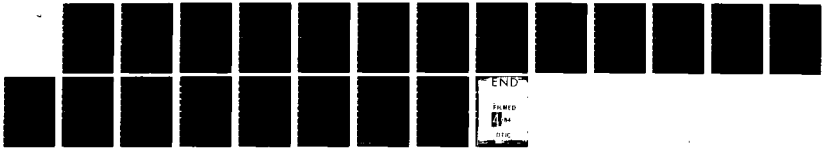

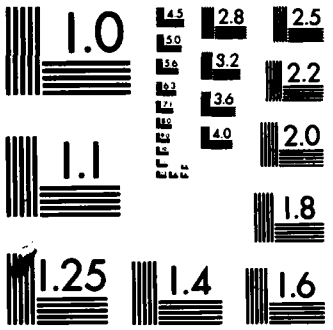

```
2400=0DGZ      = .3645649E+06,
2410=0D52      = .72E+04,
2420=0SIGTXT   = .1E+02,
2430=0BETTXT   = .33333333E-02,
2440=0$END
2450=1$FILSTAT
2460=0SIGMA    = 0.0, 0.0, 0.0, 0.0, 0.0, 0.0, 0.0, 0.0, 0.0, .1E+01, .1666667E+00,    .242E-09, .242E-09, .403E-09, .537E-04,
2470=0DALT16   = .152E+07,
2480=0SIGF16   = .5E+03,
2490=0SIGF17   = .3E-01,
2500=0BETA17   = .13888889E-03,
2510=0SIGF11   = .1E+02,
2520=0BETA11   = .138889E-03,
2530=0SIGM1    = .872E-03,
2540=0SIGM2    = .452E-07,
2550=0SIGNM1   = .537E-04,
2560=0DGZ      = .3648E+06,
2570=0SIGGZ    = .1127E-02,
2580=0DGE      = .608E+05,
2590=0SIGGE    = .8372E-03,
2600=0DGN      = .608E+05,
2610=0SIGGN    = .547E-03,
2620=0SIGARZ   = .537E-04,
2630=0$END
```

```
2640=0TIME =      0.00 - ************************************************************************************************************************
*
2650=0WHOLE VALUE USER POSITION AND VELOCITY
2660=       LON(RAD)              LAT(RAD)              ALT(FT)              VE(FPS)              VN(FPS)              V7(FPS)
2670=    -.157079632679E+01    .663225115758E+00    .275000000000E+05    .934430423263E+03    .116763904745E-10   -.326310294168E+02
2680=    -.157079393445E+01    .663227508102E+00    .275500000000E+05    .935430423263E+03    .100000000001E+01   -.325310294168E+02
2690=    -.157079393445E+01    .663227508102E+00    .275500000000E+05    .935430423263E+03    .100000000001E+01   -.325310294168E+02
2700=
2710= SQRT OF FILTER COVARIANCE DIAGONAL
2720=  2.3923E-06  2.3923E-06  5.0000E+01  1.0000E+00  1.0000E+00  1.0000E-01  1.0000E-04  1.0000E-04  5.0000E-04  5.0000E+01
2730=  2.2361E+00  1.4554E-08  1.4554E-08  2.4199E-08  1.0719E-02  5.0000E+02
2740=0ELEMENTS OF FILTER ERROR STATE VECTOR DXF
2750=  0.          0.          0.          0.          0.          0.          0.          0.          0.          0.
2760=  0.          0.          0.          0.          0.          0.
2770=0ELEMENTS OF TRUE ERROR STATE VECTOR DXT
2780=  2.3923E-06  2.3923E-06  5.0000E+01  1.0000E+00  1.0000E+00  1.0000E-01 -2.1200E-04  2.2100E-04  7.5400E-04  3.0000E-02
2790=  1.0720E-02  5.0000E+01  5.0000E-02  1.4554E-08  1.4554E-08 -1.4300E-06  4.5200E-08  4.5200E-08  4.5200E-08  4.5200E-08
2800=  4.5200E-08  4.5200E-08  1.8740E-10  1.8740E-10  1.8740E-10  3.0000E-04  3.0000E-04  1.0000E-03  1.9400E-04 -1.9400E-04
2810= -1.9400E-04  1.9400E-04  1.9400E-04 -1.9400E-04  1.6100E-03  1.6100E-03  3.2200E-03  1.5000E-04  1.5000E-04  1.5000E-04
2820= -1.4600E-04  8.7200E-04  1.4600E-04 -8.7200E-04 -1.4200E-04  1.4200E-04  5.0000E+02  8.3720E-04  5.4700E-04  1.1270E-03
2830=  2.0700E-07  1.0000E+01  1.5400E-04  2.5000E-01  3.1000E-02  3.1000E-02  3.1000E-02  1.0000E+01  1.0000E+01  1.0000E+01
2840=  1.0000E+01
2850=0ELEMENTS OF FILTER ESTIMATION ERROR XF-XT
2860=  2.3923E-06  2.3923E-06  5.0000E+01  1.0000E+00  1.0000E+00  1.0000E-01 -2.1200E-04  2.2100E-04  7.5400E-04  5.0000E+01
2870=  1.0019E+01  1.4554E-08  1.4554E-08 -1.4300E-06  6.2230E-03  1.3250E+03
2880=0HORIZON SCAN AT TIME =      0.00
2890=0DEBUG:JNUMBR= 25
2900=0DEBUG: NSEDEN(DB'S)=  -2.0200E+02
2910=0CARRIER-TO-NOISE DENSITY=    2.5139E+01
2920=0CARRIER-TO-NOISE DENSITY=    2.5042E+01
2930=0CARRIER-TO-NOISE DENSITY=    2.3996E+01
2940=0CARRIER-TO-NOISE DENSITY=    2.7335E+01
2950=0CARRIER-TO-NOISE DENSITY=    2.3157E+01
2960=0RMEAS(I)=      15.1411
2970=0RMEAS(I)=      15.1474
2980=0RMEAS(I)=      15.1975
2990=0RMEAS(I)=      14.9412
3000=0RMEAS(I)=      15.2102
3010=0THE IN VIEW SATELLITE SET IS
3020=0SATELLITE      ORBIT
3030=          1          3
3040=          1          4
3050=          2          4
3060=          2          5
3070=          3          2
3080=0THE OPTIMUM SATELLITE GROUP IS
3090=0SATELLITE      ORBIT
3100=          1          3
3110=          2          4
3120=          2          5
3130=          3          2
3140=0FOR THIS SATELLITE GROUP,GDOP =    4.7068E+00
3150=0 FOR THIS SATELLITE SET THE COST=    2.6519E+02
```

```
17660=0TIME =    600.00 - ************************************************************************************************************************
*
17670=0WHOLE VALUE USER POSITION AND VELOCITY
17680=       LON(RAD)              LAT(RAD)              ALT(FT)              VE(FPS)              VN(FPS)              VZ(FPS)
17690=   -.154239545746E+01    .663245263822E+00    .155231935410E+05    .816965122291E+03   -.213930248535E+03    .235893133900E+02
17700=   -.154239976622E+01    .663270685621E+00    .167099810937E+05    .814587380423E+03   -.213487554556E+03    .578608187920E+02
17710=   -.154239388353E+01    .663243709424E+00    .155355427488E+05    .817956771314E+03   -.214707695107E+03    .457714807283E+01
17720=
17730= SQRT OF FILTER COVARIANCE DIAGONAL
17740=  1.6749E-06  1.1028E-06  4.5412E+01  1.0712F+00  1.0815E+00  8.2243F+00  2.4241E-04  2.4264E-04  4.7187E-04  3.5620E+01
17750=  1.0692E+00  1.5710E-08  1.5710E-08  2.6134E-08  1.1082E-02  1.2671E+02
17760=0ELEMENTS OF FILTER ERROR STATE VECTOR DXF
17770= -5.8827E-06  2.6976E-05  1.1744E+03 -3.3694E+00  1.2201E+00  5.3284E+01 -7.5165E-05  9.4682E-05  1.1903E-04  1.8374E+03
17780=  6.2339E-01 -3.0324E-10  3.7469E-10  3.2403E-11 -5.6426E-02  1.1326E+03
17790=0ELEMENTS OF TRUE ERROR STATE VECTOR DXT
17800= -4.3088F-06  2.5422E-05  1.1868E+03 -2.3777E+00  4.4269E-01  3.4272E+01 -2.5358E-04  2.4465E-04  7.7302E-04  3.0000F-02
17810= -2.7173E-02  1.8356E+03  5.0124E-02  1.6841E-08  1.4912E-08 -1.4485E-06  4.5200E-08  4.5200E-08  4.5200E-08  4.5200E-08
17820=  4.5200E-08  4.5200E-08  1.8740E-10  1.8740E-10  1.8740E-10  3.0000E-04  3.0000E-04  1.0000E-03  1.9400E-04 -1.9400E-04
17830= -1.9400E-04  1.9400E-04  1.9400E-04 -1.9400E-04 -5.0804E-04  1.8065E-03  3.5325E-04  1.5000E-04  1.5000E-04  1.5000E-04
17840= -1.4600E-04  8.7200E-04  1.4600E-04 -8.7200E-04 -1.4200E-04  1.4200E-04  5.5375E+02 -1.7727E-04 -8.8620E-04  1.4889E-03
17850=  2.0700E-07  2.5223E+00  1.5400E-04  2.5000E-01  3.1000E-02  3.1000E-02  3.1000E-02 -4.9648E+00  1.8969E+01  4.2554E+00
17860= -8.6517E+00
17870=0ELEMENTS OF FILTER ESTIMATION ERROR XF-XT
17880=  1.5739E-06 -1.5544E-06  1.2349E+01  9.9165E-01 -7.7745E-01 -1.9012E+01 -1.7841E-04  1.4997E-04  6.5400E-04 -1.8138E+00
17890=  8.1555E-01  1.7144E-08  1.4537E-08 -1.4485E-06  2.7261F-02 -1.1319E+02
17900=0DEBUG: JNUMBR= 25
17910=0DEBUG: NSEDEN(DB'S)=  -2.0200E+02
17920=0CARRIER-TO-NOISE DENSITY=   2.5558E+01
17930=0CARRIER-TO-NOISE DENSITY=   2.5899E+01
17940=0CARRIER-TO-NOISE DENSITY=   2.5890E+01
17950=0CARRIER-TO-NOISE DENSITY=   2.7423E+01
17960=0CARRIER-TO-NOISE DENSITY=   3.1338E+01
17970=0RMEAS(I)=      15.1110
17980=0RMEAS(I)=      15.0832
17990=0RMEAS(I)=      15.0840
18000=0RMEAS(I)=      14.9314
18010=0RMEAS(I)=      14.5951
```

```
17660=0TIME =    600.00 - ************************************************************************************************************
*
17670=0WHOLE VALUE USER POSITION AND VELOCITY
17680=       LON(RAD)              LAT(RAD)              ALT(FT)              VE(FPS)              VN(FPS)              VZ(FPS)
17690=    -.154239545746E+01    .663245263822E+00    .155231935410E+05    .816965122291E+03   -.213930248535E+03    .235893133900E+02
17700=    -.154239976622E+01    .663270685621E+00    .167099810937E+05    .814587380423E+03   -.213487554556F+03    .578608187920E+02
17710=    -.154239388353E+01    .663243709424E+00    .155355427488E+05    .817956771314E+03   -.214707695107E+03    .457714807283E+01
17720=
17730= SQRT OF FILTER COVARIANCE DIAGONAL
17740=  1.6749E-06  1.1028E-06  4.5412E+01  1.0712E+00  1.0815E+00  8.2243E+00  2.4241E-04  2.4264E-04  4.7187E-04  3.5620E+01
17750=  1.0692E+00  1.5710E-08  1.5710E-08  2.6134E-08  1.1082E-02  1.2671E+02
17760=0ELEMENTS OF FILTER ERROR STATE VECTOR DXF
17770= -5.8827E-06  2.6976E-05  1.1744E+03 -3.3694E+00  1.2201E+00  5.3284E+01 -7.5165E-05  9.4682E-05  1.1903E-04  1.8374E+03
17780=  6.2339E-01 -3.0324E-10  3.7469E-10  3.2403E-11 -5.6426E-02  1.1326E+03
17790=0ELEMENTS OF TRUE ERROR STATE VECTOR DXT
17800= -4.3088E-06  2.5422E-05  1.1868E+03 -2.3777E+00  4.4269E-01  3.4272E+01 -2.5358E-04  2.4465E-04  7.7302F-04  3.0000F-02
17810= -2.7173E-02  1.8356E+03  5.0124E-02  1.6841E-08  1.4912E-08 -1.4485E-06  4.5200E-08  4.5200E-08  4.5200E-08  4.5200E-08
17820=  4.5200E-08  4.5200E-08  1.8740E-10  1.8740E-10  1.8740E-10  3.0000E-04  3.0000E-04  1.0000E-03  1.9400E-04 -1.9400E-04
17830= -1.9400E-04  1.9400E-04  1.9400E-04 -1.9400E-04 -5.0804E-04  1.8065E-03  3.5325E-04  1.5000E-04  1.5000E-04  1.5000E-04
17840= -1.4600E-04  8.7200F-04  1.4600E-04 -8.7200E-04 -1.4200E-04  1.4200E-04  5.5375E+02 -1.7727E-04 -8.8620E-04  1.4889E-03
17850=  2.0700E-07  2.5223E+00  1.5400E-04  2.5000E-01  3.1000E-02  3.1000E-02  3.1000E-02 -4.9648E+00  1.8969E+01  4.2554E+00
17860= -8.6517E+00
17870=0ELEMENTS OF FILTER ESTIMATION ERROR XF-XT
17880=  1.5739E-06 -1.5544E-06  1.2349E+01  9.9165E-01 -7.7745E-01 -1.9012E+01 -1.7841E-04  1.4997E-04  6.5400E-04 -1.8138E+00
17890=  8.1555E-01  1.7144F-08  1.4537E-08 -1.4485E-06  2.7261E-02 -1.1319E+02
17900=0DEBUG:JNUMBR= 25
17910=0DEBUG: NSFDEN(DB'S)=  -2.0200E+02
17920=0CARRIER-TO-NOISE DENSITY=    2.5558E+01
17930=0CARRIER-TO-NOISE DENSITY=    2.5899E+01
17940=0CARRIER-TO-NOISE DENSITY=    2.5890E+01
17950=0CARRIER-TO-NOISE DENSITY=    2.7423E+01
17960=0CARRIER-TO-NOISE DENSITY=    3.1338E+01
17970=0RMEAS(I)=      15.1110
17980=0RMEAS(I)=      15.0832
17990=0RMEAS(I)=      15.0840
18000=0RMEAS(I)=      14.9314
18010=0RMEAS(I)=      14.5951
```

```
18020=0TIME =    600.00 + ************************************************************************************************************************
*
18030= SQRT OF FILTER COVARIANCE DIAGONAL
18040=  1.2248E-06  7.1646E-07  3.2307E+01  8.1263E-01  8.2466E-01  8.2152E+00  2.4028E-04  2.4051E-04  4.7078E-04  2.7374E+01
18050=  8.9500E-01  1.5710E-08  1.5710E-08  2.6134E-08  1.1028E-02  6.6578E+01
18060=0ELEMENTS OF FILTER ERROR STATE VECTOR DXF
18070= -4.9393E-06  2.5860E-05  1.1270E+03 -4.6397E+00  6.2240E-01  5.3048E+01 -1.0704E-04  1.5065E-04  2.8357E-04  1.8787E+03
18080=  2.5633E+00 -3.4639E-10  4.6004E-10  2.5441E-10 -5.5080E-02  1.0291E+03
18090=0ELEMENTS OF FILTER ESTIMATION ERROR XF-XT
18100=  6.3058E-07 -4.3835E-07  5.9811E+01  2.2620E+00 -1.7971E-01 -1.8776E+01 -1.4654E-04  9.3998E-05  4.8946E-04 -4.3156E+01
18110= -1.1244E+00  1.7187E-08  1.4452E-08 -1.4487E-06  2.5915E-02 -9.6533E+00
18120=0HORIZON SCAN AT TIME =    600.00
18130=0DEBUG:JNUMBR= 25
18140=0DEBUG: NSEDEN(DB'S)=  -2.0200E+02
18150=0CARRIER-TO-NOISE DENSITY=   2.5558E+01
18160=0CARRIER-TO-NOISE DENSITY=   2.5899E+01
18170=0CARRIER-TO-NOISE DENSITY=   2.5890E+01
18180=0CARRIER-TO-NOISE DENSITY=   2.7423E+01
18190=0CARRIER-TO-NOISE DENSITY=   3.1338E+01
18200=0RMEAS(I)=     15.1110
18210=0RMEAS(I)=     15.0832
18220=0RMEAS(I)=     15.0840
18230=0RMEAS(I)=     14.9314
18240=0RMEAS(I)=     14.5951
18250=0THE IN VIEW SATELLITE SET IS
18260=0SATELLITE     ORBIT
18270=          1         3
18280=          1         4
18290=          2         4
18300=          2         5
18310=          3         2
18320=0THE OPTIMUM SATELLITE GROUP IS
18330=0SATELLITE     ORBIT
18340=          1         3
18350=          2         4
18360=          2         5
18370=          3         2
18380=0FOR THIS SATELLITE GROUP,GDOP =   5.2302E+00
18390=0 FOR THIS SATELLITE SET THE COST=   1.5408E-10
```

```
18020=0TIME =    600.00 + ************************************************************************************************************************
*
18030= SQRT OF FILTER COVARIANCE DIAGONAL
18040=  1.2248E-06  7.1646E-07  3.2307E+01  8.1263E-01  8.2466E-01  8.2152E+00  2.4028E-04  2.4051E-04  4.7078E-04  2.7374E+01
18050=  8.9500E-01  1.5710E-08  1.5710E-08  2.6134E-08  1.1028E-02  6.6578E+01
18060=0ELEMENTS OF FILTER ERROR STATE VECTOR DXF
18070= -4.9393E-06  2.5860E-05  1.1270E+03 -4.6397E+00  6.2240E-01  5.3048E+01 -1.0704E-04  1.5065E-04  2.8357E-04  1.8787E+03
18080=  2.5633E+00 -3.4639E-10  4.6004E-10  2.5441E-10 -5.5080E-02  1.0291E+03
18090=0ELEMENTS OF FILTER ESTIMATION ERROR XF-XT
18100=  6.3058E-07 -4.3835E-07  5.9811E+01  2.2620E+00 -1.7971E-01 -1.8776E+01 -1.4654E-04  9.3998E-05  4.8946E-04 -4.3156E+01
18110= -1.1244E+00  1.7187E-08  1.4452E-08 -1.4487E-06  2.5915E-02 -9.6533E+00
18120=0HORIZON SCAN AT TIME =    600.00
18130=0DEBUG:JNUMRR= 25
18140=0DEBUG: NSEDEN(DB'S)=  -2.0200E+02
18150=0CARRIER-TO-NOISE DENSITY=   2.5558E+01
18160=0CARRIER-TO-NOISE DENSITY=   2.5899E+01
18170=0CARRIER-TO-NOISE DENSITY=   2.5890E+01
18180=0CARRIER-TO-NOISE DENSITY=   2.7423E+01
18190=0CARRIER-TO-NOISE DENSITY=   3.1338E+01
18200=0RMEAS(I)=      15.1110
18210=0RMEAS(I)=      15.0832
18220=0RMEAS(I)=      15.0840
18230=0RMEAS(I)=      14.9314
18240=0RMEAS(I)=      14.5951
18250=0THE IN VIEW SATELLITE SET IS
18260=0SATELLITE      ORBIT
18270=          1          3
18280=          1          4
18290=          2          4
18300=          2          5
18310=          3          2
18320=0THE OPTIMUM SATELLITE GROUP IS
18330=0SATELLITE      ORBIT
18340=          1          3
18350=          2          4
18360=          2          5
18370=          3          2
18380=0FOR THIS SATELLITE GROUP,GDOP =   5.2302E+00
18390=0 FOR THIS SATELLITE SET THE COST=   1.5408E-10
```

```
31980=OTIME =    1100.00 - ********************************************************************************************************************
*
31990=OWHOLE VALUE USER POSITION AND VELOCITY
32000=       LON(RAD)              LAT(RAD)              ALT(FT)              VE(FPS)              VN(FPS)              VZ(FPS)
32010=    -.153354902831E+01    .651409423922E+00    .341540092922E+05   -.274353415334E+03   -.796730622321E+03    .608697998663E+02
32020=    -.153370170363E+01    .651435880308E+00    .356322685545E+05   -.281459710337E+03   -.797077068358E+03    .115359845547E+03
32030=    -.153354302602E+01    .651410490963E+00    .340657328228E+05   -.271240596488E+03   -.795744212447E+03    .279329379171E+02
32040=
32050= SQRT OF FILTER COVARIANCE DIAGONAL
32060=  9.4606E-07  1.0643E-06  6.0001E+01  5.7541E-01  7.2458E-01  1.3833E+01  2.7168E-04  2.6926E-04  5.2383E-04  1.8804E+01
32070=  8.9441E-01  1.6611E-08  1.6611E-08  2.7643E-08  1.1318E-07  2.6764E+02
32080=OELEMENTS OF FILTER ERROR STATE VECTOR DXF
32090= -1.5868E-04  2.5389E-05  1.5665E+03 -1.0219E+01 -1.3129E+00  8.7427E+01 -2.2715E-04 -1.0097E-04  1.7459E-04  3.4424E+03
32100=  8.7823E+00 -5.3721E-10  2.2572E-10  2.4366E-10 -7.0166E-02  1.8565E+03
32110=OELEMENTS OF TRUE ERROR STATE VECTOR DXT
32120= -1.5268E-04  2.6456E-05  1.4783E+03 -7.1063E+00 -3.4645E-01  5.4490E+01 -2.8919E-04  1.3119E-04  6.6870E-04  3.0000E-02
32130= -3.6889E-02  3.3611E+03  5.0228E-02  1.1443E-08  1.7744E-08 -1.4551E-06  4.5200E-08  4.5200E-08  4.5200E-08  4.5200E-08
32140=  4.5200E-08  4.5200E-08  1.8740E-10  1.8740E-10  1.8740E-10  3.0000E-04  3.0000E-04  1.0000E-03  1.9400E-04 -1.9400E-04
32150= -1.9400E-04  1.9400E-04  1.9400E-04 -1.9400E-04 -2.5847E-03  6.4575E-04  6.7198E-04  1.5000E-04  1.5000E-04  1.5000E-04
32160= -1.4600E-04  8.7200E-04  1.4600E-04 -8.7200E-04 -1.4200E-04  1.4200E-04  4.5780E+02  1.2356E-03 -4.7203E-04 -1.8527E-04
32170=  2.0700E-07  5.1029E+00  1.5400E-04  2.5000E-01  3.1000E-02  3.1000E-02  3.1000E-02  1.4324E+01  7.3911E+00  8.6500E+00
32180= -2.6429E+00
32190=OELEMENTS OF FILTER ESTIMATION ERROR XF-XT
32200=  6.0023E-06  1.0670E-06 -8.8276E+01  3.1128E+00  9.6641E-01 -3.2937E+01 -6.2044E-05  2.3216E-04  4.9410E-04 -8.1236E+01
32210= -4.4546E+00  1.1980E-08  1.7518E-08 -1.4554E-06  3.2641E-02 -3.7410E+02
32220=ODEBUG: JNUMBR= 25
32230=ODEBUG: NSEDEN(DB'S)=  -1.9408E+02
32240=OCARRIER-TO-NOISE DENSITY=    1.7884E+01
32250=OCARRIER-TO-NOISE DENSITY=    1.7028E+01
32260=OCARRIER-TO-NOISE DENSITY=    1.6049E+01
32270=OCARRIER-TO-NOISE DENSITY=    2.7616E+01
32280=OCARRIER-TO-NOISE DENSITY=    2.6889E+01
32290=OCARRIER-TO-NOISE DENSITY=    1.8010E+01
32300=ORMEAS(I)=      15.7519
32310=ORMEAS(I)=      16.8504
32320=ORMEAS(I)=      17.6368
32330=ORMEAS(I)=      14.9096
32340=ORMEAS(I)=      14.9891
32350=ORMEAS(I)=      15.6461
```

```
31980=0TIME =   1100.00 - ************************************************************************************************************
*
31990=0WHOLE VALUE USER POSITION AND VELOCITY
32000=      LON(RAD)              LAT(RAD)              ALT(FT)              VE(FPS)              VN(FPS)              VZ(FPS)
32010=   -.153354902831E+01    .651409423922E+00    .341540092922E+05  -.274353415334E+03  -.796730622321E+03    .608697998663E+02
32020=   -.153370170363E+01    .651435880308E+00    .356322685545E+05  -.281459710337E+03  -.797077068358E+03    .115359845547E+03
32030=   -.153354300840E+01    .651410654364E+00    .340632413932E+05  -.271224768831E+03  -.795626431947E+03    .277461265978E+02
32040=
32050= SQRT OF FILTER COVARIANCE DIAGONAL
32060=  9.4580E-07  1.0668E-06  5.9993E+01  5.7477E-01  7.2502E-01  1.3832E+01  2.7126E-04  2.6773E-04  5.2246E-04  1.8796E+01
32070=  8.9446E-01  1.6611E-08  1.6611E-08  2.7643E-08  1.1317E-02  2.6764E+02
32080=0ELEMENTS OF FILTER ERROR STATE VECTOR DXF
32090= -1.5870E-04  2.5226E-05  1.5690E+03 -1.0235E+01 -1.4506E+00  8.7614E+01 -2.6174E-04 -6.7191E-05  1.6480E-04  3.4407E+03
32100=  8.7071E+00 -6.0604E-10  2.8594E-10  2.1400E-10 -7.0298E-02  1.8616E+03
32110=0ELEMENTS OF TRUE ERROR STATE VECTOR DXT
32120= -1.5268E-04  2.6456E-05  1.4783E+03 -7.1063E+00 -3.4645E-01  5.4490E+01 -2.8919E-04  1.3119E-04  6.6870E-04  3.0000E-02
32130= -3.6889E-02  3.3611E+03  5.0228E-02  1.1443E-08  1.7744E-08 -1.4551E-06  4.5200E-08  4.5200E-08  4.5200E-08  4.5200E-08
32140=  4.5200E-08  4.5200E-08  1.8740E-10  1.8740E-10  1.8740E-10  3.0000E-04  3.0000E-04  1.0000E-03  1.9400E-04 -1.9400E-04
32150= -1.9400E-04  1.9400E-04  1.9400E-04 -1.9400E-04 -2.5847E-03  6.4575E-04  6.7198E-04  1.5000E-04  1.5000E-04  1.5000E-04
32160= -1.4600E-04  8.7200E-04  1.4600E-04 -8.7200E-04 -1.4200E-04  1.4200E-04  4.5780E+02  1.2356E-03 -4.7203E-04 -1.8527E-04
32170=  2.0700E-07  5.1029E+00  1.5400E-04  2.5000E-01  3.1000E-02  3.1000E-02  3.1000E-02  1.4324E+01  7.3911E+00  8.6500E+00
32180= -2.6429E+00
32190=0ELEMENTS OF FILTER ESTIMATION ERROR XF-XT
32200=  6.0199E-06  1.2304E-06 -9.0768E+01  3.1286E+00  1.1042E+00 -3.3124E+01 -2.7452E-05  1.9838E-04  5.0390E-04 -7.9528E+01
32210= -4.3795E+00  1.2049E-08  1.7458E-08 -1.4554E-06  3.2773E-02 -3.7920E+02
32220=0DEBUG:JNUMBR= 25
32230=0DEBUG: NSEDEN(DB'S)=  -1.9408E+02
32240=0CARRIER-TO-NOISE DENSITY=    1.7884E+01
32250=0CARRIER-TO-NOISE DENSITY=    1.7028E+01
32260=0CARRIER-TO-NOISE DENSITY=    1.6049E+01
32270=0CARRIER-TO-NOISE DENSITY=    2.7616E+01
32280=0CARRIER-TO-NOISE DENSITY=    2.6889E+01
32290=0CARRIER-TO-NOISE DENSITY=    1.8010E+01
32300=0RMEAS(I)=      15.7519
32310=0RMEAS(I)=      16.8504
32320=0RMEAS(I)=      17.6368
32330=0RMEAS(I)=      14.9096
32340=0RMEAS(I)=      14.9891
32350=0RMEAS(I)=      15.6461
```

```
 32360=0TIME =    1100.00 + ************************************************************************************************************
*
 32370= SQRT OF FILTER COVARIANCE DIAGONAL
 32380=  5.8949E-07  6.8795E-07  2.2845E+01  4.1374E-01  5.3683E-01  1.3820E+01  2.6763E-04  2.6477E-04  5.2371E-04  1.1751E+01
 32390=  6.5754E-01  1.6611E-08  1.6611E-08  2.7643E-08  1.1164E-02  6.6803E+01
 32400=0ELEMENTS OF FILTER ERROR STATE VECTOR DXF
 32410= -1.5587E-04  2.6242E-05  1.4553E+03 -9.1543E+00 -7.9969E-01  8.6440E+01 -2.1263E-04 -9.7202E-05  1.7728E-04  3.4221E+03
 32420=  9.7205E+00 -5.1051E-10  2.3397E-10  2.4738E-10 -6.6563E-02  1.7340E+03
 32430=0ELEMENTS OF FILTER ESTIMATION ERROR XF-XT
 32440=  3.1962E-06  2.1431E-07  2.2980E+01  2.0480E+00  4.5325E-01 -3.1950E+01 -7.6564E-05  2.2839E-04  4.9142E-04 -6.0958E+01
 32450= -5.3929E+00  1.1953E-08  1.7510E-08 -1.4554E-06  2.9038E-02 -2.5153E+02
 32460=0HORIZON SCAN AT TIME =    1100.00
 32470=0DEBUG;JNUMBR= 25
 32480=0DEBUG; NSEDEN(DB'S)=  -1.9408E+02
 32490=0CARRIER-TO-NOISE DENSITY=    1.7884E+01
 32500=0CARRIER-TO-NOISE DENSITY=    1.7028E+01
 32510=0CARRIER-TO-NOISE DENSITY=    1.6049E+01
 32520=0CARRIER-TO-NOISE DENSITY=    2.7616E+01
 32530=0CARRIER-TO-NOISE DENSITY=    2.6889E+01
 32540=0CARRIER-TO-NOISE DENSITY=    1.8010E+01
 32550=0RMEAS(I)=      15.7519
 32560=0RMEAS(I)=      16.8504
 32570=0RMEAS(I)=      17.6368
 32580=0RMEAS(I)=      14.9096
 32590=0RMEAS(I)=      14.9891
 32600=0RMEAS(I)=      15.6461
 32610=0THE IN VIEW SATELLITE SET IS
 32620=0SATELLITE      ORBIT
 32630=          1          3
 32640=          1          4
 32650=          2          4
 32660=          2          5
 32670=          3          2
 32680=          3          6
 32690=0THE OPTIMUM SATELLITE GROUP IS
 32700=0SATELLITE      ORBIT
 32710=          1          3
 32720=          2          5
 32730=          3          2
 32740=          3          6
 32750=0FOR THIS SATELLITE GROUP,GDOP =    3.5320E+00
 32760=0 FOR THIS SATELLITE SET THE COST=    9.8434E-10
```

```
32360=0TIME =    1100.00 + ************************************************************************************************************************
*
32370= SQRT OF FILTER COVARIANCE DIAGONAL
32380=  5.8944E-07  6.8862E-07  2.2841E+01  4.1328E-01  5.3643E-01  1.3819E+01  2.6725E-04  2.6333E-04  5.2235E-04  1.1750E+01
32390=  6.5752E-01  1.6611E-08  1.6611E-08  2.7643E-08  1.1164E-02  6.6803E+01
32400=0ELEMENTS OF FILTER ERROR STATE VECTOR DXF
32410= -1.5588E-04  2.6177E-05  1.4565E+03 -9.1646E+00 -8.7982E-01  8.6621E+01 -2.4301E-04 -6.3693E-05  1.6767E-04  3.4214E+03
32420=  9.6746E+00 -5.7166E-10  2.9403E-10  2.1799E-10 -6.6660E-02  1.7376E+03
32430=0ELEMENTS OF FILTER ESTIMATION ERROR XF-XT
32440=  3.2036E-06  2.7917E-07  2.1780E+01  2.0583E+00  5.3338E-01 -3.2130E+01 -4.6183E-05  1.9488E-04  5.0102E-04 -6.0228E+01
32450= -5.3470E+00  1.2015E-08  1.7450E-08 -1.4554E-06  2.9135E-02 -2.5521E+02
32460=0HORIZON SCAN AT TIME =    1100.00
32470=0DEBUG:JNUMRR= 25
32480=0DEBUG: NSEDEN(DB'S)=  -1.9408E+02
32490=0CARRIER-TO-NOISE DENSITY=    1.7884E+01
32500=0CARRIER-TO-NOISE DENSITY=    1.7028E+01
32510=0CARRIER-TO-NOISE DENSITY=    1.6049E+01
32520=0CARRIER-TO-NOISE DENSITY=    2.7616E+01
32530=0CARRIER-TO-NOISE DENSITY=    2.6889E+01
32540=0CARRIER-TO-NOISE DENSITY=    1.8010E+01
32550=0RMEAS(I)=      15.7519
32560=0RMEAS(I)=      16.8504
32570=0RMEAS(I)=      17.6368
32580=0RMEAS(I)=      14.9096
32590=0RMEAS(I)=      14.9891
32600=0RMEAS(I)=      15.6461
32610=0THE IN VIEW SATELLITE SET IS
32620=0SATELLITE      ORBIT
32630=          1          3
32640=          1          4
32650=          2          4
32660=          2          5
32670=          3          2
32680=          3          6
32690=0THE OPTIMUM SATELLITE GROUP IS
32700=0SATELLITE      ORBIT
32710=          1          4
32720=          2          4
32730=          2          5
32740=          3          6
32750=0FOR THIS SATELLITE GROUP,GDOP =    2.5418E+00
32760=0 FOR THIS SATELLITE SET THE COST=    1.0979E-09
```

```
37760=OTIME =   1300.00 - ************************************************************************************************************************
*
37770=OWHOLE VALUE USER POSITION AND VELOCITY
37780=      LON(RAD)              LAT(RAD)              ALT(FT)              VE(FPS)              VN(FPS)              VZ(FPS)
37790=   -.153683566988E+01    .643764744526E+00    .349011719507E+05   -.275068223173E+03   -.798806445925E+03    .590028094305E+00
37800=   -.153708093853E+01    .643787299264E+00    .366670342493E+05   -.283443408113E+03   -.799372991038E+03    .690027737411E+02
37810=   -.153683433100E+01    .643763863291E+00    .348360407527E+05   -.274946527656E+03   -.798854151366E+03   -.391258331309E+02
37820=
37830= SQRT OF FILTER COVARIANCE DIAGONAL
37840=  8.2325E-07  6.9307E-07  3.4051E+01  2.6035E-01  2.6882E-01  1.5715E+01  6.7673E-05  7.7796E-05  5.2087E-04  2.4473E+01
37850=  9.2162E-01  1.6950E-08  1.6950E-08  2.8225E-08  1.1240E-02  9.0900E+01
37860=OELEMENTS OF FILTER ERROR STATE VECTOR DXF
37870= -2.4661E-04  2.3436E-05  1.8310E+03 -8.4969E+00 -5.1884E-01  1.0813E+02 -1.6664E-04 -1.6138E-04  1.0535E-04  4.6108E+03
37880=  9.7606E+00 -4.3301E-10  9.3174E-10  2.1943E-10 -8.0483E-02  1.8851E+03
37890=OELEMENTS OF TRUE ERROR STATE VECTOR DXT
37900= -2.4527E-04  2.2555E-05  1.7459E+03 -8.3752E+00 -5.6655E-01  6.8413E+01 -2.8216E-04  7.3324E-05  6.1667E-04  3.0000E-02
37910= -4.6475E-02  4.5510E+03  5.0269E-02  6.1969E-09  1.4895E-08 -1.4548E-06  4.5200E-08  4.5200E-08  4.5200E-08  4.5200E-08
37920=  4.5200E-08  4.5200E-08  1.8740E-10  1.8740E-10  1.8740E-10  3.0000E-04  3.0000E-04  1.0000E-03  1.9400E-04 -1.9400E-04
37930= -1.9400E-04  1.9400E-04  1.9400E-04 -1.9400E-04 -2.5858E-03  3.7755E-04  1.2054E-03  1.5000E-04  1.5000E-04  1.5000E-04
37940= -1.4600E-04  8.7200E-04  1.4600E-04 -8.7200E-04 -1.4200E-04  1.4200E-04  4.5690E+02  1.4727E-03  3.5257E-04  2.7043E-04
37950=  2.0700E-07  9.0622E+00  1.5400E-04  2.5000E-01  3.1000E-02  3.1000E-02  3.1000E-02  1.7522E+01 -3.3637E-01 -1.8220E+00
37960= -1.1110E+01
37970=OELEMENTS OF FILTER ESTIMATION ERROR XF-XT
37980=  1.3389E-06 -8.8124E-07 -6.5131E+01  1.2170E-01 -4.7705E-02 -3.9716E+01 -1.1552E-04  2.3470E-04  5.1131E-04 -5.9779E+01
37990= -1.6427E+00  6.6299E-09  1.3964E-08 -1.4550E-06  3.2382E-02 -3.8118E+02
38000=ODEBUG:JNUMBR= 25
38010=ODEBUG: NSEDEN(DB'S)=  -2.0040E+02
38020=OCARRIER-TO-NOISE DENSITY=   2.4312E+01
38030=OCARRIER-TO-NOISE DENSITY=   2.3695E+01
38040=OCARRIER-TO-NOISE DENSITY=   2.1323E+01
38050=OCARRIER-TO-NOISE DENSITY=   3.4161E+01
38060=OCARRIER-TO-NOISE DENSITY=   3.3216E+01
38070=OCARRIER-TO-NOISE DENSITY=   2.5473E+01
38080=ORMEAS(I)=      15.1861
38090=ORMEAS(I)=      15.2051
38100=ORMEAS(I)=      15.1465
38110=ORMEAS(I)=      14.1511
38120=ORMEAS(I)=      14.3153
38130=ORMEAS(I)=      15.1174
```

```
37760=0TIME =   1300.00 - ************************************************************************************************************************
*
37770=0WHOLE VALUE USER POSITION AND VELOCITY
37780=       LON(RAD)              LAT(RAD)              ALT(FT)              VE(FPS)              VN(FPS)              VZ(FPS)
37790=   -.153683566988E+01    .643764744526E+00    .349011719507E+05  -.275068223173E+03  -.798806445925E+03    .590028094305E+00
37800=   -.153708093853E+01    .643787299264E+00    .346670342493E+05  -.283443408113E+03  -.799372991038E+03    .690027737411E+02
37810=   -.153683242192E+01    .643763683897E+00    .349385504146E+05  -.274129717318E+03  -.798874811965E+03   -.395526773391E+02
37820=
37830= SQRT OF FILTER COVARIANCE DIAGONAL
37840=  5.2867E-07  6.4133E-07  3.0529E+01  1.8972E-01  2.5458E-01  1.5714E+01  6.5267E-05  6.8509E-05  5.1991E-04  1.5973E+01
37850=  8.2754E-01  1.6950E-08  1.6950E-08  2.8224F-08  1.1236E-02  9.0350E+01
37860=0ELEMENTS OF FILTER ERROR STATE VECTOR DXF
37870= -2.4852E-04  2.3615E-05  1.7285E+03 -9.3137E+00 -4.9818E-01  1.0856E+02 -1.6752E-04  1.2627E-05  8.0548E-05  4.6523F+03
37880=  1.0998E+01 -5.1592E-10  1.2044E-09  1.6854E-10 -7.7856E-02  1.6686E+03
37890=0ELEMENTS OF TRUE ERROR STATE VECTOR DXT
37900= -2.4527E-04  2.2555E-05  1.7659E+03 -8.3752E+00 -5.6655E-01  6.8413E+01 -2.8216E-04  7.3324E-05  6.1667E-04  3.0000E-02
37910= -4.6475E-02  4.5510E+03  5.0269E-02  6.1969E-09  1.4895F-08 -1.4548F-06  4.5200E-08  4.5200E-08  4.5200E-08  4.5200E-08
37920=  4.5200E-08  4.5200E-08  1.8740E-10  1.8740E-10  1.8740E-10  3.0000E-04  3.0000E-04  1.0000E-03  1.9400E-04 -1.9400E-04
37930= -1.9400E-04  1.9400E-04  1.9400E-04 -1.9400E-04 -2.5858E-03  3.7755E-04  1.2054F-03  1.5000E-04  1.5000E-04  1.5000E-04
37940= -1.4600E-04  8.7200E-04  1.4600E-04 -8.7200E-04 -1.4200E-04  1.4200E-04  4.5690E+02  1.4727E-03  3.5257E-04  2.7043E-04
37950=  2.0700E-07  9.0622E+00  1.5400E-04  2.5000E-01  3.1000E-02  3.1000E-02  3.1000E-02  1.7522E+01 -3.3637E-01 -1.8220F+00
37960= -1.1110E+01
37970=0ELEMENTS OF FILTER ESTIMATION ERROR XF-XT
37980=  3.2480E-06 -1.0606E-06  3.7378E+01  9.3851E-01 -6.8366E-02 -4.0143E+01 -1.1465E-04  6.0697E-05  5.3612E-04 -1.0132F+02
37990= -2.8805E+00  6.7128E-09  1.3691E-08 -1.4549E-06  2.9755E-02 -1.6471E+02
38000=0DEBUG: JNUMBR= 25
38010=0DEBUG: NSEDEN(DB'S)=  -2.0040E+02
38020=0CARRIER-TO-NOISE DENSITY=    2.4312E+01
38030=0CARRIER-TO-NOISE DENSITY=    2.3695E+01
38040=0CARRIER-TO-NOISE DENSITY=    2.1323E+01
38050=0CARRIER-TO-NOISE DENSITY=    3.4161E+01
38060=0CARRIER-TO-NOISE DENSITY=    3.3216E+01
38070=0CARRIER-TO-NOISE DENSITY=    2.5473E+01
38080=0RMEAS(I)=      15.1861
38090=0RMEAS(I)=      15.2051
38100=0RMEAS(I)=      15.1465
38110=0RMEAS(I)=      14.1511
38120=0RMEAS(I)=      14.3153
38130=0RMEAS(I)=      15.1174
```

```
38140=0TIME =    1300.00 + ************************************************************************************************************************
*
38150= SQRT OF FILTER COVARIANCE DIAGONAL
38160=  6.6023E-07  5.5856E-07  2.4075E+01  2.2305E-01  2.3020E-01  1.5712E+01  6.1911E-05  7.3617E-05  5.2082E-04  1.7876E+01
38170=  7.0885E-01  1.6950E-08  1.6950E-08  2.8225E-08  1.1212E-02  5.3671E+01
38180=0ELEMENTS OF FILTER ERROR STATE VECTOR DXF
38190= -2.4674E-04  2.3764E-05  1.7512E+03 -8.5845E+00 -4.0713E-01  1.0770E+02 -1.4478E-04 -1.4318E-04  1.0142E-04  4.6016E+03
38200=  1.0377E+01 -3.3647E-10  1.1017E-09  2.1346E-10 -7.8118E-02  1.7704E+03
38210=0ELEMENTS OF FILTER ESTIMATION ERROR XF-XT
38220=  1.4669E-06 -1.2093E-06  1.4616E+01  2.0927E-01 -1.5943E-01 -3.9289E+01 -1.3739E-04  2.1651E-04  5.1525E-04 -5.0606E+01
38230= -2.2591E+00  6.5334E-09  1.3794E-08 -1.4550E-06  3.0017E-02 -2.6645E+02
38240=0HORIZON SCAN AT TIME =    1300.00
38250=0DEBUG:JNUMRR= 25
38260=0DEBUG: NSEDEN(DB'S)=  -2.0040E+02
38270=0CARRIER-TO-NOISE DENSITY=    2.4312E+01
38280=0CARRIER-TO-NOISE DENSITY=    2.3695E+01
38290=0CARRIER-TO-NOISE DENSITY=    2.1323E+01
38300=0CARRIER-TO-NOISE DENSITY=    3.4161E+01
38310=0CARRIER-TO-NOISE DENSITY=    3.3216E+01
38320=0CARRIER-TO-NOISE DENSITY=    2.5473E+01
38330=0RMEAS(I)=      15.1861
38340=0RMEAS(I)=      15.2051
38350=0RMEAS(I)=      15.1465
38360=0RMEAS(I)=      14.1511
38370=0RMEAS(I)=      14.3153
38380=0RMEAS(I)=      15.1174
38390=0THE IN VIEW SATELLITE SET IS
38400=0SATELLITE      ORBIT
38410=          1          3
38420=          1          4
38430=          2          4
38440=          2          5
38450=          3          2
38460=          3          6
38470=0THE OPTIMUM SATELLITE GROUP IS
38480=0SATELLITE      ORBIT
38490=          1          3
38500=          2          5
38510=          3          2
38520=          3          6
38530=0FOR THIS SATELLITE GROUP,GDOP =    3.7227E+00
38540=0 FOR THIS SATELLITE SET THE COST=    1.2029E-09
```

```
38140=0TIME =   1300.00 + ************************************************************************************************************************
*
38150= SQRT OF FILTER COVARIANCE DIAGONAL
38160=  4.1507E-07  5.1345E-07  1.9380E+01  1.6121E-01  2.1721E-01  1.5711E+01  5.9707E-05  6.5891E-05  5.1986E-04  1.0113E+01
38170=  5.8267E-01  1.6950E-08  1.6949E-08  2.8224E-08  1.1207E-02  5.2914E+01
38180=0ELEMENTS OF FILTER ERROR STATE VECTOR DXF
38190= -2.4750E-04  2.3788E-05  1.6989E+03 -9.0991E+00 -4.5079E-01  1.0837E+02 -1.5861E-04 -2.6966E-05  8.3284E-05  4.6229E+03
38200=  1.1959E+01 -4.9499E-10  1.1256E-09  1.7225E-10 -7.6923E-02  1.5226E+03
38210=0ELEMENTS OF FILTER ESTIMATION ERROR XF-XT
38220=  2.2274E-06 -1.2334E-06  6.6943E+01  7.2388E-01 -1.1576E-01 -3.9954E+01 -1.2355E-04  1.0029E-04  5.3338E-04 -7.1866E+01
38230= -3.8416E+00  6.4919E-09  1.3770E-08 -1.4550E-06  2.8822E-02 -1.8649E+01
38240=0HORIZON SCAN AT TIME =   1300.00
38250=0DEBUG:JNUMBR= 25
38260=0DEBUG: NSEDEN(DB'S)=  -2.0040E+02
38270=0CARRIER-TO-NOISE DENSITY=   2.4312E+01
38280=0CARRIER-TO-NOISE DENSITY=   2.3695E+01
38290=0CARRIER-TO-NOISE DENSITY=   2.1323E+01
38300=0CARRIER-TO-NOISE DENSITY=   3.4161E+01
38310=0CARRIER-TO-NOISE DENSITY=   3.3216E+01
38320=0CARRIER-TO-NOISE DENSITY=   2.5473E+01
38330=0RMEAS(I)=      15.1861
38340=0RMEAS(I)=      15.2051
38350=0RMEAS(I)=      15.1465
38360=0RMEAS(I)=      14.1511
38370=0RMEAS(I)=      14.3153
38380=0RMEAS(I)=      15.1174
38390=0THE IN VIEW SATELLITE SET IS
38400=0SATELLITE      ORBIT
38410=          1          3
38420=          1          4
38430=          2          4
38440=          2          5
38450=          3          2
38460=          3          6
38470=0THE OPTIMUM SATELLITE GROUP IS
38480=0SATELLITE      ORBIT
38490=          1          4
38500=          2          4
38510=          2          5
38520=          3          6
38530=0FOR THIS SATELLITE GROUP,GDOP =   2.5612E+00
38540=0 FOR THIS SATELLITE SET THE COST=  -2.3054E-09
```

Bibliography

1. YEE-81-009. NAVSTAR Global Positioning System (GPS) User's Overview. Los Angeles Air Force Station, California, Deputy for Space Navigation Systems NAVSTAR Global Positioning System Joint Program Office, September 1982.

2. Chen, Paul. "Accuracy Requirement and Cost Effectiveness of GPS-Aided INS for Tactical Fighters," IEEE National Aerospace and Electronics Conference: pp. 1212-1216 (1978).

3. Cox, D. B. Jr. "Integration of GPS with Inertial Navigation Systems," The Journal of the Institute of Navigation: pp. 144-153 (Summer 1978).

4. Kruh, Pierre. "The NAVSTAR Global Positioning System Six Plane 18-Satellite Constellation," IEEE National Aerospace Electronics Conference: pp. E9.3.1-E9.3.8 (1981).

5. Macdonald, Thomas J., et. al. GPS High Anti-Jam Performance Analysis. Final Report for the period February 1977-April 1979 (AFWAL-TR-79-1038). Wright-Patterson AFB, Ohio: Avionics Laboratory. Air Force Wright Aeronautical Laboratories, June 1979.

6. Upadhyay, Triveni N., et. al. Advanced GPS/INERTIAL Integration Technology Program (ADGINT). Final Report for the period August 1979-September 1980 (AFWAL-TR-80-1148: Volume II. Summary of Task II Results). Wright-Patterson AFB, Ohio: Avionics Laboratory. Air Force Wright Aeronautical Laboratories, September 1981.

7. Dudzinski, Edward C. Global Positioning System Satellite Selection. Final Report for the period 1 October 1979-30 November 1980 (AFWAL-TR-81-1051). Wright-Patterson AFB, Ohio: Reference Systems Branch, System Avionics Division, Avionics Laboratory. Air Force Wright Aeronautical Laboratories, 2 March 1981.

8. Jorgensen, Paul. "Combined Pseudo-Range and Doppler Positioning for the Stationary NAVSTAR User," IEEE Position, Location, and Navigation Symposium: pp. 450-458 (1980).

9. Lesher, Ronnie E. Performance Improvements of a Class of Array Processors in a Jamming Environment. MS Thesis. Wright-Patterson AFB, Ohio: Air Force Institute of Technology, 1978.

10. Hemesath, Norbert B. and William M. Hutchinson. "GPS Overview and User Equipment Anti-Jam Design," IEEE National Telecommunications Conference: pp. 41.6/1-5 (1976).

11. Brogan, William L. Improvements and Extensions of the Geometrical Dilution of Precision (GDOP) Concept for Selecting Navigation Measurements. Final Report for the period 1 May 1980 to 1 May 1981 (AFWAL-TR-81-1142). Wright-Patterson AFB, Ohio: Avionics Laboratory. Air Force Wright Aeronautical Laboratories, September 1981.

12. Brogan, William L. and A. C. Liang. Navigation of a Tactical Aircraft Using a Fully Integrated DNSS/Strapped-Down Inertial System. Aerospace Report No. TOR-0073 (3020-03)-2: pp. 28-30 (4 March 1973).

13. Liebelt, P. B. An Introduction to Optimal Estimation and Control, Addison-Wesley, 1969.

14. Meditch, J. S. Stochastic Optimal Linear Estimation and Control, McGraw-Hill, 1969.

15. Brogan, William L. Modern Control Theory, Quantum Publishers, Inc., New York, 1974.

16. Myers, Ken and Ron Butler. "Simulation Results for an Integrated GPS/Inertial Aircraft Navigation System," IEEE National Aerospace Electronics Conference: pp. 841-848 (1976).

17. IR-236. Integrated GPS/Inertial Simulator Computer Program. Cambridge, Massachusetts, Intermetrics, 26 August 1977.

18. Widnall, W. S. and P. Grundy. Inertial Navigation System Error Models. TR-03-73. Cambridge, Massachusetts, Intermetrics, 11 May 1973.

19. Carlson, N. A. "Fast Triangular Formulation of the Square Root Filter," AIAA Journal, Volume II, No. 9: p. 1259 (September 1973).

20. Shephard, William E. and Major Robert M. Edwards. Global Positioning System Jamming to Signal Ratio Analyses. Final Report for the period 27 November 1978-31 July 1979 (AFWAL-TR-80-1045). Wright-Patterson AFB, Ohio: Avionics Laboratory. Air Force Wright Aeronautical Laboratories, November 1980.

21. Maybeck, Peter S. Stochastic Models, Estimation, and Control, Volume 2, Academic Press, New York, 1982.

22. Martin, Edward H. "GPS User Equipment Error Models," IEEE National Aerospace Electronics Conference: pp. 109-118 (Summer 1978).

23. YEN-77-332. NAVSTAR Global Positioning System Navigation Signal Description. Los Angeles Air Force Station, California, Deputy for Space Navigation Systems NAVSTAR Global Positioning System Joint Program Office, 28 November 1977.

24. Musick, Stan H. PROFGEN-A Computer Program for Generating Flight Profiles. (AFWAL-TR-76-247). Wright-Patterson AFB, Ohio: Avionics Laboratory. Air Force Wright Aeronautical Laboratories, November 1976.

25. Blank, R. W. The NAVSTAR GPS Full Scale Development User Equipment Family. Cedar Rapids, Iowa, Rockwell International: Collins Gov. Avionics Division, June 1983.

26. Stark, Louis. "Microwave Theory of Phased-Array Antennas-A Review," IEEE Proceedings, Volume 62, No. 12: pp. 1661-1701 (December 1974).

27. Compton, Ralph T. Jr. "Power Optimization in Adaptive Arrays: A Technique for Interference Protection," IEEE Transactions on Antennas and Propagation, Vol. AP-28, No. 1: pp. 79-85 (January 1980).

28. LEQ2C: Linear Equation Solution-Complex Matrix-High Accuracy Solution. International Mathematical and Statistical Libraries (IMSL). Houston, Texas, IMSL, Inc., June 1982.

VITA

Peter Michael Charles Vaccaro was born on 7 June 1958 in Norwich, New York. He graduated from Amphitheater High School in Tucson, Arizona in 1976 and attended the United States Air Force Academy from which he received the degree of Bachelor of Science in Electrical Engineering in May 1980. Upon graduation, he received a commission in the USAF. He was employed as an electrical engineer in the Logistic's Directorate of the NAVSTAR Global Positioning System (GPS) Joint Program Office, Los Angeles AFS, California from June 1980 until entering the School of Engineering, Air Force Institute of Technology, in May 1982.

Permanent address: 4915 Sullinger Ave.
Tucson, Arizona 85705

UNCLASSIFIED

SECURITY CLASSIFICATION OF THIS PAGE

REPORT DOCUMENTATION PAGE

1a. REPORT SECURITY CLASSIFICATION: UNCLASSIFIED	1b. RESTRICTIVE MARKINGS
2a. SECURITY CLASSIFICATION AUTHORITY	3. DISTRIBUTION/AVAILABILITY OF REPORT: Approved for public release; distribution unlimited.
2b. DECLASSIFICATION/DOWNGRADING SCHEDULE	
4. PERFORMING ORGANIZATION REPORT NUMBER(S): AFIT/GE/EE/83D-67	5. MONITORING ORGANIZATION REPORT NUMBER(S)
6a. NAME OF PERFORMING ORGANIZATION: School of Engineering; 6b. OFFICE SYMBOL (If applicable): AFIT/ENG	7a. NAME OF MONITORING ORGANIZATION
6c. ADDRESS (City, State and ZIP Code): Air Force Institute of Technology, Wright-Patterson AFB, Ohio 45433	7b. ADDRESS (City, State and ZIP Code)
8a. NAME OF FUNDING/SPONSORING ORGANIZATION; 8b. OFFICE SYMBOL (If applicable)	9. PROCUREMENT INSTRUMENT IDENTIFICATION NUMBER
8c. ADDRESS (City, State and ZIP Code)	10. SOURCE OF FUNDING NOS. — PROGRAM ELEMENT NO. / PROJECT NO. / TASK NO. / WORK UNIT NO.
11. TITLE (Include Security Classification): See Box 19	

12. PERSONAL AUTHOR(S): Peter M. Vaccaro, B.S.E.E., 1st Lt, USAF

13a. TYPE OF REPORT	13b. TIME COVERED	14. DATE OF REPORT (Yr., Mo., Day)	15. PAGE COUNT
MS Thesis	FROM _____ TO _____	1983 December	211

16. SUPPLEMENTARY NOTATION

17. COSATI CODES			18. SUBJECT TERMS (Continue on reverse if necessary and identify by block number)
FIELD	GROUP	SUB. GR.	Global Positioning System, Inertial Navigation, Space Navigation, Navigational Aids: Navigation Satellites.
17	07		

19. ABSTRACT (Continue on reverse if necessary and identify by block number)

Title: GLOBAL POSITIONING SYSTEM SATELLITE SELECTION EVALUATION FOR AIDED INERTIAL NAVIGATION

Thesis Chairman: Robert M. Edwards, Lt. Col, USAF

LYNN E. WOLAVER 1Feb 84
Dean for Research and Professional Development
Air Force Institute of Technology (AIC)
Wright-Patterson AFB OH 45433

20. DISTRIBUTION/AVAILABILITY OF ABSTRACT	21. ABSTRACT SECURITY CLASSIFICATION
UNCLASSIFIED/UNLIMITED ☒ SAME AS RPT. ☐ DTIC USERS ☐	UNCLASSIFIED

22a. NAME OF RESPONSIBLE INDIVIDUAL	22b. TELEPHONE NUMBER (Include Area Code)	22c. OFFICE SYMBOL
Robert M. Edwards, Lt. Col, USAF	255-3576	AFIT/ENG

DD FORM 1473, 83 APR — EDITION OF 1 JAN 73 IS OBSOLETE.

UNCLASSIFIED

SECURITY CLASSIFICATION OF THIS PAGE

The navigation performance of the geometric dilution of precision (GDOP) GPS satellite selection criterion versus an alternate GPS satellite selection criterion for an integrated GPS/INS Navigator in a jamming environment is tested and analyzed.

The theoretical development of GDOP and GDOP-based satellite selection criterion are reviewed. From this review a satellite selection criterion known as the cost criterion (which is a combination of noise-weighted GDOP and the a priori covariance weighted least squares position error) is selected for performance testing against a GDOP satellite selection criterion.

Performance assessment of the two satellite selection criterion is accomplished using a modified version of the integrated GPS/INS (IGI) Computer Simulation. The IGI Simulator is modified to simulate adaptive band-width control of the satellite tracking loops, the use of a null steering antenna, the use of an alternate satellite selection criterion, and the effects due to jammers. The performance assessment is based on simulating a single F-4 Close-Air-Support Mission encountering five different jamming scenarios.

For the five test missions, the cost criterion demonstrates a performance improvement of 10-350 feet in mean radial position error with respect to GDOP performance. However, a performance degradation of 10-30 feet mean radial position error is observed for missions with rapidly varying jamming power.


FILME
4-84